

**PHYTOPLANKTON RESPONSES AS
INDICATORS OF EXPOSURE TO TOXICANTS**

by

ROSANGELA APARECIDA DEVILLA

A thesis submitted to the University of Plymouth in partial fulfilment for
the degree of

DOCTOR OF PHILOSOPHY

School of Biological Sciences
Faculty of Science

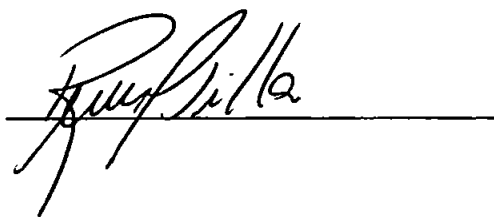
In collaboration with
Plymouth Marine Laboratory

January 2005

Copyright Statement

This copy of the thesis has been supplied on condition that anyone who consults it is understood to recognise that its copyright rests with its author and that no quotation from the thesis and no information derived from it may be published without the author's prior consent.

Signed



A handwritten signature in black ink, appearing to read "Rung Pilla", is written over a solid horizontal line.

University of Plymouth Library
Item No. 9006865418
Shelfmark THESIS 571.957 DEV

*'Gracias a la Vida que me ha dado tanto
me dio el corazón que agita su marco
cuando miro el fruto del cerebro humano,
cuando miro al bueno tan lejos del malo,
cuando miro al fondo de tus ojos claros.'*

Por: Violeta Parra

To my parents and Tobias

PHYTOPLANKTON RESPONSES AS INDICATORS OF EXPOSURE TO TOXICANTS

Rosângela Aparecida Devilla

Abstract

The use of antifouling booster biocides on boats and ships is of environmental concern as the leached products can affect non-target, highly susceptible phytoplanktonic organisms. Appropriate assessment of whether or not estuarine/marine phytoplankton are potentially at risk should include a combination of approaches, investigating toxic effects for both single species and natural phytoplankton communities and ideally include field verifications. This research addresses the application and comparison of methods to investigate toxic responses to four antifouling biocides Irgarol 1051[®], diuron, Sea-Nine 211[®] and zinc pyrithione in laboratory-based experiments with single species and using natural phytoplankton assemblages. The applicability of photosynthetic parameters and pigment:chlorophyll-*a* ratios as biomarkers was initially employed in unialgal experiments. Variations in results for pigment:chlorophyll-*a* ratios following toxic exposures indicate that care must be taken when using CHEMTAX estimations and that further research into this topic is needed.

Compositional changes in natural phytoplankton assemblages under toxicant exposure were evaluated using standard techniques (microscopy) and were compared to group-specific biomass estimation derived from CHEMTAX-High Performance Liquid Chromatography. This broad approach proved effective in detecting changes in the main phytoplankton groups, with prasinophytes and prymnesiophytes proving most susceptible and chlorophytes and dinoflagellates being comparatively resistant to the PSII inhibitor Irgarol 1051[®]. In addition, the impact of selected antifouling agents on photosynthesis and pigment chemotaxonomy was investigated for a natural phytoplankton community. Pigment signatures were determined by HPLC and growth was determined by Analytical Flow Cytometry (AFC). Primary production (estimated by ¹⁴C-uptake) was compared to photosynthetic efficiency (F_v/F_m) measured using Fast Repetition Rate Fluorescence (FRRF). Differences in species-specific sensitivity of the phytoplankton community were detected through pigment composition after 72 h exposures to zinc pyrithione (5 $\mu\text{g l}^{-1}$) and Sea-Nine 211[®] (10 $\mu\text{g l}^{-1}$). The pigment zeaxanthin was proportionally increased indicating a relative increase in Cyanophyceae.

This effect was corroborated by AFC. Both techniques (^{14}C -uptake and FRRF) were in good agreement ($r = 0.88$) suggesting the impairment of primary production and F_V/F_M following exposure to the selected toxicants.

Phytoplankton responses to toxicants may be influenced by fluctuations in a variety of environmental factors. The nutrient regime may alter the outcome of contamination by influencing the susceptibility of phytoplankton to a toxicant. A preliminary investigation of such effects on biocidal toxicity was conducted under controlled laboratory conditions to determine the extent of nutrient influence. Results indicated the influence of nutrient addition on the Irgarol 1051[®] toxic responses to cyanophytes. Besides experimental approaches, data were supplemented with a pilot survey in Plymouth coastal waters. Current concentrations of biocides together with environmental and biological data for this survey are presented and discussed as a diagnosis that provides an outline for future research.

List of Contents

Abstract	iv
List of Tables	ix
List of Figures	x
Acknowledgments	xiv
Author's declaration	xv
Acronyms	xvii
Chapter 1	
Introduction	1
1.1. Fouling organisms	1
1.2. Antifouling booster biocides in the coastal environment	2
1.3. Toxicity of antifouling booster biocides on phytoplankton	7
1.4. Parameters used to assess toxic impairment of phytoplankton	10
1.4.1. Chlorophyll fluorescence	11
1.4.1.1. Overview of photosynthetic processes	11
1.4.1.2. Fluorescence response to antifouling biocide stress	14
1.4.2. ¹⁴ Carbon incorporation	17
1.4.3. Phytoplankton composition	18
1.5. Scope of this research	24
1.6. Objectives of this research	25
1.7. Outline of the thesis	26
Chapter 2	
General Material and Methods	28
2.1. Algae and culture conditions	28
2.2. Description of the analytical reagents used	28
2.3. Glassware preparation	29
2.4. General analytical procedures	29
2.4.1. Determination of fluorescence parameters	29
2.4.2. Determination of primary production (¹⁴ C tracer method)	31
2.4.3. Determination of phytoplankton pigments	33
2.4.3.1. Sampling procedure	33
2.4.3.2. Analytical procedure	33
2.4.3.3. Quality control	35
2.4.4. Determination of Irgarol 1051 [®] and Sea-Nine 211 [®]	35
2.4.4.1. Sampling procedure	35
2.4.4.2. Analytical procedure	35
2.4.4.3. Quality control	36
2.4.5. Determination of diuron	37
2.4.6. Zinc pyrithione	41
2.4.7. Microscopic analyses	41
2.4.8. Analytical Flow Cytometry (AFC)	42
2.4.8.1. Cell enumeration	42
2.4.8.2. Protocol for Fluorescein Diacetate (FDA) staining technique	43
2.4.8.3. Determination of viable cells (FDA staining technique)	46
2.4.9. Analysis of dissolved nutrients	47

2.4.10. Suspended Particulate Matter (SPM), Carbon and Nitrogen analyses _____	48
Chapter 3	
Testing the phytoplankton response to Irgarol 1051® _____	49
3.1. The use of FDA and flow cytometry to assess cell viability as an indicator of Irgarol 1051® exposure _____	49
3.1.1. Introduction _____	49
3.1.2. Methodology _____	50
3.1.2.1. Algal culture _____	50
3.1.2.2. Algal toxicity testing _____	51
3.1.3. Results and Discussion _____	51
3.1.3.1. FDA protocol optimization _____	51
3.1.3.2. Algal toxicity testing _____	55
3.1.4. Conclusions _____	61
3.2. Flow cytometry and pigment analyses as tools to investigate the toxicity of Irgarol 1051® to natural phytoplankton communities _____	61
3.2.1. Introduction _____	61
3.2.2. Methodology _____	62
3.2.3. Results and discussion _____	62
3.2.4. Conclusions _____	66
Chapter 4	
Evaluation of techniques to measure changes in phytoplankton composition induced by Irgarol 1051® exposure _____	67
4.1. Introduction _____	67
4.2. Methods _____	68
4.2.1. Sampling and experimental design _____	68
4.2.2. Data analyses _____	69
4.2.2.1. Evaluation of phytoplankton diversity _____	69
4.2.2.2. Estimates of class-specific biomass _____	69
4.2.2.3. Comparisons between methods _____	70
4.3. Results _____	70
4.3.1. Analytical Flow Cytometry _____	70
4.3.2. Microscopy _____	71
4.3.3. Pigment composition _____	75
4.3.4. Comparisons between methods _____	76
4.3.5. Irgarol 1051® analyses _____	80
4.4. Discussion _____	80
4.5. Conclusions _____	85
Chapter 5	
Impact of a range of antifouling booster biocides on marine phytoplankton _____	86
5.1. Introduction _____	86
5.2. Methods _____	87
5.2.1. Preparation of biocide solutions _____	87
5.2.2. Unialgal, short-term experiments _____	88
5.2.2.1. Experimental organisms and culture maintenance _____	88
5.2.2.2. Experimental design for single species studies _____	88
5.2.3. Experiment with a natural phytoplankton community _____	89
5.2.3.1. Location and sampling _____	89
5.2.3.2. Experimental design for the natural phytoplankton community _____	90
5.2.4. Data analysis and statistical approach _____	91

5.3. Results	93
5.3.1. Unialgal experiments	93
5.3.1.1. Growth inhibition	93
5.3.2.2. Pigment composition	93
5.3.2.3. Antifouling biocides concentrations	97
5.3.3. Natural phytoplankton community experiment	100
5.3.3.1. Toxic effects on pigment composition	100
5.3.3.2. Toxic effect on phytoplankton growth	103
5.3.3.3. Toxic effect on photosynthesis	103
5.3.3.4. Antifouling booster biocide concentrations	108
5.4. Discussion	108
5.4.1. Unialgal experiments	108
5.4.2. Natural phytoplankton community experiment	110
5.4.2.1. Toxic impairment on pigment composition	110
5.4.2.2. Toxic effect on photosynthesis	112
5.4.2.3. FRRF versus $^{14}\text{C-HCO}_3^-$ uptake	113
5.5. Conclusions	113
Chapter 6	
(I) Effects of nutrient status on toxicity and (II) Spatial distribution patterns of antifouling biocides and phytoplankton within the Tamar Estuary	115
6.1. Influence of nutrient status on toxicity	115
6.1.1. Introduction	115
6.1.2. Methods	116
6.1.2.1. Preparation of Irgarol 1051 [®] solutions	116
6.1.2.2. Experiment with a natural phytoplankton assemblage	116
6.1.2.3. Data analysis	118
6.1.3. Results	118
6.1.4. Discussion	126
6.1.5. Conclusions	130
6.2. Spatial distribution patterns of antifouling biocides and phytoplankton structures within Plymouth waters	130
6.2.1. Introduction	130
6.2.2. Methods	133
6.2.2.1. Study area and sampling procedures	133
6.2.2.2. Data analysis and statistical approach	133
6.2.3. Results	135
6.2.3.1. Chemical-physical parameters	135
6.2.3.2. Biological parameters	135
6.2.3.3. Linking biological and environmental parameters	143
6.2.4. Discussion	143
6.2.5. Conclusions	146
Chapter 7	
General conclusions and future research	147
7.1. General conclusions	147
7.2. Future research	148
Appendices	151
References	161

List of Tables

Table 1.1. Chemical properties and specific site of action of Sea-Nine 211 [®] , Irgarol 1051 [®] , diuron and zinc pyrithione. _____	4
Table 4.1. Output matrix of marker pigment:chl- <i>a</i> ratios obtained from CHEMTAX calculations. _____	77
Table 4.2. Correlations derived from linear regression between each pigment and chlorophyll- <i>a</i> . _____	78
Table 5.1. Growth rate (μ , divisions day ⁻¹), cell numbers (cell ml ⁻¹), chlorophyll- <i>a</i> per cell (pg cell ⁻¹) and marker pigment to chlorophyll- <i>a</i> ratios for the prymnesiophyte <i>Emiliana huxleyi</i> exposed to different types and concentrations of antifouling biocides. _____	94
Table 5.2. Growth rate (μ , divisions day ⁻¹), cell numbers (cell ml ⁻¹), chlorophyll- <i>a</i> per cell (pg cell ⁻¹) and marker pigment to chlorophyll- <i>a</i> ratios for the cyanophyte <i>Synechococcus</i> sp. exposed to different types and concentrations of antifouling biocides. _____	96
Table 5.3. EC ₅₀ , NOEC, and LOEC ($\mu\text{g l}^{-1}$) at 72 h as determined from cell numbers (cell ml ⁻¹) of <i>Emiliana huxleyi</i> and <i>Synechococcus</i> sp. exposed to the four biocides tested. _____	97
Table 6.1. Mean concentrations of Irgarol 1051 [®] (ng l ⁻¹), nitrate (μM) and phosphate (μM) from day 0 (time of sampling at site L4), day 1 and day 5 (experiment). _____	125
Table 6.2. Atrazine and Irgarol 1051 [®] (ng l ⁻¹) concentrations at 9 stations from Tamar Estuary and Plymouth Sound. _____	137
Table 6.3. Pearson correlation matrix between pigments determined by HPLC (ng l ⁻¹ ; rows) and chlorophyll- <i>a</i> (ng l ⁻¹ ; columns) and cell numbers of picoeukaryotes, nanoeukaryotes, cyanophytes, cryptophytes, and total cells determined by AFC (cell ml ⁻¹ ; columns). _____	140

List of Figures

Figure 1.1. Site of action of herbicides. _____	7
Figure 1.2. Diagram of photosynthetic light reactions showing PSI and PSII components in relation to their energy level. _____	12
Figure 1.3. The Fast Repetition Rate Fluorometer. Measurements of fluorescence parameters were aquired using the dark chamber. _____	15
Figure 1.4. FRRF fluorescence signal resulted from exposure of phytoplankton to a series of microsecond flashes of blue light. _____	16
Figure 1.5. The Flow Cytometer (A) and a schematic drawing of its components (B). _____	19
Figure 1.6. Structures of selected chlorophylls and carotenoids. _____	21
Figure 1.7. An action spectrum compared to an absorption spectrum. _____	22
Figure 2.1. <i>Emiliana huxleyi</i> (92D) cell suspension. Density related changes in chlorophyll fluorescence kinetics. _____	31
Figure 2.2. Example of a typical HPLC chromatogram from a pigment extract of natural seawater. _____	34
Figure 2.3. Irgarol 1051 [®] standard calibration curve using the following concentrations: 0.226, 0.679, 1.58, 3.16, 6.33, 12.21 ng μl^{-1} . _____	37
Figure 2.4. Example of a GC-MS Total Ion Chromatogram from a standard mixture of ametryn, Sea-Nine 211 [®] and Irgarol 1051 [®] . _____	38
Figure 2.5. Mass spectra of the example showed in the Fig. 2.4 composed by the internal standard ametryn, and the standards Sea-Nine 211 [®] and Irgarol 1051 [®] obtained by GC-MS. _____	39
Figure 2.6. Examples of mass spectra of the internal standard ametryn, and the standards Sea-Nine 211 [®] and Irgarol 1051 [®] obtained by GC-MS. _____	40
Figure 2.7. Bivariate scatter-plots (AFC) of chlorophyll fluorescence versus side-angle light scatter and phycoerythrin showing phytoplankton separation for (a) nanoeukaryotes and picoeucaryotes and (b) cryptophytes and cyanophytes. _____	44
Figure 2.8. Chemical structure of fluorescein diacetate (FDA). _____	45
Figure 2.9. Frequency histograms comparing FDA accumulation in dead (thin line) and live cells (thick line). Esterase activity states are defined as normal (M1), low (M2), and intermediate (M3) activities. _____	47
Figure 3.1. Analysis of fluorescence (relative units) accumulation upon FDA addition in <i>Emiliana huxleyi</i> as revealed by flow cytometry. Diagrams show FDA fluorescence in live cells (on the left) and dead cells (on the right). _____	52
Figure 3.2. Optimization protocol for different concentrations of FDA added to <i>Emiliana huxleyi</i> cells: a) 1.2 μM , b) 4.2 μM , c) 24.0 μM , and d) 48.0 μM . _____	53
Figure 3.3. Fluorescence (relative units) accumulation under increasing incubation times of samples of <i>Emiliana huxleyi</i> after 70 μl of FDA (WS2) addition. _____	54
Figure 3.4. Fluorescence (relative units) accumulation upon 70 μl FDA (WS2) addition to different cell concentrations of <i>Emiliana huxleyi</i> . _____	54

Figure 3.5. Effects of different concentrations of Irgarol 1051 [®] (ng l ⁻¹) on cell density expressed as (A) cell ml ⁻¹ and (B) % of control of <i>E. huxleyi</i> following exposure of 72 h. _____	56
Figure 3.6. Esterase activity (FDA fluorescence) of <i>Emiliania huxleyi</i> exposed to nominal concentrations of 40, 80, 150, 250 and 500 ng l ⁻¹ of Irgarol 1051 [®] for 72 hours. _____	57
Figure 3.7. Effects of Irgarol 1051 [®] concentrations on the chlorophyll fluorescence parameters: F _o , F _v , F _m , and Sigma (σ _{PSII}) of <i>E. huxleyi</i> following exposure for (A) 6 h and (B) 72 h. ____	59
Figure 3.8. Photosynthetic efficiency (F _v /F _M) expressed as percentage of the control of <i>E. huxleyi</i> exposed to nominal concentrations of 40, 80, 150, 250 and 500 ng l ⁻¹ of Irgarol 1051 [®] for 72 hours. _____	60
Figure 3.9. Linear regression fitting between viable cells (FDA activity) and F _v /F _M at 72 h of exposure to 40, 80, 150, 250 and 500 ng l ⁻¹ of Irgarol 1051 [®] , including carrier controls (MEOH) and controls. _____	60
Figure 3.10. Cell numbers (measured by flow cytometry) of prokaryotic (<i>Synechococcus</i> sp.) and eukaryotic phytoplankton exposed to different concentrations of Irgarol 1051 [®] during a 72 hour period. _____	63
Figure 3.11. Pigment concentrations derived from HPLC pigment analyses of the phytoplankton extracts. Data are shown for the initial sample (IS = composition at the start of the experiment) and following 72 hours of exposure to concentrations of <1 (controls), 112, 331, 465, 1082, and 2020 ng l ⁻¹ of Irgarol 1051 [®] . _____	64
Figure 3.12. Pigment:chl- <i>a</i> ratios (ng l ⁻¹ : ng l ⁻¹) expressed as percentage of total. _____	64
Figure 3.13. Reductions in 19'-hexanoyloxyfucoxanthin (ng l ⁻¹) as a function of Irgarol 1051 [®] exposure concentrations (ng l ⁻¹). _____	65
Figure 4.1. Growth response of picoeukaryotes (pico), nanoeukaryotes (nano), and cyanophytes (Cyano) under exposures of 0.5 μg l ⁻¹ and 1.0 μg l ⁻¹ Irgarol 1051 [®] and the controls (no Irgarol 1051 [®] added) over a 120 h period of incubation. _____	71
Figure 4.2. Non-metric Multi-Dimensional Scaling (MDS) ordination of (A) species abundances and (B) species abundances aggregated into groups of autotrophs. _____	72
Figure 4.3. Effects of Irgarol 1051 [®] on community structure expressed as average (n = 5) Margalef's diversity index (D) and number of species (S) and groups (G) of autotrophs. ____	73
Figure 4.4. Phytoplankton response after 96 h exposure to 0.5 and 1.0 μg l ⁻¹ Irgarol 1051 [®] obtained from microscopic enumeration: (A) cell abundances and (B) carbon content estimates. _____	74
Figure 4.5. Phytoplankton response after 96 h exposure to 0.5 and 1.0 μg l ⁻¹ Irgarol 1051 [®] expressed as (A) diagnostic pigment relative abundance and (B) predicted chlorophyll- <i>a</i> from CHEMTAX calculations. _____	79
Figure 4.6. Biomass of individual algal classes expressed as chlorophyll- <i>a</i> (chl- <i>a</i>) concentration in ng l ⁻¹ estimated from CHEMTAX calculations (x-axis) and as carbon concentration in μg l ⁻¹ estimated by microscopy (y-axis). _____	81
Figure 4.7. Relationships between cell enumeration made by microscopy and analytical flow cytometry (AFC) for (A) picoeukaryotes and (B) nanoeukaryotes. _____	82
Figure 5.1. Phytoplankton composition determined by microscopy at the sampling station L4 shown as percentage of total cell numbers (A) and total carbon content in mg m ⁻³ (B). ____	91
Figure 5.2. Changes in marker pigment:chlorophyll- <i>a</i> ratios of <i>Emiliania huxleyi</i> under exposure to concentrations of diuron in μg l ⁻¹ (x-axis), controls (0 μg l ⁻¹) and solvent controls (MEOH) after 72 h. _____	98
Figure 5.3. Changes in marker pigment:cell ⁻¹ , cell numbers (cell ml ⁻¹) and growth rate (μ) of <i>Emiliania huxleyi</i> under exposure to concentrations of diuron in μg l ⁻¹ (x-axis), controls (0 μg l ⁻¹) and solvent controls (MEOH) after 72 h. _____	99

- Figure 5.4. Pigment composition (% of total) of phytoplankton after 72 h exposure to concentrations ($\mu\text{g l}^{-1}$) of zinc pyrithione (ZPT), Irgarol 1051[®] (Irgarol), diuron, Sea-Nine 211[®] (SeaNine), including control (no biocide addition) and the carrier control (MEOH). 101
- Figure 5.5. Contribution of different algal groups, as determined from pigment:chlorophyll-*a* ratios using CHEMTAX, after 72 h exposure to concentrations ($\mu\text{g l}^{-1}$) of zinc pyrithione (ZPT), Irgarol 1051[®] (Irgarol), diuron, Sea-Nine 211[®] (Sea-Nine), including the control (no biocide addition) and the carrier control (MEOH). 102
- Figure 5.6. Percentage of total cell numbers (measured by AFC) related to carrier controls (MEOH) after 24 h, 48 h and 72 h exposure to concentrations ($\mu\text{g l}^{-1}$) of zinc pyrithione (ZPT), Irgarol 1051[®] (Irgarol), diuron, and Sea-Nine 211[®] (Sea-Nine). 104
- Figure 5.7. Number of picoeukaryote, nanoeukaryote and cyanophyte cells measured (as percentage of total cells) by AFC after 72 h exposure to concentrations ($\mu\text{g l}^{-1}$) of zinc pyrithione (ZPT), Irgarol 1051[®] (Irgarol), diuron, Sea-Nine 211[®] (Sea-Nine), including the control (no biocide addition) and the methanol control (MEOH). 104
- Figure 5.8. Number of cyanophyte, picoeukaryote, nanoeukaryote cells and total cells measured by AFC after 24, 48 and 72 h of exposure to concentrations ($\mu\text{g l}^{-1}$) of zinc pyrithione (ZPT), Irgarol 1051[®] (Irgarol), diuron, Sea-Nine 211[®] (Sea-Nine), including the control (no biocide addition) and the methanol control (MEOH). 105
- Figure 5.9. Photosynthetic efficiency (F_v/F_m) of phytoplankton exposed to concentrations ($\mu\text{g l}^{-1}$) of zinc pyrithione (ZPT), Irgarol 1051[®] (Irgarol), diuron and Sea-Nine 211[®] (Sea-Nine) for the period of the experiment (72 h). 106
- Figure 5.10. A linear model relating primary production (measured as ¹⁴C-uptake) and F_v/F_m data after 24 h exposure of natural phytoplankton to Irgarol 1051[®], zinc pyrithione, Sea-Nine 211[®] and diuron ($p = 0.0001$). 107
- Figure 6.1. Experimental design to evaluate the potential influence of nitrate (N) and phosphate (P) additions on the toxicity of Irgarol 1051[®]. 117
- Figure 6.2. Phytoplankton composition determined by microscopy at the sampling station L4 shown as (A) percentage of total cell numbers and (B) percentage of total carbon content. 119
- Figure 6.3. Cell abundances (cell ml^{-1}) for picoeukaryotes, nanoeukaryotes, and cyanophytes determined by AFC in (A) controls and (B) treated with 500 ng l^{-1} Irgarol 1051[®], grown under different nutrient conditions. 120
- Figure 6.4. Cell densities (cell ml^{-1}) of controls (empty bars) and Irgarol 1051[®] treatment (filled bars) showing the effects of nutrient addition. 121
- Figure 6.5. Plots of the results of interaction analysis (two-way ANOVA) of percentages of cyanophytes, nanoeukaryotes, and picoeukaryotes to total cells grown under different nutrient regimes and exposure to Irgarol 1051[®]. 122
- Figure 6.6. Percentage of reduction related to the controls in pigment concentrations ($\mu\text{g l}^{-1}$) by exposure to Irgarol 1051[®] (500 ng l^{-1}) after 5 days of experiment conducted under different nutrient additions: NP, nitrate+phosphate; P, phosphate and N, nitrate. 124
- Figure 6.7. Sampling stations within the Tamar Estuary and Plymouth Sound area: Tamar River, Bull Point, Devonport, St. John's Lake, Mayflower Marina, Sutton Harbour, Queen Anne's Battery (QAB), Plym River, and Plymouth Sound. 134
- Figure 6.8. Mean data obtained for the 9 stations in Tamar Estuary and Plymouth Sound: (A) Suspended Particulate Material (SPM) in mg l^{-1} and C:N ratio, and (B) percentage of particulate nitrogen (%N) and organic carbon (Org C%). 136
- Figure 6.9. Total cell numbers for nanoeukaryotes + picoeucaryotes + cyanophytes measured by AFC at 9 sampling stations within Tamar Estuary and Plymouth Sound. 137
- Figure 6.10. Contribution of picoeukaryotes, nanoeukaryotes, and cyanophytes measured by AFC, to the total cell number for each surface sampling station. 138

Figure 6.11. Pigment composition on a chlorophyll-*a* basis along 8 sampling stations (surface samples). _____ 138

Figure 6.12. Multi-Dimensional Scaling (MDS) of Bray-Curtis similarities of \sqrt{x} -transformed group abundances data (graphs on the left) and of \sqrt{x} -transformed pigment composition data (graphs on the right) for 7 stations investigated (missing data for Mayflower Marina and Plym River stations). _____ 141

Acknowledgments

I would like to take this opportunity to express my heartfelt gratitude, to all the people who have helped and encouraged me throughout this period of study.

I wish to thank my supervisors Prof. J. W. Readman (Plymouth Marine Laboratory), Dr. Murray T. Brown and Dr. Maria E. Donkin for their support and advice during all this research. Particularly, I would like to gratefully acknowledge Prof. J. W. Readman for his encouragement, guidance and for resourcing my work and enabling access to facilities at PML.

I would like to acknowledge Dr. Glen Tarran, Prof. James Aiken and Dr. Ian Joint for kindly providing access and help to use techniques and instruments. I would also like to thank co-authors of the preliminary data published in Marine Environmental Research and presented in Section 3.2. My contribution to this aspect of the work concerned data analysis and interpretation.

I am also indebted to the people of EcoH group and the crew of R. V. Sepia for helping me at various stages of both laboratory and field work.

I also wish to thank the CNPq (Brazilian Ministry for Science and Technology) for resourcing my studies through a PhD studentship.

My thanks to all my friends and family for their never ending encouragement.

Author's Declaration

At no time during the registration for the degree of Doctor of Philosophy has the author been registered for any other University award without prior agreement of the Graduate Committee.

This study was financed with the aid of a studentship from the Brazilian Ministry of Science and Technology (CNPq) and was also financed by the European Commission under the ACE (Assessment of Antifouling Agents in Coastal Environments) contract. This study was carried out in collaboration with the Plymouth Marine Laboratory.

Relevant scientific seminars and conferences were regularly attended at which work was often presented. Papers have been prepared for publication in international peer-reviewed journals.

Publications:

DEVILLA, R. A., Brown, M. T., Donkin, M. E., Tarran, G., Aiken, J., Readman, J. W., 2005.

Impact of antifouling booster biocides on single microalgal species and on a natural marine phytoplankton community. *Marine Ecology Progress Series*, 286: 1-12.

DEVILLA, R. A., Brown, M. T., Donkin, M., Readman, J. W., 2005. The effects of a PSII

inhibitor on phytoplankton community structure as assessed by HPLC pigment analyses, microscopy and flow cytometry. *Aquatic Toxicology*, 71: 25-38.

Readman, J. W., DEVILLA, R. A., Tarran, G., Llewellyn, C. A., Fileman, T. W., Easton, A., Burkill, P. H., Mantoura, R. F. C., 2004. Flow Cytometry and pigment analyses as tools to investigate the toxicity of herbicides to natural phytoplankton communities. *Marine Environmental Research*, 58:353-358.

Presentation and Conferences Attended:

DEVILLA, R. A., Brown, M. T., Donkin, M. E., and Readman, J. W., 2004. *Impact of antifouling booster biocides on single microalgal species and on a natural marine phytoplankton community*. In: 14th SETAC Europe Annual Meeting, Prague, Czech Republic (poster presentation).

Short-course attended on Integrative Sampling Methods in Environment. Lead instructor: Per-Anders Bergqvist. 18th April, 2004 at SETAC Europe 14th Meeting. Prague, Czech Republic (6 hours).

Seminar presentation on Ecotoxicological Impact of Antifouling Agents on Natural Phytoplankton Communities, University of Plymouth, 27/02/2004.

DEVILLA, R. A., Readman, J. W., Brown, M. T., and Donkin, M. E., 2003. *Responses of a natural phytoplankton community to antifouling booster biocides*. In: The Third European Phycological Congress, Belfast, Northern Ireland (poster presentation).

Readman, J. W., DEVILLA, R. A., Tarran, G., Easton, A., Burkill, P. H., Mantoura, R. F. C., 2003. *Flow Cytometry and pigment analyses as tools to investigate the toxicity of herbicides to natural phytoplankton communities*. In: PRIMO 12th International Symposium, Tampa, Florida, USA (poster presentation).

Seminar presentation on 'The Impact of Antifouling Booster Biocides on Phytoplankton', Plymouth Marine Laboratory, Plymouth, UK, 07/01/2004.

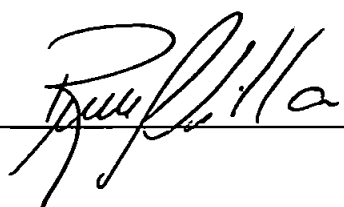
DEVILLA, R. A. and Readman, J. W., 2002. *Flow Cytometry and Fast Repetition Rate Fluorescence as tools to assess the toxicity of Irgarol 1051[®] to microalgae*. In: SETAC Latin America 5th Annual Meeting. 5-9 October, 2002. Vitória, Brazil (poster presentation).

DEVILLA, R. A., Mantoura, R. F. C., Depledge, M. H. and Readman, J. W., 2002. *Effects of four antifouling booster biocides on a natural phytoplankton community*. In: International Symposium on the Environment and Analytical Chemistry – ISEAC 32. 17-21 June 2002. Plymouth, UK (poster presentation).

Seminar presentation on Assessment of the effects of antifouling agents on phytoplankton. PML EcoH Group meeting, 15/08/2001.

Seminar presentation on 'Herbicides and marine microalgae: a study of effects and influencing factors'. University of Plymouth, 01/02/2001.

Word count of main body of thesis: 37,146

Signed: 
Date: 15/09/2005

Acronyms

AFC	Analytical Flow Cytometry
ANOSIM	Analysis of Similarities (PRIMER Software)
ANOVA	Analysis of Variance (to test for significant differences between means)
CHEMTAX	a program for estimating class abundances from pigment markers
Chl- <i>a</i>	Chlorophyll- <i>a</i>
DCMU	diuron
EC ₅₀	Effective Concentration which reduces the parameter by 50%
ELISA	Enzyme ImmunoSorbent Assay
FDA	Fluorescein Diacetate
F _M	Chlorophyll fluorescence at the light-saturated state
F _O	Chlorophyll fluorescence at the initial dark-adapted state
FRRF	Fast Repetition Rate Fluorescence
F _v	Variable chlorophyll fluorescence (F _M -F _O)
F _v /F _M	F _M -F _O /F _M , maximum quantum yield of PSII
GC-MS	Gas Chromatography and Mass Spectrometry
HPLC	High Performance Liquid Chromatography
HSE	Health and Safety Executive
HSD	Tukey Honest Significant Difference test
LOEC	Lowest Observable Effective Concentration
LDS	Least Significant Difference
MDS	Multidimensional Scaling, a multivariate statistical analysis technique
MEOH	Methanol
NOEC	Non-Observable Effective Concentration
PAR	Photosynthetic Active Radiation
PSI	Photosystem I
PSII	Photosystem II
psu	Practical salinity units
SIM mode	Selective ion monitoring mode
SIMPER	Similarity Percentages & Species Contributions (PRIMER Software)
μ	growth rate
σ _{PSII}	functional absorption cross section of PSII under dark-adapted conditions

**PHYTOPLANKTON RESPONSES AS
INDICATORS OF EXPOSURE TO TOXICANTS**

by

Rosângela Aparecida Devilla

Chapter 1

Introduction

1.1. Fouling organisms

Biofouling is the result of settlement and growth of marine organisms on submerged structures (Jacobson and Willingham, 2000). The primary colonisers of submerged surfaces are the microbiota, such as bacteria and microalgae, which generate surface biofilms. These films are characterised by an extracellular matrix (composed of water and secreted/released extracellular macromolecules) which provides architectural structure and mechanical stability for the attached population. The matrix is subjected to enzymatic and regulatory activities and external factors (fluctuations in nutrients and gaseous levels and fluid shear), which combine to produce a dynamic heterogenous microenvironment for the attached and enveloped cells (Allison, 2003).

Biofilms are of great ecological interest because they facilitate the majority of marine larval settlement and stimulate further development of fouling organisms. Such fouling organisms are components of the natural marine intertidal and subtidal communities, such as macroalgae and invertebrates (*e.g.* arthropoda, mollusca, porifera, bryozoa, coelenterata, protozoa and annelida). To prevent attachment and growth of such organisms on man-made submerged structures, such as hulls of ships or boats, buoys, fish cages, and oceanographic sensors, antifouling paints are applied. These antifouling products play an important role in the shipping industry and are of significant economic importance. It is estimated that on average, fuel consumption increases 6% for every 100 μm increase in the average hull roughness caused by fouling organisms (Liu *et al.*, 1997a; Townsin, 2003). Globally, the total annual cost due to fouling of ships is estimated at approximately US\$3 billion resulting from increased fuel consumption, cleaning costs and time expenditure associated with hydrodynamic drag and service interruption (Jacobson and Willingham, 2000). Moreover, these authors point out that the increased fuel consumption contributes to pollution, global warming and acid rain.

However, the toxic nature of these compounds has caused environmental concerns for non-target organisms.

1.2. Antifouling booster biocides in the coastal environment

Tributyltin (TBT) has been shown to be the most effective biocide compound in antifouling paints (Connelly *et al.*, 2001). However, the wide environmental distribution (Langston *et al.*, 1990) and non-selective biotoxicity (Beaumont and Newman, 1986) led the European Union (in 1989) to restrict the use of triorganotins on boats less than 25 m in length (Communauté Européenne, 1989). In 1999, the International Maritime Organization (IMO) proposed a global prohibition on the sale of organotin compounds and application to ships by January 2003, and a complete prohibition of its presence in antifouling coatings on ships by January 2008 (HSE, 2002a). Additional costs of US\$ 5.7 billion per annum to the shipping industry were estimated due to the TBT ban (Evans *et al.*, 2000). As a consequence of earlier TBT restrictions, alternative organic biocides were developed and used singly or as an additional component to Cu-based formulations (for small boats) and also occasionally in TBT-based formulations (for larger vessels) (HSE, 2002a). These organic biocides enhance the efficacy of the formulation and are referred to as 'booster' biocides (Thomas *et al.*, 2001).

Worldwide, around eighteen compounds have been used as antifouling booster biocides (Thomas, 2001). These include benzamide, chlorothalonil, copper pyrrhione, dichlofluanid, diuron, fluorofolpet, Irgarol 1051[®], Mancozeb, Polyphase, pyridine-triphenylborane, TCMTB (2-(thiocyanomethylthio)benzothiazole), TCMS pyridine (2,3,5,6-tetrachloro-4-(methylsulfonyl) pyridine), Sea-Nine 211[®], thiram, tolyfluanid, zinc pyrrhione, ziram and zineb. Some countries have already introduced legislation to restrict usage of some of these compounds.

In the UK, only biocides approved under the control of Pesticides Regulations (1986) or the Biocides Products Regulations (2001) can be used in antifouling coatings. Nine biocides have been registered for use as active ingredients in approved amateur and professional antifouling products marketed in the UK over recent years. In 2000, the Advisory Committee on Pesticides (ACP) revoked the professional use of diuron (3-(3,4-dichlorophenyl)-1,1-dimethylurea) from November 2002 and for chlorothalonil (2,4,5,6-tetrachloro-isophthalonitrile) and Irgarol 1051[®] (2-methylthio-4-tertbutylamino-6-cyclopropylamino-s-triazine) from July 2003. TCMTB (2-(thiocyanomethylthio) benzothiazole) and TCMS pyridine (2,3,5,6-tetrachloro-4-(methylsulfonyl) pyridine)

have not been supported. Only dichlofluanid (*N'*-dimethyl-*N*-phenylsulphamide), zinc pyrithione (zinc complex of 2-mercaptopyridine-1-oxide) and zineb (zinc ethylene bis dithiocarbamate), have been approved for amateur and professional use in antifouling products, although Sea-Nine 211[®], known also as Kathon 5287 (4,5-dichloro-2-*n*-octyl-4-isothiazolin-3-one) has been approved for professional use (HSE, 2002a).

A report in 2000 on the number of vessels treated with the various biocides in the UK indicated a preference for copper(I) oxide, followed by diuron, copper thiocyanate, then Irgarol 1051[®], zinc pyrithione, and finally dichlofluanid (Boxall *et al.*, 2000). A preference for one biocidal usage does not necessarily represent its dominance in the environment. Inputs and persistency in the environment depend mainly on biocide leaching rates, partition behaviour, and abiotic and biotic transformations (Jacobson and Willingham, 2000). Calculated leaching rates are higher for copper(I) oxide, followed by copper thiocyanate, zinc pyrithione, diuron, Irgarol 1051[®] and dichlofluanid (Boxall *et al.*, 2000). Large amounts of the booster biocides diuron, Irgarol 1051[®], zinc pyrithione, and dichlofluanid have been released into areas of high boating activity from vessels <25 m in length, whilst Irgarol 1051[®] and diuron have been used in sufficient quantities to be detected in the environment (Thomas *et al.*, 2001). It has been estimated that between 80-361 tonnes of biocides in antifouling paints are used on vessels in the UK each year. Of this, 0.98 to 57.1 tonnes of Irgarol 1051[®] and 11.3 to 78 tonnes of diuron are estimated to leach off UK vessels annually (Boxall *et al.*, 2000).

Environmental concentrations of Irgarol 1051[®] were first reported in 1993, in surface waters of marinas on the Côte d'Azur, France, at concentrations up to 1700 ng l⁻¹ (Readman *et al.*, 1993). Other studies have detected Irgarol 1051[®] in coastal waters of the USA, EU, Japan, Australia, Canada and Bermuda (see Konstantinou and Albanis, 2004 for a review). In the UK, the highest levels of Irgarol 1051[®] have been found in marina waters, with concentrations of up to 682 ng l⁻¹ in the Humber (Zhou *et al.*, 1996), 500 ng l⁻¹ in south-east England (Gough *et al.*, 1994), 1421 ng l⁻¹ in Southampton (locked marina), and 84 ng l⁻¹ in Plymouth (locked marina) (Thomas *et al.*, 2001). Lower levels however were found in estuarine waters, with maximum values detected in Blackwater, Essex (up to 680 ng l⁻¹) and Southampton (up to 47 ng l⁻¹) (Thomas *et al.*, 2001; Voulvoulis *et al.*, 2000) with exception of Plymouth Sound, with maximum value found of 127 ng l⁻¹ (Scarlett *et al.*, 1997). Diuron has been detected at several locations around the UK at concentrations up to 1249 ng l⁻¹ (in Southampton water). In Plymouth, maximum concentrations of 334 ng l⁻¹ for diuron have been reported (Thomas *et al.*,

Table 1.1. Chemical properties and specific site of action of Sea-Nine 211[®], Irgarol 1051[®], diuron and zinc pyrithione. BCF: bioconcentration factor.


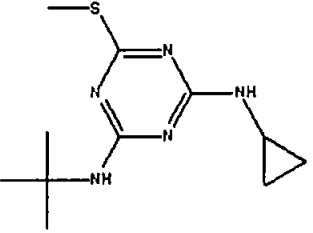
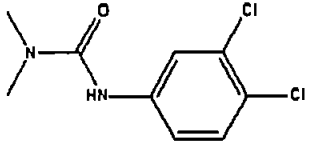
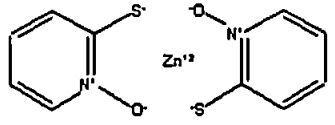
COMPOUND	SEA-NINE 211 [®]	IRGAROL 1051 [®]	DIURON	ZINC PYRITHIONE
GROUP	Isothiazolone	Triazine	Phenylurea	Organo-metal
ACTIVE SUBSTANCE	4,5-dichloro-2- <i>n</i> -octyl-3-(2H)-isothiazolin-3-one (DCOI)	<i>N</i> '-tert-butyl- <i>N</i> -cyclopropyl-6-(methylthio)-1,3,5-triazine-2,4-diamine	1-(3,4-dichlorophenyl)-3,3-dimethylurea	<i>bis</i> (1hydroxy-2(1H)-pyridethionato-O,S)-T-4 zinc
FORMULA				
LOG K _{OC}	3.2 ⁽¹⁾	3.0 (marine sediment) ^(3,9) , 3.1 (freshwater sediment) ⁽⁹⁾	2.4-3.0 (soil) ⁽³⁾	2.9-4.0 ⁽⁴⁾
LOG K _{OW}	2.8 ⁽²⁾	3.95 ⁽³⁾	2.8 ⁽³⁾	0.97 ⁽⁴⁾
RELEASE RATE	13 mg m ⁻² d ⁻¹ (calculated leaching – in harbour) 25 mg m ⁻² d ⁻¹ (calculated leaching - when sailing)	5 µg cm ⁻² d ⁻¹ (ISO test system) ⁽³⁾ 2.6 µg cm ⁻² d ⁻¹ (flume system) ⁽³⁾ 0.12-3.4 µg cm ⁻² d ⁻¹ (calculated) ⁽⁷⁾	0.8 µg cm ⁻² d ⁻¹ (17)	21 mg m ⁻² d ⁻¹ (calculated leaching – in harbour) 41 mg m ⁻² d ⁻¹ (calculated leaching – when sailing)
SPECIFIC SITE OF ACTION	PS II inhibitor; react with thiol-containing enzymes	PS II inhibitor (high affinity to Q _B -binding site)	PS II inhibitor (high affinity to Q _B -binding site)	Inhibitor of bacterial ATP synthesis; inhibitor of membrane transport ⁽⁵⁾

Table 1.1. *Continued*

COMPOUND	SEANINE 211 [®]	IRGAROL 1051 [®]	DIURON	ZINC PYRITHIONE
BCF FACTOR	600 for whole fish (130-200 muscle; 700-1,100 for internal organs) ^(13,14)	160-250 for fish ⁽⁹⁾	Unlikely to be significant	Low with uncertainty
PHOTOLYSIS	½ life 13.4 days	Stable. ½ life of 35.9-84.8 days ⁽⁸⁾ ½ life of 273 days ⁽¹⁶⁾	60 days	½ life of 17.5 days ⁽¹¹⁾
HYDROLYSIS	½ life 9-12.5 days	½ life > 200 days	Stable	yes
BIODEGRADATION	½ life < 24h	½ life 201 days ⁽¹⁵⁾	< 1% in 42 days ⁽¹⁷⁾	>50% in less than 24 h
DEGRADATION PRODUCT	N-(n-octyl)malonamic acid; N-(n-octyl)b hydroxypropionamide	GS 26575 or (1,3,5-triazine-2,4-diamine,N-(1,1-dimethylethyl)-6-methylthio))	N-(3,4-dichlorophenyl)-N'; N'-formylmethylurea; demethylated products	Omadine sulfonic acid; pyridine sulfonic acid; NP1 and NP2 ⁽¹²⁾
EC50 ALGAE (µg l ⁻¹)	13.9-36	0.058-2.14 (96 h)	2.1-2.8 ⁽⁶⁾	28

¹Howard, 1991; ²Jacobson, 1993; ³Thomas, 2001; ⁴Olin, 1997; ⁵Dinning et al, 1998; ⁶Eriksson, 2001; ⁷Boxall et al., 2000; ⁸Ciba-Geigy Corporation 1996; ⁹Williams and Hargadine, 1990; ¹⁰Shade et al., 1993; ¹¹Reynolds, 1995; ¹²Ritter, 1999; ¹³Forbis et al., 1985; ¹⁴Derbyshire et al., 1991; ¹⁵Schmidt and Head, 1991; ¹⁶Boxall et al., 1998; ¹⁷Thomas et al., 2002; Other data compiled from Hall et al. (1999) and Ranke and Jarstorff (2000).

2001). Sediments collected from Southampton water showed maximum concentrations of $3.5 \mu\text{g kg}^{-1}$ for Irgarol 1051[®] and $6.2 \mu\text{g kg}^{-1}$ for diuron (Thomas *et al.*, 2002). Other antifouling biocides such as Sea-Nine 211[®], chlorothalonil, dichlofluanid, and TCMTB were analysed but were not been detected at sites investigated around UK (Thomas *et al.*, 2002). A clear seasonal pattern in antifoulant contamination has been observed: enclosed marinas exhibit peak concentrations in January, whilst open marinas show one mid-summer peak (Thomas *et al.*, 2001). A description of the main physico-chemical properties of the most used booster biocides in the UK (diuron and Irgarol 1051[®]) and the presently approved ones (Sea-Nine 211[®] and zinc pyrithione) are shown in Table 1.1.

Besides being used in antifouling coatings, some biocides have other applications. Chlorothalonil, dichlorofluanid, and diuron are widely used in agriculture and on amenity and other non-cropped areas. Diuron, for instance, is principally employed for selective control of germinating grass and broad-leaved weeds in many crops, but is also used for weed control on roads, railways and parks (Tixier *et al.*, 2001). Isothiazolone compounds (*e.g.* Sea-Nine 211[®]) are used in a variety of applications, such as cooling water, paper, cosmetics and textiles (Laopaiboon *et al.*, 2001). Zinc pyrithione is also a component in some anti-dandruff shampoos, possibly leading to inputs from effluent discharges (Thomas *et al.*, 2001).

Alternatives to the use of antifouling biocides have been proposed. There are non-biocidal methods available that can utilise coatings with a mixture of enzymes or microorganisms which retard the growth of fouling organisms. For example, coating applications containing organisms that outcompete, organisms that exudate antibiotics, organisms that remove critical nutrients, or coatings containing extracellular enzymes that disrupt proteins and polysaccharides attacking the surface film (Selvig *et al.*, 1999). Others function by physical means, *e.g.* silicone-based paints that make it difficult for organisms to settle; and sonic wave antifouling systems (HSE, 2002b) have also been developed. Additionally, antifouling properties have been discovered from a macroalgal natural product (Hellio *et al.*, 2001; Da Gama *et al.*, 2002) as an alternative to synthetic compounds. Nevertheless, cost-effective, efficient and environmentally acceptable alternatives to synthetic herbicides are not yet available (Faber *et al.*, 1998), which makes booster biocides the most popular means of controlling fouling due to their effectiveness and rapid performance. However, the environmental risk remains an issue

due to the lack of detailed information on their toxicity to non-target, natural populations.

1.3. Toxicity of antifouling booster biocides on phytoplankton

Antifouling paints act by continuously releasing active chemicals to the surrounding waters. They generally remain active for approximately 1-2 years after painting (HSE 2002b). Biocidal leaching from the matrix of the paints causes toxic effects not only to the fouling organisms but also to other 'non-target' biota. The extent of impact of each toxicant released into the environment to organisms varies according to its leaching rate, time of exposure, degradation rates, sorptive behaviour, water movements, and the number of vessels in the water. It is expected that these chemicals may have a significant impact on natural non-target communities, potentially altering diversity and biomass and leading to possible changes in ecosystem functioning. Therefore, the toxicity of booster biocides to a number of species needed to be assessed in order to fully evaluate the risks to non-target organisms.

Phytoplankton are highly susceptible to herbicidal antifouling compounds which impair photosynthesis (Fig. 1.1). Due to their short generation times and differential species responses and susceptibilities to biocides, algae can be affected over time scales from hours to days (McCornick and Cairns, 1994; Jørgensen and Christoffersen, 2000),

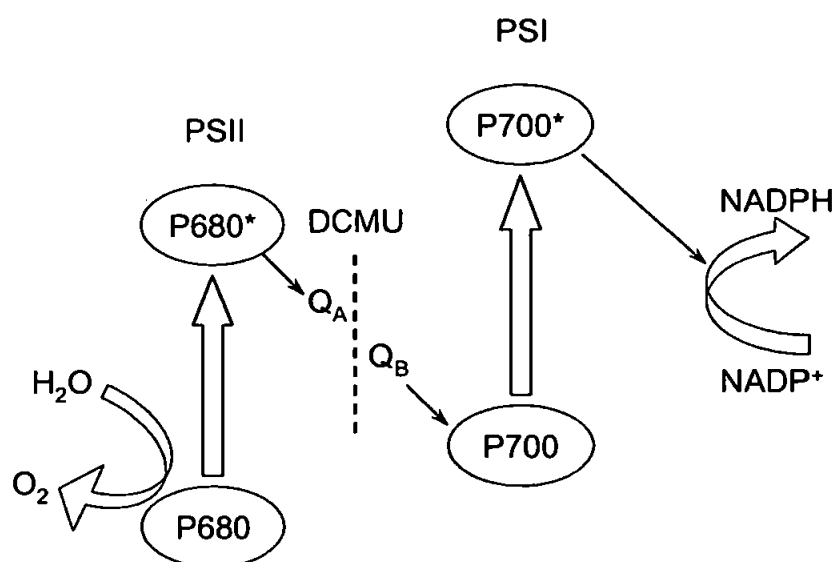


Figure 1.1. Site of action of herbicides. Many herbicides, such as DCMU (diuron) and Irgarol 1051[®] act by blocking electron flow at the quinone acceptors of photosystem II, by competing for the binding site of plastoquinone that is normally occupied by Q_B. (From <http://www.plantphys.net>)

leading to changes in community structure (Hamilton *et al.*, 1988). Because of their ecological importance, algae have been widely used as biomonitors of environmental change; they indicate the quality of the environment mainly from modifications in their density and diversity (Lewis, 1995). Moreover, they can influence the speciation and transport of pollutants in natural waters (Millard *et al.*, 1993). Such characteristics make phytoplankton ideal candidates for evaluating the potential impacts of these biocides to marine ecosystems.

Toxicity testing is used to establish links between adverse ecological effects and the toxicity of environmental chemicals (Lytle and Lytle, 2001). Toxicity to phytoplankton has typically been assessed using traditional methods of algal growth inhibition, using single species grown in artificial culture media (see Walsh, 1988). The use of standard algal tests is more appropriate for screening the toxicity of compounds than for predicting their environmental impact. Therefore, single species tests cannot be used to predict toxic levels for natural plankton communities (Brown and Lean, 1995), since synergistic or antagonistic effects of other stressors or environmental factors (*e.g.* light, individual chemicals, nutrient status, outcompetition) could result in changing the sensitivities of different species to the tested chemicals (Pinckney *et al.*, 2002; Folt *et al.*, 1999). Experiments conducted in micro- and meso-cosms provide information about effects at a higher level of biological organization and take account of interacting populations of different trophic status and different taxonomic groups (Jak *et al.*, 1998). Thus, it provides a more realistic evaluation of adverse ecological effects associated with the toxicity of environmental chemicals (Lytle and Lytle, 2001).

Toxic responses of phytoplankton communities might be influenced by fluctuations of a variety of environmental and intrinsic factors. These factors can alter the outcome of contamination by chemically changing the contaminant and modifying its toxicity, affecting the bioavailability of the contaminant, and by affecting the tolerance that organisms have towards a contaminant. Examples of factors that can affect toxicity include physical-chemical characteristics of the water (temperature, pH, light), mixtures of individual chemicals present, nutrient status, and algal competition. Temperature affects the chemical activity of contaminants and the physiological processes of the organisms, thus affecting toxicity. The pH of surface water or groundwater can affect the form, reactivity, solubility, and toxicity of some contaminants. Photo-enhanced toxicity may be caused by photosensitisation (formation of reactive species) and photo-modification (formation of oxygenated products). The interaction between individual

chemicals can result in concentration-additive effects, more-than-additive (synergistic effects) or less-than-additive (antagonistic effects) (Franklin *et al.*, 2002; Faust *et al.*, 2003). Moreover, the trophic state of an ecosystem plays an important role in its susceptibility to toxic effects (McCarthy and Bartell, 1988) because it controls phytoplankton survival, productivity, and structure as well as toxic chemical availability. The nutrient regime can affect the bioconcentration of hydrophobic organic contaminants by altering microalgae lipid content (Halling-Sørensen *et al.*, 2000), potentially affecting pesticide toxicity (DeLorenzo *et al.*, 2001). Nutrient status has also affected the recovery capacity of microbial communities following toxic stress (Lozano and Pratt, 1994; Pratt and Barreiro, 1998), and the toxicant disappearance rate (Pratt and Barreiro, 1998). Evidence of high, as well as insignificant influences, of pesticide/herbicide toxicity to microbial communities and phytoplankton under nutrient-enriched conditions has been reported (deNoyelles *et al.*, 1982; DeLorenzo *et al.*, 2002; Pratt and Barreiro, 1998). Algae may also compete for available nutrients (Kayser, 1979) or produce exudates that are toxic to other algal species (Sharp *et al.*, 1979; De Jong and Admiraal, 1984; Metaxas and Lewis, 1991). Such stresses may have a greater effect on algal growth and algal sensitivity to toxicants than toxicant concentration and solution speciation alone (Franklin *et al.*, 2004).

Toxicity data concerning microorganisms and pesticides are, in general, limited (see DeLorenzo *et al.*, 2001), with the majority restricted to studies on single species of microalgae (*e.g.* Tang *et al.*, 1998; Behra *et al.*, 1999; Nelson *et al.*, 1999; Leboulanger *et al.*, 2001; Pennington and Scott, 2001; Rioboo *et al.*, 2002). There are fewer investigations involving natural phytoplankton (*e.g.* Brown and Lean, 1995; DeLorenzo, *et al.*, 1999; Pollehne *et al.*, 1999; Pinckney *et al.*, 2002; Seguin *et al.*, 2002) and the use of pollution induced community tolerance (PICT) techniques (*e.g.* Gustavson and Wängberg, 1995; Nyström *et al.*, 2000; Bérard and Benninghoff, 2001). Scarce information has been reported about the influence of community trophic status on the toxic effects of contaminants (Pratt and Barreiro, 1998), or the effects of antifouling booster biocides on natural phytoplankton assemblages (Dahl and Blanck, 1996; Nyström *et al.*, 2002; Larsen *et al.* 2003).

Non-routine methodological approaches have been developed including field-and laboratory-based measurements of changes in community structure (such as species succession, diversity reduction, dominance by opportunist species) or function (ecosystem processes, such as primary production, respiration, decomposition, nutrient

cycling) (e.g. Schindler, 1987; Gray, 1989; Pratt and Cairns, 1996). There is no consensus yet on whether structural or functional effects are the most appropriate endpoints for ecotoxicological studies.

1.4. Parameters used to assess toxic impairment of phytoplankton

Microalgae respond rapidly to a wide range of pollutants, and the effects can be measured at different levels of organization. Algal cells exhibit several responses to toxicants, including morphological modifications, growth inhibition and stimulation, and physiological changes (Lewis, 1995). The most reported effect is that of growth inhibition (at population level), based on changes in biomass, which can be determined or estimated by several techniques including dry weight, cell counting, chlorophyll-*a* concentration, deoxyribonucleic acid (DNA) content, adenosine triphosphate (ATP) activity. Changes in cellular composition, cell pigment content and composition, fluorescence and ^{14}C -uptake have also been observed following exposure to surfactants, metals, pesticides and land-based discharges (e.g. Rioboo *et al.*, 2002; Seguin *et al.*, 2002; Lytle and Lytle, 2001) and these may be useful early warning parameters to predict damage to phytoplankton. At a higher organizational level, the structure of algal communities has been reported to be very sensitive to environmental contaminants (Goldsborough and Robinson, 1986) and algal assemblages have been successfully used to monitor the impacts of aquatic stressors (Hoagland *et al.*, 1996; Wilson and Elkaim, 1991), and to assess the biotic integrity of aquatic ecosystems. To assess compositional changes of planktonic communities, several parameters have been used. The most common technique to identify species is by microscopic examination. Recently, indirect estimates of species composition have been generated through pigment composition analyses. Also, direct discrimination between major algal groups can be determined by analytical flow cytometry. However, relationships between these parameters and those of population growth and community structure in natural phytoplankton assemblages has not been well established.

To assess physiological changes as a measure of the health state of phytoplankton at either population or community levels, chlorophyll-*a* fluorescence has been widely used. As the majority of the booster biocides studied here affect the PSII photosystem, an overview of photosynthesis processes and relevant fluorescence parameter determinations are given below.

1.4.1. Chlorophyll fluorescence

1.4.1.1. Overview of photosynthetic processes

The energy to drive photosynthesis is derived from the conversion of the photochemical excitation energy to electro-chemical energy in the reaction centres (Suggett *et al.*, 2001). Light is absorbed by the antenna pigments in the photosynthetic apparatus and the excitation energy is transferred to the reaction centres of PSI and PSII, leading to a charge separation (Krause and Weiss, 1991; Kolber and Falkowski, 1993). The reaction centre in PSII consists of a primary electron donor, a special chlorophyll-*a* molecule, designated as P680, and a primary electron acceptor, a quinone designated as Q_A .

Upon exposure to light, P680 is oxidized to $P680^+$, and the quinone Q_A is reduced to Q_A^- . Hence, the reaction centres cannot utilize a subsequent excitation for photochemical charge separation and is said to be closed (Kolber *et al.*, 1993), until a low energy electron is drawn from the water oxidation system *via* intermediate molecules (Fig. 1.2). The photo-electron transport generates a charge separation in PSII and the energy to drive all subsequent reactions of photosynthesis (ATP synthesis and CO_2 fixation). In the dark, P680 is reduced whilst Q_A is oxidized, and the reaction centre is said to be open (Kolber *et al.*, 1993). The Q_A^- is oxidized by a secondary acceptor, Q_B (a plastoquinone) which, upon receiving two electrons, physically dissociates from the reaction centre protein complex to become part of the plastoquinone (PQ) pool. The vacated binding site on the protein is then occupied by another PQ. Electrons from the PQ pool are transferred *via* cytochromes to PSI. These two photosystems differ in their functions, PSII splits water to form oxygen, while only PSI transfers electrons to the final electron acceptor, $NADP^+$ (Lodish *et al.*, 2004).

Chlorophyll fluorescence is the phenomena of chlorophyll-*a* naturally absorbing a specific wavelength of light (460 nm for *in vivo* analysis) and almost instantaneously emitting a longer wavelength of light (685 nm). The ratio of light emitted as fluorescence to light absorbed is defined as the quantum yield of chlorophyll fluorescence (Falkowski and Raven, 1997) and it is controlled by the ability of the phytoplankton to utilize light for photosynthesis. This ability varies due to environmental factors such as nutrient and trace metals availability, temperature, and exposure to high irradiance and/or UV content in the ambient light. It is also controlled

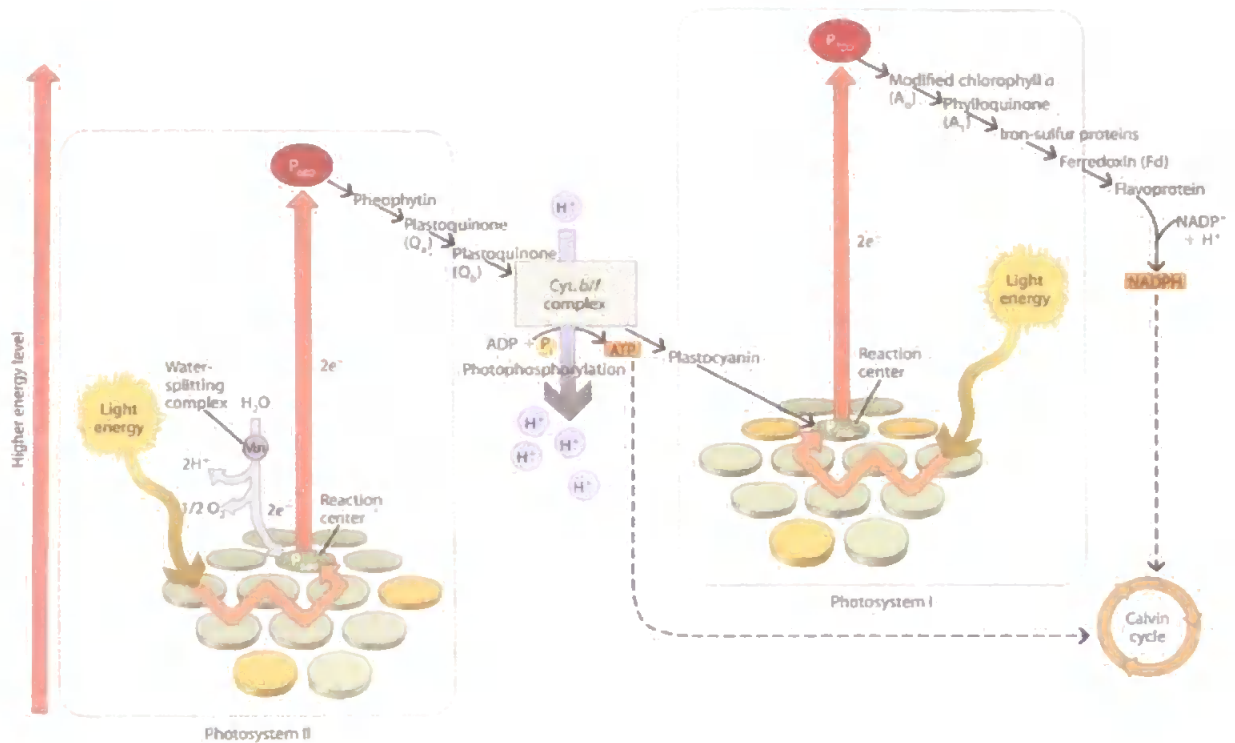


Figure 1.2. Diagram of photosynthetic light reactions showing PSI and PSII components in relation to their energy level. (From Vinebrooke, 2003)

by internal mechanisms of cell division and diel cycle. At physiological temperature, most fluorescence is emitted from chlorophyll-*a* in PSII (Barber *et al.*, 1989). This can be explained by the relative stability of P700 (PSI) in the oxidized state compared with P680⁺ (PSII), which is readily returned to the ground state by electron donation (Krause and Weis, 1991). When a photon excites a chlorophyll-*a* molecule, an electron is transferred from low to high energy (excited). This is an unstable state molecule, which returns to ground state by means of several competing processes. Photochemical reactions (K_P) and the emission of fluorescence are competing processes for deactivation of excited chlorophyll-*a* (K_F) (Krause and Weis, 1991). The thermal deactivation (K_D), or the transfer to non-fluorescent pigments (K_T) are alternative pathways for the dissipation of energy from the excited chlorophyll molecule (Campbell *et al.*, 1998). Maximum fluorescence yield is observed when all reaction centres of PSII are 'closed' and minimum fluorescence yield is when all reaction centres are in active 'open' state. When all Q molecules are oxidized the maximum quantum yield for photochemistry is reached, and when all Q molecules are reduced, the maximum quantum yield for fluorescence occurs (Falkowski and Raven, 1997). Thus, the quantum yields of

photochemistry (ϕP) (equation 1) and fluorescence (ϕF) (equation 2) are inversely related to each other.

$$\phi P = \frac{K_P}{(K_F + K_D + K_T + K_P)} \quad \text{Eq. (1)}$$

$$\phi F = \frac{K_F}{(K_F + K_D + K_T + K_P)} \quad \text{Eq. (2)}$$

In low light, under optimal conditions, the primary photosynthetic energy conversion occurs with high efficiency, with more than 90% of absorbed light quanta utilized by photosynthesis. The maximum fluorescence yield in the photosynthetic apparatus (ϕF_M) is only around 3% of the absorbed light. Upon illumination of the photosynthetic apparatus by actinic light in a dark-adapted state, an increase in fluorescence begins. Several parameters can be determined from the kinetics of the fluorescence emission, each describing the efficiency of a photochemical reaction or processes within the photosynthetic apparatus.

The induction signal represents a complex polyphasic process (Krause and Weis, 1991). When Q_A reduction is faster than re-oxidation of Q_A the maximum fluorescence yield (F_M) state is reached, representing full reduction of Q_A . As the proportion of closed reaction centres increases relative to the total number of reaction centres, the efficiency of light conversion into photosynthesis decreases, resulting in increased chlorophyll fluorescence. As electrons pass from Q_A^- via Q_B to plastoquinone (PQ), the fluorescence rise is also related to the reduction of these electron carriers and is used to determine the size of the PQ pool. The true F_M can only be reached when the PQ pool becomes reduced. The rate of its re-oxidation depends on electron transfer via PSI and on the final consumption of reducing equivalents in carbon metabolism and other metabolic reactions. The typical fluorescence induction signal exhibits a relatively fast rise from F_0 to F_I (I = inflection) followed by a plateau (F_D) and a slower rise to the fluorescence maximum (F_M) (Krause and Weis, 1991).

The variable fluorescence ratio F_V/F_M , which describes the maximum efficiency of PSII photochemistry, is calculated from the minimum fluorescence (F_0) in the dark and the maximum fluorescence (F_M) on application of 'saturating' light to the dark-adapted plant (Maxwell and Johnson, 2000). Under ideal conditions, F_V/F_M would be expected to

be equal to 1, reflecting the fluorescence when all reaction centres are open, and with F_0 equal to zero. In fact, this is not observed since inefficiencies in energy transfer and charge recombination within the reaction centres occurs (Kolber and Falkowski, 1993). Variations in F_V/F_M are due to changes in the efficiency of non-photochemical quenching (described below).

Following an increase in the yield of fluorescence, fluorescence quenching occurs. It reflects all processes that lower the fluorescence yield below its maximum (Krause and Weis, 1991). The resolution of quenching components provides important information on the functional state of the photosynthetic apparatus, and more specifically on the efficiency of PSII (Krause and Weis, 1991). Due mainly to light induced-activation of enzymes involved in carbon metabolism, an increase in the rate at which electrons are transported away from PSII takes place, *i.e.*, photochemical quenching. This reflects a lowering of fluorescence below maximal levels through photochemical competition with fluorescence emission. At the same time, there is an increase in the efficiency with which energy is converted to heat and this process is termed non-photochemical quenching (Maxwell and Johnson, 2000). The non-photochemical quenching of fluorescence is due to a number of biophysical and biochemical mechanisms that dissipate excess excitation energy in the pigment antenna to protect PSII from overexcitation (see Krause and Weis, 1991; Kolber and Falkowski, 1993; Maxwell and Johnson, 2000). The major contributor to non-photochemical quenching is thought to be essential in protecting the cell from light-induced damage (Maxwell and Johnson, 2000), which requires the presence of a low pH in the lumen of the thylakoid and involves the light-induced formation of the carotenoid zeaxanthin (Demming-Adams, 1990). Photoprotective processes with long relaxation times have been related to the presence of zeaxanthin and are thought to occur in the light-harvesting antenna of PSII (Horton *et al.*, 1996). A second process that relaxes over a time scale of a few minutes (but only makes a small contribution to overall quenching) involves the reversible phosphorylation of light-harvesting proteins and are thought to be important in balancing the distribution of light energy between PSI and PSII at low light.

1.4.1.2. Fluorescence response to antifouling biocide stress

Although fluorescence measurements may provide a useful measure of the photosynthetic performance, fluorescence can also provide insights into the ability of algae to tolerate environmental stresses and into the extent of damage of the

photosynthetic apparatus. Analysis of chlorophyll fluorescence is a sensitive and early indicator of damage to the photosynthetic apparatus (Krause and Weis, 1991) and is, therefore, suitable for monitoring the effects of biocides. Environmental stresses that affect PSII efficiency lead to a characteristic decrease in F_V/F_M . Chlorophyll fluorescence responses have been successfully employed to detect the effects of antifouling biocide exposures in phytoplankton, periphyton and plants (Nyström *et al.*, 2000; Jones and Kerswell, 2003; Chesworth *et al.*, 2004).

The development of methods for measuring chlorophyll fluorescence (20 years ago) led to two distinct approaches for measuring the photosynthetic quantum yield in actinic light: a pulse amplitude modulation (PAM) fluorometer and the fast repetition rate (FRR) approach. Both fluorometers are fundamentally distinct in the way in which they 'perturb' the redox state of photosystem II with each flash of light (see Kromkamp and Forster, 2003). The PAM technique generates multiple photochemical charge separations (multiple turnover) and fully reduces Q_A , the secondary acceptor (Q_B) and plastoquinone (PQ). In contrast, the FRR technique fully reduces the primary electron acceptor, Q_A , and allows a simultaneous, single closure event (single turnover) of all PSII reaction centres (Suggett *et al.*, 2003). Fast Repetition Rate fluorimetry (FRRF) (Fig. 1.3) is a technological development from an earlier pump-and-probe¹ technique

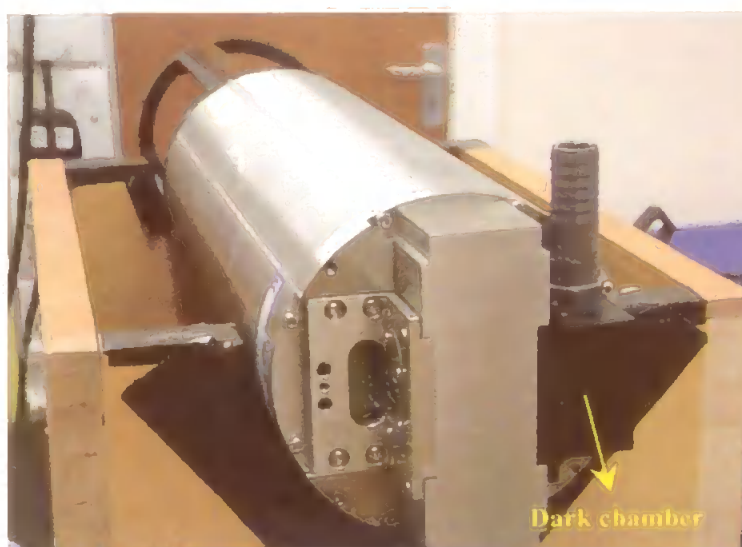


Figure 1.3. The Fast Repetition Rate Fluorometer. Measurements of fluorescence parameters were acquired using the dark chamber.

¹ This technique compares the fluorescence before and after single-turnover actinic or saturating pump flashes to measure the kinetics of the electron transfer in PSII (Kolber and Falkowski, 1993), and uses brief flashes to cumulatively saturate the reaction centre within a single photochemical reaction (Falkowski and Raven, 1997).

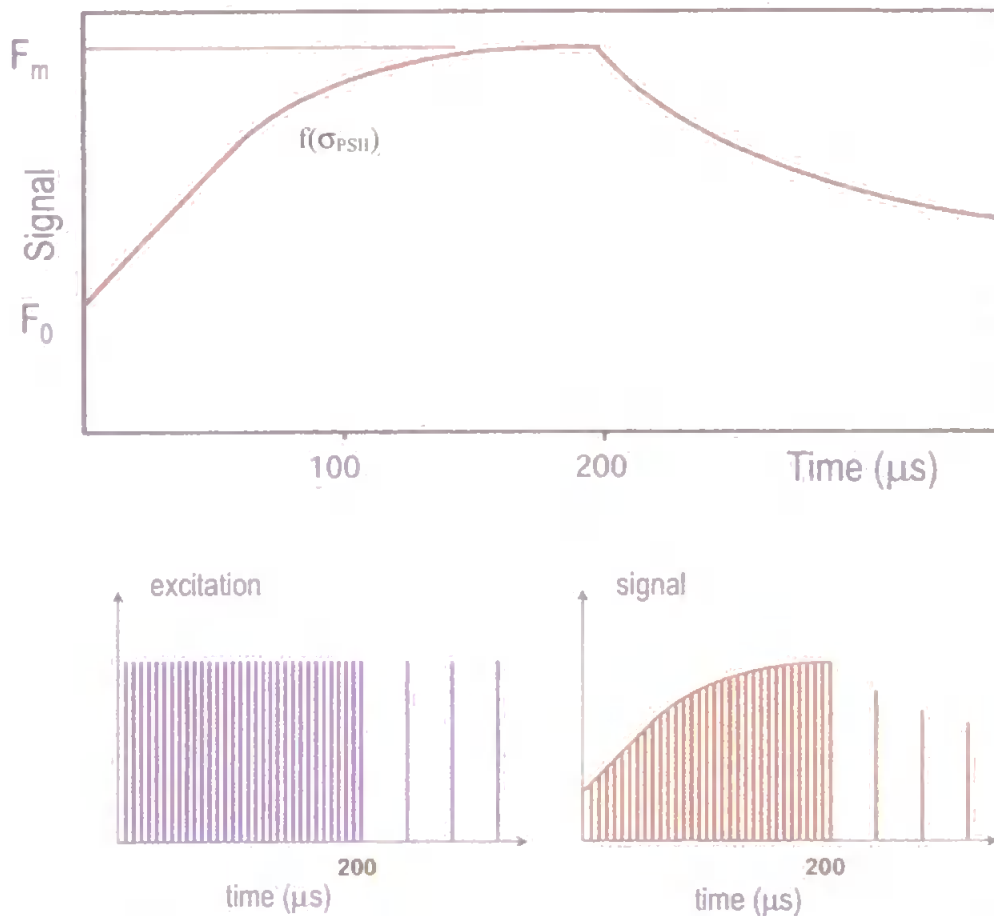


Figure 1.4. FRRF fluorescence signal resulted from exposure of phytoplankton to a series of microsecond flashes of blue light. The saturation profile of PSII variable fluorescence is used to derive the following parameters used in this study: $F_M - F_0 / F_M$: photochemical quantum efficiency (F_V / F_M); σ_{PSII} : functional absorption cross section of PSII. (Diagram modified from Chelsea Technologies Group).

(Kolber *et al.*, 1998), based on similar principles.

The basis of the Fast Repetition Rate (FRR) technique is to measure fluorescence transients induced by a rapid train of sub-saturating excitation flashes, where the intensity, duration, and time delay between flashes can be individually controlled (Kolber *et al.*, 1998). Thus, it provides measurements of the progressive closure of PSII reaction centres (Sakshaug *et al.*, 1997) in response to flashes of excitation energy (Fig. 1.4). As with FRR, the PAM and the pump-and-probe techniques measure photosynthesis in a non-destructive and rapid way and can be performed in real-time. The FRR and PAM estimates of photochemical efficiency of photosystem II (F_V' / F_M' under light exposure) are non-linearly related, reflecting the differences in techniques (Suggett *et al.*, 2003). However, the FRRF provides a better signal to noise ratio and allows more robust measurements in low chlorophyll samples (Suggett *et al.*, 2001),

such as cultures impacted by toxicants as well as oceanic samples. FRR fluorescence was utilised in this investigation as a tool to detect impairment of phytoplankton photosynthesis under exposure to antifouling compounds. Although it can provide endpoints for dark- and light-adapted samples, owing to the instrumentation available, only dark- adapted algae responses were used in this study.

1.4.2. ^{14}C Carbon incorporation

In stressed environments it is essential to measure primary production and photosynthetic capacity to determine the extent to which inorganic carbon is fixed and made available to higher trophic levels. The ^{14}C method is the most commonly used technique for the measurement of phytoplankton production (Longhurst *et al.*, 1995; Falkowski and Raven, 1997) because of its sensitivity, relative ease of measurement and apparent simplicity (Williams *et al.*, 1996). The method allows for the estimation of dissolved inorganic carbon uptake from water by planktonic algae as they photosynthesise. The carbon incorporated either remains in the algae as particulate organic carbon or is excreted into the water as dissolved organic carbon (Peterson, 1980). The method was first introduced by Steemann Nielsen in 1952 and has been described and explained by many authors (see Peterson, 1980 and Strickland and Parsons, 1972). The technique is based on the amount of radioactive carbon incorporated into the algae after being spiked with a known amount of ^{14}C (usually as $\text{NaH}^{14}\text{CO}_3$) under specific incubation conditions. Primary production is calculated from the amount of radioactive carbon incorporated into particulate (and sometimes dissolved) organic matter, and is a measure of total carbon uptake during the period of incubation. It may be normalised to carbon, cell number or chlorophyll concentration as a measure of biomass.

Compared to the natural environment, interpretation under experimental conditions are influenced during the incubations by a series of processes which involve: 1) loss of fixed ^{14}C by autotrophic respiration, excretion or passive diffusion of dissolved organic carbon (Raven, 1993), grazing activities, heterotrophic respiration (Harris, 1986); and 2) bottle effects due to the isolation of a population from external physical, chemical and biological influences from its natural environment (Li and Goldman, 1981).

In this study, two techniques, *in vivo* fluorescence (F_V/F_M) and ^{14}C incorporation were compared to investigate their suitability as measures of the response to antifouling

booster biocides. Even though both parameters measure slightly different phases of the photosynthetic process, similar responses are expected since biocidal effects occur at the PSII electron transfer. Toxicity assessments on phytoplankton determined by *in vivo* chlorophyll fluorescence and/or ^{14}C -tracer methods have been described previously (Marwood *et al.*, 2001; Dahl and Blanck, 1996). A comparison between both Pulse Amplitude Modulated and ^{14}C -tracer methods have recently been made in order to assess the sensitivity of freshwater periphyton to atrazine and isoproturon (Dorigo and Leboulanger, 2001; Nyström *et al.*, 2002). Comparisons between marine phytoplankton production using FRR fluorescence and traditional techniques such as *in vitro* ^{14}C assimilation and *in situ* O_2 evolution have also been applied in oceanographic studies (Suggett *et al.*, 2001; Kolber and Falkowski, 1993). However, use of the FRR technique in toxicological studies has only recently been applied (Marino Balsa *et al.*, 2003; this thesis).

1.4.3. Phytoplankton composition

In this section, the methods used to measure phytoplankton composition: light microscopy, analytical flow cytometry and HPLC-chemotaxonomy are described.

Several techniques have been employed to investigate phytoplankton community composition. Light microscopy is the classical method for identifying and enumerating phytoplankton, allowing estimations of carbon content from biovolume determinations (Strathmann, 1967; Montagnes and Franklin, 2001). Whilst detailed information about species and size can be acquired, this method is very time consuming and requires considerable taxonomic expertise. Moreover, light microscopy examination does not easily lend itself to identification of small-sized organisms (e.g. nanoplanktonic flagellates). Furthermore, fixation can alter the structure of fragile cells of many species (Gieskes and Kraay, 1983; Simon *et al.*, 1994), making the identification even more difficult.

Analytical flow cytometry (AFC) is an ideal tool for studying aquatic microbial populations because of its rapid enumeration and quantification of both structural and functional properties of individual cells. It has become indispensable for the identification and enumeration of picoplankton ($< 2 \mu\text{m}$), which are very important in oceanic food webs. This has afforded a better understanding of the roles played by individual organisms. Since the early 1980s, applications of flow cytometry in marine

(A)



(B)

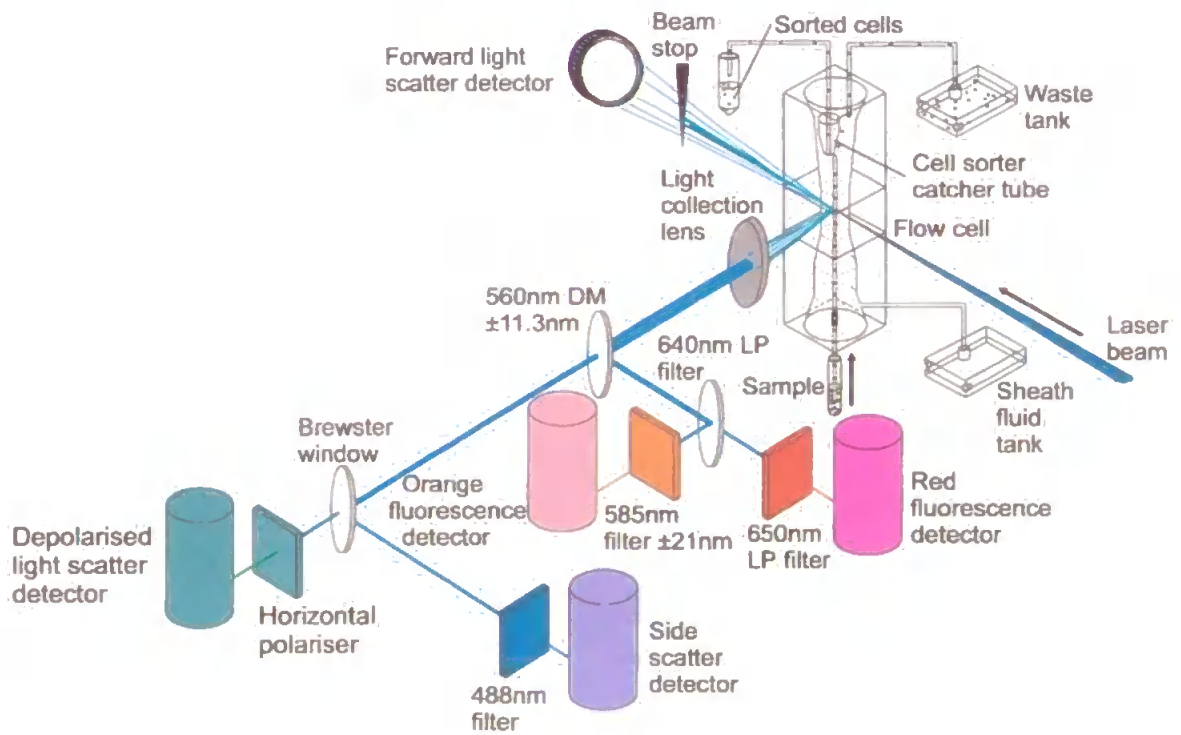


Figure 1.5. The Flow Cytometer (A) and a schematic drawing of its components (B). (The diagram is a courtesy of Glen Tarran, Plymouth Marine Laboratory).

microbial ecology have increased exponentially (Campbell, 2001). Numerous applications have resulted from using the technique for the determination of species specific growth rates (Carpenter and Chang, 1988) of microbial populations (Vaulot *et al.*, 1995; Liu *et al.*, 1997b, 1998); grazing studies and trophic dynamics (Cucci *et al.*, 1989; Landry *et al.*, 1995); bacterial and phytoplankton community structure, composition and activity (Collier and Campbell, 1999); and, most recently, the toxicity of xenobiotics on phytoplankton (Readman *et al.*; 2004, Devilla *et al.*, *in press*; Franklin *et al.*, 2001a).

Flow cytometric analysis consists of individual cells passing through a laser beam at high speed (Fig. 1.5A and Fig. 1.5B). Analytical Flow Cytometry (AFC) separates different groups of phytoplankton through optical properties of the cell, such as light scatter, diffraction and fluorescence parameters, which are measured on individual cells at rates of up to 10^3 cells s^{-1} (Burkill and Mantoura, 1990). AFC allows precise estimates, requires a small volume of sample and provides a rapid assessment and quantification of phytoplankton communities. It also is applicable for environmentally realistic cell densities of around 10^2 to 10^3 cells ml^{-1} (Franklin *et al.*, 2002). This unique characteristic of flow cytometry enables bioassays to better simulate the composition of algae in natural assemblages, which usually have a few dominant species and several sub-dominant taxa, all at low cell densities. The large number of events (10000 or more) acquired for each analysis using AFC provides results with a greater level of statistical significance than the traditional epifluorescence microscopy. However, it lacks detailed taxonomic resolution as given by light microscopy. Another limitation lies in the detection of larger sized cells (approximately $> 50 \mu m$). Based on the optical properties of cells, AFC can discriminate phytoplankton communities into picoplanktonic prokaryotes, picoeukaryotes, and nanoeukaryotes (Readman *et al.*, 2004).

A chemotaxonomic approach has provided an additional tool that overcomes some of the limitations of microscopy and AFC. Based on analyses of pigments using high performance liquid chromatography (HPLC), taxon-specific markers, such as chlorophylls (Fig. 1.6A) and carotenoids (Fig. 1.6B), can discriminate between the main algal classes contributing to the phytoplankton community (e.g. Barlow *et al.*, 1993; Jeffrey *et al.*, 1997). For example, peridinin has been used as a diagnostic pigment marker for dinoflagellates, 19'-hexanoyloxyfucoxanthin for prymnesiophytes, alloxanthin for cryptophytes, while other pigments are shared within more than one algal

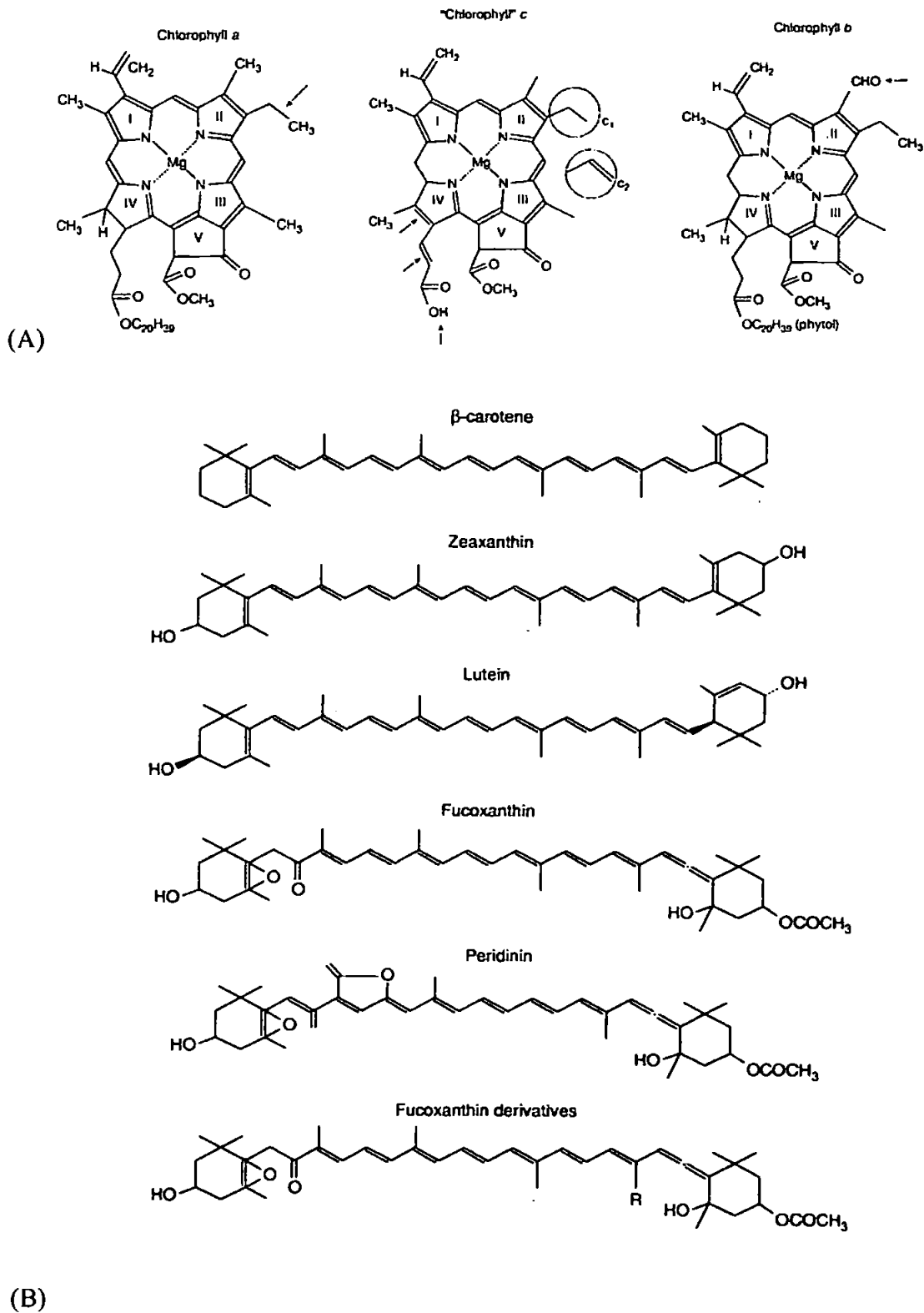


Figure 1.6. Structures of selected chlorophylls and carotenoids. (A) The chlorophyll-*a* molecule is found in all photoautotrophs. The chlorophylls *b* and *c* function as accessory pigments. All chlorophylls are made of four pyrroles and a Mg atom. Whereas in chlorophyll *c* a double bond is present, true chlorophylls have a saturated single bond in ring 4, leading to large absorption bands at lower energy states (red region of the spectrum). Arrows indicate differences between structures. (B) The basic structure of carotenoids is a conjugated isoprene backbone with cyclic-6-carbon side groups. Oxygenation of the side groups confers hydrophylicity, and such carotenoids are called xanthophylls. (From Falkowski and Raven, 1997).

class, e.g. chlorophyll *b* which occurs in chlorophytes, prasinophytes and prochlorophytes (Andersen *et al.*, 1996; Jeffrey *et al.*, 1997).

Carotenoids represent an extremely large group of biological chromophores that, depending on subtle structural changes (Fig. 1.6), can demonstrate a remarkable range of spectral characteristics (Rau, 1988). Spectrally, the major carotenoids display blue and/or blue-green absorption bands that partially overlap with chlorophyll (Fig. 1.7) and they may either facilitate the transfer of excitation energy to, or remove excitation from, chlorophyll (Falkowski and Raven, 1997). In addition, they play an important role in protecting photosynthetic organisms from damage resulting from the photochemical generation of oxygen radicals (Sandmann *et al.*, 1993).

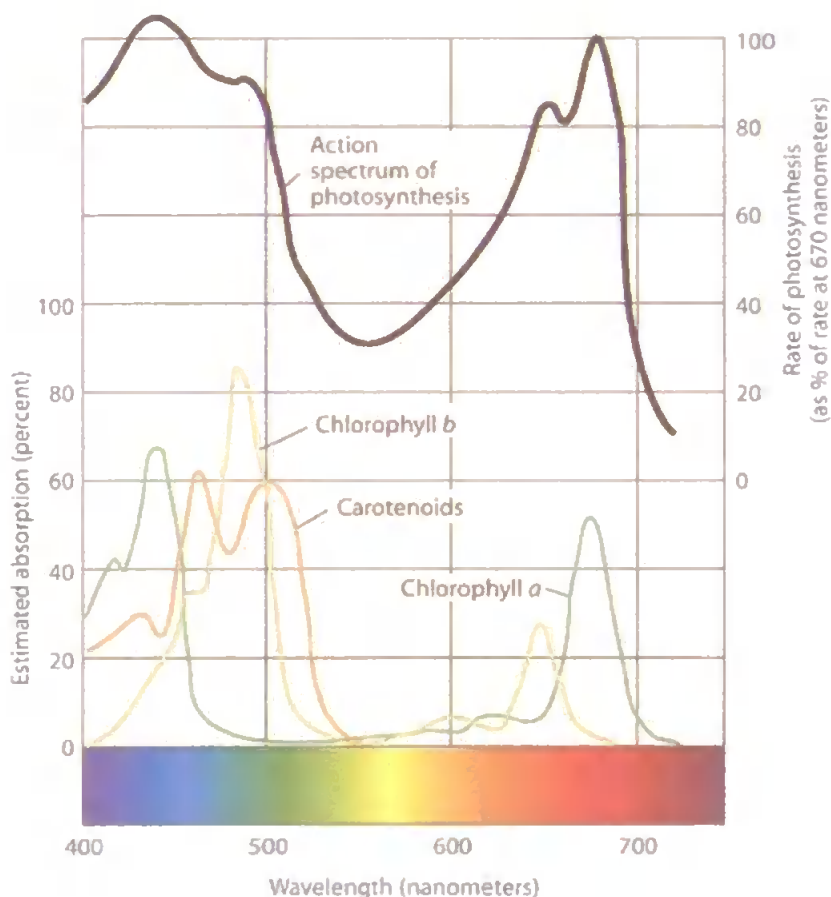


Figure 1.7. An action spectrum compared to an absorption spectrum. An action spectrum is measured by plotting a response to light (such as the rate of photosynthesis), as a function of wavelength. If the pigments used to obtain the absorption spectrum are the same as those that cause the response, the absorption and action spectra would match, indicating that light absorption by the chlorophylls mediates oxygen evolution. Discrepancies are found in the region of carotenoid absorption (from 450 to 550 nm), indicating that energy transfer from carotenoids to chlorophylls is not as effective as energy transfer between chlorophylls.

In the past, chlorophylls and carotenoids have generally been measured using simple spectrophotometric techniques. The application of HPLC allows far more accurate measures of chlorophyll-*a* (Chl-*a*) and the quantification of up to 50 additional chloro-pigments and carotenoids in marine plankton (Jeffrey *et al.*, 1997). Chlorophylls and associated carotenoid pigments are being used to map the chemotaxonomic composition of phytoplankton in the oceans and also to track the flux, transformation and fate of phyto-genic carbon (Jeffrey *et al.*, 1997). Disappearance of native pigments and formation of degradation products (*e.g.* peripherally modified cyclic tetrapyrroles², linear tetrapyrroles³) have also been used to quantify grazing by micro- and macro-zooplankton (Porra *et al.*, 1997; Burkill *et al.*, 1987; Kleppel *et al.*, 1988). However, the use of specific biomarkers in coastal waters is more complicated than in the open ocean, since inland inputs can change chemical, physical and consequently biological characteristics of water. In contrast to oligotrophic and oceanic areas, the HPLC method has only rarely been used to estimate phytoplankton compositions in eutrophic and coastal marine areas (*e.g.* Bennett *et al.*, 2000; Pinckney *et al.*, 2002).

To estimate the biomass of phytoplankton groups from pigment concentrations, Mackey *et al.* (1996) introduced the CHEMTAX program, which utilises factor analysis and steepest decent algorithms to allocate a best fit to the data. It is based on suggested accessory pigment:chl-*a* ratios for both diagnostic pigments and pigments present in several phytoplankton groups. Since concentrations of carotenoids and Chl-*a* are influenced by irradiance and nutrient limitation (Goericke and Montoya, 1998), knowledge of their influence on pigment:Chl-*a* ratios is essential for the application of CHEMTAX. These ratios have been determined for species which are prevalent in estuaries and coastal areas under varying light, climate and nutrient limitation (Schlüter *et al.*, 2000).

Identification and enumeration of phytoplankton species by microscopic analyses is laborious, time-consuming, and abundance estimates can be uncertain. A combination of Analytical Flow Cytometry used to measure pico- and nano-phytoplankton and High Performance Liquid Chromatography (HPLC) providing pigment signature data overcomes many of these problems. Several recent studies have compared microscopic and chemotaxonomic approaches to assess natural communities (Breton *et al.*, 2000;

2 *e.g.*, degraded by chlorophyllase, Mg dechelatase.

3 *e.g.*, degraded from oxidative cleavage of Chlorophyll macrocycles

Rodriguez *et al.*, 2002; Carreto *et al.*, 2003; Garibotti *et al.*, 2003; Fietz and Nicklish, 2004), with some also including flow cytometric analyses (e.g. Gin *et al.*, 2003). These have demonstrated that HPLC pigment analysis is a valuable tool for phytoplankton studies and that it can generate a good approximation of carbon biomass. However, more research is needed to assess the chemotaxonomic approach, since the use of chlorophyll-*a* as a biomass indicator must be undertaken with caution as it is susceptible to changes in environmental conditions. To date, few investigations on community changes under anthropogenic stressors have been reported (Pinckney *et al.*, 2002; Larsen *et al.*, 2003; Readman *et al.*, 2004).

1.5. Scope of this research

The use of antifouling booster biocides is of environmental concern as they can affect non-target organisms. Phytoplankton are potentially highly susceptible to antifouling biocides because most of the formulations contain herbicides. If primary production as well as key phytoplankton species are significantly depressed or altered by antifoulant exposures, the food resource to higher consumers may be reduced. Also, opportunistic species may take over in detriment of sensitive species, possibly causing nuisance to the environment (e.g. toxic blooms). The question arises as to whether estuarine/marine ecosystems are potentially at risk to antifouling biocidal inputs.

In order to simulate how phytoplankton are affected by antifouling booster biocides in natural environments, the following needs to be addressed:

- Biocides impair photosynthesis and may affect non-target species to different extents, potentially modifying the structure of phytoplankton communities;
- A comparison of methods that would indicate sensitive parameters to assess physiological and compositional effects;
- Estuaries and coastal areas are eutrophic environments and the influence of environmental factors, such as nutrients, may influence the toxicity of contaminants;
- Current levels of antifouling booster biocides need to be re-evaluated in potentially impacted areas and compared to non-impacted ones, and such

levels contrasted with variations in local phytoplankton community compositions. Long-term changes in phytoplankton community structure resulting from biocidal exposure may be revealed. For example, in impacted areas, phytoplankton communities may be dominated by more resistant individuals.

1.6. Objectives of this research

The main objectives of this research are:

- To evaluate a suite of techniques available for detecting toxic effects of antifouling biocides on single microalgal species and on natural phytoplankton community compositions.
- To investigate changes in biochemical and physiological function of selected microalgal species and to the compositional structure of a marine phytoplankton community, induced by exposure to relevant antifouling biocides. These biocides selected included two that have been detected in Plymouth waters (diuron and Irgarol 1051[®]) and two which are being increasingly used (Sea-Nine 211[®] and zinc pyrithione).
- To compare and contrast changes in community structure as determined by HPLC-class specific pigment analyses, optical microscopy and AFC and use of these techniques to monitor the effects of Irgarol 1051[®] in microcosms.
- To investigate the influence of nutrients (nitrate and phosphate) on the toxic response of a natural phytoplankton community exposed to Irgarol 1051[®].
- To characterise the distribution of phytoplanktonic pigments and abundances, antifouling booster biocides, and related physico-chemical parameters (salinity, turbidity, particulate carbon and nitrogen) in a coastal environment (the Tamar Estuary and Plymouth Sound). This preliminary study would provide data on spatial variability in phytoplankton communities and would attempt to assess whether or not exposure to sources of pollutants might influence distribution patterns.

1.7. Outline of the thesis

The aim of this thesis is to address aspects of the toxicity of antifouling booster biocides to marine phytoplankton. Specifically, application and comparisons of methods to investigate toxic responses to phytoplankton (Chapters 3 and 4), the level of impact of different biocides on single species and on natural phytoplankton assemblages (Chapter 5), and preliminary data involving both an evaluation of the influence of macronutrients on biocide toxicity (Chapter 6; section 6.1) and a field investigation of the current levels of biocides and their association with phytoplankton (Chapter 6, section 6.2).

The most appropriate way to analyse the toxic effects of booster biocides on marine phytoplankton entails a combination of approaches, for both single species and natural phytoplankton experiments, and a field characterization. The search for a rapid and sensitive endpoint is crucial for determining reliable indicators of environmental stress. Physiological endpoints could provide valuable early warning indicators of stress from antifouling biocides. The applicability of photosynthetic parameters and pigment:chlorophyll-*a* ratios as biomarkers was first employed in unialgal experiments, as described in Chapters 3 and 5. Also described in these chapters and also Chapter 4 are the studies undertaken on phytoplankton composition and biomass, that provide information on the extent to which the structural changes in the community occur, and the implications of this for grazers and the ecosystem as a whole. Such information is also of relevance to establishing safe environmental regulations for water quality. Only limited information is available on the toxicological effects on phytoplankton of the most widely used booster biocides (Irgarol 1051[®] and diuron) and those becoming increasingly used (Sea-Nine 211[®] and zinc pyrithione).

Toxic responses of phytoplankton may be influenced by fluctuations in a variety of environmental factors which can alter the outcome of contamination. An example is the nutrient status of an ecosystem, which may play an important role in its susceptibility to toxic effects. An unbalanced nitrate and phosphate ratio can affect the physiology of phytoplankton which alters their vulnerability to toxicants and can affect the bioaccumulation of contaminants and the recovery capacity of a community after stress. In Chapter 6, an investigation of such effects on biocidal toxicity was conducted under laboratory controlled conditions to determine the extent of nutrient influence. Thus, the response of biotic communities to xenobiotics is directly affected by changes in environmental characteristics, in which anthropogenic discharges play a significant

role in regulating chemical/physical alterations. These alterations, both individually and interactively, induce responses in communities that are complex and not easily discerned with experimental manipulations under laboratory conditions.

Because environmental effects are integrated by community structure, *in situ* biological monitoring is a useful alternative approach for assessing disturbance and pollution in aquatic ecosystems. Manipulative approaches, as described in the chapters 3, 4, 5 and 6 (section 6.1), should be supplemented with survey data wherein many sites are sampled and analysed using measurements of community structure as response variables. Also in the Chapter 6 (section 6.2), a pilot field study of the current concentrations of biocides together with selected environmental parameters and biological data are presented. Although survey data are complex, multivariate statistical methods have been applied to extract patterns at regional scales relevant to environmental management and identify the main environmental stressors.

To complete this thesis, Chapter 7 draws the information together, providing the key conclusions reached and suggests directions for future research.

Chapter 2

General Material and Methods

2.1. Algae and culture conditions

Unialgal culture studies were carried out on two species, a prymnesiophyte *Emiliania huxleyi* and a cyanophyte *Synechococcus* sp.. Detailed descriptions of culture conditions for experimentation are outlined in the relevant chapters. Unialgal cultures were grown and maintained in an enriched medium F/2, according to Guillard (1975), by transferring aliquots (1-2 ml) of old culture into a new fresh medium F/2 (~150 ml). This medium was prepared with natural offshore seawater collected from the Eddystone Reef, Plymouth, UK. This site is situated 10 miles offshore on a flood tide (50°10'N; 4°15'W), where not much coastal influence is observed. Seawater was stored in a 2,500 litres capacity tank, with approximately 50% of the capacity replenished on a monthly basis. Water quality was maintained by continuous aeration, mixing (three times a day), and filtration through 10 µm, 1 µm and 0.45 µm porosity sized filters.

2.2. Description of the analytical reagents used

All solvents (*e.g.* methanol, ethyl acetate, acetone, and dichloromethane) used for preparation of stock solutions and for analytical procedures were of HPLC grade and supplied by Rathburn Chemicals (UK) and Fisher Scientific (UK).

Authentic analytical standards were acquired: Irgarol 1051[®] (N'-Tert-Butyl-N-cyclopropyl-6-(Methylthio)-1,3,5-Triazine-2) was supplied by Ciba-Geigy Ltd.; diuron pestanal[®] ([3-(3,4-Dichlorophenyl)-1,1 dimethyl-urea]; 99% purity; C₉H₁₀Cl₂N₂O; 233.10 g Mol⁻¹), and Ametryn pestanal[®] (2-ethylamino-4-isopropylamino-6-methylthio-1,3,5-triazine; 227.33 g Mol⁻¹) were supplied by Riedel-de Haën; Sea-Nine 211[®] (4,5-dichloro-2-n-octyl-4-isothiazolin-3-one) was kindly supplied by the Institute for Environmental Science, Netherlands; zinc pyrithione (1-Hydroxypyridine-2-thione (pyrithione) zinc salt; C₁₀H₈N₂O₂S₂Zn; FW 317.7; approximately 95% purity) was obtained from Sigma Chemical Co. (UK).

Analytical standards for HPLC pigment calibration were purchased from the International Agency for ^{14}C Determination DHI-Water and Environment (Hørsholm, Denmark) and Sigma-Aldrich Co. (UK) and were: chlorophylls *a*, *b*, *c*₁*c*₂, and *c*₃, peridinin, 19'-butanoyloxyfucoxanthin, fucoxanthin, 19'-hexanoyloxyfucoxanthin, prasinoxanthin, violaxanthin, neoxanthin, diadinoxanthin, alloxanthin, zeaxanthin, lutein, apo-carotenal, and β -carotene.

2.3. Glassware preparation

All glassware used in the experimental and analytical procedures was cleaned by soaking overnight in 5% Decon (phosphate-free detergent) followed by soaking in 5% nitric acid and then thorough rinsing with tap water. Specific glassware treatment was tailored for its particular use prior each specific analytical procedure, such as rinsing with methanol for antifouling biocide analysis, and rinsing with Milli-Q water for microalgal culturing.

2.4. General analytical procedures

2.4.1. Determination of fluorescence parameters

The FAST^{tracka} fluorimeter (Chelsea Instruments) was developed to measure phytoplankton photosynthetic parameters, *in situ*, rapidly and non-destructively (Aiken *et al.*, 2004). It enables the measurement of the absorption cross section of Photosystem II, the rate of photosynthetic electron transport and the level of photochemical quenching by delivering a rapid series of high frequency (200 kHz) flashes. Deployed in the ocean, this measurement occurs optically, in real time and *in situ*, and the simultaneous measurement of photosynthetically active radiation (PAR) by the FAST^{tracka} allows estimates to be made of phytoplankton primary production. The optical head has dual sample chambers allowing comparisons to be made of ambiently-irradiated and dark adapted phytoplankton samples. The fluorescence emission and flash excitation data obtained provide fluorescence yield data which is then used to calculate the biophysical parameters related to photosynthesis. These parameters are stored on an internal memory card, from where data can be downloaded to a computer, for subsequent data analysis (manufacturer's technical reference).

For the purpose of this study, the FAST^{tracka} fluorimeter (FRRF) was operated as a benchtop unit, which employs an excitation protocol of 100 'flashlets' of sub-saturating

intensity (1.1 μs duration and 2.8 μs interval) (Suggett *et al.*, 2001; Aiken *et al.*, 2004). The FRRF was configured with only the dark chamber activated, with 20 discrete acquisitions (8 sequences per acquisition) and an auto-ranging mode gain to allow maximum sensitivity for each sample. The FRRF could therefore detect changes in chlorophyll fluorescence yield between the initial dark-adapted state (F_0), when all functional PSII reaction centres are oxidized, and the light-saturated state (F_M), when all PSII reaction centres are photochemically reduced. Samples (25 ml) were dark-adapted for 30 minutes prior to measurement to ensure complete opening of PSII reaction centres. Data were downloaded from the FRRF in binary format and were analysed by the FRRF software FRS 1.8 (Chelsea Instruments, UK) to provide values given as instrument units for F_0 , F_M , the functional absorption cross section of PSII (σ_{PSII} ; $\text{\AA}^2 \text{ quanta}^{-1}$), and the non-dimensional maximum quantum yield of PSII (F_v/F_M). σ_{PSII} is derived from the slope of the fluorescence-yield curve from F_0 to F_M by fitting an exponential function to the data. F_v/F_M was calculated as a ratio of variable to maximum fluorescence as shown in equation 1.

$$\frac{F_v}{F_M} = \frac{F_M - F_0}{F_M} \quad \text{Eq. (1)}$$

The instrument calibration was performed by Chelsea Instruments. However, instrumental saturation limits of chlorophyll fluorescence were checked by performing a test using different cell concentrations of *E. huxleyi* (strain 92D). Assuming similar chlorophyll-*a*:cell ratios, saturation points were obtained with approximately 2×10^4 cell ml^{-1} (Fig. 2.1). More accurate results were obtained when cell concentrations in each sample were within this range. Culture conditions of *E. huxleyi* were similar to those described for the unialgal experiments with this species (Chapter 5), where similar fluorescence was expected. Blanks were run as culture medium only (without cells) and measures did not provide positive results, *i.e.*, below the instrument detection limits.

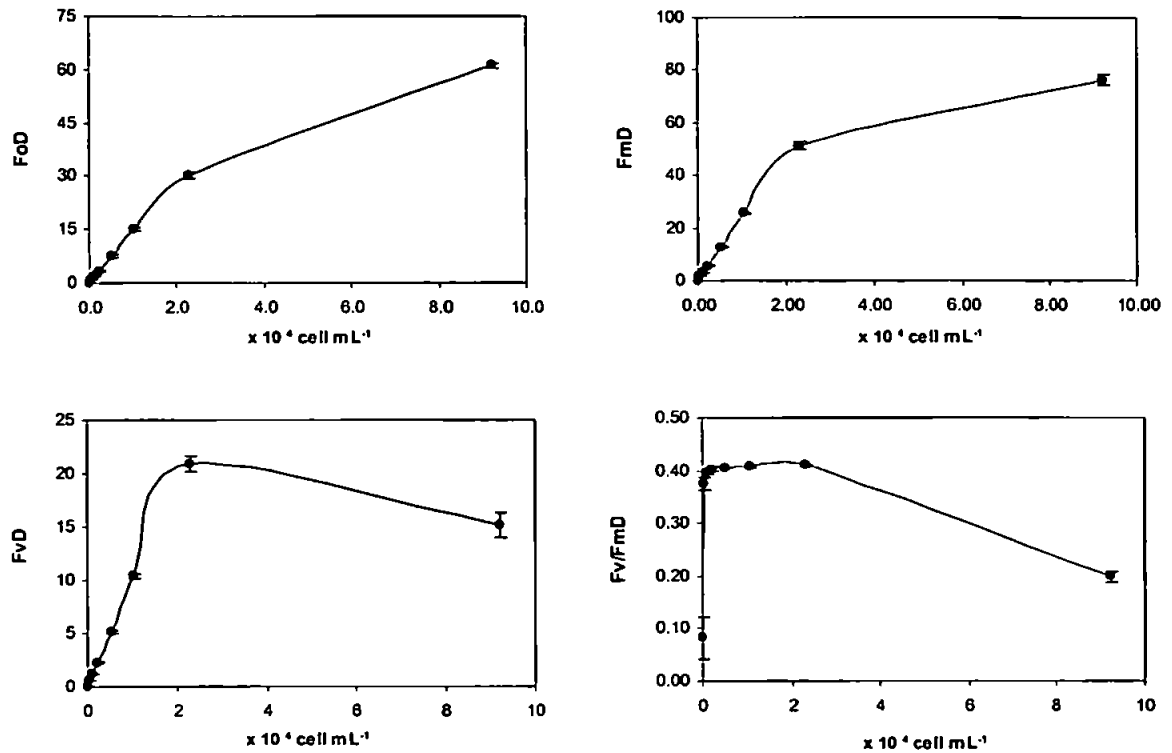


Figure 2.1. *Emiliana huxleyi* (92D) cell suspension. Density related changes in chlorophyll fluorescence kinetics. Mean values \pm standard deviation ($n = 3$). (F_0D) Minimum fluorescence yield measured in the dark (arbitrary units), ($F_M D$) maximum fluorescence yield measured in the dark (arbitrary units), ($F_V D$) variable fluorescence ($F_M - F_0$) (arbitrary units), and ($F_V/F_M D$) maximum quantum yield of PSII (dimensionless).

2.4.2. Determination of primary production (^{14}C tracer method)

The rate of carbon fixation was estimated from the incorporation of ^{14}C -bicarbonate (Peterson, 1980). Seawater samples containing the natural phytoplankton community ($<63 \mu m$) were transferred to 60 ml transparent polycarbonate bottles. Ampoules containing 0.5 ml of $NaHCO_3$ with a radioactivity of 37 MBq (1 mCi) were obtained from Amersham Pharmacia Biotech Ltd. A diluted $^{14}C-HCO_3^-$ solution was prepared from the 1 mCi stock to a final volume of 10 ml of pre-filtered sterile seawater, resulting in a radioactivity of $3.7 MBq ml^{-1}$ ($0.1 \mu Ci \mu l^{-1}$). Dilution was carried out using a Pasteur pipette to ensure complete removal of the radioactive liquid from the ampoule to the volumetric flask. Aliquots of radioactive diluted solution (50 μl) were then added to each 60 ml bottle containing the seawater sample, giving a final activity of 5 μCi $^{14}C-HCO_3^-$ per bottle. The same volume of $NaHCO_3$ was added to 10 ml of a carbon dioxide absorber (Carbo-Sorb E supplied by Packard) to determine the total radioactivity added

to each bottle. Estimates of dark $^{14}\text{C-HCO}_3^-$ fixation were obtained by covering the polycarbonate bottles with aluminium foil.

Incubations were terminated by filtration through Nuclepore polycarbonate membrane filters (0.2 μm pore size). Non-incorporated inorganic ^{14}C was eliminated in a fuming HCl atmosphere for approximately 4 min, and filters were transferred to vials, dried and stored in a desiccator for at least 12 h. A 2.5 ml volume of scintillation cocktail (Wallac OptiPhase 'Hi Safe'3) was then added to the vials and samples were counted in a liquid scintillation counter (LKB Wallac 1219 Rackbeta LSC) for 2.5 minutes. The efficiency was determined with an external standard with a channels ratio method⁴. Carbon fixation rates were calculated using equation 2, where PP is the primary production ($\text{mgC m}^{-3} \text{d}^{-1}$), dpm_{SAMPLE} is the radioactivity of the sample (disintegrations per minute), dpm_{ADDED} is the total radioactivity added to the sample as measured from the carbon dioxide absorber (equation 3), TCO_2 is the total weight of carbon dioxide present (in mgC m^{-3}), as shown in equation 4, and the incubation time d (day) corresponds to a 12/12 h light/dark cycle. The factor 1.05 accounts for the isotope discrimination factor – the preferential uptake of ^{12}C over ^{14}C by plants (Strickland and Parsons, 1968).

$$PP (\text{mgC} \cdot \text{m}^{-3} \cdot \text{d}^{-1}) = \frac{dpm_{\text{SAMPLE}} \times \text{TCO}_2 \times 1.05}{dpm_{\text{ADDED}} \times \text{IncubationTime}} \quad \text{Eq. (2)}$$

where:

$$dpm_{\text{ADDED}} = dpm_{\text{CarboSorb}} \times \text{dilutionfactor} \quad \text{Eq. (3)}$$

$$\text{TCO}_2 = \{[(\text{salinity} \times 0.067) - 0.05] \times 0.96 \times 12.01\} \times 1000 \quad \text{Eq. (4)}$$

where the factor 0.067 converts salinity (in psu) to total alkalinity (in meq l^{-1}), the subtraction of 0.05 converts total alkalinity to carbonate alkalinity (in meq l^{-1}), multiplication by 0.96 converts carbonate alkalinity into total carbon dioxide (in meq l^{-1}), and multiplications by 12.01 and 1000 converts the units to mgC m^{-3} .

⁴ The scintillation photons produced in the vials are detected by the photomultiplier tubes and, by comparing the number of counts in two different energy windows, a ratio called External Standard Ratio (ESR) can be obtained. A calibration curve with those parameters (efficiency and ESR) is made and saved under a specific measuring program later used when measuring unknown samples.

2.4.3. Determination of phytoplankton pigments

2.4.3.1. Sampling procedure

Phytoplankton samples (0.5-2 l) were concentrated under gentle vacuum (< 20 psi) onto 25 mm GF/F Whatman filters and were then frozen in liquid nitrogen (-196 °C). Pigments were extracted into 2 ml of 90% acetone:10% Milli-Q water (v/v) solution (containing an internal standard; ~200 ng ml⁻¹ apo-carotenal or canthaxanthin) with the aid of an ultrasonication probe (20 s; 60 W). Extracts were centrifuged for 5 min at 3000 rpm followed by 2 min at 14000 rpm to remove debris and clarify the extract. Extracts were transferred to 2 ml amber screw top vials sealed with PTFE septa and were placed in a controlled temperature autosampler (set at 0 °C).

2.4.3.2. Analytical procedure

Supernatants were mixed with 1M ammonium acetate (50%:50% v/v) before injection into an High Performance Liquid Chromatograph (HPLC). Analyses of pigments were conducted using the reverse phase HPLC procedure outlined by Barlow *et al.* (1997) using a 3 µm Hypersil MOS2 C-8 column (100 mm x 4.6 mm; Alltech Associates Ltd.) on a Shimadzu HPLC system (Thermoseparation products) or an Agilent HPLC system coupled with a diode array spectrophotometer detector. Analyses were run under a solvent gradient of 70:30 MEOH:1M ammonium acetate (v/v) solution (solvent A) and 100% MEOH (solvent B). Pigments were separated at a flow rate of 1 ml min⁻¹ by a linear gradient programmed as follows: 0 min, 75%A:25%B; 1 min, 50%A:50%B; 20 min, 30%A:70%B; 25 min, 100%B; 32 min, 100%B; 39 min, 75%A:25%B.

Carotenoids were detected by absorbance at 440 nm using a UV-Visible detector. Chlorophylls were determined by fluorescence (430 nm excitation and 668 nm emission). Data were stored, processed, and peak integrations were performed using the ChromQuest software version 5.21 (Shimadzu HPLC system) or LC Chemstation Software (Agilent HPLC system). Peaks were identified by comparing the retention times and online absorption UV-visible spectra (300-750 nm) from those of authentic standards (Fig. 2.2). Pigments were quantified from their peak areas relative to the internal standard *via* relative response factors.

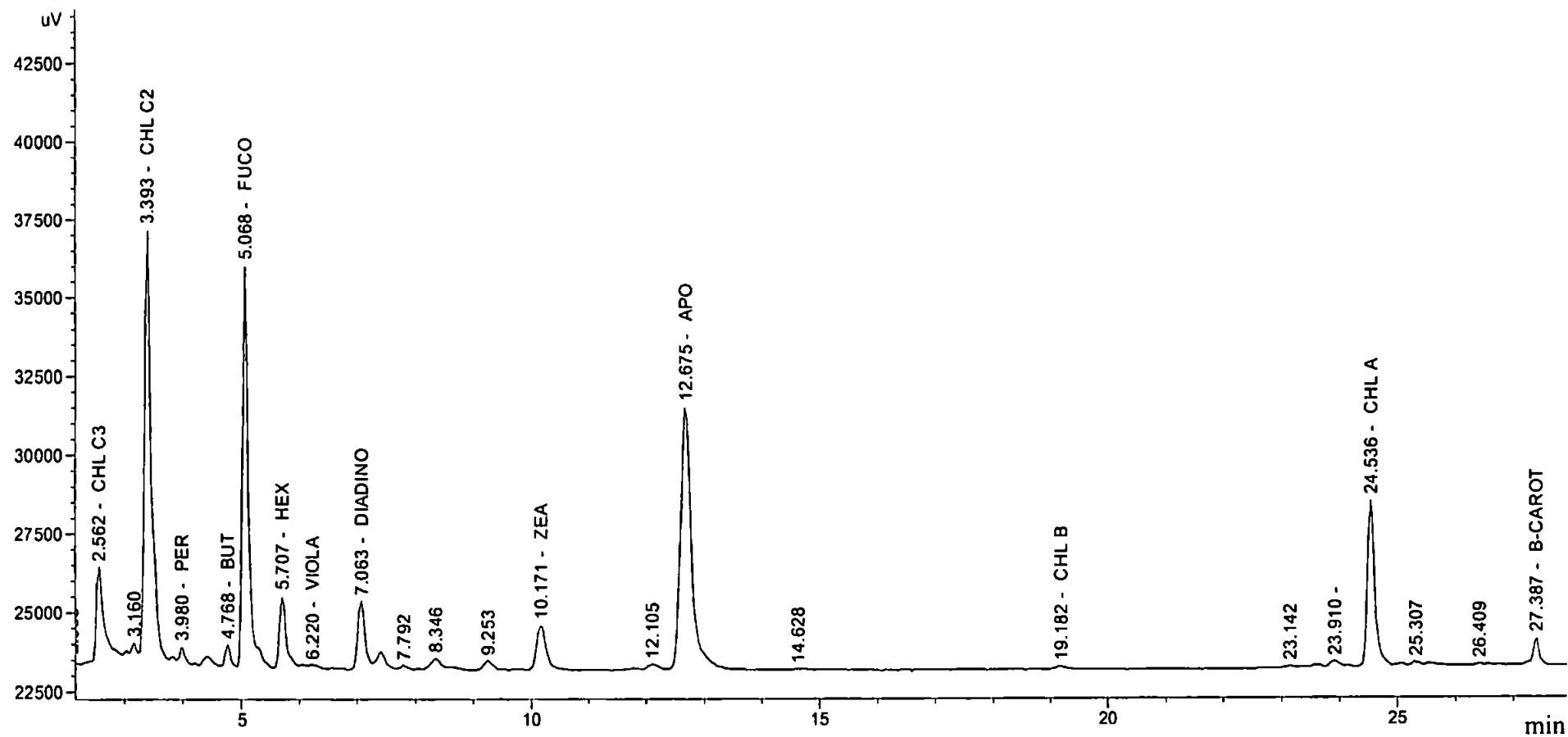


Figure 2.2. Example of a typical HPLC chromatogram from a pigment extract of natural seawater. Pigment identifications and retention times (min) are shown. Chlorophyll c_3 , Chlorophyll c_1c_2 , peridinin, 19'-butanoyloxyfucoxanthin, fucoxanthin, 19'-hexanoyloxyfucoxanthin, violaxanthin, diadinoxanthin, zeaxanthin, apocarotenal, chlorophyll b , chlorophyll a and β -carotene.

2.4.3.3. Quality control

Quality assurance included the running of calibration standards (apo-carotenal or canthaxanthin and chlorophyll-*a*) and instrumental blanks (90% acetone) with every batch of samples. The system was calibrated at intervals of approximately 6 months using all the authentic standards (International Agency for ¹⁴C Determination, DHI, Denmark and Sigma-Aldrich Co., UK) and the response factors were calculated relative to the internal standard (ametryn or apo-carotenal). Calibration was performed by analysing three replicate standards for each of the three to five concentrations of the 17 pigments acquired.

2.4.4. Determination of Irgarol 1051[®] and Sea-Nine 211[®]

2.4.4.1. Sampling procedure

Environmental seawater samples (2.7 litres) were collected from 0.5 m depth using dark glass bottles with PTFE-lined screw-capped lids (Law *et al.*, 1988; Zhou *et al.*, 1996). Sample bottles were mounted in a weighted stainless steel frame and deployed by means of a nylon rope. After collection, bottles were taken to the laboratory for analysis. Seawater samples from the microcosms were collected into 2 l borosilicate bottles. All samples were spiked with aliquots of internal standard solution (Ametryn Pestanal or Atrazine-d₅ solutions in methanol) and stored at 4 °C to await extraction within 48 h (Thomas *et al.*, 2001).

2.4.4.2. Analytical procedure

Extractions and analyses of Irgarol 1051[®] and Sea-Nine 211[®] (and atrazine, which is described in Chapter 6) were based on the methods described in Zhou *et al.* (1996) for solid-phase extraction (SPE) or Sargent *et al.* (2000) for liquid-liquid extraction. Solid phase extractions (SPE) were carried out using Env+ cartridges (200 mg; 6 ml), pre-rinsed sequentially with ethyl acetate, methanol and ultra-pure Milli-Q water. Cartridges were eluted with 3.5 ml ethyl acetate for 5 minutes. Solvent extracts were blown down to < 1 ml under a N₂ atmosphere in a Turbo-Evaporator (Zymark Turbo Vap[®] LV) set at 30 °C with 2.5 psi N₂.

Liquid-liquid extraction was performed using glass separation funnels and dichloromethane as the extracting solvent. The funnel was rinsed twice with methanol

followed by dichloromethane, prior to extraction. Extractions were performed twice by shaking the sample plus solvent for 2 min. The extracts were transferred into a 120 ml dark glass bottle containing dichloromethane washed Na₂SO₄, and the aqueous phase discarded. Water-free extracts plus the internal standard were sequentially concentrated down to 1 ml in a rotary-evaporator (Büchi Rotavapor R-205; 30-35 °C) and to 200 µl using the Turbo-Evaporator under a gentle stream of pure nitrogen gas.

Extracts (1-2 µl) were injected in splitless mode into a Gas Chromatograph – Mass Spectrometer (GC-MS) (6890 N Network GC System coupled with a 5973 Network Mass Selective Detector, Agilent Technologies, UK). The GC system was fitted with an HP-5MS capillary column (Agilent 19091S-433, 0.25 mm x 30 m x 0.25 µm). Helium carrier gas was maintained at a constant flow rate of 1 ml min⁻¹. The column temperature was programmed from 40 °C to 170 °C at 20 °C min⁻¹, 170 °C to 220 °C at 3 °C min⁻¹, and 220 °C to 320 °C at 20 °C min⁻¹. The instrument was operated in selective ion monitoring (SIM) mode using m/z values of 182 for Irgarol 1051[®], 169 for Sea-Nine 211[®], and 227 for Ametryn or 205 for Atrazine-d₅. Analytes were identified by comparing their retention times and mass spectra with authentic standards. Sea-Nine 211[®] and Irgarol 1051[®] concentrations were quantified from their peak areas relative to internal standard *via* relative response factors (RRF), according to the equation 5:

$$RRF = \frac{M_S}{M_{IS}} \times \frac{A_{IS}}{A_S} \quad \text{Eq. (5)}$$

where M_S is the mass of the sample, M_{IS} is the mass of the internal standard, A_{IS} is the peak area of the internal standard and A_S is the peak area of the sample.

2.4.4.3. Quality control

Prior to analysing a sample set, performance and calibration of the GC-MS system were verified for all analytes. The mass spectrometer was tuned on a regular basis using the system's operating software programs (Autotune) with perfluorotributylamine (PFTBA) calibration gas. Quality assurance included the running of calibration standards, instrumental blanks, procedural blanks (using ultra pure Milli-Q water) and matrix spikes (using seawater) with every batch of samples. Calibrations were achieved by making serial dilutions with authentic standards in dichloromethane and the resulting calibration curves displayed a determination coefficient of R² = 0.98-0.99 (Fig. 2.3). Injections were performed automatically (splitless mode) using an autosampler set to either 1 µL or 2 µL. Mass chromatograms were generated and ions were chosen by their

specificity and relevance from each of the analytical standard peaks (see Fig. 2.4, Fig. 2.5 and Fig. 2.6). Peak integrations were performed using a software package (HSD Chemstation). Recoveries of the analysed compounds were 85% ($\pm 3\%$; $n = 5$) for Sea-Nine 211[®] and 81% ($\pm 6\%$; $n = 5$) for Irgarol 1051[®]. Detection limits derived from replicate procedural blanks (taken as 6 times baseline noise) were $< 3 \text{ ng l}^{-1}$.

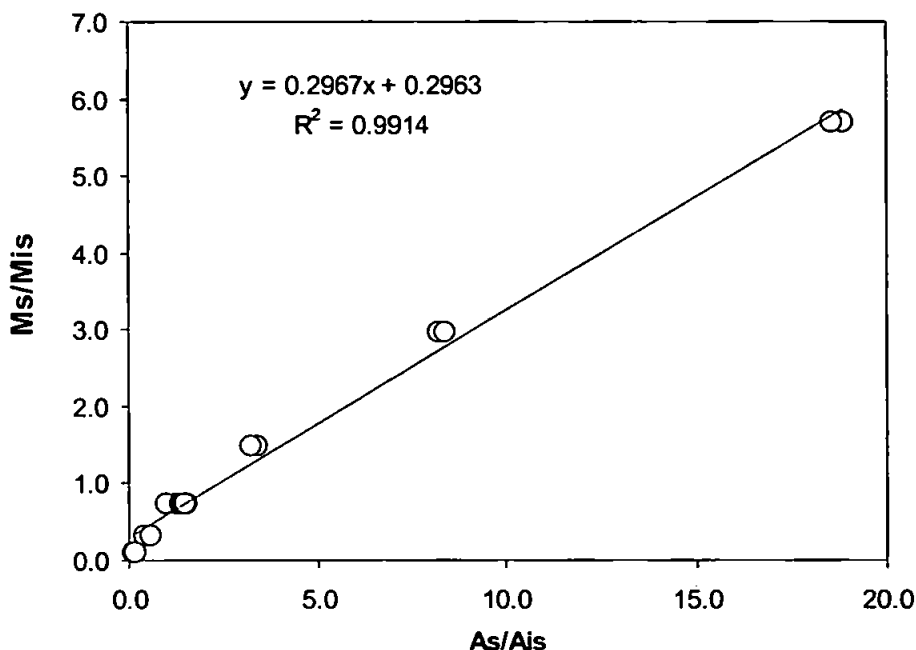


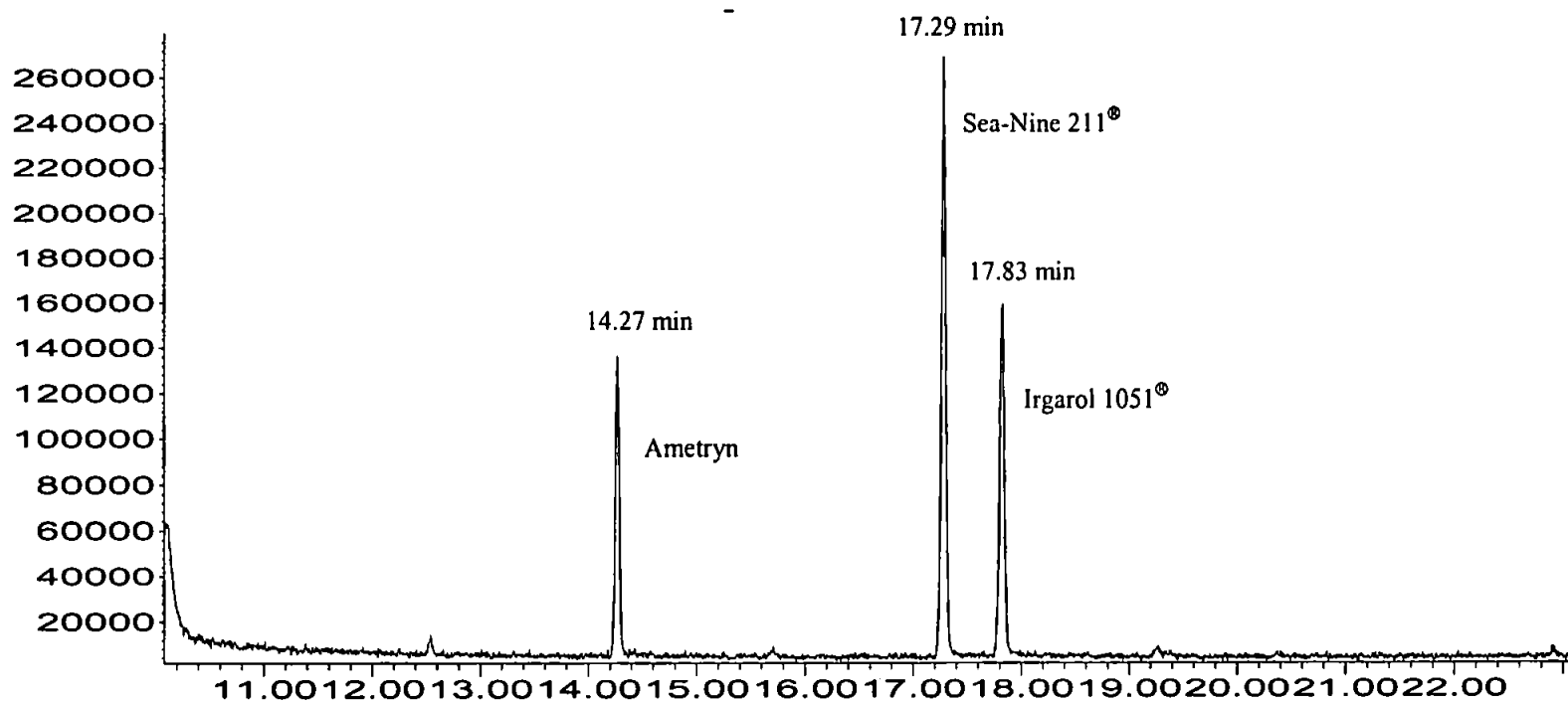
Figure 2.3. Irgarol 1051[®] standard calibration curve using the following concentrations: 0.226, 0.679, 1.58, 3.16, 6.33, 12.21 $\text{ng } \mu\text{l}^{-1}$. $n = 16$. M_S/M_{IS} and A_S/A_{IS} are the response factors for the standard.

2.4.5. Determination of diuron

Samples for diuron determination were analysed using a commercially available Enzyme-Linked ImmunoSorbent Assay (ELISA) kit (Sension GmbH, Germany). The test is based on the recognition of diuron by specific antibodies immobilized onto paramagnetic particles situated on the plate. Diuron present in the water sample and a phenylurea-enzyme conjugate compete for the binding sites of the antibodies.

Water samples were stored in borosilicate vials and kept frozen ($-20 \text{ }^\circ\text{C}$) until analysis. Analytical procedures followed the manufacture's instructions. Diuron ELISA kits were stored at $4 \text{ }^\circ\text{C}$ and standards and samples were allowed to adjust to room temperature ($20\text{-}25 \text{ }^\circ\text{C}$) before initiating the test. Samples were analysed in triplicate or duplicate together with standard calibrations and blanks. Defined volumes of samples,

Abundance



Time-->

Figure 2.4. Example of a GC-MS Total Ion Chromatogram from a standard mixture of ametryn, Sea-Nine 211[®] and Irgarol 1051[®].

Abundance

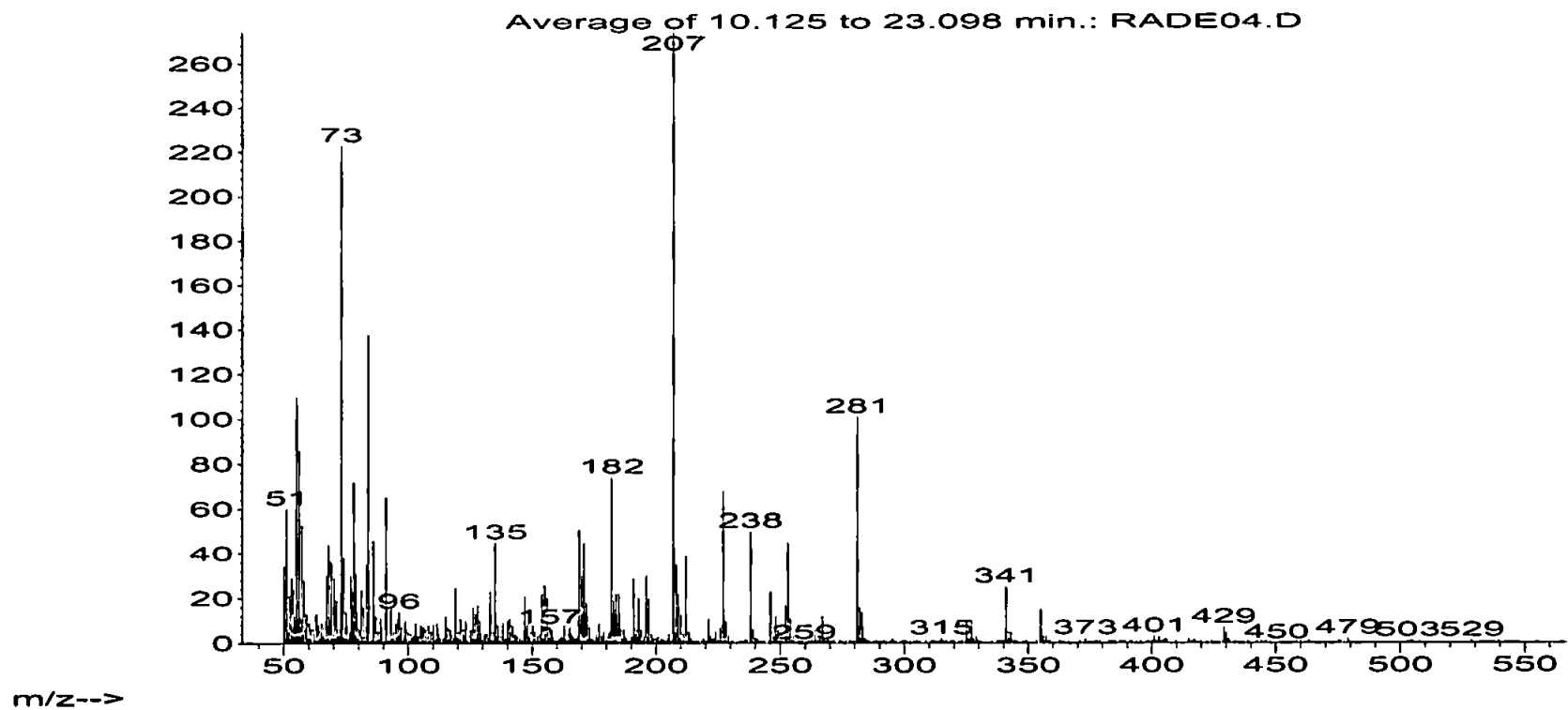


Figure 2.5. Mass spectra of the example showed in the Fig. 2.4 composed by the internal standard ametryn, and the standards Sea-Nine 211[®] and Irgarol 1051[®] obtained by GC-MS.

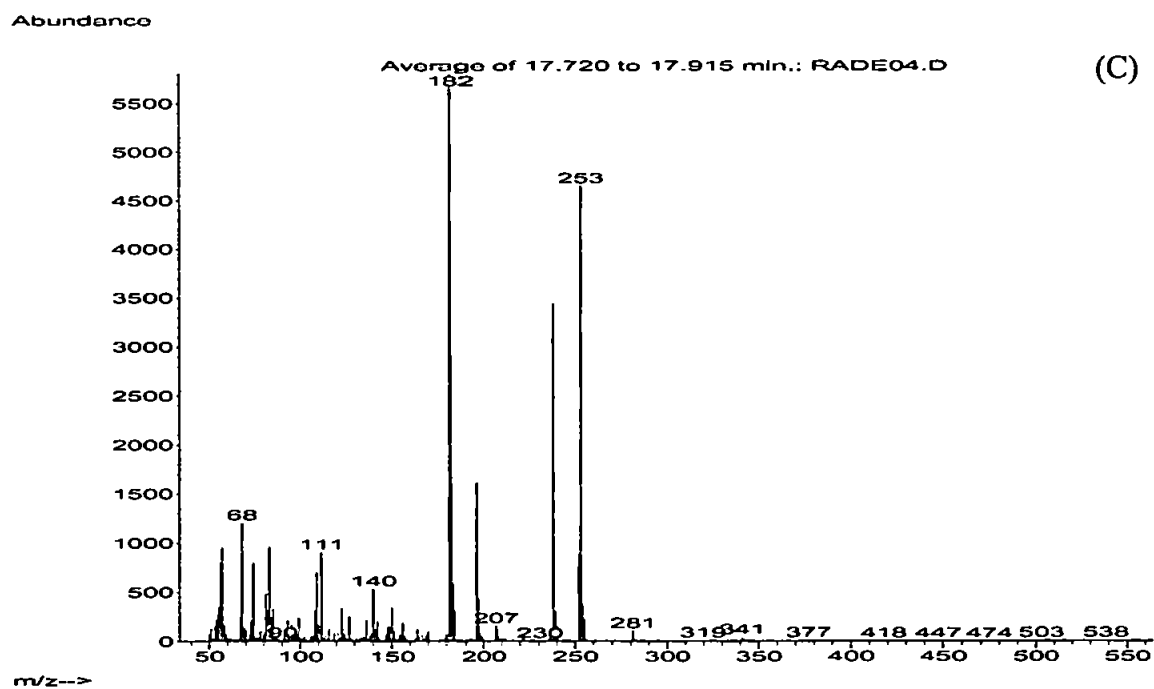
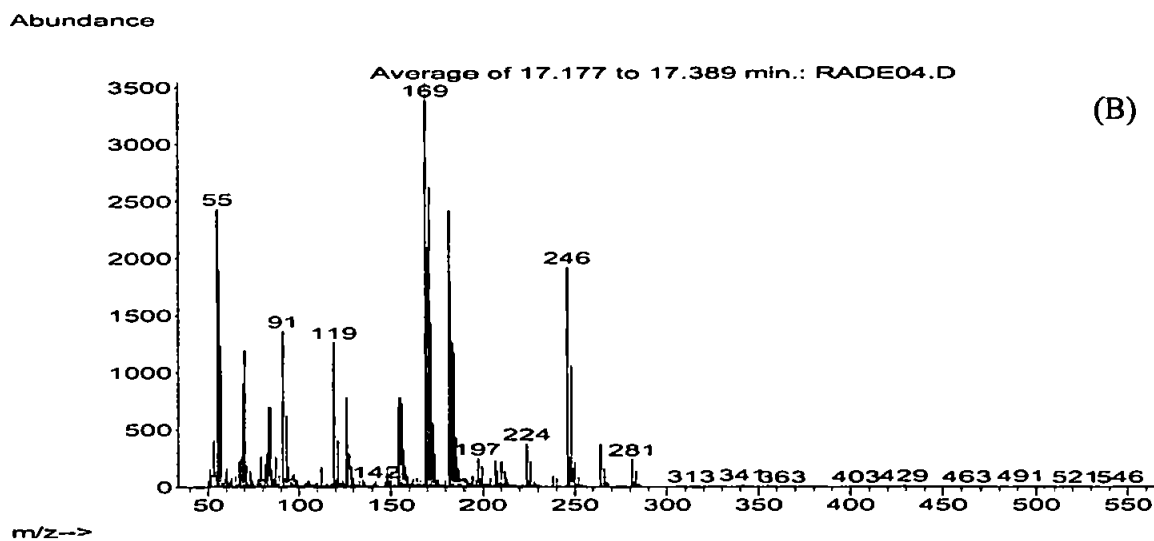
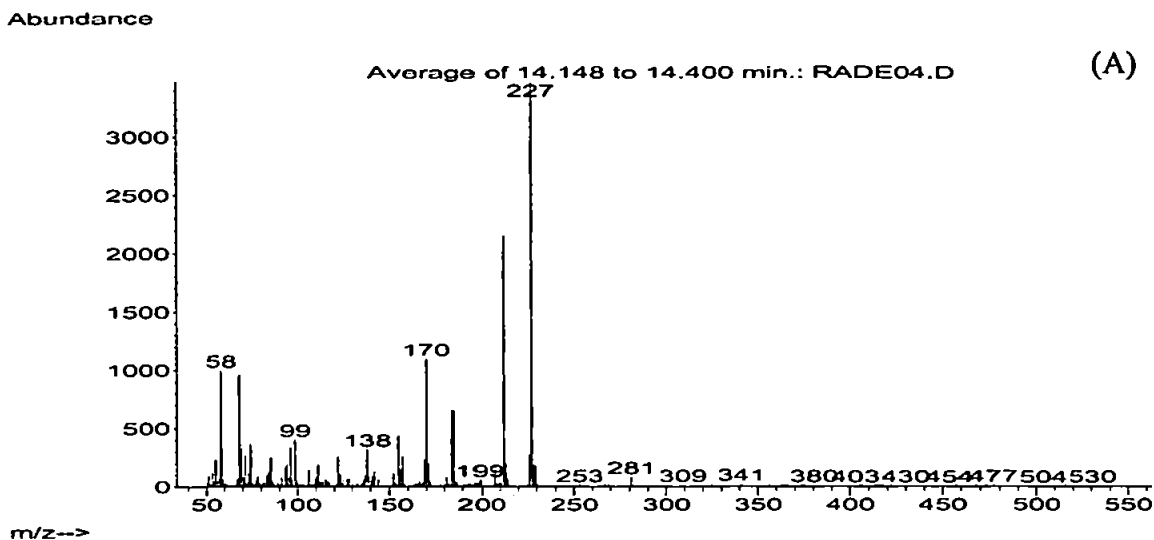


Figure 2.6. Examples of mass spectra of the internal standard ametryn (A), and the standards Sea-Nine 211[®] (B) and Irgarol 1051[®] (C) obtained by GC-MS.

controls, standards, and enzyme tracer solutions were mixed and incubated to allow recognition of diuron by antibodies. Plate wells were washed three times with the kit buffer solution and then the substrate solution (tetramethylbenzidine) was added producing a colour signal. The colour reaction was stopped after 25-30 min of incubation in the dark by adding defined amounts of sulphuric acid (2 M). The resulting colour was measured at 450 nm using an Anthos Labtec HT2 microplate reader (version 1.02). The standard curve was a linear regression of the logarithm of concentration against $\log_{it} B/B_0$, which is calculated from equation 6:

$$\log_{it} B/B_0 = \ln \left[\frac{(B/B_0)}{(100 - B/B_0)} \right] \quad \text{Eq. (6)}$$

where B/B_0 is the quotient obtained from the mean absorbance value of standard or sample and the zero standard.

Sample concentrations were determined by interpolation of their absorbance using the standard curve of 0, 0.03, 0.1, 0.3, 1.0 and 3.0 $\mu\text{g l}^{-1}$ diuron. Calibrations for all the kits used resulted in very similar standard curves ($R^2 = 0.98$; slope = -0.5401; y -axis interception = -5.916). A detection limit of 0.027 $\mu\text{g l}^{-1}$ was calculated as the average of 5 blank determinations minus 3 standard deviations. The standard curve for diuron was linear between 0.1 and 3 $\mu\text{g l}^{-1}$. The 50% B/B_0 (concentration required to inhibit one-half of the colour produced by the negative control) was at 0.25 $\mu\text{g l}^{-1}$. This method yielded a recovery of 80-110% and no matrix effects were determined (manufacturer's reference). Samples assumed to have higher concentrations than the highest standard were diluted to permit determination of more accurate results. Sample concentrations are given in $\mu\text{g l}^{-1}$ and were corrected for dilutions, when applied.

2.4.6. Zinc pyrithione

Zinc pyrithione is notoriously difficult to analyse (Thomas, 1999) and for this reason nominal concentrations have been used throughout.

2.4.7. Microscopic analyses

Phytoplankton samples were preserved with Lugol's iodine solution to a final concentration of 2%. Counting was carried out on settled (Utermöhl counting chambers) 100 ml samples using an inverted microscope at magnifications of 187 \times and 750 \times . Algal cells were identified to species level when possible, except for the small fragile cells,

such as nanoplanktonic flagellates, for which only genus or class was recorded. Carbon estimates for each species were derived from volume determinations according to Kovala and Larrance (1966) (see in UNESCO, 1974) and the cell volume:carbon relationships were obtained from Eppley *et al.* (1970) except for the ciliates whose conversion factors were derived from Beers *et al.* (1975).

2.4.8. Analytical Flow Cytometry (AFC)

2.4.8.1. Cell enumeration

A flow cytometer measures light scatter and fluorescence of particles passing a zone of laser light (monochromatic, with ultraviolet, visible or near infrared lines), carried and centred inside a high speed water jet. The cells are pumped in a single file through the analysis point generating the scattering and fluorescence signals which are detected by photomultiplier tubes or photodiodes. Signals are converted by the electronics interface and data are presented as distributions or multivariate scatterplots. Mixed cultures or field samples appear as several clusters, more or less separated, and represent groups with different optical properties (Dubelaar and Jonker, 2000).

Phytoplankton samples were enumerated and size classified using a Becton Dickinson FACSort™ flow cytometer as described in Readman *et al.* (2004). Samples were fixed with 1-2 % glutaraldehyde (final concentration; microscopy grade – Merck) (Vaulot *et al.*, 1989) for approximately 10 min, fast-frozen in liquid nitrogen and then stored at -80 °C in darkness to preserve their fluorescence (Jeffrey *et al.*, 1997). *In vivo* samples derived from the unialgal cultures were analysed immediately after sample collection and, therefore, did not require fixation.

The FACSort™ counted particles and measured chlorophyll fluorescence (>650 nm), phycoerythrin fluorescence (585 nm ± 21 nm) and side scatter (light scattered at 90° to the plane of a vertically polarised argon ion laser exciting at 488 nm). The optical alignment of the FACSort™ was checked for each run of samples using Coulter™ FlowSet™ calibration fluorospheres (3.6 µm diameter). Data acquisition was triggered on red fluorescence, using the optical characteristics of *Synechococcus* sp. to set rejection gates for background noise. Samples were analysed for three minutes at a flow rate of 100 µl min⁻¹. The flow rate was calibrated daily by weighing samples of Milli-Q water for three or four minutes at high flow rate at the beginning and end of the analysis of a batch of samples. Data were stored in listmode format and read using WinMDI (Windows Multiple Document Interface) flow cytometry analysis software (version 2.8,

created by Joseph Trotter, 1998) to produce scatter- plots of phycoerythrin versus chlorophyll fluorescence and side scatter versus chlorophyll fluorescence. *Synechococcus* sp. which contains phycoerythrin, was discriminated from the eukaryotic phytoplankton using the phycoerythrin *versus* chlorophyll fluorescence scatter plot. Cyanophytes (*e.g.* *Synechococcus* sp.) were enumerated by drawing a gate around the population and calculating the abundance using the WinMDI software. The same gate was used to exclude cyanophytes (*Synechococcus* sp.) from the scatter plot of side scatter versus chlorophyll fluorescence, enabling simple enumeration of the eukaryotic phytoplankton based on their side scatter and chlorophyll fluorescence characteristics. Cryptophytes were also discriminated by phycoerythrin properties, but as a component of the nanoplankton. Commercial flow cytometers can only measure cells up to 50 μm (Peperzak *et al.*, 2000), which allows microplankton to be viewed. However, accurate abundances were only discriminated for prokaryote and eukaryote picophytoplankton and eukaryote nanophytoplankton (< 20 μm) (Fig. 2.7).

The abundance N (cell ml^{-1}) for each population in a field sample was calculated from equation 7:

$$N = \frac{C}{(T \times R) \times CF \times 1000 \mu\text{l} . \text{ml}^{-1}} \quad \text{Eq. (7)}$$

where C is the number of events acquired (cells) for a specified population, T is the duration of analysis (min), R is the sample flow rate ($\mu\text{l min}^{-1}$), and CF is a correction factor to account for sample dilution owing to preservation or staining. The efficiency of counting was assured by a sample acquisition at a rate of below 1000 events s^{-1} for greatest accuracy.

2.4.8.2. Protocol for Fluorescein Diacetate (FDA) staining technique

Cell viability can be used as a quantitative parameter to assess the cytotoxicity of exogenous substances. This method compares intact viable, competent cells with dead cells by fluorescence analysis through detection of active cell metabolism using fluorescein diacetate (FDA). FDA is a non-polar, non-fluorescent substance which can pass through the cell membrane whereupon non-specific intracellular esterases (*eg.* lipase and acylase but not acetylcholinesterase) break the FDA molecule producing the highly fluorescing fluorescein and two acetate molecules (Fig. 2.8). The highly polar fluorescein will accumulate in cells which possess intact membranes so the green

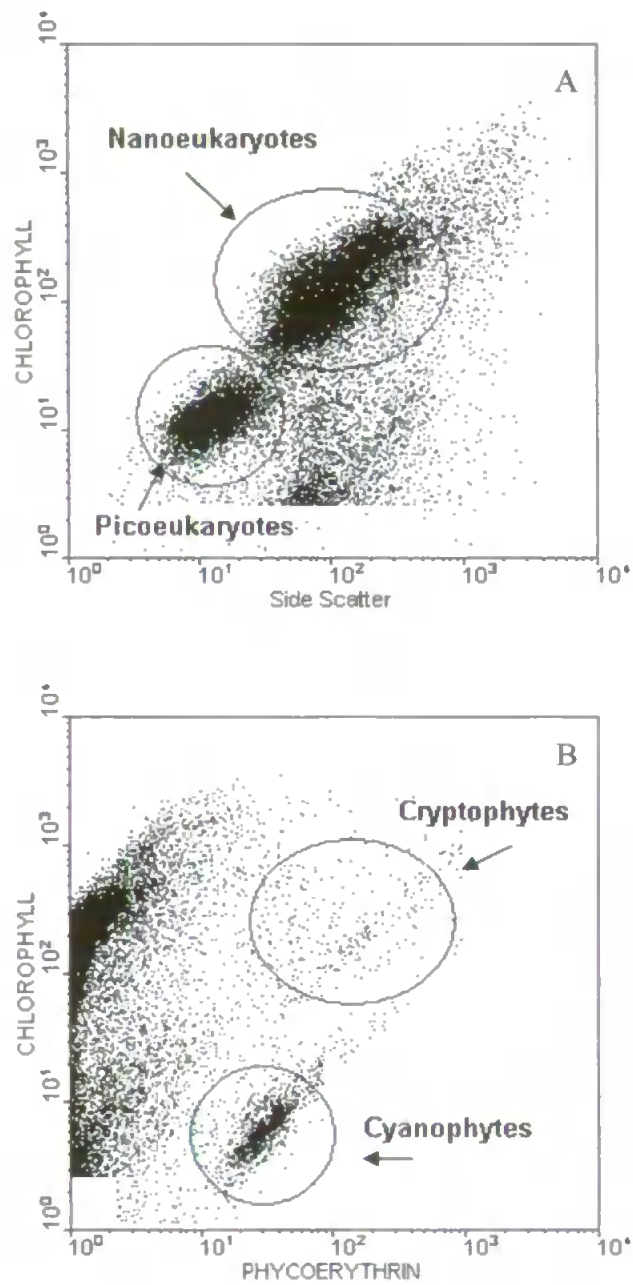


Figure 2.7. Bivariate scatter-plots (AFC) of chlorophyll fluorescence versus side-angle light scatter and phycoerythrin showing phytoplankton separation for (A) nanoeukaryotes and picoeukaryotes and (B) cryptophytes and cyanophytes.

fluorescence can be used as a marker of cell viability. Cells which do not possess an intact cell membrane or an active metabolism may not accumulate the fluorescent product and, therefore, do not exhibit green fluorescence (Jochem, 2000). FDA stained cells fluoresce at a higher intensity than the unstained or formaldehyde-treated cells, in which esterases are inactivated.

Cell metabolic activity of *E. huxleyi* cultures was measured using FDA-staining protocol for fluorescein diacetate based on Jochem (1999). The optimal FDA incubation time and concentration for *E. huxleyi* were determined by manipulating the FDA incubation time and working solution concentrations. Distinctions between live and dead cells were confirmed by analyzing samples containing untreated cells and fixative-treated cells (formaldehyde plus hexamine solution; 2% v/v). Therefore, unstained and FDA-stained deactivated (formaldehyde fixed) cells were included as negative controls. The fluorescein fluorescence was also tested for different concentrations of live cells and compared to the same concentration of dead cells.

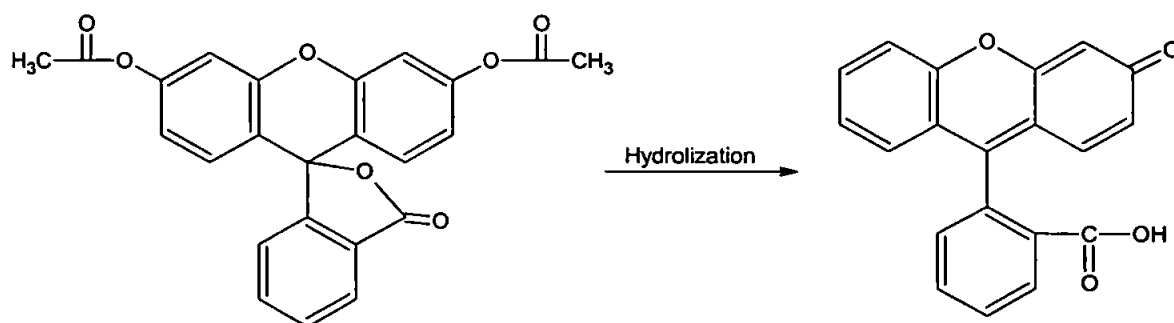


Figure 2.8. Chemical structure of fluorescein diacetate (FDA) (left) and its hydrolyzation by esterases generating fluorescein molecule (right) and acetic acid.

Initial FDA ($C_{24}H_{11}O_7$) stock solutions were prepared by dissolving 50 mg FDA (Sigma Chemicals F-7378) in reagent grade DMSO to 20 ml, giving a concentration of 2.5 mg ml^{-1} . The FDA was completely dissolved and the stock solution stored at $4 \text{ }^\circ\text{C}$ (DMSO freezes at $18 \text{ }^\circ\text{C}$). The stock solution was thawed and working solutions were prepared by diluting aliquots of the FDA stock solution to 50 ml of Milli-Q water, resulting in 20-fold ($WS1 = 125 \text{ } \mu\text{g ml}^{-1}$) and 50-fold ($WS2 = 50 \text{ } \mu\text{g ml}^{-1}$) dilutions. Due

to the slightly low FDA solubility in water (tends to flocculate at $> 1 \mu\text{g ml}^{-1}$), working solutions were prepared with ice-cold water and mixed quickly (Jochem, 1999). Thus, flocculation was prevented, even though working solutions appeared slightly opaque. The working solutions were kept on ice to minimize FDA degradation (Jochem 1999) and were discarded after every 45 min approximately and fresh ones prepared. Aliquots of 20, 70, and 400 μl from WS2 and 320 μl from WS1 were added to 2 ml samples containing identical cell densities of *E. huxleyi* resulting in final FDA concentrations of 0.5, 1.75, 10, and 20 $\mu\text{g ml}^{-1}$ in the samples. Analyses were performed in a Becton Dickinson FACSort™ flow cytometer as described in section 2.4.8.1 for cell enumeration. Green fluorescein fluorescence (absorption maximum at 494 nm; emission maximum at 518 nm) was measured on a log scale. The instrument settings were saved and used in subsequent experiments.

Samples (dead and live cells) were analyzed for 26 min in medium flow rate ($\sim 33.3 \mu\text{l min}^{-1}$) and scatter plots of green fluorescence against time were produced to determine the FDA incubation time for every concentration of FDA tested. Cells were analysed according to size (side scatter) and chlorophyll-*a* fluorescence to prevent interference from cell fragments, bacteria and dust particles. Data were collected and displayed in one-dimensional histograms of green fluorescence. Dead cells were excluded from the analyses by gating on green fluorescence positioned to the left of the distribution of healthy control cells.

2.4.8.3. Determination of viable cells (FDA staining technique)

Cell metabolic activity was measured as the rate of fluorescein production following incubation in FDA and expressed as the FDA conversion rate with units of fluorescence $\text{cell}^{-1} \text{min}^{-1}$. A 70 μl volume of FDA working solution (4.2 μM) was added to 2 ml culture samples and incubated at room temperature in the dark for 20 min. Samples were analysed in the flow cytometer for 3 min. All FDA fluorescence measurements were taken using the same settings, so that FDA fluorescence readings are comparable between experiments. Negative controls (*i.e.*, formaldehyde-treated cells and unstained cells) were included in each experiment. Frequency histograms of green fluorescence were generated to measure viable cells falling into M1 (*i.e.*, metabolic activity state) and compared with stained control cells. The M2 region corresponded to non-viable cells, defined by formaldehyde-treated cells, whilst M3 was an intermediate state (Fig. 2.9).

The percentage of cells in M1 relative to controls (%M1) was of primary importance in this study as it indicated that the water sample exerted a toxic effect.

Finally, mean cell metabolic activity was compared with photosynthetic capacity measured with a FRRF fluorometer. The number of cells in the activity state (M1) was defined according to the frequency distribution of fluorescence for individual cells.

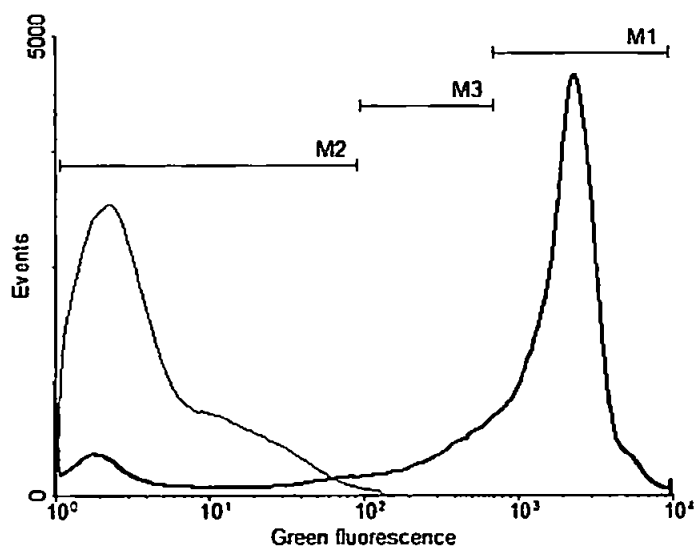


Figure 2.9. Frequency histograms comparing FDA accumulation in dead (thin line) and live cells (thick line). Esterase activity states are defined as normal (M1), low (M2), and intermediate (M3) activities.

2.4.9. Analysis of dissolved nutrients

Seawater samples were filtered on 0.45 μm Millipore MFTM - membrane filters (nitrocellulose), previously soaked overnight in HCl 10%, and sequentially rinsed with Milli-Q water and water sample. Filtered samples (70 ml) were stored in Nalgene translucent high-density polyethylene bottles and were frozen (-20°C) until analyses. The segmented flow autoanalyser system used at the Plymouth Marine Laboratory is a Technicon AAll system, an *in-house* constructed system which allows flexibility in the choice of analytical techniques.

The analytical methodology for phosphate determination was based on Kirkwood (1989) and involves the production of the phosphor-molybdenum-blue complex by reaction with molybdate and ascorbic acid, and a catalyst of potassium antimony tartrate (Woodward, 1994). Nitrate was measured based on Brewer and Riley (1965) and

modified for increased sensitivity (Woodward, 1994). Nitrite was detected by the Grasshoff (1976) method. A copper/cadmium column is used to reduce nitrate to nitrite. Nitrite ions react with an acidic sulphanilamide solution to form a diazo compound, which reacts with N-1-naphthylethylenediamine dihydrochloride, to form a reddish purple azo dye. The concentration of nitrate is obtained by subtracting the nitrite concentration from the nitrate and nitrite combined concentration.

2.4.10. Suspended Particulate Matter (SPM), Carbon and Nitrogen analyses

Measured volumes of seawater samples were filtered through a GF/C Whatman filter that was previously combusted (500 °C for 3 h) and weighed. After washing with ultra-pure water (Milli-Q system), filters were dried at approximately 35 °C and stored in a desiccator. Dried filters were reweighed to provide the weight of the suspended particulate matter (SPM) by difference, then divided by the volume of filtered seawater and expressed as mg l⁻¹. Filters were cut into two sub-circles of known diameter. One sub-circle was placed overnight in a desiccator under a sulphur dioxide atmosphere in order to eliminate the inorganic carbon. The other sub-circle did not require further treatment and was used for total particulate carbon determination (inorganic plus organic carbon).

Samples for particulate nitrogen, particulate organic carbon and total particulate carbon were then weighed into tin foil boats, previously cleaned with chloroform, acetone and ultra-pure water. Procedure blanks (tin foil boats), pre-weighed Acetiniide OAS standards (Elemental Microanalysis Ltd, UK), pre-weighed marine reference sediment material (NRC-CNRC, Canada) and samples were analysed using a Carlo-Elba CHN Elemental Analyser operated according to the manufacturer instructions.

Chapter 3

Testing the phytoplankton response to Irgarol 1051®

This chapter describes the use of selected parameters as ecotoxicological indicators of stress imposed by exposure of microalgae to a single antifouling compound, Irgarol 1051®. The effects of Irgarol 1051® on single algal cultures and phytoplankton composition within natural phytoplankton community are evaluated. Since toxicants directly affect cells, the measurement of individual cells is desirable. In the section 3.1, the impact of Irgarol 1051® on a representative of a sensitive phytoplankton group (*Emiliania huxleyi*; Prymnesiophyceae) was measured using rapid and simple techniques. Fluorescein diacetate (FDA) staining was used to assess cell viability using analytical flow cytometry and photosynthetic efficiency was investigated using fast repetition rate fluorescence (FRRF). In section 3.2, a natural phytoplankton population was exposed to Irgarol 1051® and algal composition responses were measured using flow cytometry and pigment composition. These latter studies generated a manuscript that was published in *Marine Environmental Research* (Readman *et al.*, 2004).

3.1. The use of FDA and flow cytometry to assess cell viability as an indicator of Irgarol 1051® exposure

3.1.1. Introduction

Antifouling biocide exposures of phytoplankton can change the cellular metabolic activity as a result of induced stress. Metabolic activity of phytoplankton is often assessed by use of parameters associated with photosynthesis such as adenosine triphosphate (ATP) formation, ¹⁴C assimilation, oxygen evolution and fluorometry. There are, however, stains used to assess microbial viability and activity, which are suitable for use with phytoplankton (Dorsey *et al.*, 1989). Enzyme inhibition measurements in microalgae (*e.g.*, peroxidases, β -galactosidases, esterases) are becoming increasingly popular indicators of environmental stress because they offer a rapid and sensitive endpoint (Blaise and Menard, 1998).

Fluorescein diacetate (FDA) is a suitable metabolic probe because it is readily absorbed by cells and metabolised by esterases (*i.e.*, enzymes involved in phospholipids turnover). The resultant conversion to fluorescein has been used as a measure of esterase activity, indicating cell viability under pollution stress, *e.g.* in the freshwater microalga *Selenastrum* (Arsenault *et al.*, 1993; Gala and Giesy, 1994; Blaise and Menard, 1998; Franklin *et al.*, 2001a, 2001b), *Chlamydomonas eugametos* (Franqueira *et al.*, 2000), *Chlorella* sp. (Franklin *et al.*, 2001a, 2001b) and in the marine microalgae *Phaeodactylum tricornutum* (Franqueira *et al.*, 2000; Franklin *et al.*, 2001a, 2001b), *Dunaliella tertiolecta* (Franklin *et al.*, 2001a, 2001b), and *Entomoneis punctulata*, *Nitzschia paleacea*, *Tetraselmis* sp. (Franklin *et al.*, 2001b). The use of this technique needs to be tested for suitability for each microalgal species and toxicant studied, since responses of different microalgal species or toxicants could vary. For instance, the ability of microalgae to accumulate fluorescein under exposure to copper caused a shift to either a lower or higher esterase activity level, depending on the copper concentration and duration of exposure (Arsenault *et al.*, 1993). Therefore, enzyme activity could be used as an alternative endpoint to detect chemical toxicity in acute and chronic tests. As an indicator of toxic effects on the activity of esterases in the cell, FDA fluorescence can easily distinguish dead from live, viable cells, thus determining inhibition of the cell growth.

The aim of this research was to apply and test the suitability of a staining technique to rapidly assess the metabolic activity of microalgal cells in cultures of the prymnesiophyte *Emiliana huxleyi* following exposure to the antifouling biocide Irgarol 1051®. Results are then compared with other endpoints such as *in vivo* chlorophyll-*a* fluorescence.

3.1.2. Methodology

3.1.2.1. Algal culture

The prymnesiophyte *Emiliana huxleyi* (strain 96A) was obtained from the Plymouth Culture Collection, UK. Non-axenic cultures were kept in a controlled temperature room and, before the experiment, were maintained under the test conditions for at least one growth cycle to ensure cell acclimatization. The cultures were maintained in f/2 culture medium (Guillard, 1975), slightly modified by omitting silicate and Trizma, and prepared with filtered (0.45 µm) offshore seawater. Salinity and initial pH

were 35 PSU and 8.3, respectively, and were measured using a WTW Multiline P4 pH-meter/salinometer. Sterile techniques were used for all culture work in an attempt to minimize bacterial growth.

3.1.2.2. Algal toxicity testing

The prymnesiophyte *Emiliana huxleyi* was exposed to nominal concentrations of 40, 80, 150, 250, and 500 ng l⁻¹ Irgarol 1051®. A working solution of Irgarol 1051® was prepared by diluting 25 µl of stock solution (1 µg l⁻¹; dissolved in methanol) into 50 ml of sterile seawater. Experiments were conducted in 500 ml borosilicate Erlenmeyer flasks containing 400 ml of culture medium spiked with aliquots of the biocide working solutions, in triplicate. Exponentially growing cells were inoculated into the medium giving a final cell concentration of approximately 0.5×10⁴ cells ml⁻¹. The controls consisted of cells without Irgarol 1051® and the carrier controls consisted of cells incubated with methanol (at the same concentration present in the Irgarol 1051® treated flasks). Final concentrations of methanol for each treatment did not exceed 0.00005% (v/v). *E. huxleyi* was grown on a 12:12 light:dark cycle at 15.5 ± 2.5 °C under an average irradiance of 174 µmol photons m⁻² s⁻¹ photosynthetic active radiation (PAR), provided by cool white light bulbs (Sylvania; 70W). The air around the culture flasks was ventilated with a fan, which ensured an even temperature distribution even close to the light sources. Static culture conditions were maintained throughout the tests. Esterase activity was measured daily, using the FDA staining method. The experiment was terminated after 72 h of incubation.

3.1.3. Results and Discussion

3.1.3.1. FDA protocol optimization

For optimization and standardization of the FDA staining protocol, accumulation of fluorescein was followed continuously for 26 min after FDA addition in pre-tests (Fig. 3.1). Amongst the concentrations of FDA tested, 4.2 µM was the most appropriate, giving a clear separation between dead and live cells and the highest fluorescence (Fig. 3.2). After addition, FDA readily penetrated into the cells, and green fluorescence increased for 8 min. Thereafter, cellular fluorescence remained stable until

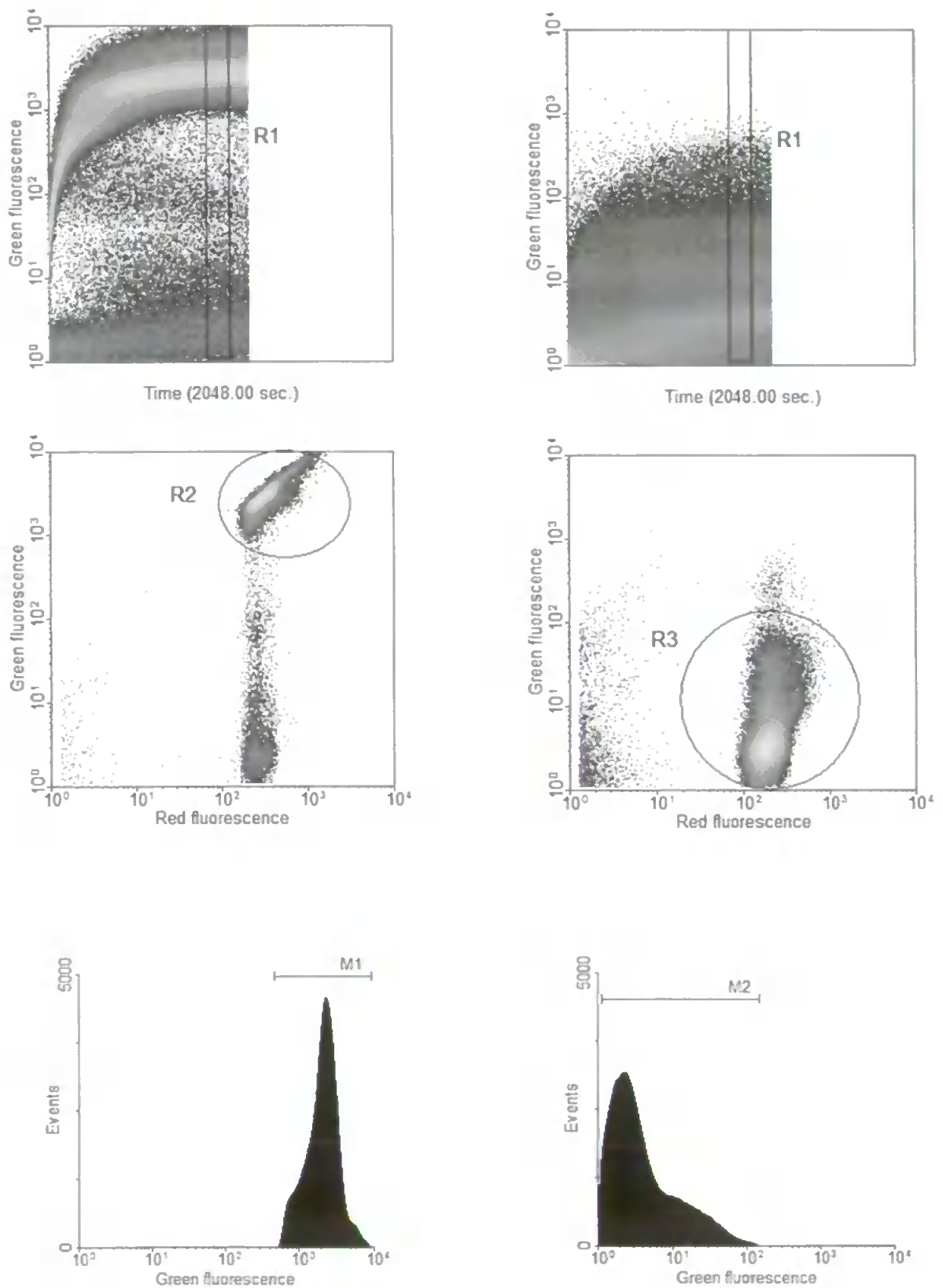


Figure 3.1. Analysis of fluorescence (relative units) accumulation upon FDA addition in *Emiliana huxleyi* as revealed by flow cytometry. Diagrams show FDA fluorescence in live cells (on the left) and dead cells (on the right).

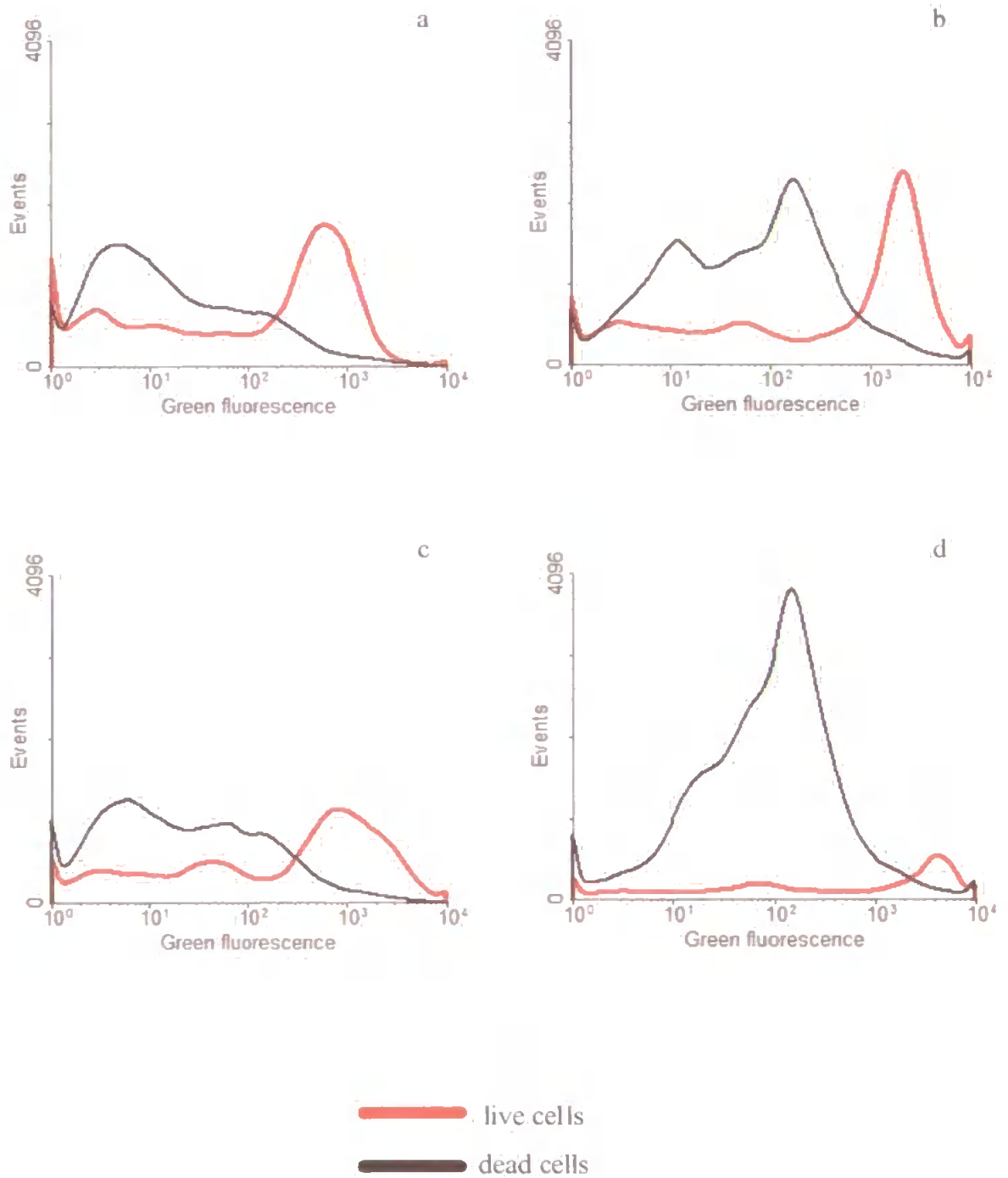


Figure 3.2. Optimization protocol for different concentrations of FDA added to *Emiliana huxleyi* cells: a) 1.2 μM , b) 4.2 μM , c) 24.0 μM , and d) 48.0 μM .

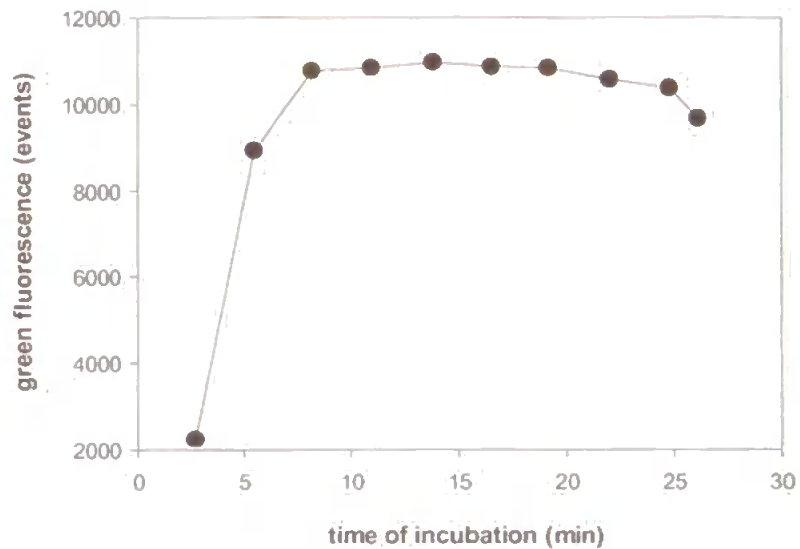


Figure 3.3. Fluorescence (relative units) accumulation under increasing incubation times of samples of *Emiliania huxleyi* after 70 μ l of FDA (WS2) addition.

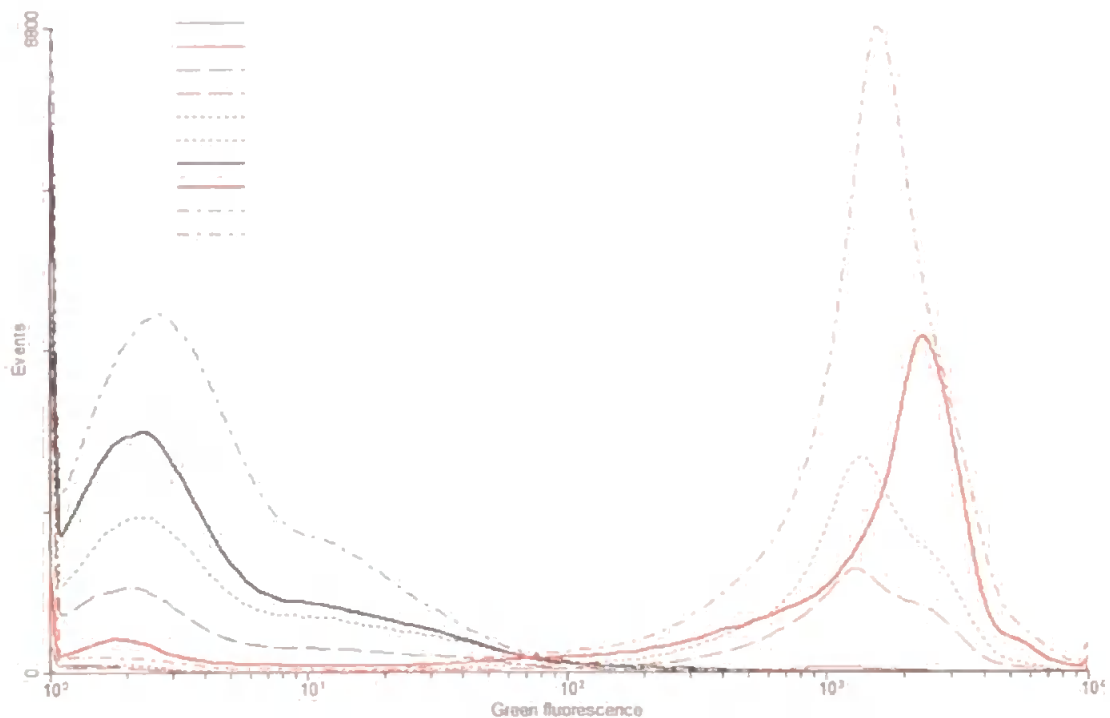


Figure 3.4. Fluorescence (relative units) accumulation upon 70 μ l FDA (WS2) addition to different cell concentrations of *Emiliania huxleyi*. Time of incubation = 20 min. Cell concentration 1 = 1.64×10^4 ; 2 = 27.2×10^4 ; 3 = 53.4×10^4 ; 4 = 75.7×10^4 ; and 5 = 132.4×10^4 cell ml^{-1} .

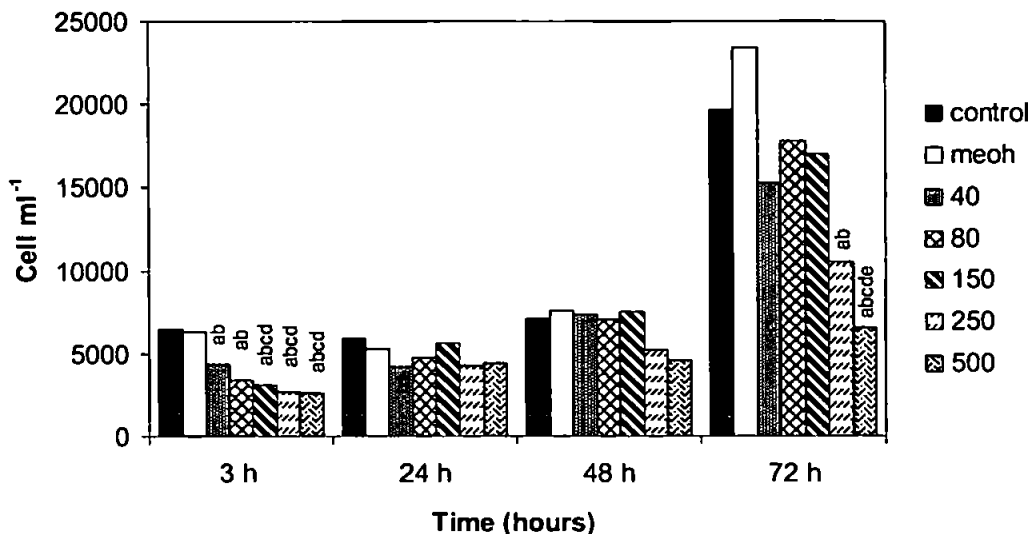
approximately 20 min after FDA addition, and eventually leakage of fluorescein out of the cells began to reduce the cellular fluorescence (Fig. 3.3). For the subsequent experiments, FDA incubation time was set at exactly 20 min after FDA addition. This timing gave a good compromise of reasonably low variation in fluorescence readings and high fluorescence yields from FDA cleavage. Hence, cells with fluorescence readings at M1 (see section 2.4.8.3) were considered FDA positive, viable cells and, when compared to the controls, were of primary importance in this study to indicate reductions in viable cells following exposure to Irgarol 1051® (Fig. 3.1). The number of events with FDA fluorescence increased with increasing cell concentrations and saturation of cell numbers was not observed under sample incubation with 70 µl FDA (Working Solution 2 – WS2) for the cell concentrations tested (Fig. 3.4).

According to the results given, the FDA staining protocol was validated for the marine alga *E. huxleyi*, so that dead cells could be easily distinguished from live, viable cells, and therefore used to determine inhibition of cell numbers. FDA fluorescence is an indicator of toxicant effects on the activity of esterases in the cell and is demonstrated to be an alternative and sensitive endpoint to detect toxicity of the PSII inhibitor Irgarol 1051®.

3.1.3.2. Algal toxicity testing

Results obtained by exposing cells of *Emiliania huxleyi* to different levels of Irgarol 1051® indicate that concentrations as low as 40 ng l⁻¹ can affect the number of viable cells (as measured by FDA fluorescence) and photosynthetic parameters (*in vivo* fluorescence) during the selected exposure time. Cell numbers were significantly reduced with increasing toxicant concentrations at 3 h and 72 h of experiment ($p < 0.05$) (Fig. 3.5A). Irgarol 1051® concentrations of 155 and 222 ng l⁻¹ reduced cell numbers by 50% following 3 h and 72 h exposure, respectively (Fig. 3.5B). Viable cells, as measured by FDA fluorescence, were significantly reduced from low to high concentrations ($p < 0.05$) (Fig. 3.6). After 3 h, concentrations of 40 ng l⁻¹ reduced viable cells by 42% and 500 ng l⁻¹ Irgarol 1051® reduced by approximately 90%, compared to the carrier controls. After 72 h exposure, concentrations of 250 ng l⁻¹ or higher completely reduced the number of viable cells. By using the equations given in Figure 3.6, calculated reductions in 50% of viable cells were observed over 78 and 71 ng l⁻¹ Irgarol 1051® after 3 h and 72 h, respectively.

(A)



(B)

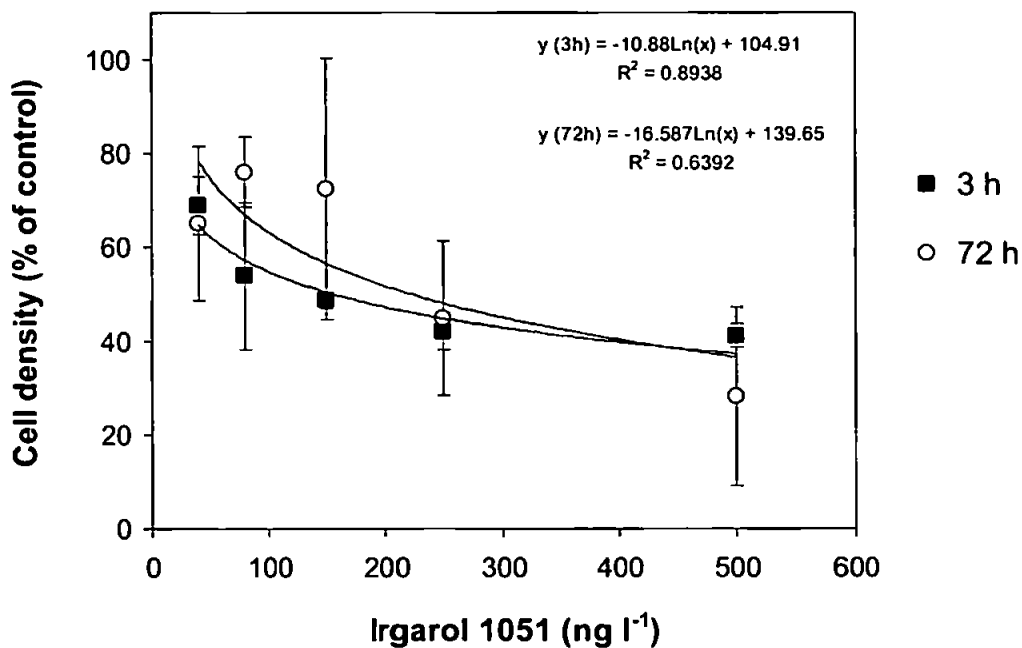


Figure 3.5. Effects of different concentrations of Irgarol 1051[®] (ng l⁻¹) on cell density expressed as (A) cell ml⁻¹ and (B) % of control of *E. huxleyi* following exposure of 72 h. Letters designate statistically significant differences amongst (a) control, (b) MEOH, (c) 40 ng l⁻¹, (d) 80 ng l⁻¹, (e) 150 ng l⁻¹ using ANOVA one-way followed by LSD *post hoc* test ($\alpha = 0.05$). 3 h ($p < 0.0001$); 24 h ($p = 0.4133$); 48 h ($p = 0.3173$); 72 h ($p = 0.1268$). $n = 3$.

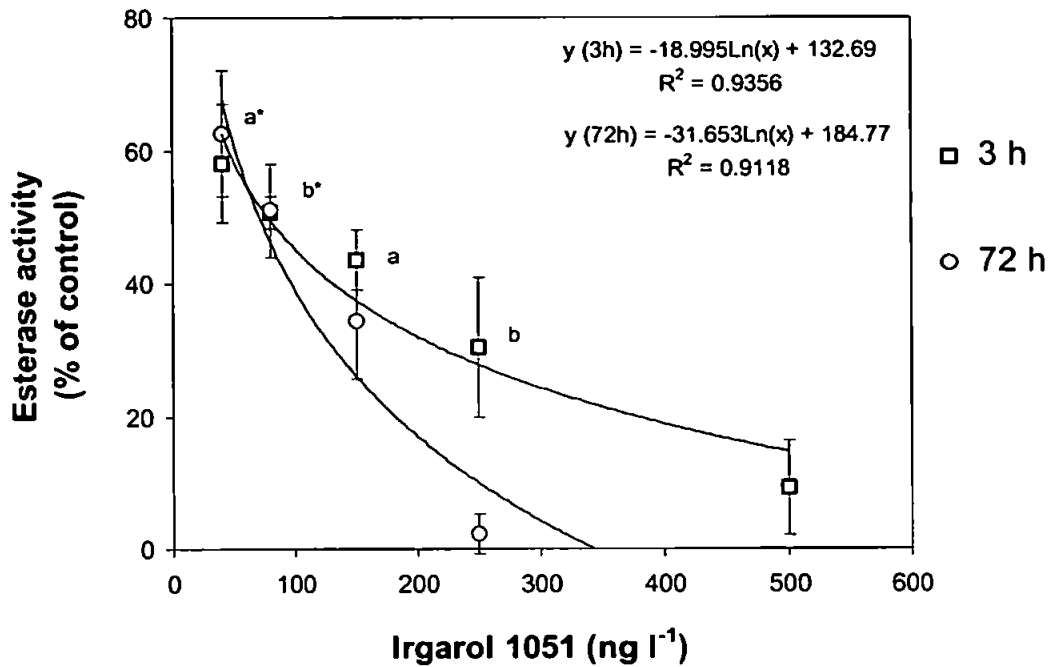


Figure 3.6. Esterase activity (FDA fluorescence) of *Emiliana huxleyi* exposed to nominal concentrations of 40, 80, 150, 250 and 500 ng l⁻¹ of Irgarol 1051[®] for 72 hours. ANOVA one-way followed by LSD *post hoc* test. Letters designate non-significant differences from 80 ng l⁻¹ (a) and from 150 ng l⁻¹ (b) at 3 h. All other treatments are significantly different from each other ($p < 0.05$). $n = 3$. *72 h time exposure

The sensitivity of FDA fluorescence measurements was about four times greater than that for growth (as indicated by cell numbers) following 3 h exposures to Irgarol 1051[®]. Also, exposure time appeared to have influenced growth (cell numbers) more than FDA fluorescence. Reductions in cell numbers following Irgarol 1051[®] exposure were more pronounced in the short (3 h) rather than the long (72 h) exposures, possibly relating to cell recovery. Reductions in FDA fluorescence, however, were similar at both exposure times (3 h and 72 h) for the lowest toxicant concentration.

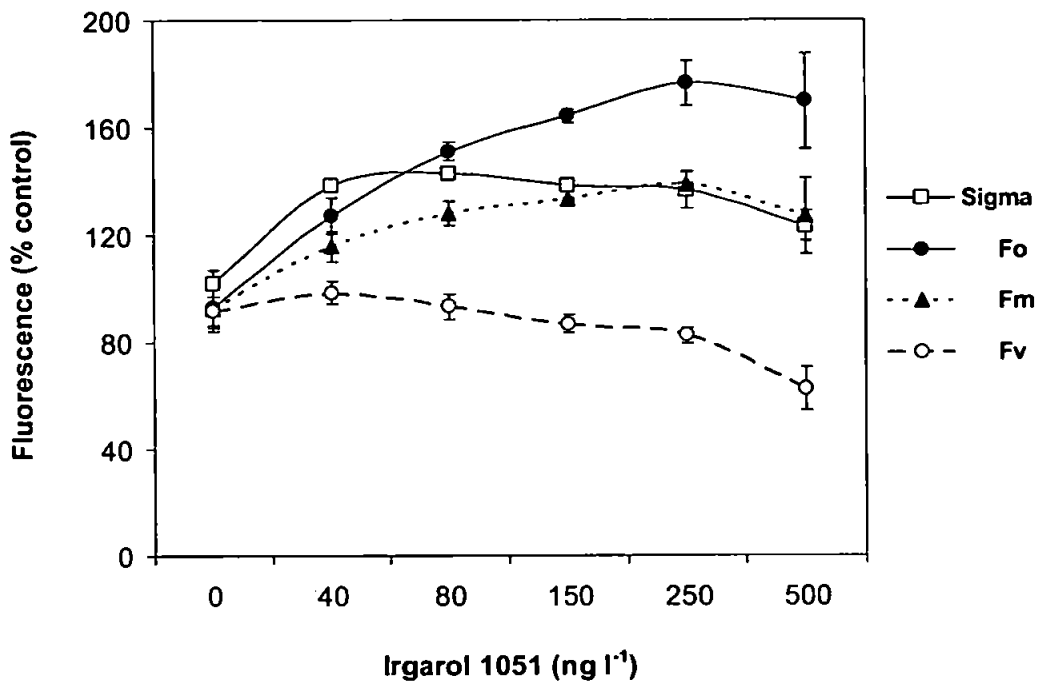
In addition to high sensitivity observed in this study, the measure of the esterase activity using FDA as a fluorogenic probe gives the technique a rapid measure of phytoplankton activity (Regel *et al.*, 2002). The degree of fluorescence depends on the physical and metabolic state of the cell and has proved a reliable indicator of the toxic effects of pollutants (Bentley-Mowat, 1982), including Irgarol 1051[®]. Such probes can also demonstrate differences in response among different species, enhancing our understanding on how biodiversity is sustained on a cellular level (Jochem, 2000).

Other studies have also demonstrated the use of flow cytometry to detect toxicity in freshwater and marine microalgae, e.g. following exposure to copper and the herbicide paraquat (Franklin *et al.*, 2001a; Franqueira *et al.*, 2000). Numerous probes have also been developed for environmental monitoring of water quality using flow cytometry (Jochem, 2000). The application of FDA as described in this study is a relatively recent technique and its fluorescence reflects the activity of esterases and cell membrane integrity (Berglund and Eversman, 1988), both of which indicate cell viability (Blaise and Ménard, 1998). The use of FDA for detecting the viability of marine phytoplankton in pollution studies was first reported using fluorescence microscopy (Bentley-Mowat, 1982). Later, detection of the fluorescein fluorescence by flow cytometry was applied to assess microalgal toxicity of heavy metals (Arsenault *et al.*, 1993; Franklin *et al.*, 2001a; Regel *et al.*, 2002), and pesticides and herbicides (Gilbert *et al.*, 1992). Whereas reduced esterase activity in terms of FDA fluorescence accumulation in *Selenastrum capricornutum* has been documented for high ($450 \mu\text{g l}^{-1}$) concentrations of copper, lower concentrations can actually induce an increase in esterase activity (Arsenault *et al.*, 1993).

In the present study, *in vivo* fluorescence, as measured by FRRF, was also assessed during the exposure period. Parameters measured were F_0 , F_M , F_V , Sigma (or σ_{PSII} , *i.e.*, functional absorption cross section of PSII under dark-adapted conditions) and F_V/F_M (Fig. 3.7; Fig. 3.8). Results showed that, compared to the controls, percentage values of F_M , F_0 and σ_{PSII} tended to increase significantly with increasing concentrations of Irgarol 1051® following 6 h of exposure (Fig. 3.7A). Following 72 h of exposure, the parameters measured are shown to decrease ($p < 0.01$; LSD *post hoc* test) (Fig. 3.7B). During the time period from 6 h to 72 h of Irgarol 1051® exposure, F_V/F_M was significantly reduced ($p < 0.01$; LSD *post hoc* test) at all concentrations tested, when compared to the controls (Fig. 3.8). Although a significant inhibition in photosynthetic efficiency (F_V/F_M) was noticed at earlier hours of incubation (6 and 24 h), longer Irgarol 1051® exposure times (48 and 72 h) affected F_V/F_M most.

Results for this toxicity test showed that the presence of the carrier control (methanol) did not affect the fluorescence parameters ($p > 0.01$). The pH drift detected was less than 0.3 over the 72 hours, which is within test-acceptability limits (± 1 pH units). Acceptable limits for growth for determination of EC_{50} were not satisfied, since the cell density in the controls did not increase by factor of 16 in 72 h (Lewis, 1995).

(A)



(B)

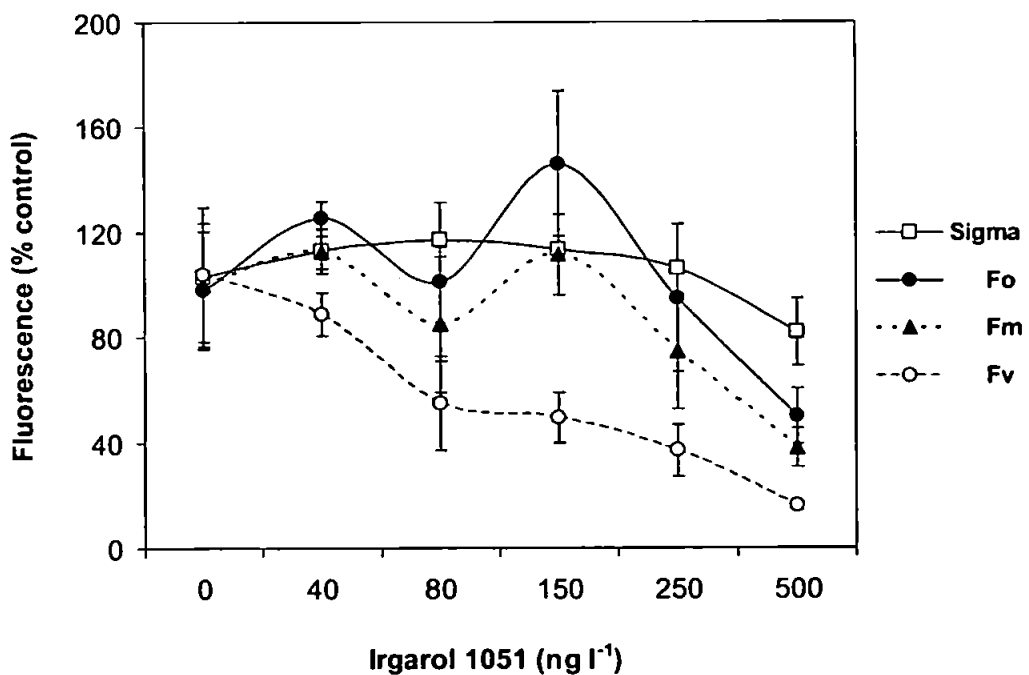


Figure 3.7. Effects of Irgarol 1051[®] concentrations on the chlorophyll fluorescence parameters: F_o, F_v, F_m and Sigma (σ_{PSII}) of *E. huxleyi* following exposure for (A) 6 h and (B) 72 h. Bars are \pm standard deviation of mean values (n = 3).

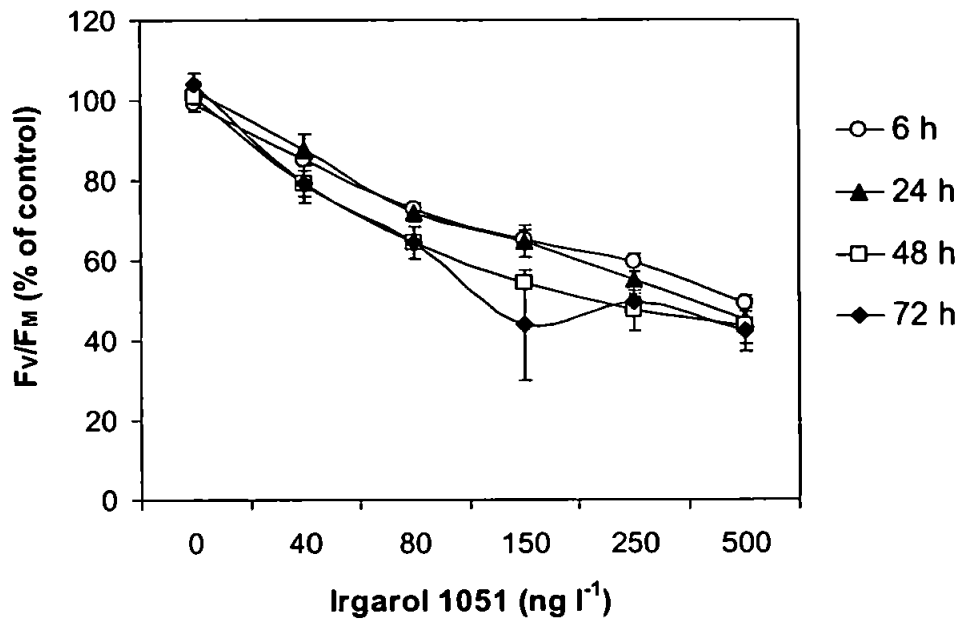


Figure 3.8. Photosynthetic efficiency (F_v/F_M) expressed as percentage of the control of *E. huxleyi* exposed to nominal concentrations of 40, 80, 150, 250 and 500 ng l⁻¹ of Irgarol 1051[®] for 72 hours. n = 3.

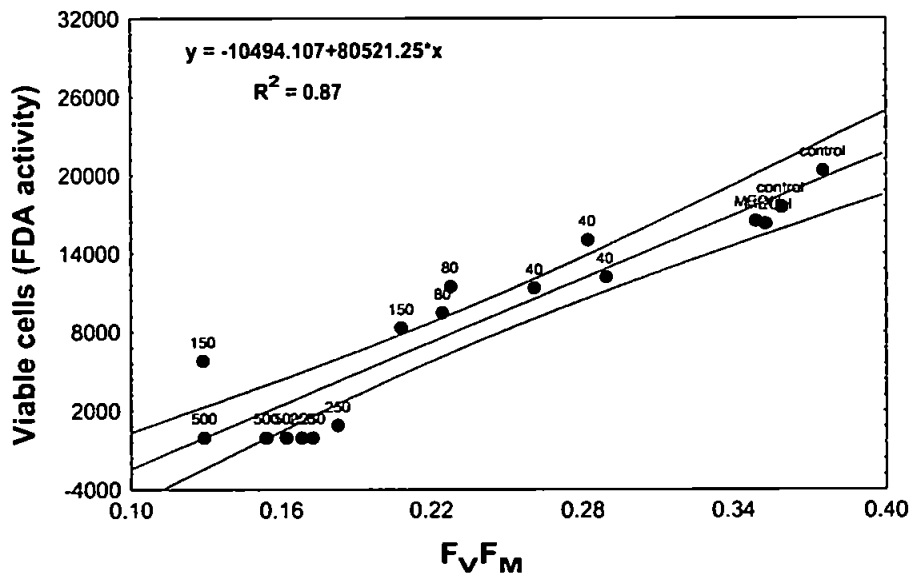


Figure 3.9. Linear regression fitting between viable cells (FDA activity) and F_v/F_M at 72 h of exposure to 40, 80, 150, 250 and 500 ng l⁻¹ of Irgarol 1051[®], including carrier controls (MEOH) and controls. n = 17.

However, comparisons between the selected parameters to evaluate sensitivity of responses are still valid.

The detection of FDA activity following Irgarol 1051® exposure was supported by *in vivo* chlorophyll fluorescence measurements. A good correlation between viable cells (FDA activity) and photosynthetic efficiency (F_V/F_M) was observed following 72 h exposures ($R^2 = 0.87$; $p < 0.0001$). This indicates that *E. huxleyi* responded similarly for both parameters at this time (Fig. 3.9). The rate of FDA conversion to fluorescein is correlated with photosynthetic capacity in many marine microalgal species (Dorsey *et al.*, 1989), validating the use of this assay in the assessment of metabolic activity in cells exposed to PSII inhibitors.

3.1.4. Conclusions

The combined use of metabolic probes, such as FDA, with the analytical speed and flexibility of flow cytometry enable rapid tests of algal responses to toxic substances in water. As with FDA activity measurements, fluorescence kinetics measurements also permit rapid examination of toxic effects at an early stage, soon after exposing test organisms to a toxic compound. In particular, the F_V/F_M ratio, which has been used extensively to detect toxic impairment in algae, provides a reliable assessment of photosynthetic efficiency in phytoplankton.

3.2. Flow cytometry and pigment analyses as tools to investigate the toxicity of Irgarol 1051® to natural phytoplankton communities⁵

3.2.1. Introduction

Flow cytometry affords a rapid and precise method to quantify and characterise phytoplankton within natural populations (Carr *et al.*, 1996). Chemotaxonomic assessments through high performance liquid chromatographic analyses offer a complementary technique to characterise phytoplanktonic communities (Jeffrey *et al.*, 1997). Although increasingly applied in oceanographic research, negligible data is available relating to the application of either technique in toxicological assessment of

⁵ An article of this section has been published in *Marine Environmental Research*.

natural phytoplankton populations. In this section, a report on the combined use of both techniques to monitor toxicological effects of Irgarol 1051® is presented.

3.2.2. Methodology

Bulk (40 litres) near shore (3 km) sub-surface sea water samples were taken and filtered through a 63 µm sieve to remove zooplankton and minimise grazing of the phytoplankton. Following thorough mixing, sub-samples were decanted into 2 L clear glass Winchester. Sub-samples were removed for flow cytometric analyses to demonstrate homogeneity. Samples were also analysed for Irgarol 1051® to confirm lack of contamination. The vessels were then spiked with Irgarol 1051® (in methanol) to provide concentrations ranging from 100 to 2000 ng l⁻¹ (adding the same quantity of methanol to each vessel, including controls). Triplicate samples were run to assess variability. Sub-samples (5 ml) were removed immediately after spiking for flow cytometry and, thereafter, twice daily. Sample bottles (maintained under ambient laboratory conditions) were individually mixed by gentle turning (1 min) immediately prior to sampling. After the third day, the experiments were terminated and Irgarol 1051® concentrations were measured using solid phase extraction followed by gas chromatography - selective ion monitoring mass spectrometry (Scarlett *et al.*, 1997). Sub-samples were also taken for pigment analyses and following filtration (0.7 µm GF/F), phytoplankton were extracted and pigments analysed by high performance liquid chromatography (HPLC) with diode array detection (Barlow *et al.*, 1997). The abundance of eukaryotic phytoplankton (<20 µm) and *Synechococcus* sp. (prokaryotic picoplankton) was measured by analytical flow cytometry (AFC). Samples taken for AFC were maintained at approximately 4 °C in the dark and were analysed within one hour using a Becton Dickinson FACSort™ flow cytometer.

3.2.3. Results and discussion

Flow cytometric results are plotted in Fig. 3.10. The data demonstrates that addition of Irgarol 1051® at the concentrations selected had an insignificant effect on eukaryotic phytoplankton during the initial 23 hours. After 23 hours, however, the control incubations, without Irgarol 1051® grew steadily, tripling their abundance towards the end of the experiment. Conversely, eukaryote growth was significantly inhibited in all incubations exposed to Irgarol 1051®. At an exposure concentration of 112 ng l⁻¹, growth was inhibited to the extent that eukaryote abundance was less than half that of the

controls at the end of the experiment. In all other incubations, Irgarol 1051® had even more of an effect, causing eukaryote abundance to decrease below initial concentrations. It is interesting to note that Irgarol 1051® had negligible effect on the abundance of prokaryotic cyanobacteria of the genus *Synechococcus* (Fig. 3.10). This might relate to D1 exchange and the Photosystem II repair cycle (Campbell *et al.*, 1996).

High resolution pigment analyses were performed at the end of the experiments. Pigments can be specific for certain taxonomic groups e.g. zeaxanthin is indicative of prokaryotes (such as cyanobacteria), peridinin of dinoflagellates, 19'-hexanoyloxyfucoxanthin of prymnesiophytes (and some dinoflagellates) whilst fucoxanthin is present in diatoms, prymnesiophytes, raphidophytes, chrysophytes and several dinoflagellates. Chlorophyll-*a* is found in all photosynthetic microalgae. Results from this experiment revealed that with the exception of zeaxanthin, all pigments were significantly reduced with increasing Irgarol 1051® concentrations (Fig. 3.11). Percentages of each pigment:chlorophyll-*a* ratio to total are shown in Fig. 3.12. Highest

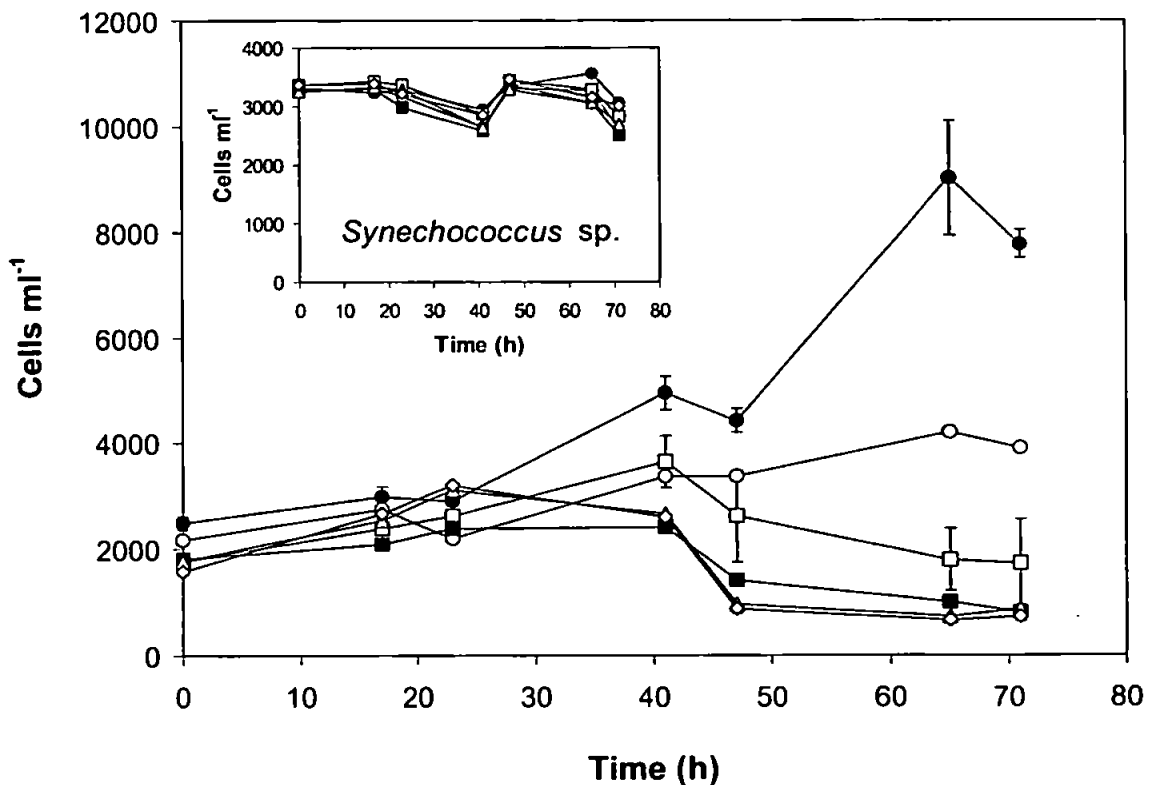


Figure 3.10. Cell numbers (measured by flow cytometry) of prokaryotic (*Synechococcus* sp.) and eukaryotic phytoplankton exposed to different concentrations of Irgarol 1051® during a 72 hour period. Symbols indicate: ● < 1 ng l⁻¹ (controls); ○ 112 ng l⁻¹; □ 331 ng l⁻¹; ■ 465 ng l⁻¹; Δ 1082 ng l⁻¹; ◇ 2020 ng l⁻¹.

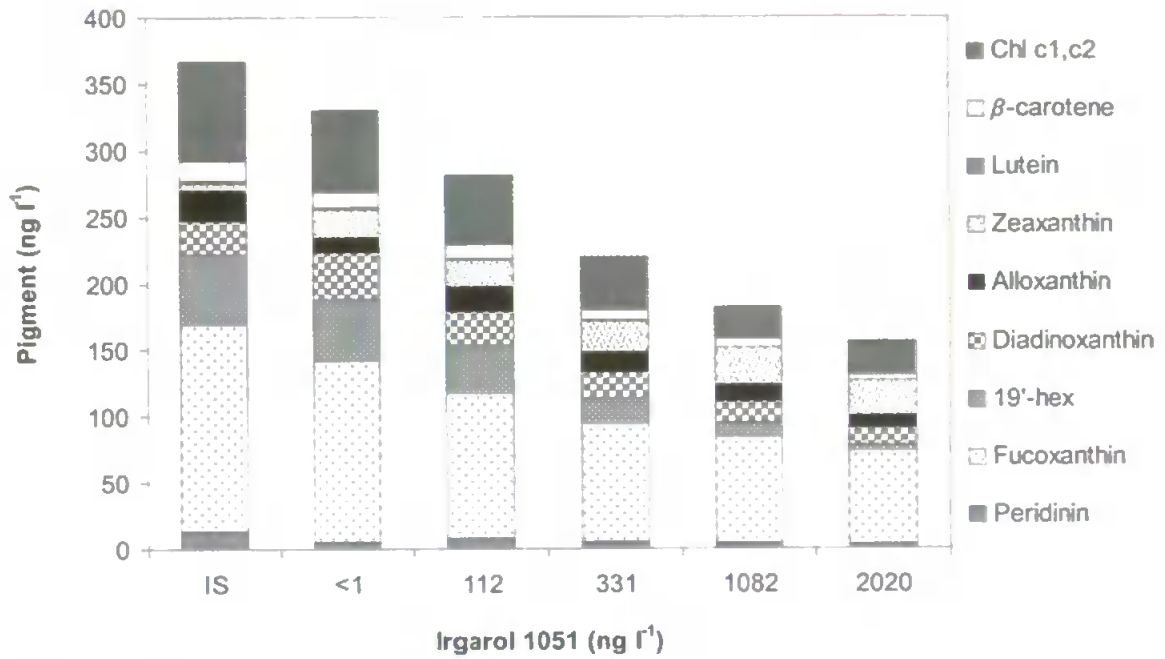


Figure 3.11. Pigment concentrations (ng l^{-1}) derived from HPLC pigment analyses of the phytoplankton extracts. Data are shown for the initial sample (IS = composition at the start of the experiment) and following 72 hours of exposure to concentrations of <1 (controls), 112, 331, 465, 1082, and 2020 ng l^{-1} of Irgarol 1051[®]. Note: 19'-hexanoyloxyfucoxanthin is abbreviated to 19'-hex in the key.

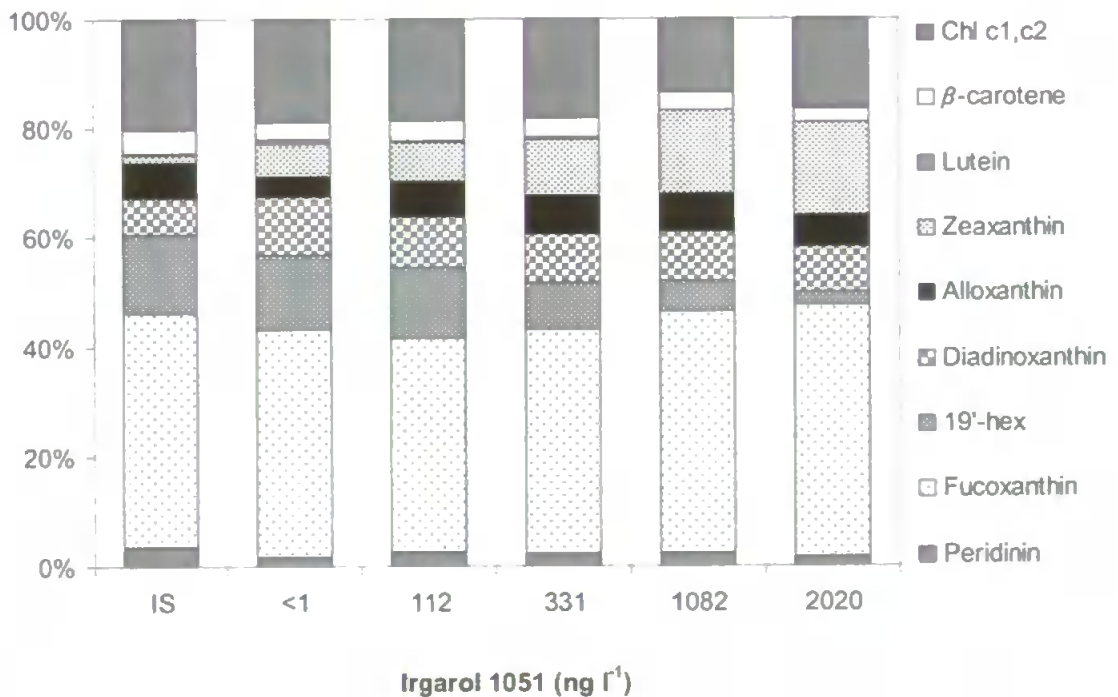


Figure 3.12. Pigment:chl-*a* ratios ($\text{ng l}^{-1}:\text{ng l}^{-1}$) expressed as percentage of total. Ratios are shown for the initial sample (IS = composition at the start of the experiment) and following 72 hours of exposure to concentrations of <1 (controls), 112, 331, 465, 1082, and 2020 ng l^{-1} of Irgarol 1051[®]. Note: 19'-hexanoyloxyfucoxanthin is abbreviated to 19'-hex in the key.

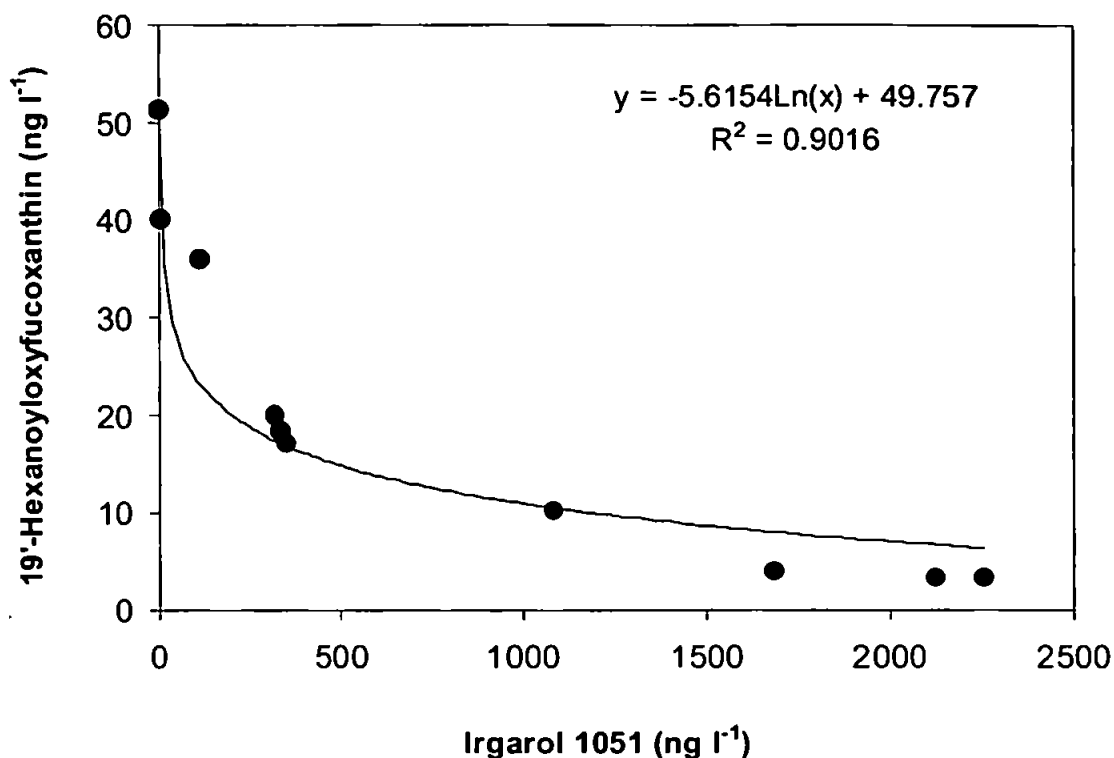


Figure 3.13. Reductions in 19'-hexanoyloxyfucoxanthin (ng l⁻¹) as a function of Irgarol 1051® exposure concentrations (ng l⁻¹). Exposure time = 72 h.

reductions in concentrations were demonstrated for 19'-hexanoyloxyfucoxanthin (Fig. 3.13). Calculations indicate EC₅₀(72h) values of between 70 to 200 ng l⁻¹ for phytoplankton containing this pigment (primarily the prymnesiophytes).

To date, there is very little published data on the effects of booster herbicides on natural phytoplanktonic communities. However, Dahl and Blank (1996) have reported an EC₅₀ of 200 ng l⁻¹ of Irgarol 1051® (for a decrease in photosynthetic activity in periphyton) with the most sensitive long term effects being detected between 63 and 250 ng l⁻¹. Also, macroalgal reproduction-related processes are affected at low concentrations (120 ng l⁻¹) with significant inhibition of growth of *Enteromorpha intestinalis* spores (Scarlett *et al.*, 1997). Even vascular plants in the marine environment (*Zostera marina*) have been shown to be affected by 200 ng l⁻¹ of Irgarol 1051® (Scarlett *et al.*, 1999). To place these levels into an environmental perspective, concentrations of Irgarol 1051® in coastal waters have been reported to range from < 2 to 500 ng l⁻¹ (Southern UK coast; Gough *et al.*, 1994), < 5 to 1700 ng l⁻¹ (Côte d'Azur, Mediterranean; Readman *et al.*, 1993) and 7 to 325 ng l⁻¹ (Spanish Coast; Ferrer *et al.*, 1997).

With these reported EC₅₀ values estimated at such low concentrations, effects are likely to occur at much lower concentrations than these. Implications for phytoplankton populations and ecosystem changes could ensue. In addition, the presence of other antifouling booster biocides and agricultural herbicides would contribute to potential environmental effects. This research demonstrates the applicability and sensitivity of flow cytometry and high resolution pigment analyses to quantitatively investigate toxic effects on natural phytoplanktonic communities.

3.2.4. Conclusions

Flow cytometric analyses coupled with HPLC pigment determinations were demonstrated to be useful and rapid tools to investigate phytoplankton community changes induced by the antifouling biocide Irgarol 1051®. Such techniques are very important to detect changes in small sized phytoplankton (<20 µm), where optical microscopy is deficient and time consuming. Pigment composition has a great potential to be used to estimate phytoplankton groups by the use of statistical tools. However, investigations are needed that take into account pigment content variability under stress conditions. Also, validation of the use of these techniques with phytoplankton responses to other toxicants is necessary to validate their use as ecotoxicological endpoints.

Chapter 4

***Evaluation of techniques to measure changes in phytoplankton composition induced by Irgarol 1051[®] exposure*⁶**

4.1. Introduction

Several techniques have been employed to investigate phytoplankton community composition. Light microscopy is the classical method, but is very time consuming, requires considerable taxonomic expertise and has limitations in identifying small-sized organisms (e.g. nanoplanktonic flagellates). Conversely, Analytical Flow Cytometry (AFC) provides a more rapid assessment and quantification of phytoplankton communities, but lacks detailed compositional information, discriminating phytoplankton communities into bigger groups: picoplanktonic prokaryotes, picoeukaryotes, and nanoeukaryotes (Readman *et al.*, 2004). To overcome some of the limitations of microscopy and AFC, the chemotaxonomic approach provides discrimination between the main algal classes, which is based on taxon-specific pigment markers analysed by HPLC (Barlow *et al.*, 1993; Jeffrey *et al.*, 1997).

Several recent studies have compared microscopic and chemotaxonomic approaches on natural communities (Breton *et al.*, 2000; Rodriguez *et al.*, 2002; Carreto *et al.*, 2003; Garibotti *et al.*, 2003; Fietz and Nicklish, 2004), with some also including flow cytometry analyses (e.g. Gin *et al.*, 2003). Studies have demonstrated that HPLC pigment analysis is a valuable tool for phytoplankton studies and that it can generate a good approximation of carbon biomass. However, more research is needed to assess the chemotaxonomic approach, since the use of chlorophyll-*a* as a biomass indicator must be undertaken with caution as it is susceptible to changes in environmental conditions. To date, few investigations on community changes under anthropogenic stressors have been reported (Readman *et al.*, 2004). Data on single species exposures and preliminary data on natural phytoplankton community changes have been reported by Devilla *et al.* (*in press*). In this Chapter, the consequences of environmental disturbances on phytoplankton composition by manipulating a natural algal community in microcosms

⁶ An article of this chapter has been published in *Aquatic Toxicology*.

exposed to the PSII inhibitor Irgarol 1051[®] are examined. The aim is to compare and contrast changes in community structure as determined by HPLC-class specific pigment analyses, optical microscopy and AFC and use these techniques to monitor the effects of Irgarol 1051[®] in microcosms.

4.2. Methods

4.2.1. Sampling and experimental design

One hundred litres of coastal surface water was collected from the well characterised L4 station (Pingree, 1978; Rodríguez *et al.*, 2000), off Plymouth, UK (50°15' N, 04°13' W) on August 11th, 2003. The *in situ* temperature was 16 °C and salinity was 35 PSU. At the laboratory, the seawater was filtered through a 150 µm nylon mesh net and 4 litres were transferred into each of 15 microcosms comprising 5-L borosilicate glass Erlenmeyer flasks. All flasks were previously cleaned in 5% Decon followed by 5% acid soaking, rinsed three times with Milli-Q water and sterilized by autoclaving (20 min; 121 °C/15 psi).

A stock solution of 0.503 µg µl⁻¹ Irgarol 1051[®] (N'-Tert-Butyl-N-cyclopropyl-6-(Methylthio)-1,3,5-Triazine-2) was prepared by dissolution in methanol (HPLC grade). The working solution (1 µg ml⁻¹) was prepared at the start of the experiment from dilutions of the stock solution into filtered (0.45 µm) and autoclaved seawater to reduce carrier solvent concentration. Microcosms were spiked with aliquots of the Irgarol 1051[®] working solution to give nominal concentrations of 0.5 and 1.0 µg l⁻¹ (which were selected from a preliminary scaling experiment). It was ensured that all microcosms (including the controls) were spiked with the same amount of methanol. Final concentrations of methanol for each treatment did not exceed 0.0002% (v/v). There were five replicate microcosms for each treatment and control. Flasks were randomly placed in a walk-in controlled temperature room on a 12:12 h light:dark cycle under an average temperature of 17 °C and an irradiance of 160 µmol photons m⁻² s⁻¹ photosynthetic active radiation (PAR), provided by cool white fluorescent light bulbs (Sylvania; 70W). The experiment was conducted over 120 hours. After 48 h, the water in all microcosms was partially renewed with the original seawater (sterilized by filtration through 0.2 µm Track-Etch membrane filters following collection, with or without Irgarol 1051[®] addition) to compensate for any nutrient depletion. This was adjusted to result in a

dilution of phytoplankton content of 1.4 times. To minimise changes due to light variability, flasks were randomly repositioned each day. Flasks were swirled by hand once daily prior to sample removal. Samples for AFC were taken daily to monitor phytoplankton growth (section 2.4.8). Samples for pigments (section 2.4.3), microscopic enumeration and identification (section 2.4.7), and Irgarol 1051[®] analyses (section 2.4.4) were taken at 0, 48 and 96 h of the experiment.

4.2.2. Data analyses

4.2.2.1. Evaluation of phytoplankton diversity

Comparisons of the effects of Irgarol 1051[®] on community structure were performed using average Margalef's diversity index (Margalef, 1958) and the number of species or groups of autotrophs were enumerated by microscopy. The diversity index was calculated from equation 8, where D is the Margalef's Diversity Index, S is the number of species in a sample, and N is the number of individuals in a community.

$$D = \frac{(S - 1)}{\ln N} \quad \text{Eq. (8)}$$

A matrix using Bray-Curtis dissimilarity was generated using fourth root transformed abundance data from microscopy observations. Subsequently, non-metric multi-dimensional scaling (MDS) ordinations were conducted for species abundances and species were aggregated into groups (diatoms, dinoflagellates, Chlorophyceae, Chrysophyceae, Cryptophyceae, Prasinophyceae, Prymnesiophyceae, unidentified flagellates). These analyses were performed using the statistical software PRIMER for Windows v 5.2.9 (Plymouth, UK).

4.2.2.2. Estimates of class-specific biomass

Estimates of biomass from chlorophyll-*a* for each phytoplankton group were obtained using the matrix factorisation program CHEMTAX run under MATLAB[™] (Mackey *et al.*, 1996). Algal classes were selected according to the phytoplankton composition obtained from microscopic analysis. The pigment:chl-*a* ratio input matrix was derived from the literature (Mackey *et al.*, 1996; Irigoien *et al.*, 2000). In addition to the dinoflagellates, a separate initial marker pigment:chlorophyll-*a* ratio was required for the dinoflagellate *Karenia mikimotoi* (formerly *Gyrodinium aureolum*) (80% carbon),

because its pigment composition differs from the normal pigment composition of dinoflagellates, which have peridinin as the marker carotenoid (Wright and Jeffrey, 1997). *K. mikimotoi* has 19'-hexanoyloxyfucoxanthin and fucoxanthin instead of peridinin (Johnson and Sakshaug, 1993). The light protecting carotenoids β -carotene, diadinoxanthin, diatoxanthin and other pigments only detected in trace amounts were excluded from the matrix, as recommended by Mackey *et al.* (1996).

4.2.2.3. Comparisons between methods

Linear regression models between chlorophyll-*a* biomass estimated through CHEMTAX and carbon content obtained from microscopy for each phytoplankton group were obtained using the statistical package Statistica for Windows version 5.1 (1996 edition, StatSoft Inc., Tulsa, USA). Regressions were significant at a level of 0.05. The effects of Irgarol 1051[®] exposures were analysed by one-way ANOVA followed by the least significant difference test (LSD; $\alpha = 0.05$). All data were tested for homocedasticity (Cochran's test) and normality (χ^2 test) and transformed ($\log x+1$; rank) when necessary to meet the assumptions for parametric tests.

4.3. Results

4.3.1. Analytical Flow Cytometry

Growth of nanophytoplankton and picophytoplankton was monitored by AFC for 120 h. Nanoplanktonic cryptophytes were in insignificant numbers and were, therefore, omitted from the results. Picoeukaryotes were exponentially growing until 96 h in the controls (Fig. 4.1), therefore data obtained from this day were selected for comparisons. Results showed a decline in cell numbers relative to controls with increasing concentrations of Irgarol 1051[®] throughout the experimental period. After 96 h, relative to the controls, picoeukaryotes exposed to 0.5 and 1.0 $\mu\text{g l}^{-1}$ Irgarol 1051[®] were significantly ($p < 0.05$) inhibited by 38% and 73% respectively, and nanoeukaryotes were inhibited by 52% and 78% respectively. Cyanophyceae cell numbers steadily declined throughout the experimental period, with cell numbers being reduced by 53% following a 96 h exposure to 1.0 $\mu\text{g l}^{-1}$ Irgarol 1051[®] (Fig. 4.1).

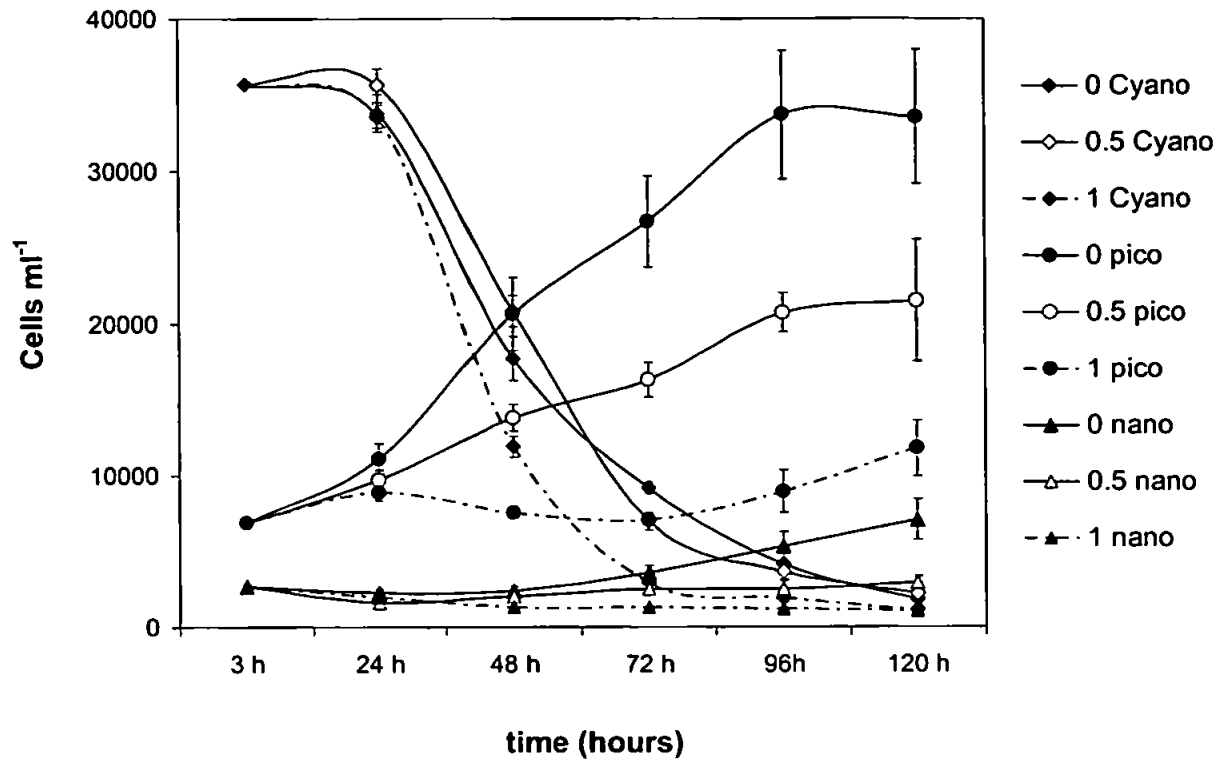


Figure 4.1. Growth response of picoeukaryotes (pico), nanoeukaryotes (nano), and cyanophytes (Cyano) under exposures of 0.5 $\mu\text{g l}^{-1}$ and 1.0 $\mu\text{g l}^{-1}$ Irgarol 1051[®] and the controls (no Irgarol 1051[®] added) over a 120 h period of incubation. Data are expressed as mean cell abundances (measured by AFC). Bars indicate standard deviations. $n = 5$.

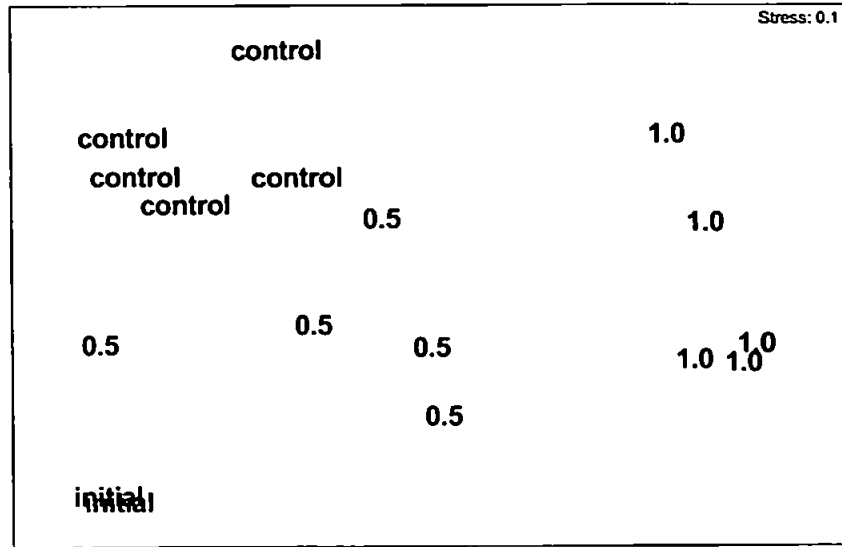
4.3.2. Microscopy

A 96 h exposure to concentrations of 0.5 and 1.0 $\mu\text{g l}^{-1}$ Irgarol 1051[®] induced changes in autotroph composition by modifying either phytoplankton species or group compositions (Fig. 4.2). Similar species composition could be readily separated into 3 clusters representing the different treatments and controls at 96 h of incubation (Fig. 4.2A). For similar group composition, clustering only isolated the 1.0 $\mu\text{g l}^{-1}$ exposure (Fig. 4.2B). All treated and control clusters after 96 h of incubation were different from the 'initial' composition, *i.e.*, time 0 of incubation (Fig. 4.2A and Fig. 4.2B).

Microscopy observations revealed that the number of autotrophic species (S) and autotrophic groups (G) significantly declined ($S = 36$; $G = 7$) relative to the controls ($S = 45$; $G = 9$) following 96 h exposure to 1.0 $\mu\text{g l}^{-1}$ Irgarol 1051[®] ($p < 0.01$) (Fig. 4.3). A significant reduction in the Margalef's diversity index was also observed for the

(A)

Species (autotrophs)



(B)

Group (autotrophs)

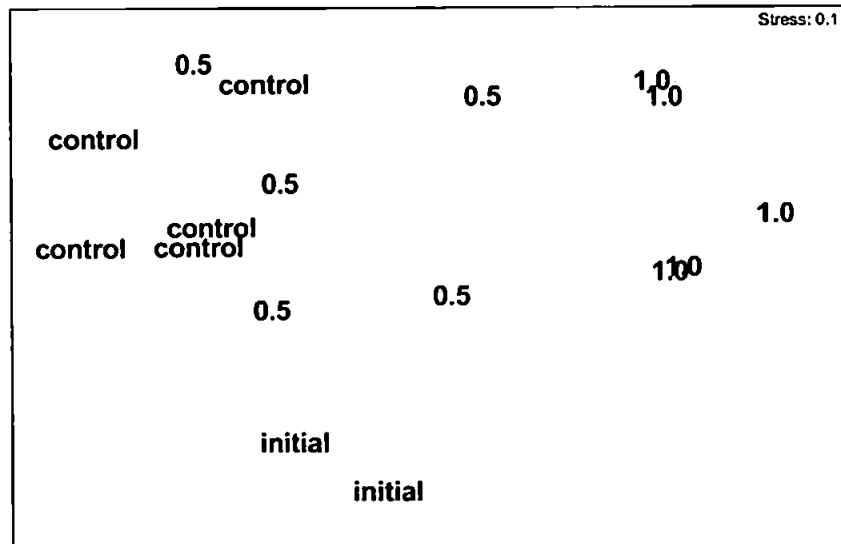


Figure 4.2. Non-metric Multi-Dimensional Scaling (MDS) ordination of (A) species abundances and (B) species abundances aggregated into groups of autotrophs. Data were fourth root-transformed for Bray-Curtis dissimilarities analysis. Autotrophs present in the controls (no Irgarol 1051[®] added) and in the microcosms treated with 0.5 $\mu\text{g l}^{-1}$ and 1.0 $\mu\text{g l}^{-1}$ Irgarol 1051[®] at 96 h of experiment (5 replicates). Autotrophs at time of collection (time 0) is expressed as 'initial'. Small distances between observations indicate high similarity in community structure. Stress levels (above each graph) indicate a good representation of the relationship between observations.

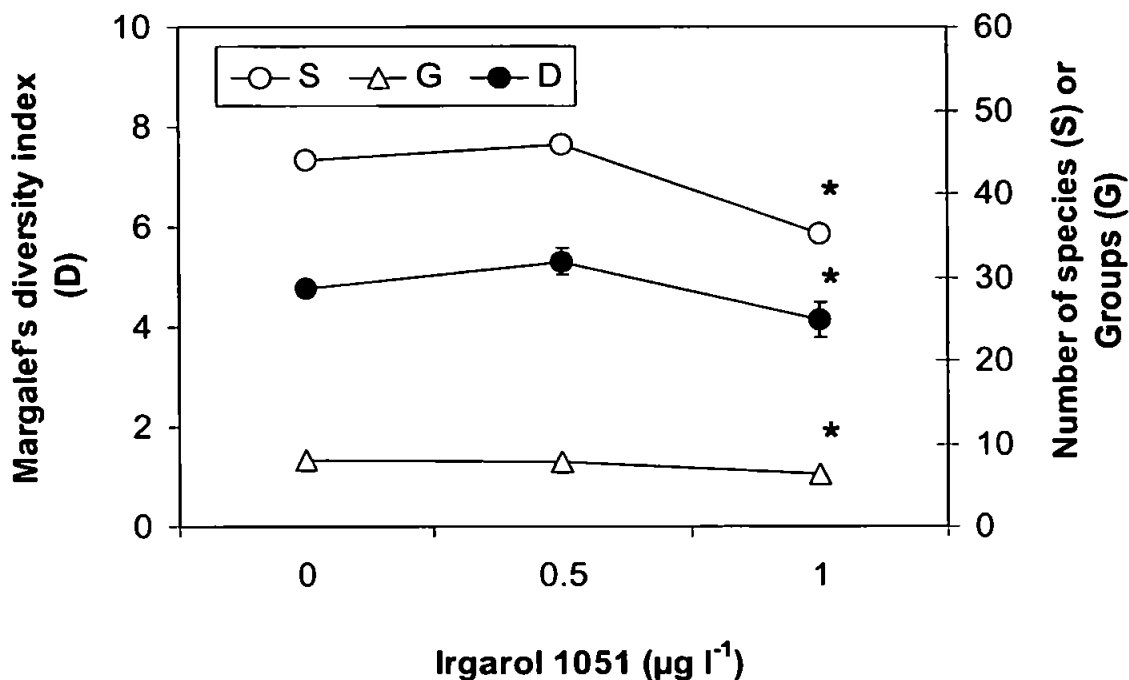
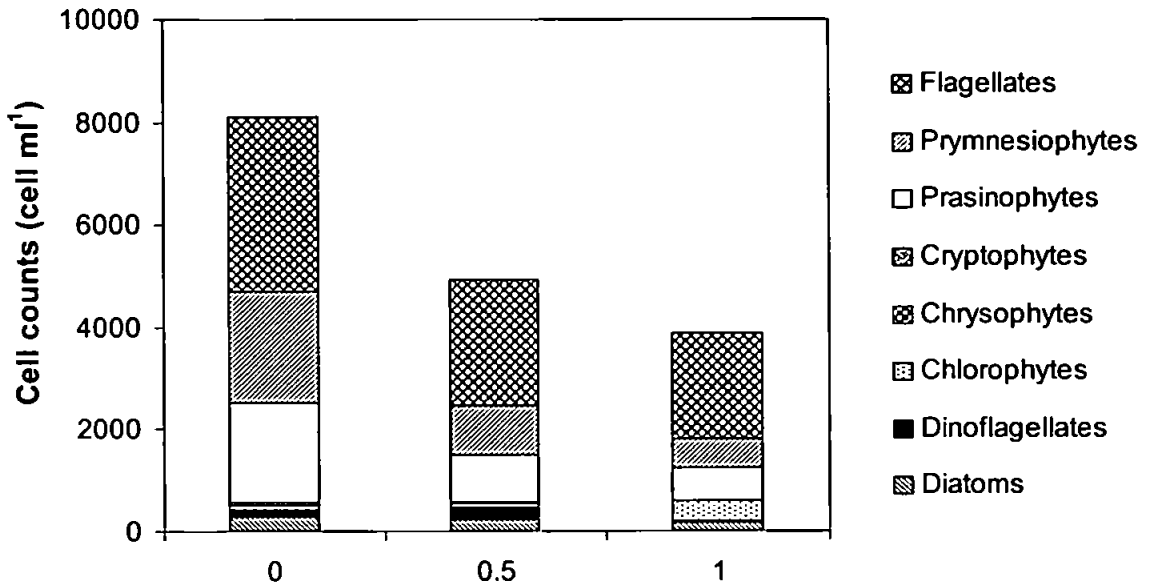


Figure 4.3. Effects of Irgarol 1051[®] on community structure expressed as average ($n = 5$) Margalef's diversity index (D) and number of species (S) and groups (G) of autotrophs. Data obtained from microscopy observations at 96 h of experimental period.

*Significant difference compared to controls (i.e. no addition of Irgarol 1051[®]). One-way ANOVA followed by LSD post hoc comparison of means ($p < 0.01$; data were rank transformed for the parameter S)

community studied under exposure to $1.0 \mu\text{g l}^{-1}$ Irgarol 1051[®] ($p < 0.01$) (Fig. 4.3). Both parameters also showed significant differences between 0.5 and $1.0 \mu\text{g l}^{-1}$ Irgarol 1051[®] ($p < 0.05$). Relative to the controls, autotroph species abundances were significantly reduced by 39% and 52% following exposure to 0.5 and $1.0 \mu\text{g l}^{-1}$ Irgarol 1051[®], respectively ($p < 0.05$). No significant difference in autotroph abundance was, however, found between the Irgarol 1051[®] treatments ($p > 0.05$). Abundance of prasinophytes and prymnesiophytes were significantly reduced after exposure to 0.5 and $1.0 \mu\text{g l}^{-1}$ Irgarol 1051[®] ($p < 0.05$) when compared to the controls (Fig. 4.4A). Diatoms, dinoflagellates, cryptophytes, and unidentified flagellates were significantly reduced only under $1.0 \mu\text{g l}^{-1}$ Irgarol 1051[®]. In contrast, chlorophyte abundances significantly increased following exposure to this concentration ($p < 0.05$) (Fig. 4.4A). No significant differences ($p > 0.05$) were observed for diatoms, dinoflagellates, chlorophytes, chrysophytes, cryptophytes and unidentified flagellates exposed to $0.5 \mu\text{g l}^{-1}$ Irgarol 1051[®]. Also, no changes were observed for chrysophytes at either exposure concentrations ($p > 0.05$).

(A)



(B)

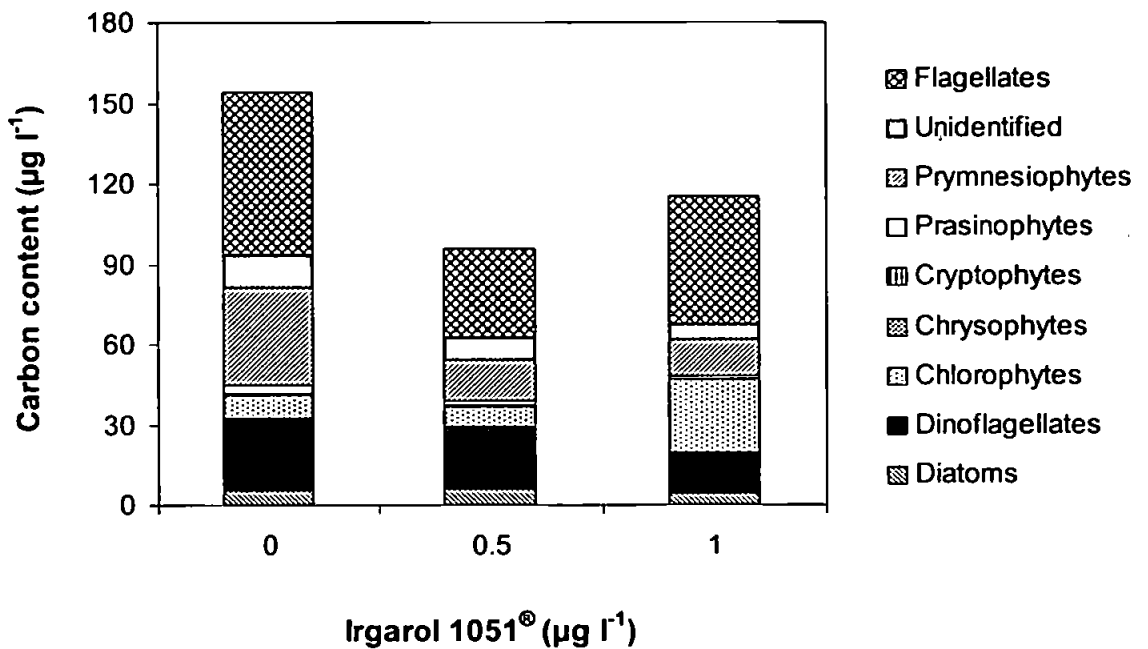


Figure 4.4. Phytoplankton response after 96 h exposure to 0.5 and 1.0 µg l⁻¹ Irgarol 1051[®] obtained from microscopic enumeration: (A) cell abundances (cell ml⁻¹) and (B) carbon content estimates (µg l⁻¹); n = 5.

Carbon estimates indicated similar patterns of response amongst groups to both Irgarol 1051[®] exposures, except for diatoms, for which the carbon content did not differ between treatments. The relative carbon contribution of chlorophytes increased from 6% (controls) to 24% ($1.0 \mu\text{g l}^{-1}$ Irgarol 1051[®]) and dinoflagellates increased from 18% (controls) to 24% ($0.5 \mu\text{g l}^{-1}$ Irgarol 1051[®]). Reductions in the relative proportion of carbon content were observed mainly for the prymnesiophytes from 23% (controls) to 11% ($1.0 \mu\text{g l}^{-1}$ Irgarol 1051[®]). Heterotrophs, however, increased in numbers under $1.0 \mu\text{g l}^{-1}$ Irgarol 1051[®] ($p < 0.05$), whilst no difference was observed in their carbon content ($p > 0.05$) (data not shown). Carbon content of total autotrophs exposed to 0.5 and $1.0 \mu\text{g l}^{-1}$ Irgarol 1051[®] decreased significantly relative to the controls ($p = 0.0034$ and $p = 0.0338$, respectively), but no significant difference was observed between Irgarol 1051[®] treatments ($p = 0.236$) (Fig. 4.4B). A value of 80% of the carbon content relative to dinoflagellates was attributed to *Karenia mikimotoi*.

4.3.3. Pigment composition

The output matrix, *i.e.*, the final marker pigment:chlorophyll-*a* ratios obtained using the CHEMTAX program and used to calculate the group specific chlorophyll-*a* concentration is shown in Table 4.1.

All diagnostic pigments were significantly correlated to chlorophyll-*a* ($p < 0.05$; Table 4.2). The highest correlations were found for fucoxanthin ($R^2 = 0.96$), alloxanthin ($R^2 = 0.84$), chlorophyll *c*₃ ($R^2 = 0.73$), chlorophyll *b* ($R^2 = 0.62$), 19'-hexanoyloxyfucoxanthin ($R^2 = 0.55$), and 19'-butanoyloxyfucoxanthin ($R^2 = 0.52$) ($p < 0.01$). Zeaxanthin proved to be an exception to this pattern, being inversely proportional to chlorophyll-*a* ($R^2 = 0.73$; $p < 0.0001$) (Table 4.2). It is demonstrated, therefore, that chlorophyll-*a* biomass is linearly related to prymnesiophytes, chrysophytes and diatoms (fucoxanthin-containing groups), the cryptophytes (alloxanthin), and the chlorophytes (chlorophyll *b*). Other phytoplankton diagnostic pigments presented weak correlations with chlorophyll standing stocks.

After 96 h, an apparent 10% increase in chlorophyll-*a* was observed under $0.5 \mu\text{g l}^{-1}$ Irgarol 1051[®] ($p > 0.05$), with a subsequent significant decrease of 30% at $1.0 \mu\text{g l}^{-1}$ Irgarol 1051[®] ($p < 0.05$) compared to the controls (Fig. 4.5A). No pattern of strong dominance of a specific pigment was observed in the microcosms. Fucoxanthin was the

main pigment and constituted 26% of the total pigments in the controls, followed by 19'-hexanoyloxyfucoxanthin, which constituted 17%. In the treated microcosms (0.5 and 1.0 $\mu\text{g l}^{-1}$ Irgarol 1051[®]), zeaxanthin and antheraxanthin proportionally increased up to twice and six times, respectively, relative to the controls (Fig. 4.5A).

Estimation of the community structure using the CHEMTAX calculations identified four groups as the main contributors to the total chlorophyll-*a* biomass of the phytoplankton community. Dinoflagellates '1' (as discriminated by *K. mikimotoi*), chrysophytes, cryptophytes, and prymnesiophytes contributed to 36%, 21%, 18%, 11%, respectively, for the chlorophyll-*a* biomass in the controls after 96 h (Fig. 4.5B). The contribution of chlorophytes estimated by CHEMTAX increased with increasing concentrations of Irgarol 1051[®], from 4% of the total biomass in the controls to 21% at 1.0 $\mu\text{g l}^{-1}$ ($p < 0.05$) (Fig. 4.5B). Also, the relative contributions of diatoms and dinoflagellates increased with increasing exposure to Irgarol 1051[®], from 5% (controls) to 18% (1.0 $\mu\text{g l}^{-1}$) and from 4% (controls) to 6% (1.0 $\mu\text{g l}^{-1}$), respectively. The dinoflagellate *Karenia mikimotoi*, for which the main diagnostic carotenoid is 19'-hexanoyloxyfucoxanthin instead of peridinin, was confirmed by CHEMTAX analyses to be a major contributor to the dinoflagellate biomass. The biomass of prymnesiophytes, chrysophytes and dinoflagellates '1' was significantly reduced with increasing concentrations of Irgarol 1051[®] (Fig. 4.5B) with reductions from 11% (controls) to 7% (1.0 $\mu\text{g l}^{-1}$), from 21% (controls) to 1% (1.0 $\mu\text{g l}^{-1}$), and from 36% (controls) to 31% (1.0 $\mu\text{g l}^{-1}$), respectively for the three groups.

4.3.4. Comparisons between methods

Comparisons of CHEMTAX estimates of chlorophyll-*a* and phytoplankton carbon (from microscopy) showed agreement mainly for chlorophytes ($R^2 = 0.53$; $p = 0.002$), cryptophytes ($R^2 = 0.51$; $p = 0.003$) and dinoflagellates (discriminated as *K. mikimotoi*) ($R^2 = 0.48$; $p = 0.004$) (Fig. 4.6). Unidentified flagellates enumerated by microscopy also showed agreement with prymnesiophytes ($R^2 = 0.56$; $p = 0.001$), chrysophytes ($R^2 = 0.54$; $p = 0.002$), and prasinophytes ($R^2 = 0.64$; $p < 0.001$) as estimated by CHEMTAX (Fig. 4.6). However, discrepancies were observed for cryptophytes, which did not show a correlation with unidentified flagellates enumerated by microscopy. Also, no correlation was observed between total carbon and total chlorophyll-*a*.

Table 4.1. Output matrix of marker pigment:chl-*a* ratios obtained from CHEMTAX calculations. Dinoflagellates_1 corresponds to ratios for *Karenia mikimotoi*. Chl_: chlorophylls *a*, *b*, *c*₁*c*₂ or *c*₃; PER: peridinin; BUT: 19'-butanoyloxyfucoxanthin; FUCO: fucoxanthin; HEX: 19'-hexanoyloxyfucoxanthin; ANTH: antheraxanthin; VIOLA: violaxanthin; ALLO: alloxanthin; ZEA: zeaxanthin.

	Chl_ <i>c</i> ₃	Chl_ <i>c</i> ₁ <i>c</i> ₂	PER	BUT	FUCO	HEX	ANTH	VIOLA	ALLO	ZEA	Chl_ <i>b</i>	Chl_ <i>a</i>
Prasinophytes	0.000	0.000	0.000	0.000	0.000	0.000	0.004	0.071	0.000	0.071	0.498	0.356
Dinoflagellates_1	0.116	0.082	0.000	0.000	0.130	0.110	0.000	0.000	0.000	0.000	0.000	0.562
Dinoflagellates	0.000	0.153	0.282	0.000	0.000	0.000	0.000	0.000	0.000	0.000	0.000	0.565
Cryptophytes	0.000	0.027	0.000	0.000	0.000	0.000	0.000	0.000	0.074	0.000	0.000	0.899
Chrysophytes	0.000	0.000	0.000	0.000	0.117	0.000	0.007	0.125	0.000	0.038	0.000	0.712
Haptophytes	0.009	0.142	0.000	0.164	0.216	0.215	0.000	0.000	0.000	0.000	0.000	0.254
Chlorophytes	0.000	0.000	0.000	0.000	0.000	0.000	0.200	0.048	0.000	0.143	0.000	0.609
Cyanophytes	0.000	0.000	0.000	0.000	0.000	0.000	0.000	0.000	0.000	0.600	0.000	0.400
Diatoms	0.000	0.085	0.000	0.000	0.348	0.000	0.000	0.000	0.000	0.000	0.000	0.567

Table 4.2. Correlations derived from linear regression between each pigment and chlorophyll-*a*. Data were obtained from all treatments (control, 0.5 and 1.0 $\mu\text{g l}^{-1}$ Irgarol 1051[®]) at 96 h of experiment. *n* = 15. Chl: chlorophylls *b*, *c*₁*c*₂ or *c*₃; PER: peridinin; BUT: 19'-butanoyloxyfucoxanthin; FUCO: fucoxanthin; HEX: 19'-hexanoyloxyfucoxanthin; ANTH: antheraxanthin; VIOLA: violaxanthin; ALLO: alloxanthin; ZEA: zeaxanthin, DIATO: diatoxanthin, DIADINO: diadinoxanthin, β -CAR: β -carotene.

	Chl <i>c</i> ₃	Chl <i>c</i> ₁ <i>c</i> ₂	PER	BUT	FUCO	HEX	ANTH	VIOLA	ALLO	ZEA	Chl <i>b</i>	DIATO	DIADINO	β -CAR
R ²	0.73	0.94	0.41	0.52	0.96	0.55	0.48	0.29	0.84	0.73	0.62	0.50	0.29	0.90
p	0.0000	0.0000	0.0096	0.0025	0.0000	0.0016	0.0041	0.0038	0.0000	0.0000	0.0005	0.0030	0.0378	0.0000

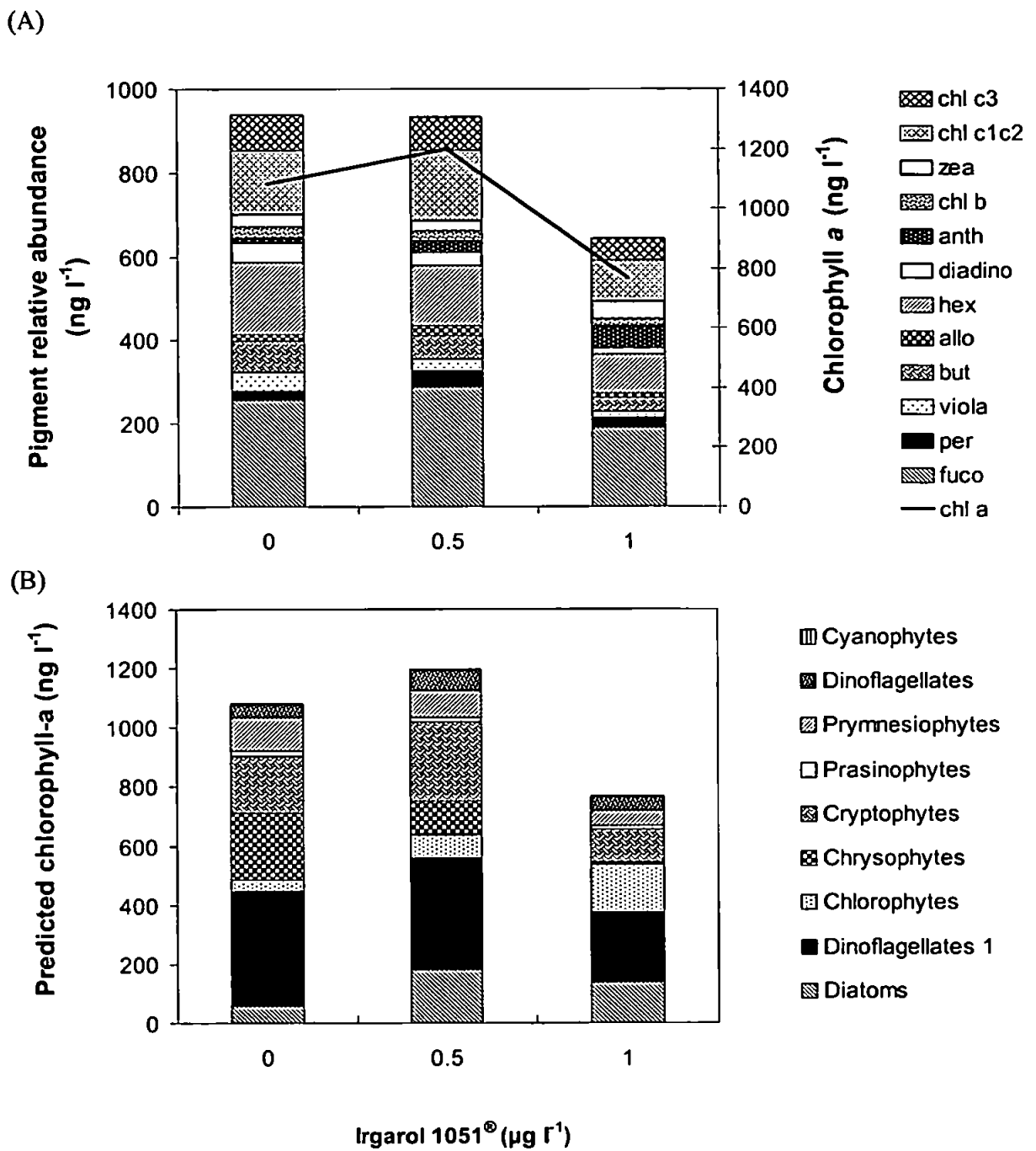


Figure 4.5. Phytoplankton response after 96 h exposure to 0.5 and 1.0 $\mu\text{g l}^{-1}$ Irgarol 1051[®] expressed as (A) diagnostic pigment relative abundance and (B) predicted chlorophyll-*a* from CHEMTAX calculations ($n = 5$). Chl: chlorophylls *a*, *b*, *c*₁*c*₂ or *c*₃; per: peridinin; but: 19'-butanoyloxyfucoxanthin; fuco: fucoxanthin; hex: 19'-hexanoyloxyfucoxanthin; anth: antheraxanthin; viola: violaxanthin; allo: alloxanthin; zea: zeaxanthin, diadino: diadinoxanthin (A). 'Dinoflagellates 1' correspond to *Karenia mikimotoi* (B).

Comparisons of cell enumeration by microscopy and by flow cytometry revealed good agreement for nanoeukaryotes ($R^2 = 0.80$; $p < 0.001$), although a lower coefficient of determination was found for picoeukaryotes ($R^2 = 0.43$; $p = 0.011$) (Fig. 4.7).

4.3.5. Irgarol 1051[®] analyses

At the beginning of the experiment, measured concentrations of Irgarol 1051[®] were $0.61 \mu\text{g l}^{-1}$ and $1.16 \mu\text{g l}^{-1}$ for the two dosing concentrations. Following replenishment of the sea water (after 48 h), concentrations were measured to be $0.60 \mu\text{g l}^{-1}$ and $1.20 \mu\text{g l}^{-1}$. At the end of the experiment, measured concentrations were $0.58 \mu\text{g l}^{-1}$ and $1.13 \mu\text{g l}^{-1}$. Concentrations measured for the controls were close to the limit of detection of the method.

4.4. Discussion

Addition of the PSII inhibitor Irgarol 1051[®] to the microcosms induced marked changes in the phytoplankton community as revealed by microscopy, class-specific pigments and AFC. Nanoeukaryotes appeared to be more affected by Irgarol 1051[®] than picoeukaryotes. This higher sensitivity could be related to the presence of species- or class-specific algae which are more vulnerable to antifoulant stress. The decline in cyanophytes with time, as measured by AFC, may have resulted from the experimental conditions giving optimal conditions for other groups to develop. According to optical microscopy, chrysophytes were not sensitive to Irgarol 1051[®], whilst chlorophytes were stimulated with increasing Irgarol 1051[®] exposure concentrations. Despite efforts to reduce the heterotrophs present in the microcosms, their presence might have influenced the abundances of some classes due to selective herbivory. Prasinophytes and prymnesiophytes were the most sensitive groups to Irgarol 1051[®]. The sensitivity of prymnesiophytes to this biocide was also detected in recent studies (Readman *et al.*, 2004; Devilla *et al.*, *in press*).

Optical microscopy and class-specific pigment techniques identified changes in dominant microalgal groups amongst controls and treated microcosms. Significant correlations were found between chlorophyll-*a* biomass and the diagnostic pigments. CHEMTAX-HPLC pigment data were used to quantify the contribution of the individual phytoplankton groups to total chlorophyll-*a*. Estimation of phytoplankton composition using CHEMTAX indicated structural changes relative to the controls following

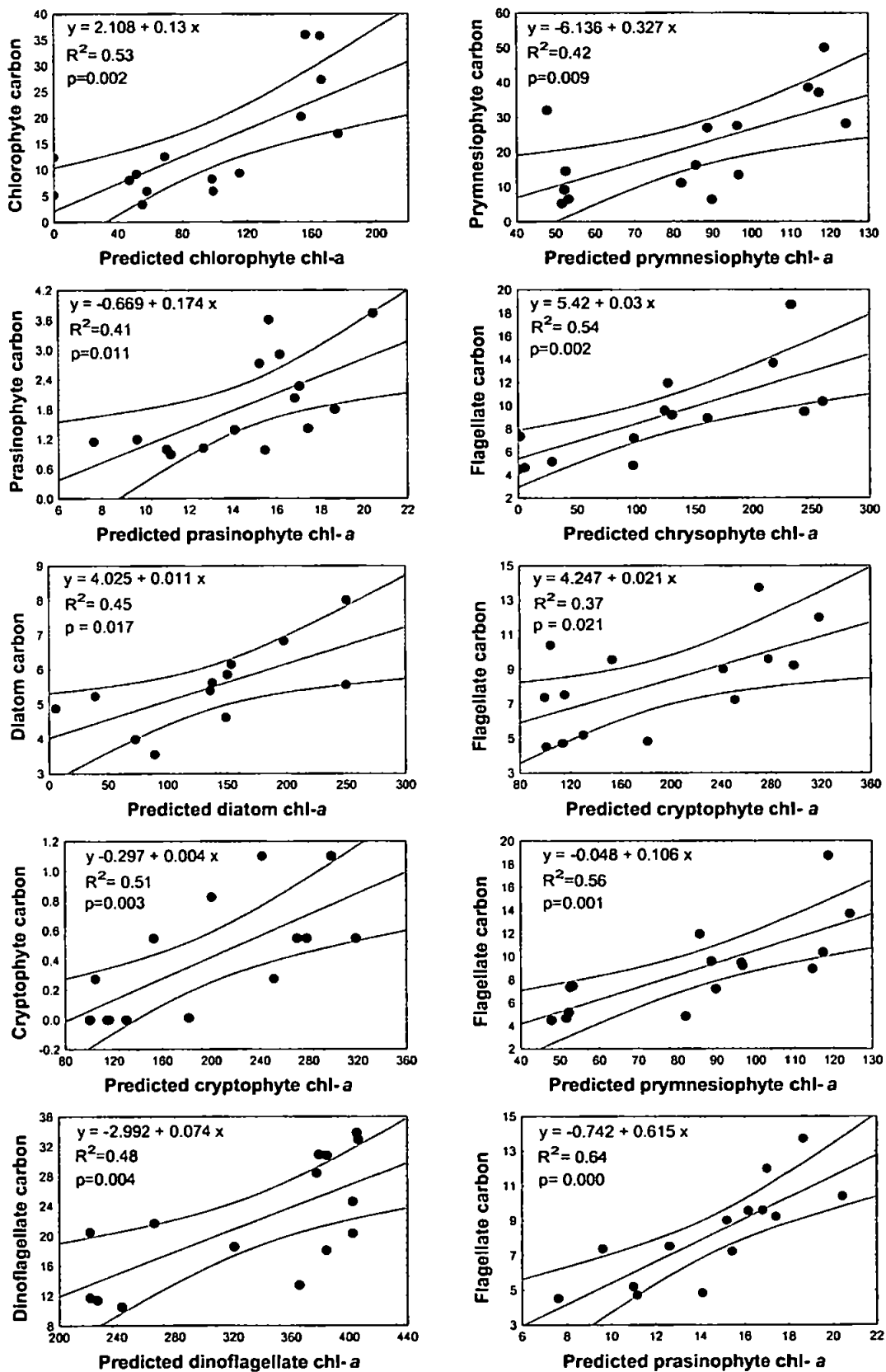
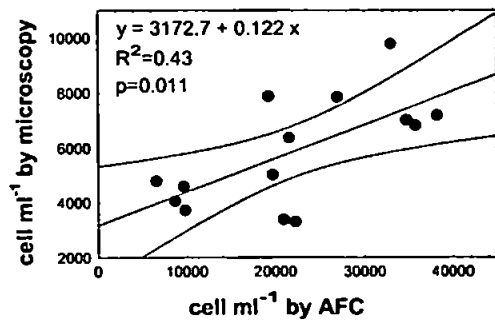


Figure 4.6. Biomass of individual algal classes expressed as chlorophyll-*a* (chl-*a*) concentration in ng l^{-1} estimated from CHEMTAX calculations (*x*-axis) and as carbon concentration in $\mu\text{g l}^{-1}$ estimated by microscopy (*y*-axis). Linear regressions are significant ($p < 0.05$) between biomass estimations ($n = 15$). Data are rank transformed (diatoms) and log ($x+1$) transformed (cryptophyte \times flagellate).

(A)



(B)

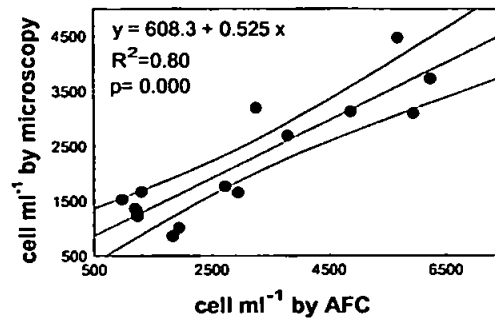


Figure 4.7. Relationship between cell enumeration made by microscopy and analytical flow cytometry (AFC) for (A) picoeukaryotes and (B) nanoeukaryotes. Regressions are significant ($p < 0.05$; $n = 15$).

exposures to Irgarol 1051[®]. Significant correlations were found between the group-specific chlorophyll-*a* of several phytoplankton groups and their respective carbon biomass as estimated from optical microscopy. Results indicated an agreement between carbon content and chlorophyll biomass of chlorophytes ($R^2 = 0.53$). Significant amounts of 19'-hexanoyloxyfucoxanthin could be attributed to a particular species of dinoflagellate (*Karenia mikimotoi*), which was shown by optical microscopy to comprise 80% of the dinoflagellate carbon content. Good agreement was demonstrated between the two techniques for inhibition of this particular dinoflagellate following exposure to $1.0 \mu\text{g l}^{-1}$ Irgarol 1051[®]. *Karenia mikimotoi* did not, however, show significant inhibition at the lower Irgarol 1051[®] concentration tested ($0.5 \mu\text{g l}^{-1}$), as shown by both microscopy and CHEMTAX estimations.

Light microscopic analyses confirmed the presence of phytoplankton groups which corresponded to the diagnostic pigments for dinoflagellates (mainly *K. mikimotoi*, which contains 19'-hexanoyloxyfucoxanthin), diatoms (fucoxanthin), prymnesiophytes (19'-hexanoyloxyfucoxanthin), chlorophytes and prasinophytes (chlorophyll *b*). Following exposure, marked reductions in prymnesiophyte and flagellate carbon contents (estimated from microscopy) were observed, whilst chlorophytes increased in cell numbers and carbon content (compared to the controls) with increasing concentrations of Irgarol 1051[®]. A large quantity of small phytoflagellates (nanoplankton flagellates) could not be taxonomically identified by microscopy. These flagellates probably belong mostly to prasinophytes, haptophytes and chrysophytes. This is supported by the significant correlation found between small flagellate abundance and the CHEMTAX estimates.

Microscopy observations, together with AFC, did not corroborate the presence of cryptophytes as estimated by CHEMTAX. A possible explanation for this disagreement could be either problems in sample preservation which render microscopic observations difficult, or the presence of dinoflagellates or the ciliate *Mesodinium rubrum*, which can contain cryptophytes as endosymbionts (Gieskes and Kraay, 1983; Jeffrey and Veski, 1997).

In general, correlations between carbon biomass and concentrations of the respective pigment marker co-vary between phytoplankton communities (Breton *et al.*, 2000). The more an algal group is homogeneous in composition and size, the better is the

correlation (Breton *et al.*, 2000). Even though positive correlations were found between chlorophyll-*a* and carbon content for some individual microalgal groups, quantitative comparison of total chlorophyll-*a* to total carbon concentration indicated discrepancies. Total carbon and chlorophyll-*a* decreased significantly under high ($1.0 \mu\text{g l}^{-1}$) Irgarol 1051[®] exposure. Under low exposure ($0.5 \mu\text{g l}^{-1}$), however, both parameters showed opposite trends, where chlorophyll biomass was not shown to be affected, whereas the carbon content decreased. Irgarol 1051[®] is known to impair photosynthesis by displacing a plastoquinone (Q_B) from its binding site in the D1 protein of photosystem II (Cremlyn, 1991), and is considered to be one of the most potent photosynthetic inhibitors (Dahl and Blanck, 1996). Cellular amounts of light-harvesting pigments may, however, increase under moderate photosynthetic inhibition by a herbicide, simulating the effects of light limitation (Plumley and Davis, 1980). Although cell densities were significantly reduced with increasing concentrations of Irgarol 1051[®], total carbon did not differ between concentrations of 0.5 and $1.0 \mu\text{g l}^{-1}$ Irgarol 1051[®], probably owing to a volume increase relating to delayed cell division. As a consequence, no linear correlation between total carbon and total chlorophyll-*a* was found.

Investigating the influence of toxicants in coastal areas requires rapid methods to detect subtle modifications in community structure. Flow Cytometry and HPLC are both rapid methods that can identify changes in community and, with the aid of microscopy can yield a comprehensive description which can be used to assess the effects of toxicants. Measuring pigment composition by HPLC affords a more rapid discrimination of algal types than does microscopic analyses, especially for small-sized cells that are difficult to visualise. Group-specific chlorophyll-*a* estimations may afford a good approximation of carbon biomass from HPLC pigment analyses (Breton *et al.*, 2000), but algal class biomass estimations from pigment data in coastal waters should be treated cautiously since pigment per chlorophyll-*a* measures can vary due to anthropogenic stressors (Devilla *et al.*, *in press*). Cellular-intrinsic or environmental parameters can also influence this parameter (Mackey *et al.*, 1996).

Cross-correlation analyses between diagnostic pigments and the presence of specific algal groups are necessary to understand the accuracy of chemotaxonomic estimations. Biomass estimations from pigments require a stable physiological state, which is difficult to achieve in the environment. Thus, variations in pigment content per chlorophyll-*a* and carbon per chlorophyll-*a* hampers class-specific biomass estimations.

Even though a number of class-specific pigment ratios are available in the literature (Mackey *et al.*, 1996; Goericke and Montoya, 1998; Schlüter *et al.*, 2000; Henriksen *et al.*, 2002), more research to evaluate the influence of environmental parameters on pigment:chlorophyll-*a* ratios would enable more accurate predictions, especially when considering coastal areas with herbicidal inputs (Devilla *et al.*, *in press*). Different responses for the various pigment:chlorophyll-*a* ratios have been reported within the same phytoplankton group and even between species (Goericke and Montoya, 1998; Henriksen *et al.*, 2002), where inter-species variability exceeded the differences in the ratios caused by the varying growth conditions (Schlüter *et al.*, 2000). Besides the influences of irradiance, nutritional state and growth phase, it is also necessary to understand the xenobiotic influences regulating dynamics in phytoplankton community-structures in coastal areas.

4.5. Conclusions

The toxicity of the PSII inhibitor Irgarol 1051[®] towards the phytoplankton community studied induced a restructuring of the community and, therefore, changes in taxonomic composition. Group-specific sensitivity was detected through microscopy and was corroborated with CHEMTAX estimations. Results revealed that chlorophytes and dinoflagellates are comparatively resistant to Irgarol 1051[®]. Estimates from HPLC-CHEMTAX pigment analyses were correlated with chlorophytes ($R^2 = 0.53$), which increased in both abundance and carbon content under exposures to Irgarol 1051[®]. Both CHEMTAX-HPLC analyses and microscopy revealed that prasinophytes and prymnesiophytes are the groups most affected by exposure to Irgarol 1051[®]. Abundances determined by microscopy afforded good agreement with AFC in measuring nanoeukaryotes ($R^2 = 0.8$), but microscopy was shown to underestimate picoeukaryotes.

Monitoring phytoplankton responses to toxicants benefits from the assessment of a relatively large number of samples. Less time-consuming methods that evaluate all phytoplankton sizes are, therefore, beneficial. The use of class-specific pigment determinations combined with AFC and some microscopic screening is demonstrated to provide a comprehensive evaluation of the effects on a phytoplankton community under the stress of a PSII inhibitor.

Chapter 5

Impact of a range of antifouling booster biocides on marine phytoplankton⁷

5.1. Introduction

Concerns over the biological impact of antifouling booster biocides have been increasing since TBT restrictions were introduced in the late 1990's (HSE 2002a) and their use has become more widespread. Among the biocides, Irgarol 1051[®] and diuron were, until recently, the most commonly used booster biocides in the UK (Thomas *et al.*, 2002), with levels up to 1421 ng l⁻¹ and 6742 ng l⁻¹ respectively being reported in marinas (Thomas *et al.*, 2001). Maximum concentrations in Plymouth waters, for example, have been recorded as 334 ng l⁻¹ diuron and 127 ng l⁻¹ Irgarol 1051[®] (Scarlett *et al.*, 1997, Thomas *et al.*, 2001, Thomas *et al.*, 2002). Such concentrations have raised concerns about the environmental impact on indigenous organisms (Readman *et al.*, 1993).

To date, effects of antifouling agents on phytoplankton and periphyton have been detected mainly from measurements of photosynthetic activity, species composition, and pigment signatures (*e.g.* Dahl and Blanck, 1996; Readman *et al.*, 2004) and it has been demonstrated that community structure and community tolerance are very sensitive parameters for long-term exposure (Nyström *et al.*, 2002). Therefore, toxicological studies on phytoplankton are particularly relevant to establish safe environmental regulations. While typically based on unialgal tests (Brown and Lean, 1995), toxic responses of natural phytoplankton communities are more environmentally relevant. Only limited information is available on the toxicological effects of the most recently used booster biocides. Although diuron (also known as DCMU) has been extensively investigated due to its widespread agricultural use (*e.g.* Furuya and Li, 1992; Molander and Blanck, 1992; Molander *et al.*, 1992), literature concerning the effects of antifouling biocides on naturally occurring phytoplankton communities is still scarce (*e.g.* Dahl and

⁷ An article of this chapter has been published in *Marine Ecology-Progress Series*.

Blanck, 1996; Nyström *et al.*, 2002; Larsen *et al.*, 2003; Readman *et al.*, 2004). Moreover, the impact of the currently approved biocides in the UK (HSE 2002a), such as Sea-Nine 211[®] and zinc pyrithione has not been adequately investigated.

The aims of this study were to investigate changes in biochemical and physiological function of selected microalgal species and to the composition of a marine phytoplankton community, induced by exposure to four antifouling biocides, two of which have been reported in Plymouth waters (diuron and Irgarol 1051[®]) and two of which are in common usage (Sea-Nine 211[®] and zinc pyrithione). Diuron and Irgarol 1051[®] are PSII inhibitors and impair photosynthesis by displacing a plastoquinone (Q_B) from its binding site in the D1 protein of photosystem II (Cremlyn 1991). Sea-Nine 211[®] has a broad spectrum activity (e.g. against fungi, algae, bacteria and marine invertebrates) and reacts with thiol-containing enzymes (Collier *et al.*, 1990). Zinc pyrithione inhibits bacterial ATP synthesis and membrane transport (Dinning *et al.*, 1998) and generates hydroxyl radicals when photolysed with visible or UV light (Aveline *et al.*, 1996). Since the detection of sensitive toxicological endpoints is crucial for accurately determining toxic effects on communities, this study also assesses the suitability of several biomarkers: growth, photosynthesis, pigment:chlorophyll-*a* ratios and chemotaxonomy. A range of techniques was employed to test their applicability as biomarkers of stress imposed by the selected biocides and to compare their toxicological properties. Initially, experiments were performed on unialgal cultures to investigate changes in growth and marker pigment:chlorophyll-*a* ratios. Subsequently, the impact on a natural phytoplankton community was assessed by measuring photosynthetic inhibition, growth and by using chemotaxonomy.

5.2. Methods

5.2.1. Preparation of biocide solutions

Stock solutions of Irgarol 1051[®], diuron pestanal[®] and Sea-Nine 211[®] were prepared by ultrasonication in methanol. The zinc pyrithione stock was prepared in filtered (0.45 µm) and autoclaved seawater. Working solutions were prepared from dilutions of the stock solutions into filtered (0.45 µm) and autoclaved seawater. All working solutions and the zinc pyrithione stock solution were prepared on the same day of the experiment.

5.2.2. Unialgal, short-term experiments

5.2.2.1. Experimental organisms and culture maintenance

The prymnesiophyte *Emiliana huxleyi* (PCC 92D) and the cyanophyte *Synechococcus* sp. (PCC 543) were obtained from the Plymouth Culture Collection, UK. *Emiliana huxleyi* is a widespread component of the nanoplankton in coastal and oceanic waters. It is an important contributor to the total phytoplankton when blooms develop (Holligan *et al.*, 1993) and it has been demonstrated to be sensitive to Irgarol 1051[®] exposures (Readman *et al.*, 2004). *Synechococcus* sp. is an important component of the marine picoplankton in coastal and oceanic waters (Weisse, 1993) and it has been demonstrated to be tolerant to Irgarol 1051[®] (Readman *et al.*, 2004).

Non-axenic cultures of both species were maintained in *f/2* culture medium (Guillard 1975), slightly modified by omitting silicate and Trizma, and prepared with filtered (0.45 μm) offshore seawater. Salinity and initial pH were 33 PSU and 8.3-8.4 respectively and were measured using a WTW Multiline P4 pH-meter/salinometer. Experimental ideal growth rates (~ 1 division day^{-1}) were achieved by varying culture conditions in both species. *Emiliana huxleyi* was grown on a 12:12 light:dark cycle at 15.5 ± 2.5 °C under an average irradiance of $160 \mu\text{mol photons m}^{-2} \text{s}^{-1}$ photosynthetic active radiation (PAR), provided by cool white light bulbs (Sylvania; 70W). The air around the culture flasks was ventilated with a fan, which ensured even temperature distribution close to the light source. *Synechococcus* sp. was grown on a 12:12 light:dark cycle at 20.5 ± 1.5 °C under an average irradiance of $80 \mu\text{mol photons m}^{-2} \text{s}^{-1}$ PAR, provided by white light bulbs (Thorn; 30W). Prior to experimentation, cultures were grown for at least 4 days to ensure cell acclimatisation. Sterile techniques were used for all culture work in an attempt to minimize bacterial growth.

5.2.2.2. Experimental design for single species studies

Experiments were conducted using 2 l borosilicate bottles containing 1 l of culture medium spiked with aliquots of biocide working solutions. *Emiliana huxleyi* was exposed to the nominal concentrations of 0.2, 0.4, 0.6, 0.8, 1.0 $\mu\text{g l}^{-1}$ zinc pyriithione; 0.4, 0.8, 1.5 $\mu\text{g l}^{-1}$ Sea-Nine 211[®]; 0.1, 0.2, 0.5 $\mu\text{g l}^{-1}$ Irgarol 1051[®]; and 0.2, 0.5, 5.0, 10, 50 $\mu\text{g l}^{-1}$ diuron. *Synechococcus* sp. was exposed to 0.4, 0.6, 1 $\mu\text{g l}^{-1}$ zinc pyriithione; 0.2, 0.4, 0.9 $\mu\text{g l}^{-1}$ Sea-Nine 211[®]; 0.2, 0.5, 1 $\mu\text{g l}^{-1}$ Irgarol 1051[®]; 0.2, 0.4, 2.2 and 3.3 $\mu\text{g l}^{-1}$ diuron. Exponentially growing cells were inoculated into bottles to obtain $\sim 1 \times 10^4$ cells

ml⁻¹. Controls and carrier controls were included in all experiments. Final concentrations of methanol for each treatment did not exceed 0.00036% (v/v). All experiments were carried out in triplicate over 72 h, without renewing the culture medium. The flasks were gently swirled by hand once daily. Samples for pigment analyses and biocide determinations were taken at the beginning and end of the experiments, while samples for Flow Cytometry were taken daily.

5.2.3. Experiment with a natural phytoplankton community

5.2.3.1. Location and sampling

The L4 site is situated 10 nautical miles south-west of Plymouth, in the western English Channel (50°15' N, 04°13' W) and has been very well characterised (Pingree 1978, Rodríguez *et al.*, 2000). This site was previously considered to be uninfluenced by local riverine inputs, but recent studies have shown that it is sporadically subjected to inputs of diluted river water, especially at spring tides during times of high river run-off (Siddorn *et al.*, 2003).

In the summer, this station is situated between stratified and transitional mixed-stratified waters and on some occasions represents the margin of the tidal front characteristic of this region (Pingree, 1978). Conceptual trophic models in the tidal frontal zone in summer reflects a multivorous web, where the large amount of phytoplanktonic biomass fuels high rates of bacterial production. Nutrient regeneration is likely to be intense due to, presumably, elevated activity of the microbial web (Rodríguez *et al.*, 2000). The seasonal phytoplankton cycle is characterised by a spring diatom bloom and a summer dinoflagellate bloom. The diatom dominated spring bloom differs annually, whilst the dinoflagellate bloom is intense and is usually dominated by *Karenia mikimotoi* (former *Gyrodinium aureolum*), which usually comprises >95% of phytoplankton carbon at its peak. The development of cyanobacterial populations appear to be favoured during phases of transition in vertical stability (November, March and August) and also during periods of high input of freshwater into the coastal zone (increases in Tamar River run-off paralleled high cyanobacterial biomass during October-November) (Rodríguez *et al.*, 2000).

Coastal water was collected from L4 station in August, 2001. The *in situ* temperature was 15 °C and salinity was 33 PSU. Phytoplankton composition⁸ on the day of sampling (21st August 2001), as characterised by cell abundance, was 15.6% flagellates (< 15 µm), 3.5% diatoms (mainly contributed by *Chaetoceros similis*, *Leptocylindrus mediterranea*, *Nitzschia delicatissima*), 2.2% colourless Dinophyceae (*Karenia* sp.), 0.2% Dinophyceae (*Heterocapsa minuta*, *Mesoporos perforatus*), 0.05% coccolithophorids, and 78.5% picoplankton. Highest carbon biomass was attributed to Dinophyceae (35%), flagellates (24%), colourless Dinophyceae (16%), diatoms (18%), and picoplankton (6%) (Fig. 5.1).

5.2.3.2. Experimental design for the natural phytoplankton community

A range of techniques was employed to characterize the effect of the selected biocides. Structural changes were identified using Analytical Flow Cytometry (AFC) to quantify cyanophytes, picoeukaryotes and nanoeukaryotes. This was coupled with High Performance Liquid Chromatography (HPLC) pigment signature data. Many pigments have strong chemotaxonomic association, which can be exploited to characterise abundance and composition of phytoplankton communities (Jeffrey *et al.*, 1997; Mackey *et al.*, 1996, 1998). The physiological state of the phytoplankton community was determined by the variable fluorescence ratio F_v/F_m , *i.e.*, the maximum efficiency of PSII photo-chemistry (Maxwell and Johnson, 2000), measured using a Fast Repetition Rate Fluorimeter (Kolber *et al.*, 1998; Suggett *et al.*, 2001). Here, we compare results with the additional technique of ¹⁴C-HCO₃⁻ incorporation (Peterson, 1980) and discuss the advantages and disadvantages.

One hundred litres of coastal surface water were collected and filtered through a 63 µm nylon mesh net to minimise zooplankton grazing. The experiment was performed by transferring volumes of 2 l of phytoplankton suspension (<63 µm) into 2 l borosilicate glass bottles and spiking with biocide working solutions. The nominal concentrations tested were selected from results of preliminary scaling experiments and were: 0.03 and 0.05 µg l⁻¹ Irgarol 1051[®], 0.5 and 5 µg l⁻¹ zinc pyrithione, 1 and 10 µg l⁻¹ diuron, and 1 and 10 µg l⁻¹ Sea-Nine 211[®]. All concentration exposures were run in triplicate, including controls and carrier controls. Bottles were randomly placed in a walk-in controlled temperature room on a 12:12 h light:dark cycle under an average temperature and irradiance of 17 °C and 230 µmol photons m⁻² s⁻¹ PAR, respectively, for 72 h.

⁸ Data obtained from the Plymouth Marine Laboratory dataset (<http://www.pml.ac.uk/L4/Index.htm>)

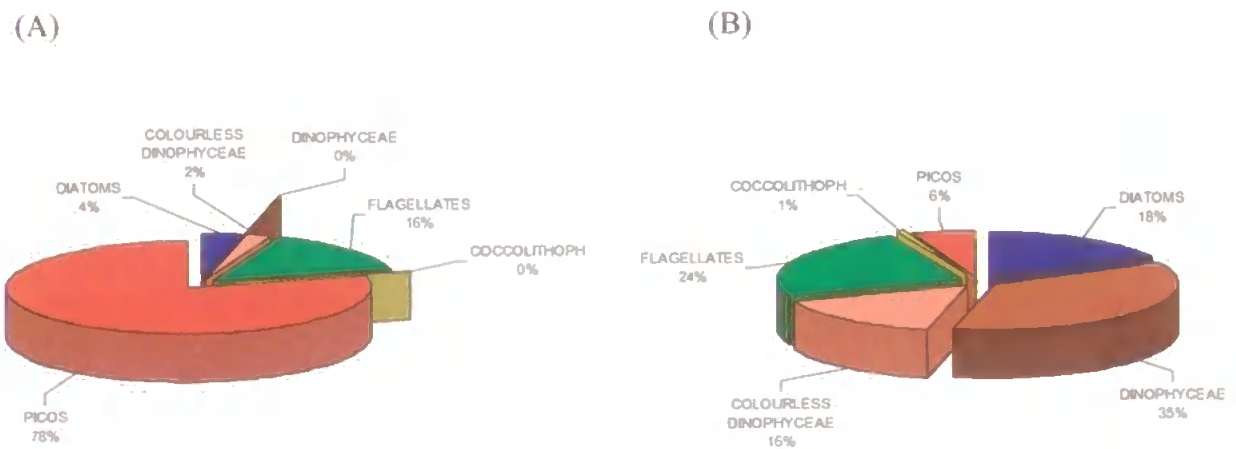


Figure 5.1. Phytoplankton composition determined by microscopy at the sampling station L4 shown as percentage of total cell numbers (A) and total carbon content in mg m^{-3} (B). Data obtained from L4 dataset (Plymouth Marine Laboratory).

To minimise any differences in phytoplankton response due to light variability on the shelves, bottles were randomly repositioned each day. Bottles were swirled by hand once daily prior to sample removal. Samples for AFC and photosynthetic efficiency determinations were taken daily. After 72 h, the experiment was terminated and variable volumes of 0.5-1.5 l of seawater were filtered for pigment determination. Samples for biocide determination were taken at the beginning and end of the experiment. Sub-surface (0.5 m depth) seawater samples (2.7 l) were also collected from the L4 station to check for biocide contamination. A set of 60 ml transparent polycarbonate bottles containing the phytoplankton community ($<63 \mu\text{m}$) under the same concentrations was also incubated to determine carbon dioxide fixation by $^{14}\text{C-HCO}_3^-$ uptake.

5.2.4. Data analysis and statistical approach

For the unialgal experiments, the effective concentration which reduces growth (cell numbers) by 50% (EC_{50}) was calculated using a graphical interpolation method (Walsh *et al.*, 1987; Walsh, 1988). Values were obtained from concentration-response curves between the percentage of the parameter inhibition (cell numbers) and the logarithm of the toxicant concentration. The lowest observable effective concentration (LOEC) and the non-observable effective concentration (NOEC) values after 72 h exposure to biocides were determined by one-way ANOVA, and followed by Tukey honest significant difference test (HSD; $\alpha = 0.05$) means contrast, in which LOEC represented

$p < 0.05$ and NOEC represented $p > 0.05$. Growth rates (μ) were estimated from the slope of a linear fitting curve between \log_2 of cell number *versus* time and are expressed as divisions day^{-1} (div day^{-1}). Pigment:chl-*a* ratio data were analysed by one-way ANOVA followed by the Tukey HSD test ($\alpha = 0.05$). All data were tested for homocedasticity (Cochran's test) and normality (χ^2 test) and 'rank' values transformed when necessary to meet the assumptions for parametric tests. These tests were available in the statistical package Statistica for Windows version 5.1 (1996 edition, StatSoft Inc., Tulsa, USA).

For the experiment with natural phytoplankton, a distance matrix (Bray Curtis similarity) was generated using fourth root transformed pigment data. Subsequently, this matrix was submitted to an analysis of similarities (ANOSIM analysis) and the contribution of individual pigments to each biocide exposure was determined by SIMPER analysis (Similarity Percentages - species contributions) by using the statistical software PRIMER for Windows version 5.2.9 (Clarke and Gorley, 2001).

Estimates of biomass as chlorophyll-*a* (chl-*a*) referring to each phytoplankton group were obtained using the matrix factorisation program CHEMTAX run under MATLAB™ (Mackey *et al.*, 1996). The pigment:chl-*a* ratios used to create the initial matrix were derived from published literature (Mackey *et al.*, 1996; Schlüter *et al.*, 2000) as well as from the unialgal culture data obtained in this study. The pigment data were run under three different pigment:chl-*a* ratios for Prymnesiophytes, obtained from the *E. huxleyi* cultures exposed to biocides (Table 5.1). For Cyanophyceae, zeaxanthin:chl-*a* ratios were constant throughout the different concentrations of biocides, as determined for *Synechococcus* sp. (Table 5.1). The pigments β -carotene, diadinoxanthin and chlorophyll *c*₁*c*₂ were excluded from the matrix as recommended by Mackey *et al.* (1996). Algal classes were selected according to the phytoplankton composition on the day of sampling (see 5.2.3.1).

5.3. Results

5.3.1. Unialgal experiments

5.3.1.1. Growth inhibition

Cell numbers of *Emiliana huxleyi* exposed to all four biocides tested significantly decreased with increasing concentrations ($p < 0.05$) (Table 5.1). The EC_{50} (72 h) values for cell numbers of *E. huxleyi* indicated differences in the sensitivity to the four biocides. EC_{50} values were $2.26 \mu\text{g l}^{-1}$ for diuron, $0.54 \mu\text{g l}^{-1}$ for zinc pyriithione, $0.35 \mu\text{g l}^{-1}$ for Sea-Nine 211[®] and of $0.25 \mu\text{g l}^{-1}$ for Irgarol 1051[®] (Table 5.3). At concentrations of $0.5 \mu\text{g l}^{-1}$ diuron and $0.2 \mu\text{g l}^{-1}$ zinc pyriithione, no effect was observed at 72 h (NOEC) ($p > 0.05$) (Table 3). The LOEC was $0.4 \mu\text{g l}^{-1}$ for zinc pyriithione and $0.1 \mu\text{g l}^{-1}$ for Irgarol 1051[®] ($p < 0.05$), both corresponding to 21% of inhibition in *E. huxleyi* cell numbers.

Under the selected experimental conditions, *Synechococcus* sp. growth rates and cell numbers were not inhibited by zinc pyriithione or Sea-Nine 211[®] exposures ($p > 0.05$), whereas exposure to diuron and Irgarol 1051[®] significantly inhibited these endpoints ($p < 0.05$) (Table 5.2). Estimated EC_{50} (72 h) values for *Synechococcus* sp. were $0.55 \mu\text{g l}^{-1}$ for diuron and $0.16 \mu\text{g l}^{-1}$ for Irgarol 1051[®]. The NOEC was $0.21 \mu\text{g l}^{-1}$ for diuron, $1.0 \mu\text{g l}^{-1}$ for zinc pyriithione, and $0.9 \mu\text{g l}^{-1}$ for Sea-Nine 211[®] ($p > 0.05$) (Table 5.3). For all exposure experiments with *Synechococcus* sp. the controls were not significantly different from the methanol carrier controls ($p > 0.05$). Results indicated that the carrier solvent did not significantly influence growth compared to the controls ($p > 0.05$).

5.3.2.2. Pigment composition

For *E. huxleyi*, all marker pigment to chl-*a* ratios changed significantly when exposed to diuron and zinc pyriithione ($p < 0.05$); whereas chlorophyll-*c*₃:chl-*a*, fuco:chl-*a* (fucoxanthin:chl-*a*) and 19'-hex:chl-*a* (19'-hexanoyloxyfucoxanthin:chl-*a*) varied with Sea-Nine 211[®] concentrations, and only fuco:chl-*a* ratio varied with Irgarol 1051[®] concentrations ($p < 0.05$) (Table 5.1). Values calculated for the pigment ratios in *E. huxleyi* controls varied from 0.423 to 0.595 for fuco:chl-*a* ratio, 0.146 to 0.193 for 19'-hex:chl-*a* ratio, and 0.111 to 0.191 for diadino:chl-*a* (diadinoxanthin:chlorophyll-*a*) ratio. A pattern of reduction in pigment to chl-*a* ratio was observed with increasing exposure to biocides, except for 19'-hex:chl-*a*, diadino:chl-*a* and chlorophyll-*c*₃:chl-*a* ratios, which increased at intermediate concentrations of biocides, followed by a decline

Table 5.1. Growth rate (μ , divisions day⁻¹), cell numbers (cell ml⁻¹), chlorophyll-*a* per cell (pg cell⁻¹) and marker pigment to chlorophyll-*a* ratios for the prymnesiophyte *Emiliana huxleyi* exposed to different types and concentrations of antifouling biocides. Data represent means of three replicated cultures.

Species	Biocide	Biocide ($\mu\text{g l}^{-1}$)	μ ^a div day ⁻¹	Cell ml ⁻¹	Chl- <i>a</i> :Cell	Chl _{c₁} :Chl- <i>a</i>	Chl _{c₂} :Chl- <i>a</i>	Fuc:Chl- <i>a</i>	19'-Hex:Chl- <i>a</i>	Diad:Chl- <i>a</i>	β -Car:Chl- <i>a</i>
<i>Emiliana huxleyi</i> (Prymnesiophyceae)	Diuron	0	1.12	72277	0.401	0.277	0.201	0.595	0.186	0.174	0.032
		MEOH	1.11	74784	0.400	0.268	0.202	0.566	0.182	0.165	0.032
		0.2	1.05	63795	0.371	0.257	0.217	0.502	0.246	0.158	0.030
		0.5	1.02	65415	0.259	0.247	0.218	0.475	0.274	0.169	0.031
		5	0.51	22255	0.254	0.238	0.210	0.483	0.269	0.171	0.029
		12	0.42	17421	0.226	0.230	0.213	0.505	0.241	0.176	0.031
		50	0.38	16975	0.155	0.157	0.191	0.446	0.233	0.185	0.025
		*	*	*	*	*	*	*	*	*	*
Zinc pyrithione	0	1.15	58589	0.458	0.237	0.108	0.423	0.193	0.191	0.022	
		0.2	1.13	56252	0.518	0.228	0.105	0.389	0.202	0.185	0.024
		0.4	1.06	45466	0.233	0.236	0.124	0.367	0.308	0.345	0.022
		0.6	0.84	25401	0.162	0.194	0.171	0.230	0.355	0.377	0.026
		0.8	0.18	6877	0.106	1.366	0.612	1.977	3.265	0.939	0.004
		1	-0.62	1228	0.116	4.700	1.252	7.053	10.367	2.087	0.000
		*	*	*	*	*	*	*	*	*	*

Table 5.1. (Cont.)

Species	Biocide	Biocide ($\mu\text{g l}^{-1}$)	μ^x div day ⁻¹	Cell ml ⁻¹	Chl- <i>a</i> :Cell	Chl _{c₂} :Chl- <i>a</i>	Chl _{c₃} :Chl- <i>a</i>	Fuc:Chl- <i>a</i>	19'-Hex:Chl- <i>a</i>	Diad:Chl- <i>a</i>	β -Car:Chl- <i>a</i>
<i>Emiliana huxleyi</i> (Prymnesiophyceae)	SeaNine 211 [®]	0	1.17	30245	0.807	0.248	0.174	0.505	0.146	0.111	0.024
		MEOH	1.13	29072	0.801	0.231	0.122	0.584	0.187	0.139	0.019
		0.4	0.74	12355	0.686	0.262	0.135	0.449	0.222	0.123	0.023
		0.8	-1.33	182	0.760	0.192	0.066	0.431	0.349	0.160	0.011
			*	*			*	*	*		
	Irgarol 1051 [®]	0	1.17	30245	0.807	0.248	0.174	0.505	0.146	0.111	0.024
		MEOH	1.13	29072	0.801	0.231	0.122	0.584	0.187	0.139	0.019
		0.1	1.02	23251	0.371	0.823	0.295	2.153	0.830	0.281	0.009
		0.2	0.86	16147	0.457	0.211	0.172	0.393	0.228	0.133	0.022
		0.5	0.52	7964	0.400	0.308	0.157	0.715	0.346	0.236	0.015
			*	*	*			*			

^x μ was estimated by taking into account the three days of the experiment.

* Significant differences in pigment ratios and growth rates due to different concentrations of biocides for each marked column ($p < 0.05$).

Table 5.2. Growth rate (μ , divisions day⁻¹), cell numbers (cell ml⁻¹), chlorophyll-*a* per cell (pg cell⁻¹) and marker pigment to chlorophyll-*a* ratios for the cyanophyte *Synechococcus* sp. exposed to different types and concentrations of antifouling biocides. Data represent means of three replicated cultures.

Species	Biocide	Biocide ($\mu\text{g l}^{-1}$)	μ^x div day ⁻¹	Cell ml ⁻¹	Chl- <i>a</i> :Cell	β -Car:Chl- <i>a</i>	Zea:Chl- <i>a</i>
<i>Synechococcus</i> <i>sp.</i> (Nostocophyceae)	Diuron	0	1.23	128481	0.0033	0.115	0.608
		MEOH	1.26	118869	0.0034	0.120	0.645
		0.2	1.03	87601	0.0037	0.137	0.643
		0.4	1.07	78281	0.0043	0.117	0.555
		2.2	0.53	29648	0.0025	0.183	0.637
		3.3	0.29	17994	0.0035	0.130	0.647
			*	*			
	Zinc pyrithione	0	1.18	53745	0.0049	0.106	0.709
		0.4	1.18	51503	0.0042	0.129	0.642
		0.6	1.15	70953	0.0046	0.106	0.663
		1	1.02	47627	0.0054	0.107	0.637
SeaNine 211 [®]	0	1.18	53745	0.0049	0.106	0.709	
	MEOH	1.19	51503	0.0045	0.107	0.680	
	0.2	1.23	56008	0.0042	0.120	0.685	
	0.4	1.18	66977	0.0040	0.122	0.673	
	0.9	0.91	36115	0.0046	0.109	0.710	
Irgarol 1051 [®]	0	1.13	83867	0.0036	0.139	0.745	
	MEOH	0.97	61145	0.0050	0.134	0.829	
	0.2	0.58	30670	0.0022	0.214	0.650	
	0.5	0.08	10795	0.0037	0.116	0.708	
	1	-0.10	7732	0.0031	0.144	0.806	
		*	*	*	*		

^x μ was estimated by taking into account the three days of the experiment.

* Significant differences in pigment ratios and growth rates due to different concentrations of biocides for each marked column ($p < 0.05$).

Table 5.3. EC_{50} , NOEC, and LOEC ($\mu\text{g l}^{-1}$) at 72 h as determined from cell numbers (cell ml^{-1}) of *Emiliania huxleyi* and *Synechococcus* sp. exposed to the four biocides tested. Numbers in parentheses indicate the percentage of inhibition at the given concentration.

	<i>E. huxleyi</i>			<i>Synechococcus</i> sp.		
	EC_{50}	NOEC	LOEC	EC_{50}	NOEC	LOEC
Zinc pyrethione	0.54	0.2	0.4 (21%)	nd	1.0	nd
Diuron	2.26	0.54	nd	0.55	0.21	0.43 (45%)
Irgarol 1051 [®]	0.25	nd	0.1 (21%)	0.16	nd	nd
Sea-Nine 211 [®]	0.35	nd	nd	1.25	0.9	nd

nd: not determined due to insufficient data

at the highest concentrations (particularly for 19'-hex:chl-*a* and chlorophyll-*c*₃:chl-*a* ratios at concentrations $\geq 5 \mu\text{g l}^{-1}$ diuron) (Table 5.1, Fig. 5.2). However, when these ratios were normalised to the number of cells, a general pattern of decreased pigment per cell with increasing toxicant concentrations was apparent (Fig. 5.3). Values calculated for *E. huxleyi* varied from 0.194-0.467 for fuco:cell, 0.074-0.149 for 19'-hex:cell, and 0.066-0.116 for diadino:cell in the control treatments.

For *Synechococcus* sp., there was no significant difference in marker pigment to chl-*a* ratios within the concentration range of the biocides tested ($p > 0.05$) except for Irgarol 1051[®], where significant differences in β -carotene:chl-*a* and chl-*a*:cell were recorded ($p < 0.05$) (Table 5.2). Values calculated for the pigment ratios in *Synechococcus* sp. controls varied from 0.106 to 0.139 for β -carotene:chl-*a* ratio and 0.608 to 0.745 for zeaxanthin:chl-*a* ratio (Table 5.2).

5.3.2.3. Antifouling biocides concentrations

In the experiments with *Synechococcus* sp., initial Irgarol 1051[®] concentrations were 0.209, 0.537, and $1.10 \mu\text{g l}^{-1}$ and after 72 h were 0.204, 0.512, and $1.081 \mu\text{g l}^{-1}$. Concentrations in the controls were $< 0.013 \mu\text{g l}^{-1}$. Initial concentrations measured in experiments with diuron were 0.21, 0.43, 2.26, and $3.26 \mu\text{g l}^{-1}$ and no change was

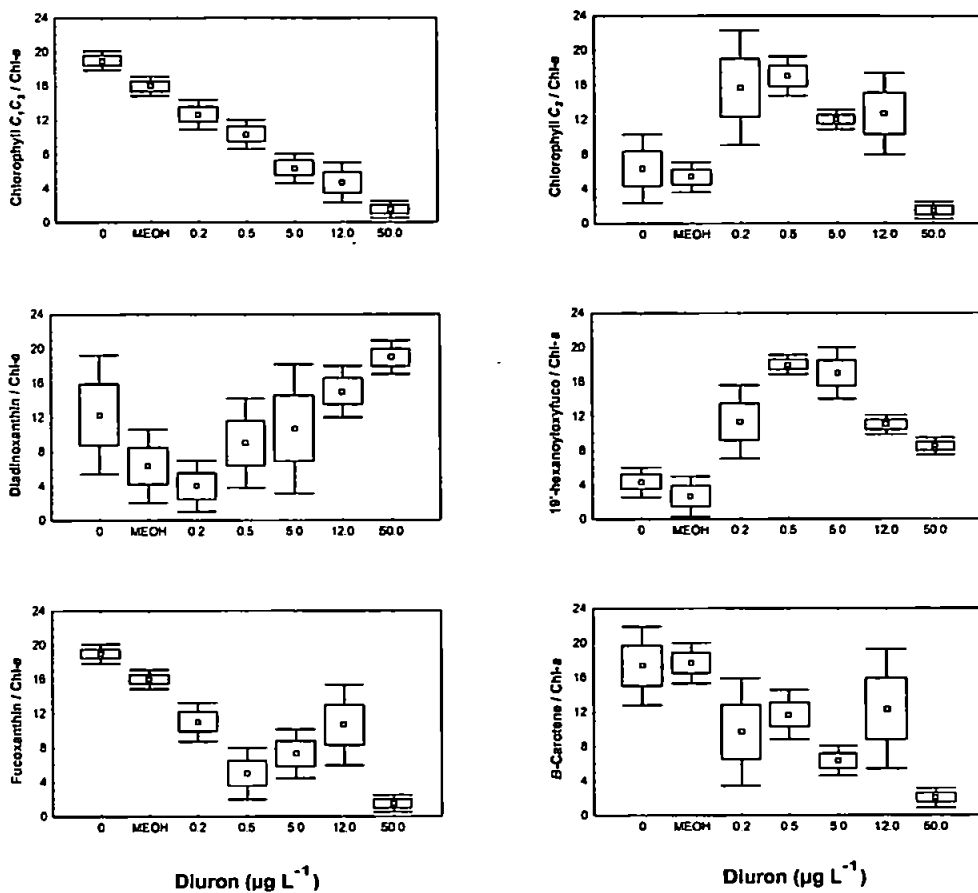


Figure 5.2. Changes in marker pigment:chlorophyll-*a* ratios of *Emiliana huxleyi* under exposure to concentrations of diuron in $\mu\text{g l}^{-1}$ (*x*-axis), controls ($0 \mu\text{g l}^{-1}$) and solvent controls (MEOH) after 72 h. Means (markers), $\pm 1.00 \times$ standard error (boxes) and $\pm 1.96 \times$ standard error (lines) of 'rank' transformed data (ANOVA one-way; Tukey HSD test as the *post hoc* comparison of means; $p < 0.05$).

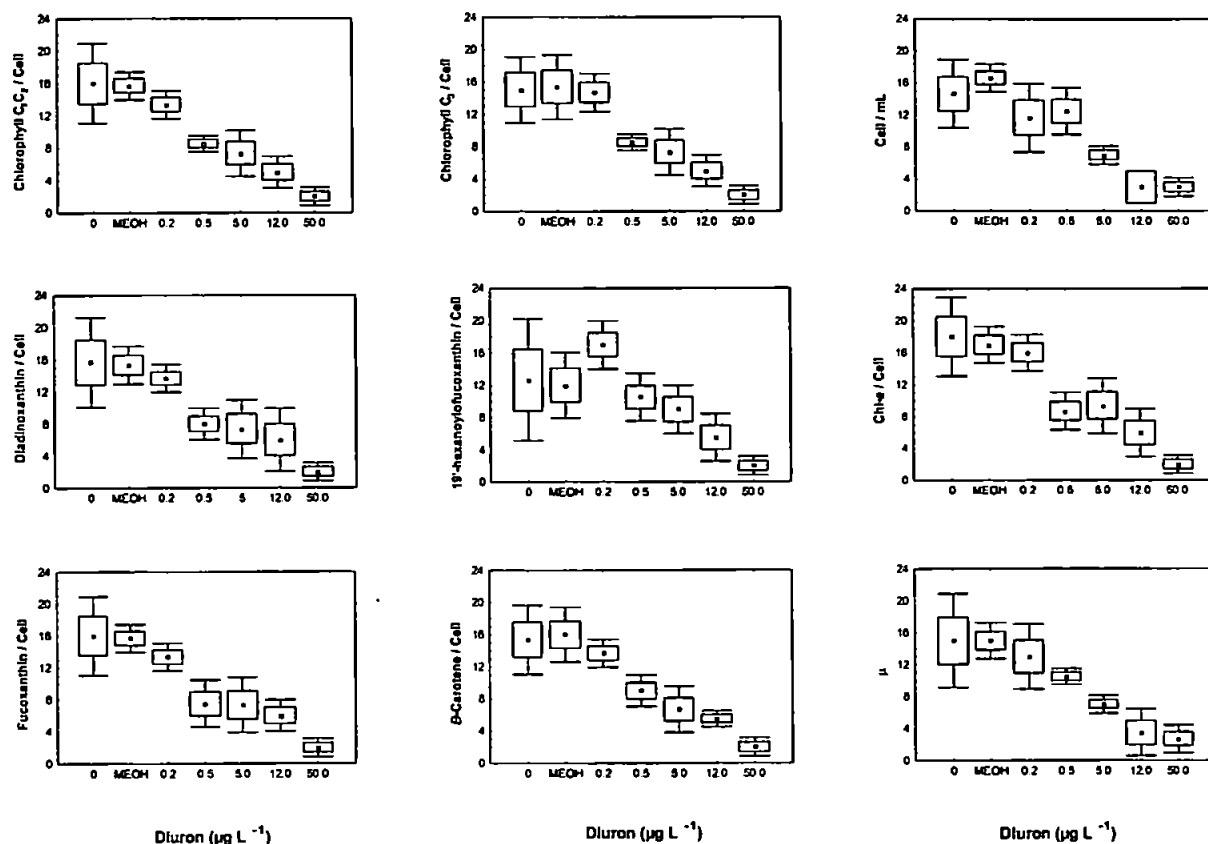


Figure 5.3. Changes in marker pigment:cell⁻¹, cell numbers (cell ml⁻¹) and growth rate (μ) of *Emiliana huxleyi* under exposure to concentrations of diuron in $\mu\text{g l}^{-1}$ (x axis), controls (0 $\mu\text{g l}^{-1}$) and solvent controls (MEOH) after 72 h. Means (markers), $\pm 1.00 \times$ standard error (boxes) and $\pm 1.96 \times$ standard error (lines) of 'rank' transformed data (ANOVA one-way; Tukey HSD test as the *post hoc* comparison of means; $p < 0.05$).

observed after 72 h (0.23, 0.42, 1.95, and 3.14 $\mu\text{g l}^{-1}$). Measured initial Sea-Nine 211[®] concentrations were 0.038, 0.12, and 0.45 $\mu\text{g l}^{-1}$ respectively. Those are lower than the nominal concentrations and probably relate to the rapid degradation of Sea-Nine 211[®] ($\frac{1}{2}$ life < 24 h). Indeed, after 72 hours no Sea-Nine 211[®] was detected in the samples. Therefore, nominal concentrations were used for the calculations of toxicological endpoints for the *Synechococcus* sp. and *E. huxleyi* experiments.

In the experiments with *E. huxleyi*, measured concentrations of Irgarol 1051[®] were 0.098, 0.195, and 0.47 $\mu\text{g l}^{-1}$ at time zero with little change after 72 h (0.087, 0.19, and 0.46 $\mu\text{g l}^{-1}$). Controls and carrier controls did not show any contamination. Diuron concentrations were 0.23, 0.54, 5.0, 12.0 and 56.0 $\mu\text{g l}^{-1}$ at the start and did not change substantially after 72 h (0.24, 0.51, 5.0, 13.2, and 55.3 $\mu\text{g l}^{-1}$).

5.3.3. Natural phytoplankton community experiment

5.3.3.1. Toxic effects on pigment composition

A comparison of the percentage each pigment contributed to the total pigment across biocide exposures is shown in Figure 5.4. Biocide treatments significantly affected the pigment composition ($R = 0.477$; $p = 0.001$; ANOSIM analysis). No significant difference was found between the lowest concentrations of all compounds tested and the controls. However, the greatest differences in pigment proportions were found at concentrations of $5 \mu\text{g l}^{-1}$ zinc pyriithione and $10 \mu\text{g l}^{-1}$ Sea-Nine 211[®]. Whilst the contribution of chl-*a* to total pigments was reduced drastically, zeaxanthin levels either increased (Sea-Nine 211[®] exposure) or remained unchanged (zinc pyriithione exposure) resulting in an increase in its relative contribution (Fig. 5.4).

There was a trend towards dissimilarity ($> 40\%$) between untreated samples and those treated with $5 \mu\text{g l}^{-1}$ zinc pyriithione and $10 \mu\text{g l}^{-1}$ Sea-Nine 211[®] (SIMPER analysis). The pigments chlorophyll-*c*₃, fucoxanthin, 19'-butanoyloxyfucoxanthin and 19'-hexanoyloxyfucoxanthin contributed to 54% of the dissimilarity between $5 \mu\text{g l}^{-1}$ zinc pyriithione and controls; whilst fucoxanthin, chlorophyll-*c*₃, alloxanthin, peridinin and 19'-hexanoyloxyfucoxanthin contributed to 54% of the dissimilarity between $10 \mu\text{g l}^{-1}$ Sea-Nine 211[®] and the controls. Dissimilarities amongst treatments ($> 30\%$) were observed for concentrations of: a) $5 \mu\text{g l}^{-1}$ zinc pyriithione with diuron (0.4 and $10 \mu\text{g l}^{-1}$), Irgarol 1051[®] ($0.03 \mu\text{g l}^{-1}$), Sea-Nine 211[®] ($1 \mu\text{g l}^{-1}$) and zinc pyriithione ($0.5 \mu\text{g l}^{-1}$); and b) $10 \mu\text{g l}^{-1}$ Sea-Nine 211[®] with zinc pyriithione ($0.5 \mu\text{g l}^{-1}$), Irgarol 1051[®] ($0.03 \mu\text{g l}^{-1}$), diuron (0.4 and $10 \mu\text{g l}^{-1}$) and Sea-Nine 211[®] ($1 \mu\text{g l}^{-1}$). All other comparisons showed dissimilarities lower than 30%. High similarities (71% to 98%) were observed between replicates, showing zeaxanthin (for the highest concentrations of zinc pyriithione and Sea-Nine 211[®]) or fucoxanthin (for all other concentrations) as the main pigment contributing to this similarity.

Estimation of the community structure using the CHEMTAX identified diatoms, dinoflagellates, prymnesiophytes and cyanophytes as the main contributors to the total chlorophyll-*a* biomass of the phytoplankton community. The presence of zeaxanthin indicated a relative increase in cyanophytes at the highest concentrations of zinc pyriithione and Sea-Nine 211[®] (Fig. 5.5), contributing to 74% and 79% to the total

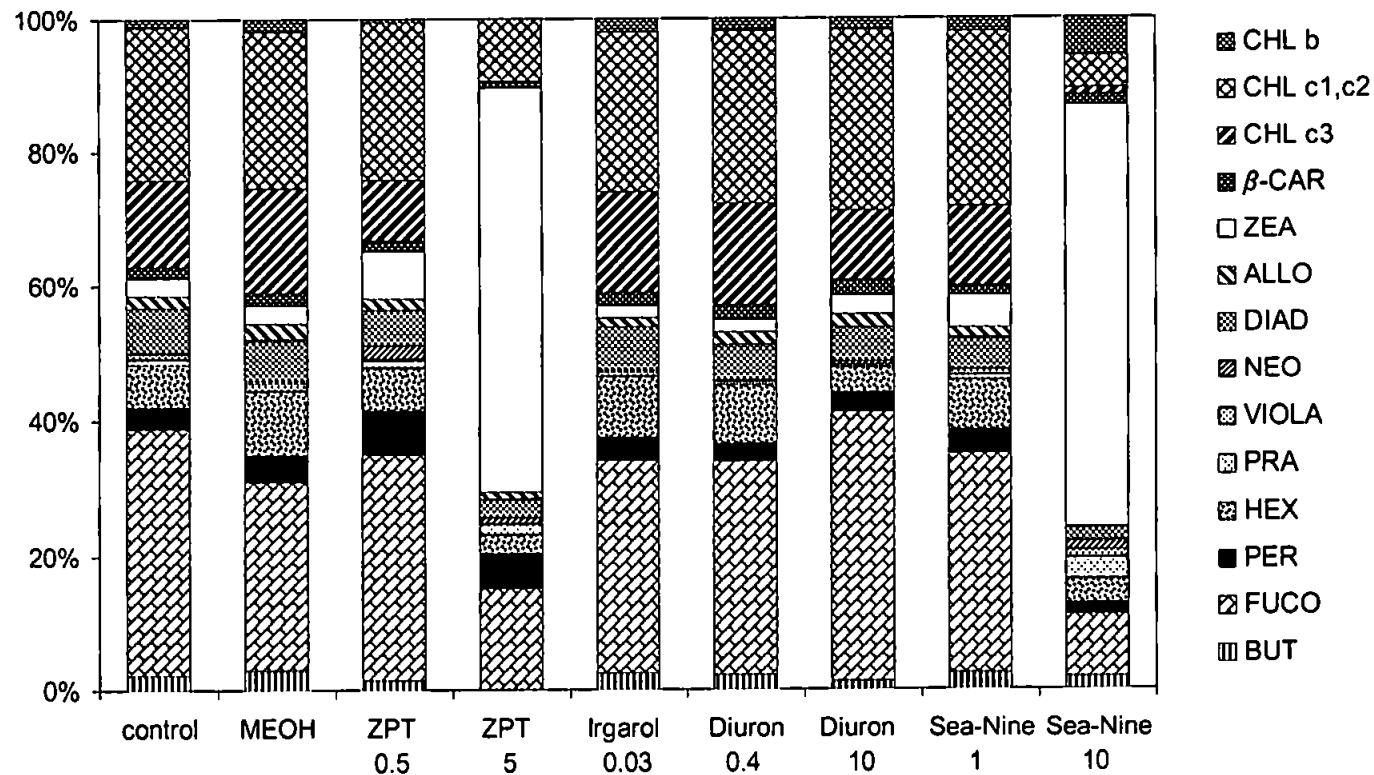


Figure 5.4. Pigment composition (% of total) of phytoplankton after 72 h exposure to concentrations ($\mu\text{g l}^{-1}$) of zinc pyriithione (ZPT), Irgarol 1051[®] (Irgarol), diuron, Sea-Nine 211[®] (SeaNine), including control (no biocide addition) and the carrier control (MEOH). Data are mean values ($n = 3$). Samples from the $0.05 \mu\text{g l}^{-1}$ Irgarol 1051[®] were lost during analyses. CHL b: chlorophyll-*b*, CHL c1,c2: Chlorophyll *c*₁,*c*₂; CHL c3: Chlorophyll *c*₃; β-CAR: β-carotene; ZEA: zeaxanthin; ALLO: alloxanthin; DIAD: diadinoxanthin; NEO: neoxanthin; VIOLA: violaxanthin; PRA: prasinoxanthin; HEX: 19'-hexanoyloxyfucoxanthin; PER: peridinin; FUCO: fucoxanthin; BUT: 19'-butanoyloxyfucoxanthin.

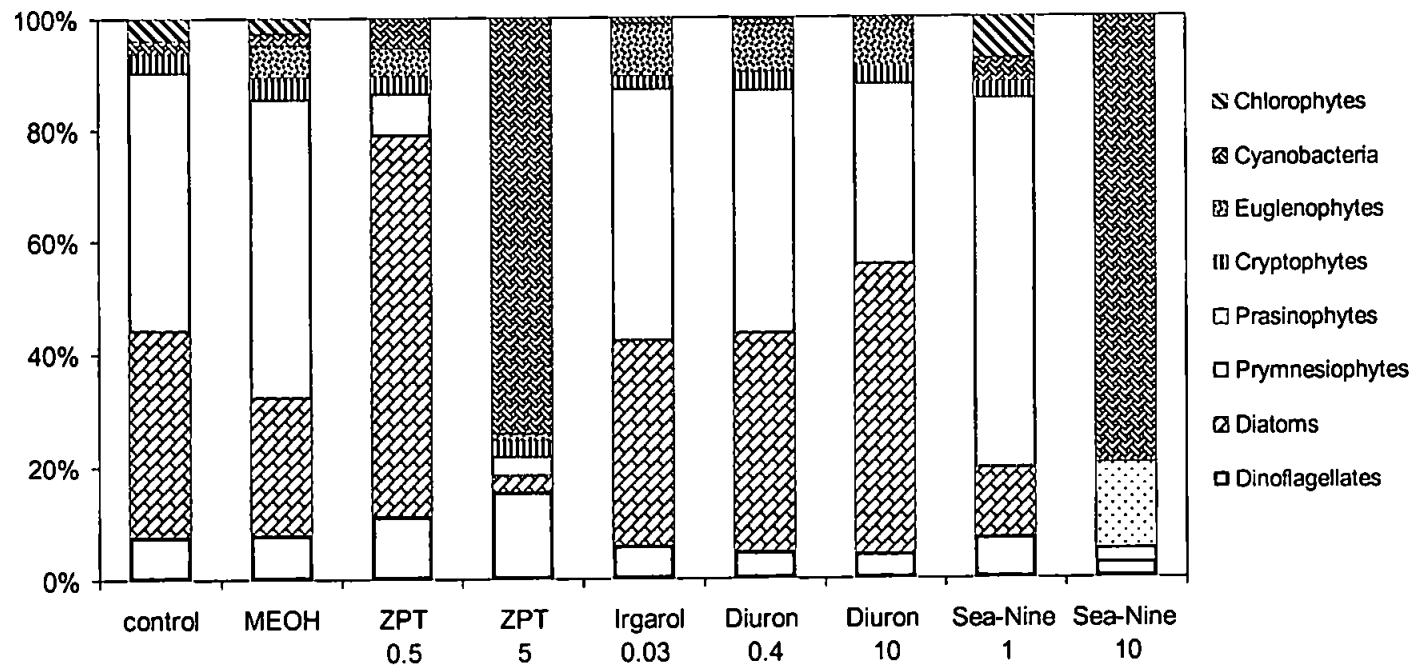


Figure 5.5. Contribution of different algal groups, as determined from pigment:chlorophyll-*a* ratios using CHEMTAX, after 72 h exposure to concentrations ($\mu\text{g l}^{-1}$) of zinc pyriothione (ZPT), Irgarol 1051[®] (Irgarol), diuron, Sea-Nine 211[®] (Sea-Nine), including the control (no biocide addition) and the carrier control (MEOH).

biomass (as chlorophyll-*a*), respectively. The contribution of dinoflagellates to the biomass (chlorophyll-*a*) appeared to increase under exposures to 0.5 and 5 $\mu\text{g l}^{-1}$ zinc pyrithione (11% and 15%, respectively) when compared to the controls (8%), although it remained almost unchanged under the other biocide exposures. At concentrations of 10 $\mu\text{g l}^{-1}$ diuron and 0.5 $\mu\text{g l}^{-1}$ zinc pyrithione, indications of a reduction in prymnesiophytes (33% and 8%) and an increase in diatoms (51% and 68%) relative to controls (48% and 30%, respectively) were observed. At 1 $\mu\text{g l}^{-1}$ Sea-Nine 211[®], a reduction in diatoms and an increase in prymnesiophytes were observed.

5.3.3.2. Toxic effect on phytoplankton growth

AFC results demonstrated reductions between total cell numbers as percentage compared to the controls under different biocide concentrations after 72 h exposure ($p < 0.05$); no reductions, however, were found for 0.03 $\mu\text{g l}^{-1}$ Irgarol 1051[®] and 0.4 $\mu\text{g l}^{-1}$ diuron ($p > 0.05$; One-way ANOVA, Least Significant Difference *post hoc* test) (Fig. 5.6). Cell numbers fell by 7% on exposure to 50 ng l^{-1} Irgarol 1051[®], were reduced by 66% and 95% at 0.5 and 5 $\mu\text{g l}^{-1}$ of zinc pyrithione, respectively, by 38% and 79% at 1 and 10 $\mu\text{g l}^{-1}$ of Sea-Nine 211[®], and were reduced by 40% at 10 $\mu\text{g l}^{-1}$ of diuron (Fig. 5.6).

The relative contribution of cyanophyte, nanoeukaryote and picoeukaryote cell numbers to the population for each biocide treatment is shown in Figure 5.7. The relative contributions of cyanophytes to the population increased at the highest concentrations of zinc pyrithione and Sea-Nine 211[®]; picoeukaryotes appeared to contribute similarly (5 $\mu\text{g l}^{-1}$ zinc pyrithione) or more (10 $\mu\text{g l}^{-1}$ Sea-Nine 211[®]) compared to the controls, whilst the contribution of nanoeukaryotes decreased (Fig. 5.7). Compared to controls, results of absolute cell numbers indicated a decrease in nanoeukaryotes following exposures to zinc pyrithione, Sea-Nine 211[®] and 10 $\mu\text{g l}^{-1}$ diuron ($p < 0.05$), a reduction in picoeukaryote numbers in all biocide exposures ($p < 0.05$) except for 1 $\mu\text{g l}^{-1}$ Sea-Nine 211[®], and no change in cyanophyte abundances under all treatments ($p > 0.05$), except for 10 $\mu\text{g l}^{-1}$ diuron (Fig. 5.8).

5.3.3.3. Toxic effect on photosynthesis

The development of the phytoplankton community was followed daily using *in vivo* chlorophyll fluorescence. All four antifouling biocides impaired photosynthesis at the

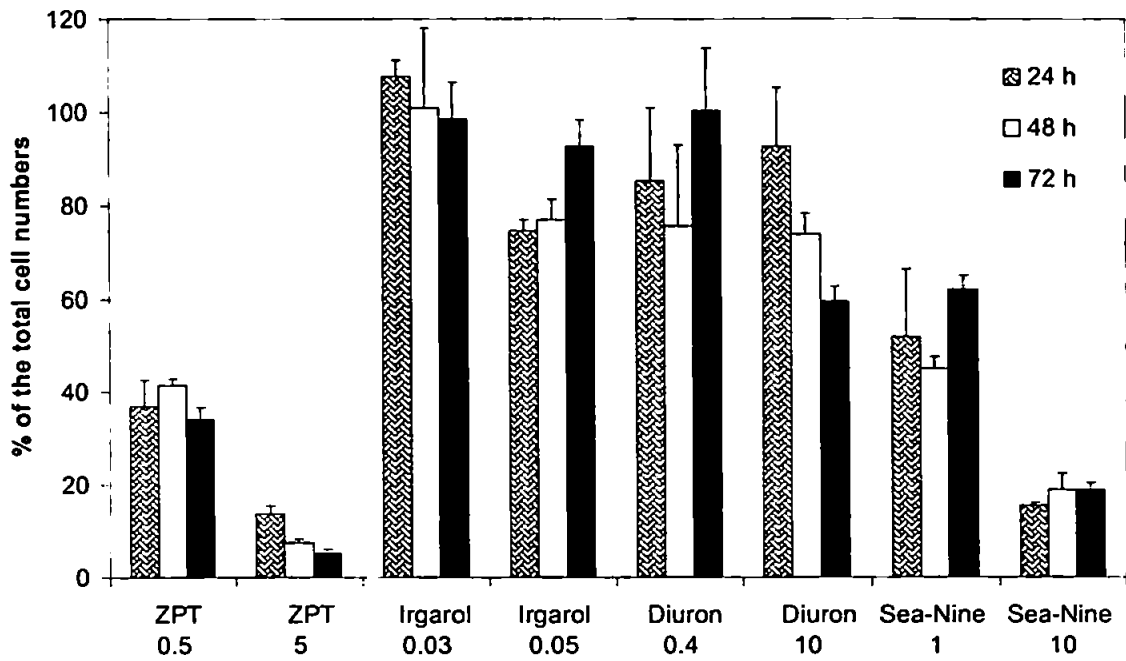


Figure 5.6. Percentage of total cell numbers (measured by AFC) related to carrier controls (MEOH) after 24 h, 48 h and 72 h exposure to concentrations ($\mu\text{g l}^{-1}$) of zinc pyriothione (ZPT), Irgarol 1051[®] (Irgarol), diuron, and Sea-Nine 211[®] (Sea-Nine). Data are mean values \pm SD (n = 3).

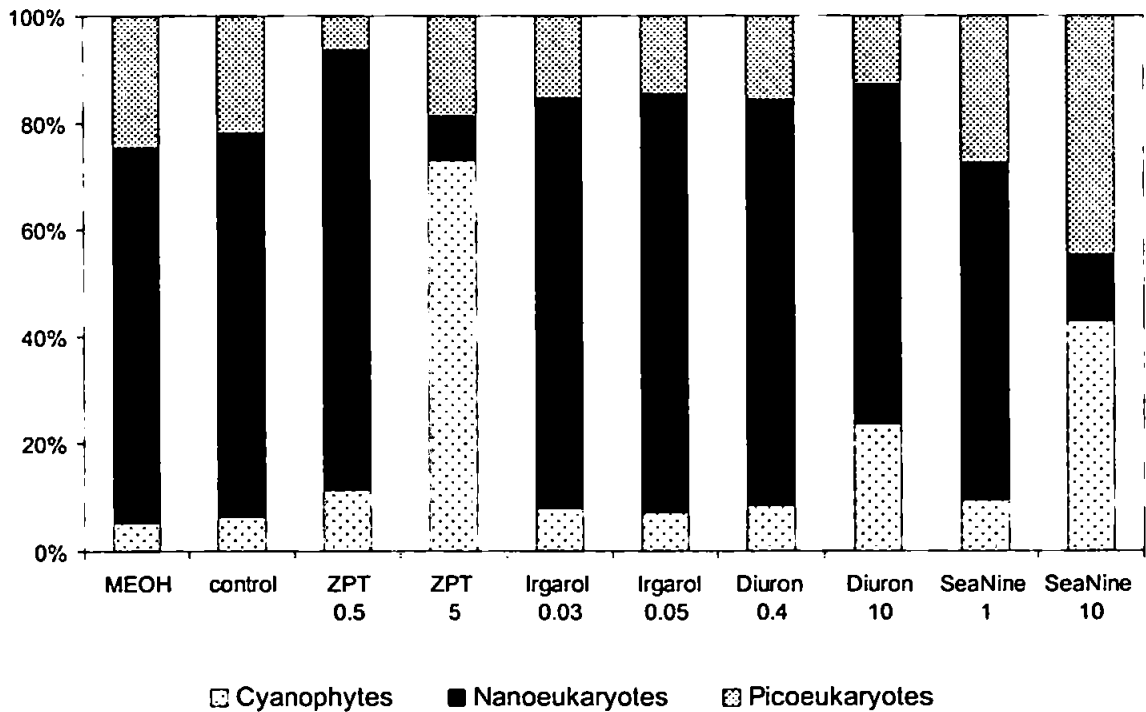


Figure 5.7. Number of picoeukaryote, nanoeukaryote and cyanophyte cells (as percentage of total cells) measured by AFC after 72 h exposure to concentrations ($\mu\text{g l}^{-1}$) of zinc pyriothione (ZPT), Irgarol 1051[®] (Irgarol), diuron, Sea-Nine 211[®] (Sea-Nine), including the control (no biocide addition) and the methanol control (MEOH). Data are mean values (n = 3).

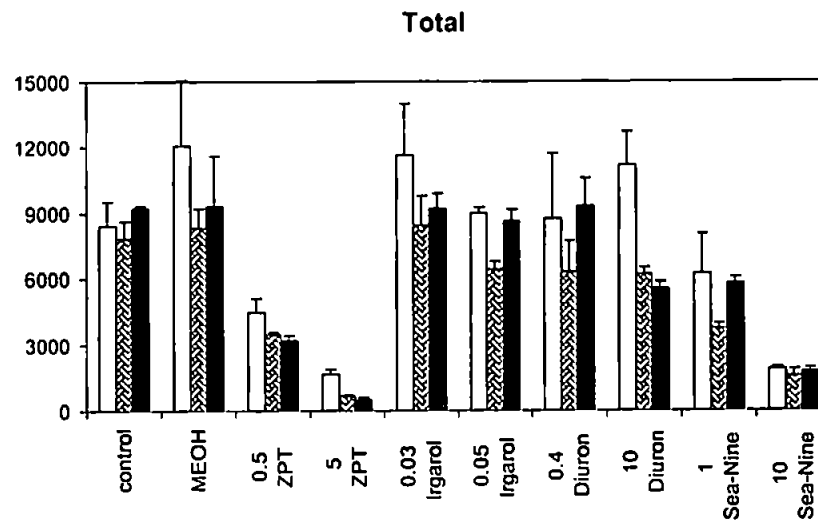
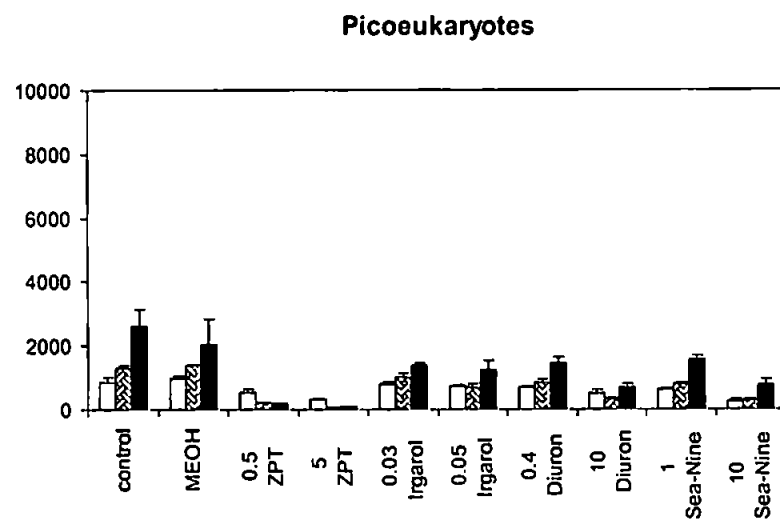
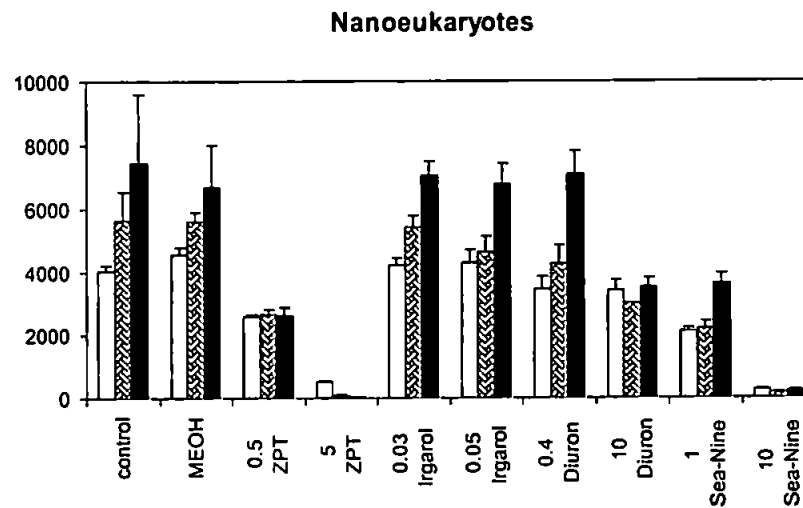
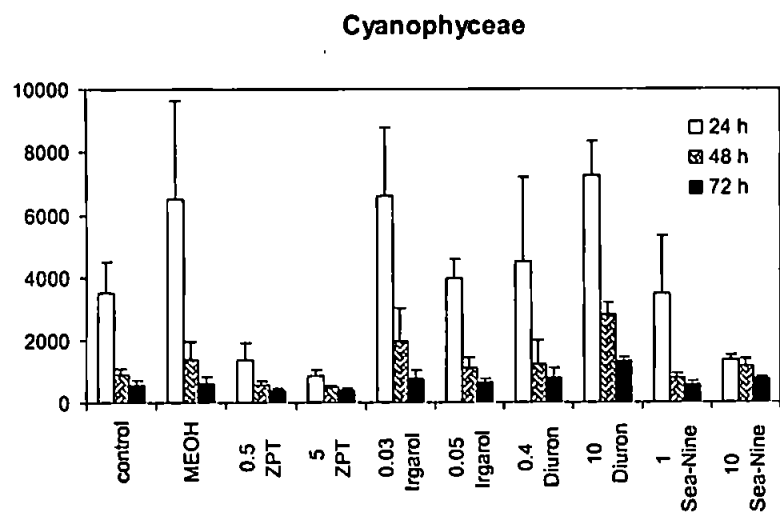


Figure 5.8. Number of cyanophyte, picoeukaryote, nanoeukaryote cells and total cells measured by AFC after 24, 48 and 72 h of exposure to concentrations ($\mu\text{g l}^{-1}$) of zinc pyriothione (ZPT), Irgarol 1051[®] (Irgarol), diuron, Sea-Nine 211[®] (Sea-Nine), including the control (no biocide addition) and the methanol control (MEOH). Data are mean values ($n = 3$).

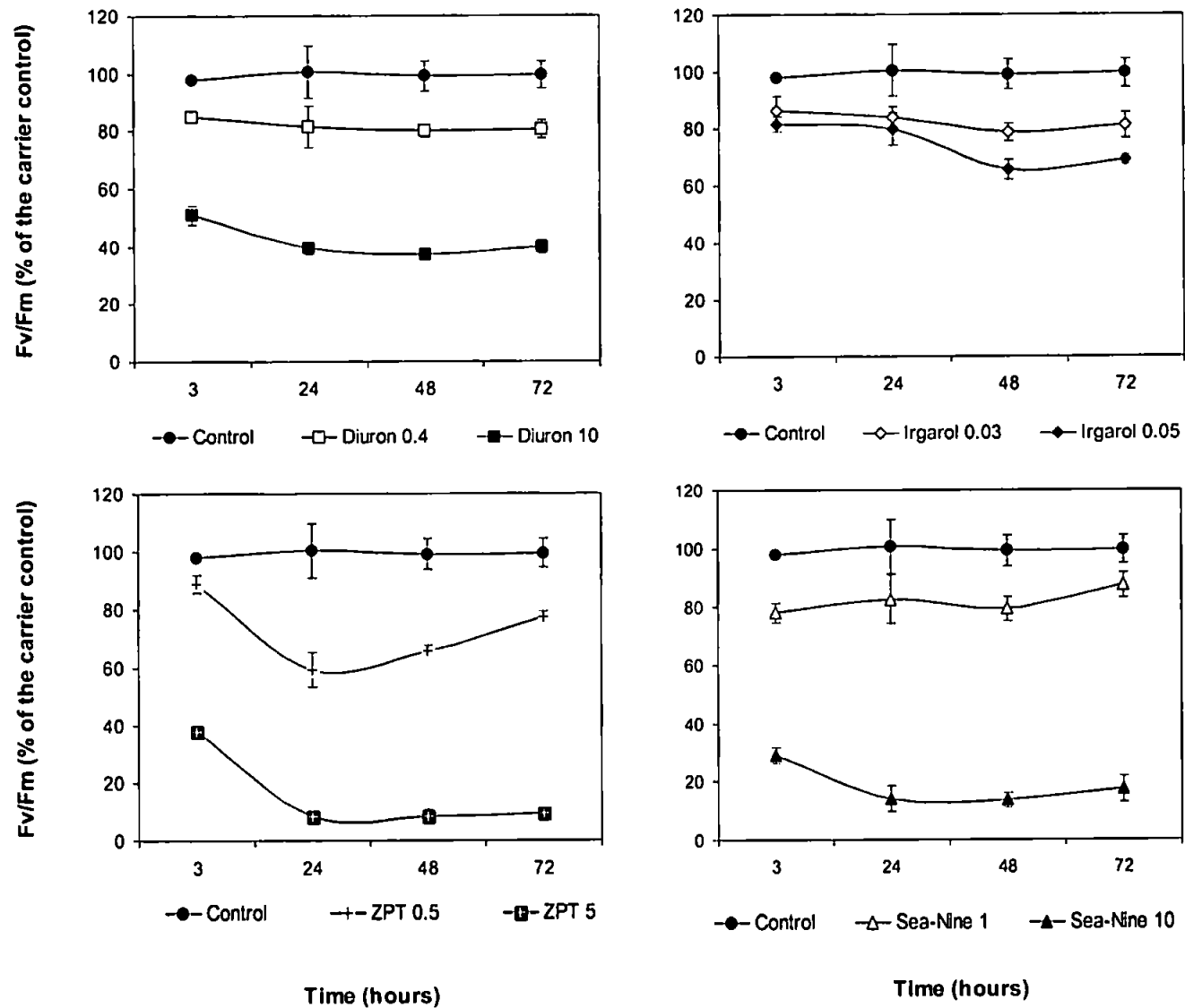


Figure 5.9. Photosynthetic efficiency (F_v/F_m) of phytoplankton exposed to concentrations ($\mu\text{g l}^{-1}$) of zinc pyriithione (ZPT), Irgarol 1051[®] (Irgarol), diuron and Sea-Nine 211[®] (Sea-Nine) for the period of the experiment (72 h). Data are mean values \pm SD ($n = 3$).

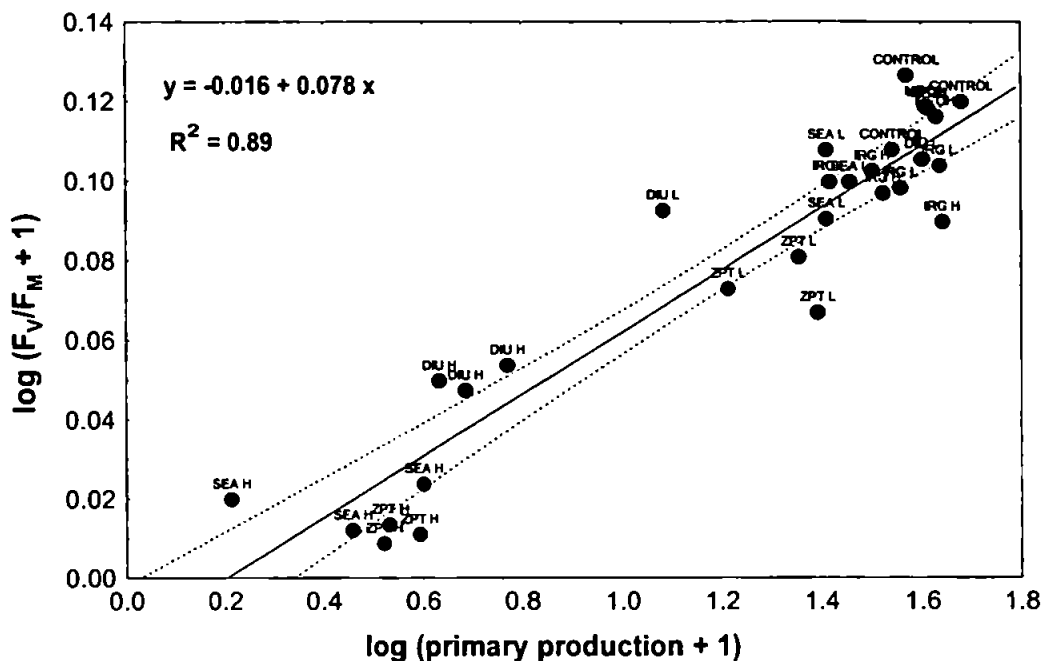


Figure 5.10. A linear model relating primary production (measured as ^{14}C -uptake) and F_v/F_M data after 24 h exposure of natural phytoplankton to Irgarol 1051[®], zinc pyriithione, Sea-Nine 211[®] and diuron ($p = 0.0001$). The confidence intervals (95%) correspond to the outer bounds on the graph. Controls, carrier controls (MEOH), diuron $0.4 \mu\text{g l}^{-1}$ (DIU L) and $10 \mu\text{g l}^{-1}$ (DIU H), Irgarol 1051[®] $0.03 \mu\text{g l}^{-1}$ (IRG L) and $0.05 \mu\text{g l}^{-1}$ (IRG H), zinc pyriithione $0.5 \mu\text{g l}^{-1}$ (ZPT L) and $5 \mu\text{g l}^{-1}$ (ZPT H), Sea-Nine 211[®] $1 \mu\text{g l}^{-1}$ (SEA L) and $10 \mu\text{g l}^{-1}$ (SEA H).

concentrations tested. After 72 h, results indicated severe damage in F_v/F_M compared to controls at $10 \mu\text{g l}^{-1}$ Sea-Nine 211[®] and $5 \mu\text{g l}^{-1}$ zinc pyriithione (Fig. 5.9), with reductions of 83% and 91%, respectively. The lower exposure concentrations of zinc pyriithione ($0.5 \mu\text{g l}^{-1}$) and Sea-Nine 211[®] ($1 \mu\text{g l}^{-1}$) inhibited F_v/F_M by 23% and 13%, respectively. Concentrations of 0.4 and $10 \mu\text{g l}^{-1}$ diuron reduced F_v/F_M by 20% and 60%, whilst 0.03 and $0.05 \mu\text{g l}^{-1}$ Irgarol 1051[®] reduced the same parameter by 19% and 31%. At the lowest concentrations of the biocides tested, F_v/F_M appeared to increase with time of exposure particularly with zinc pyriithione and Sea-Nine 211[®]. Inhibition by zinc pyriithione was most pronounced after 24 h exposure, contrasting with Sea-Nine 211[®], where the inhibition decreased with time of exposure (Fig. 5.9). Reversibility of impairment of the phytoplankton was faster for zinc pyriithione than for Sea-Nine 211[®], recovering 18% of the photosynthetic efficiency within 48 h of exposure to $0.5 \mu\text{g l}^{-1}$ (Fig. 5.9).

In vivo inhibition of fluorescence measured using FRRF was compared with inhibition of $^{14}\text{C-HCO}_3^-$ incorporation following 24 h of incubation. A linear regression indicates a coefficient of determination of 0.89 ($p = 0.0001$) (Fig. 5.10).

5.3.3.4. Antifouling booster biocide concentrations

No Irgarol 1051[®] was detected at the sampling site ($n = 3$) or in the control treatments ($n = 3$). Concentrations of Irgarol 1051[®] in the carrier controls on day one of the experiment were close to the detection limit. Initial Irgarol 1051[®] concentrations were within $\pm 5\%$ of the nominal concentrations ($n = 2$). Diuron concentrations on day one were 0.4 and 9.7 $\mu\text{g l}^{-1}$ and after 72 h were 0.4 and 6.0 $\mu\text{g l}^{-1}$, respectively. Due to Sea-Nine 211[®] degradation, nominal concentrations were reported.

5.4. Discussion

5.4.1. Unialgal experiments

The effects of four antifouling biocides on growth and pigmentation of two species of algae were assessed using unialgal cultures. For *E. huxleyi* growth, Irgarol 1051[®] was the most toxic ($\text{EC}_{50} = 0.25 \mu\text{g l}^{-1}$) and diuron the least toxic ($\text{EC}_{50} = 2.26 \mu\text{g l}^{-1}$). Although Sea-Nine 211[®] is known to be readily degraded (Jacobson and Willingham, 2000), and is therefore suggested to be less harmful to non-target species, it actually impaired *E. huxleyi* growth to a similar extent to that of Irgarol 1051[®] ($\text{EC}_{50} = 0.35 \mu\text{g l}^{-1}$). Values of NOEC for Sea-Nine 211[®] and zinc pyrithione in *Synechococcus* sp. were higher than the EC_{50} s calculated for *E. huxleyi*, which suggests that *Synechococcus* sp. is more resistant to these two biocides. Comparing the EC_{50} s of the two species, *Synechococcus* sp. was more sensitive to diuron than *E. huxleyi*, whereas both showed similar sensitivities to Irgarol 1051[®]. Our data indicate higher sensitivities in the species tested than those reported for the freshwater alga *Selenastrum capricornutum* exposed to Sea-Nine 211[®] ($\text{EC}_{50} = 3 \mu\text{g l}^{-1}$), diuron ($\text{EC}_{50} = 45 \mu\text{g l}^{-1}$), and Irgarol 1051[®] ($\text{EC}_{50} = 11 \mu\text{g l}^{-1}$) (Fernández-Alba *et al.*, 2002). Differences in sensitivities observed in this study and compared to the literature are probably related to the species studied, culture conditions and the measures of toxic response, and are further discussed.

In cultures of *E. huxleyi*, changes in pigment:chlorophyll-*a* ratios were reported following exposures to the antifouling biocides. Changes in 19'-

hexanoyloxyfucoxanthin, diadinoxanthin and chlorophyll c_3 with increasing concentrations of biocides showed opposite trends when normalised to chlorophyll- a or cell numbers (Fig. 5.2 and Fig. 5.3), resulting from the relative reduction of chlorophyll- a . When, however, chlorophyll- a is removed from the assessment and effects are related to cell numbers, overall reductions in the phytoplankton pigments with increasing concentrations of biocides are clearly apparent. 19'-hexanoyloxyfucoxanthin is a light-harvesting pigment and its relative increase might be related to hydroxylation of fucoxanthin to 19'-hexanoyloxyfucoxanthin, causing a reduced efficiency of energy supply by the light harvesting complex (Vanleeuwe and Stefels, 1998). This coincides with a decrease in fucoxanthin:chl- a and an increase in 19'-hex:chl- a ratios under diuron exposure in this study. Increases in 19'-hex:chl- a and diadino:chl- a ratios have also been reported by Schlüter *et al.* (2000) for *Phaeocystis* sp. and *E. huxleyi* following exposure to increasing light levels.

In contrast to *E. huxleyi*, *Synechococcus* sp. showed no overall differences in pigment to chlorophyll- a ratios at the concentrations of biocides tested, owing mostly to the lack of inhibition on growth (zinc pyrithione and Sea-Nine 211[®]). For Irgarol 1051[®], however, where growth inhibition was more pronounced, the changes in β -carotene:chl- a and chl- a :cell ratios might have been related to protective mechanisms. When exposed to PSII inhibitors (such as Irgarol 1051[®] and diuron), algae decrease their electron transport capacity and increase the production of oxy-radicals, giving rise to destructive effects when the protective mechanisms are overwhelmed (Dahl and Blanck, 1996). In contrast to algae, cyanobacteria lack the zeaxanthin cycle-dependent antenna quenching, and so other mechanisms of energy dissipation, such as D1 exchange might be involved in cell protection (Sane *et al.*, 2002). The unialgal culture studies reported here indicated that, under the selected experimental conditions, *Synechococcus* was more sensitive to PSII inhibitors than *E. huxleyi*. Elucidating why the biochemical mechanisms appear more susceptible to PSII inhibitors in *Synechococcus* sp. requires further investigation.

The values of pigment to chl- a ratios obtained for controls of *Emiliania huxleyi* (0.423-0.595 for fuco:chl- a , 0.146-0.193 for 19'-hex:chl- a , 0.111-0.191 for diadino:chl- a) and *Synechococcus* sp. (0.60-0.74 for zeaxanthin:chl- a) were in close agreement with those reported in the literature (Schlüter *et al.*, 2000, Henriksen *et al.*, 2002). Schlüter *et al.* (2000) found values from 0.106-0.722 for fuco:chl- a ratios, 0.230-0.504 for 19'-hex:chl- a ratios, and 0.136-0.276 for diadino:chl- a ratios in cultures of *E. huxleyi*, and values of 0.673 were reported for zeaxanthin:chl- a in *Synechococcus* sp. cultures

(Henriksen *et al.*, 2002). While it is well documented that changes in natural environmental conditions (e.g. nutrient-limitation, irradiance and cell growth phase) can alter pigment to chl-*a* ratios (Schlüter *et al.*, 2000; Henriksen *et al.*, 2002), our results indicate that anthropogenically derived substances such as biocides can also influence pigment to chl-*a* ratios and therefore must be taken into account when estimating phytoplankton composition from group-specific pigment ratios used in programmes such as CHEMTAX.

5.4.2. Natural phytoplankton community experiment

5.4.2.1. Toxic impairment on pigment composition

Estimation of phytoplankton composition using CHEMTAX provides an indication of the compositional changes following exposures to biocides. Our results showed a selective toxicity to the natural phytoplankton assemblage, especially following exposure to the highest concentrations of zinc pyriithione and Sea-Nine 211[®] tested. A relative increase in peridinin indicated an increase of dinoflagellates and a relative increase in zeaxanthin denoting a greater proportion of cyanophytes present in the community under exposure to zinc pyriithione. Similar structural changes to these were also noted at 10 $\mu\text{g l}^{-1}$ Sea-Nine 211[®], although the relative proportion of peridinin in this case remained almost unchanged. Such tolerance to both biocides (zinc pyriithione and Sea-Nine 211[®]) is corroborated by the lack of sensitivity found in *Synechococcus* sp. toxicity experiments.

Under almost all biocide exposures, cyanophycean cell numbers remained unchanged compared to controls, even though marked reductions in other phytoplankton groups occurred. For instance, picoeukaryotes were sensitive to almost all biocide treatments, possibly as a result of their large surface:volume ratio, absorbing more chemical per body mass. The selective reduction of other groups resulted in a relative increase in cyanophytes abundance mainly under zinc pyriithione and Sea-Nine 211[®] exposure. Moreover, AFC results and CHEMTAX estimates were in good agreement in detecting these changes in cyanophytes. Such relative lack of sensitivity of cyanophytes in comparison to other groups could possibly lead to development of potentially toxic Cyanophyceae species with environmental consequences.

Cyanophycean cell numbers increased under exposure to 10 $\mu\text{g l}^{-1}$ diuron; this was not detected from the pigment results, due probably to them being masked by major

algal groups. *Synechococcus* sp. has been reported to be capable of exchanging the D1:1 and D1:2 proteins, triggered by diuron treatments (Campbell *et al.*, 1996), therefore conferring resistance to PSII inhibitors. Cells containing the D1:2 form generally have a higher quantum yield of oxygen evolution and lower non-photochemical quenching than cells containing only D1:1 protein (Campbell *et al.*, 1996). The transient exchange of the D1:1 protein, which appears to be the initial response, may thus provide the time required for full cellular acclimation to an increased excitation pressure by modification in protein and lipid composition. This mechanism might have aided cyanophytes to outcompete other algal groups in the community, when exposed to high diuron concentrations.

Although the concentrations of Irgarol 1051[®] tested were too low to induce any detectable impact under the selected experimental conditions, it is likely that environmental concentrations (of up to 1.42 $\mu\text{g l}^{-1}$; Thomas *et al.*, 2001) would modify phytoplankton composition (Readman *et al.*, 2004). Other studies have demonstrated that, depending on the concentrations, Irgarol 1051[®] (0.07 to 2.5 $\mu\text{g l}^{-1}$) can modify algal community composition, by reductions in prymnesiophytes and development of pennate diatoms, cryptophytes, chrysophytes and cyanophytes (Bérard *et al.*, 2003; Readman *et al.*, 2004). A similar pattern was observed in this study for 0.5 $\mu\text{g l}^{-1}$ zinc pyrithione and 10 $\mu\text{g l}^{-1}$ diuron, where the relative contribution of diatoms increased while prymnesiophytes (indicated by 19'-hexanoyloxyfucoxanthin) were reduced. Reported environmental concentrations of diuron (up to 6.74 $\mu\text{g l}^{-1}$; Thomas *et al.*, 2001) also pose a threat to phytoplankton, as indicated in this study. Very little data is available on environmental concentrations of Sea-Nine 211[®] and zinc pyrithione (www.pml.ac.uk/ace).

Phytoplankton have been shown to be more sensitive to antifoulants than other planktonic groups, such as bacteria and crustaceans (Fernández-Alba *et al.*, 2002). The toxic responses of phytoplankton, such as compositional changes and low productivity, might lead to an indirect impact on grazers by reducing their food resources. These compositional changes also affect nutrient cycling through the microbial food web and subsequent flow to higher trophic levels (Goldman *et al.*, 1987). Bioaccumulation and consequent trophic transfer of antifoulants is unlikely to be of major significance, given their partition coefficients (Konstantinou and Albanis, 2004). In addition, the rapid degradation of Sea-Nine 211[®] and zinc pyrithione reduce exposure concentrations with time (Jacobson and Willingham, 2000; Turley *et al.*, 2000).

5.4.2.2. Toxic effect on photosynthesis

The quantum efficiency of PSII (F_v/F_M) was diminished by all concentrations of all biocides tested on the natural phytoplankton community. Diminished F_v/F_M can indicate a large proportion of inactive PSII reaction centres due to oxidation, degradation of D1 proteins (Anderson *et al.*, 1997) or severely reduced pigment concentrations (Marwood *et al.*, 2001). Based on F_v/F_M measurements, the phytotoxicity of the biocides for the natural phytoplankton community can be ranked: Irgarol 1051[®] > zinc pyrithione ~ Sea-Nine 211[®] > diuron. However, it should be borne in mind that variations in this toxicity ranking of biocides might differ for other communities depending on species composition or physiological state.

Irgarol 1051[®] affected F_v/F_M at very low ($0.03 \mu\text{g l}^{-1}$) and environmentally relevant concentrations. Even though a higher concentration of diuron was required to impair photosynthesis (0.4 and $10 \mu\text{g l}^{-1}$), similar levels (up to $6.74 \mu\text{g l}^{-1}$) have been detected in the environment (Thomas *et al.*, 2001). Degradation products of diuron (photoproducts and metabolites) can also pose a toxic threat to the environment (Tixier *et al.*, 2001). However, since Irgarol 1051[®] and diuron are not easily degraded, exposures and toxicity were not significantly reduced over time during the experiments in this study. Zinc pyrithione and Sea-Nine 211[®] are, however, transformed more rapidly than diuron and Irgarol 1051[®] (Thomas, 2001) reducing exposure concentrations and toxic response. Zinc pyrithione and Sea-Nine 211[®] have low partition coefficients and hence less affinity to bind to organic sediments, thus leading to a larger proportion of dissolved compound potentially affording enhanced exposure to phytoplankton.

Reversibility of F_v/F_M impairment was faster for zinc pyrithione than for Sea-Nine 211[®], which was observed at the lower concentrations tested, most likely due to the fact that these compounds undergo degradation within hours. Biological processes appear to be more important than abiotic processes for the transformation of the active substance of Sea-Nine 211[®] (DCOI) with half-lives varying from < 1 h to 24 h according to the matrices and temperature investigated (Jacobson and Willingham, 2000). In contrast to Sea-Nine 211[®], zinc pyrithione is rapidly transformed by photolysis with a half-life of < 1 h in natural seawater (Turley *et al.*, 2000). It is assumed that zinc pyrithione is transformed *via* the structurally comparable omadine disulphide, which is rapidly transformed to heterocyclic compounds with one ring under environmentally realistic test conditions. Toxicity of metabolites is lower than zinc pyrithione and omadine

sulphide (Turley *et al.*, 2000; Olin, 1997) and this may have contributed to the F_V/F_M recovery observed after 24 h exposure. Algal survival mechanisms might be triggered when moderate stress is induced and the physiological processes are returned to normal following cessation of exposure.

5.4.2.3. FRRF versus $^{14}\text{C-HCO}_3^-$ uptake

Photosynthesis-related endpoints are sensitive measures for assessing short-term responses to the antifouling biocides studied. Although quantum efficiency of PSII (F_V/F_M) and $^{14}\text{C-HCO}_3^-$ -uptake measure different phases of the photosynthetic process, a good correlation between both methods was reported ($r^2 = 0.89$).

Analysis of chlorophyll fluorescence is a sensitive and early indicator of damage to the photosynthetic apparatus (Krause and Weis, 1991) whilst $^{14}\text{C-HCO}_3^-$ -uptake measures the end result of the photosynthetic process, i.e., carbon assimilation (Williams, 1993). Compared to other fluorescence techniques, FRRF provides a better signal to noise ratio and allows more robust measurements in low chlorophyll samples (Suggett *et al.*, 2001). A 1:1 relationship between $^{14}\text{C-HCO}_3^-$ measurements and FRRF estimates of carbon fixation has been reported by the originators of the technique (Kolber and Falkowski, 1993). Good comparability between a pulse-amplitude modulated fluorometer and $^{14}\text{C-HCO}_3^-$ -based primary production has also been reported by Dorigo and Leboulanger (2001) for freshwater periphyton exposed to herbicides and for natural phytoplankton exposed to Irgarol 1051[®] (Nyström *et al.*, 2002).

5.5. Conclusions

The differential toxicity of the tested biocides to algae induced modifications to the community structure of the natural phytoplankton under investigation, which resulted in changes to the taxonomic composition of natural seawater. The cyanophyte *Synechococcus* sp. was more resistant than the prymnesiophyte *Emiliana huxleyi* to zinc pyriithione and Sea-Nine 211[®] in culture experiments. In contrast, *Synechococcus* sp. was more sensitive than *E. huxleyi* to diuron, while exposure to Irgarol 1051[®] showed a similar impact on both species. Irgarol 1051[®] toxicity was up to twice that of zinc pyriithione and Sea-Nine 211[®], whilst diuron was the least toxic of the biocides studied.

The biocides impacted on the selected natural phytoplankton community and the differences in group-specific sensitivity were detected through pigment composition.

Following exposure to zinc pyrithione and Sea-Nine 211[®], the pigment zeaxanthin proportionally increased indicating a relative increase in cyanophytes, which was corroborated with AFC results. The Cyanophyceae is a group of particular concern given their occurrence as toxic blooms (Jacoby *et al.*, 2000). Thus, consequences of biocide pollution on marine diversity during conditions which promote toxic blooms require further investigation in mesocosm-type studies. As identified in this study, further investigations should also be conducted on inter-species variations in pigment to chlorophyll-*a* ratios following exposure to toxicants. Using the correct pigment ratios for the ambient environmental conditions would improve accuracy in applying CHEMTAX to estimate phytoplankton group-specific biomass.

Biocidal effects at very low concentrations were also detected through physiological impairment as measured by ¹⁴C-HCO₃⁻ uptake and F_V/F_M. F_V/F_M is considered to be a sensitive and rapid endpoint to assess the impact of antifouling booster biocides. The Fast Repetition Rate Fluorometer is a comparatively new technology and has many advantages in research of pollution effects on phytoplankton.

Concentrations of antifouling booster biocides in the environment are still a matter for concern. In the UK, the use of Irgarol 1051[®] was revoked by legislation in July 2003. While both Sea-Nine 211[®] and zinc pyrithione are readily degradable, my results suggest that the consequences of continuous use, providing persistent contamination, could be environmentally damaging. The effects of acute versus chronic exposure need to be researched further.

Chapter 6

(I) Effects of nutrient status on toxicity and (II) Spatial distribution patterns of antifouling biocides and phytoplankton within Plymouth waters

6.1. Influence of nutrient status on toxicity

6.1.1. Introduction

In addition to xenobiotic contamination, environmental problems can also be associated with eutrophication, particularly in areas with excessive nutrient loading and/or restricted water exchange, such as estuaries, bays, or marinas. The trophic state of an ecosystem is of significance in its susceptibility to toxic effects. Inputs of nutrients or organic matter stimulate productivity and provide a rich source of particulate and dissolved material in eutrophic systems (McCarthy and Bartell, 1988).

Different nutrient regimes can affect the bioconcentration of hydrophobic organic contaminants by altering microalgal lipid content (Halling-Sørensen *et al.*, 2000). Studies have suggested that periphyton communities with the lowest biomass tend to be more sensitive to stress (Blanck, 1985) and that the capacity of recovery from the toxic stress is affected by trophic status (Pratt and Barreiro, 1998). However, it remains unclear if communities of different trophic status can differ in sensitivity to toxic stress for reasons other than chemical interactions (*e.g.* different species composition and diversity, different biomass) (Lozano and Pratt, 1994). Studies have shown some influence of nutrient status on the intensity of diquat and arsenate toxic actions (Wängberg and Blanck, 1990; Lozano and Pratt, 1994; Pratt and Barreiro, 1998). Phosphorus and nitrogen are essential nutrients required by algae and bacteria in aquatic ecosystems. Phosphorus is present in deoxyribonucleic acid (DNA), ribonucleic acid (RNA), membrane lipids, and nucleotide phosphates, and is stored as energy-rich polyphosphate. Nitrogen, however, is used for amino acid synthesis. The uptake and

assimilation of both P and N by algal cells require the expenditure of energy as adenosine triphosphate (ATP) and/or reducing equivalents (Beardall *et al.*, 2001).

An experiment was designed to make a preliminary assessment of toxic stress induced by the PSII inhibitor Irgarol 1051[®] on natural phytoplankton communities under different nutrient conditions. To characterise such influences, phytoplankton structure was estimated through pigment composition and cell abundances of major groups (cyanophytes, cryptophytes, pico- and nanoeukaryotes) following a short-term exposure to Irgarol 1051[®]. Irgarol 1051[®] was chosen as the stress inducing toxicant as it inhibits photosynthesis by binding to the D1 protein in the PSII, and it is also known to be highly toxic to phytoplankton (see chapters 3, 4 and 5).

6.1.2. Methods

6.1.2.1. Preparation of Irgarol 1051[®] solutions

A stock solution of $2 \mu\text{g } \mu\text{l}^{-1}$ was prepared by dissolving 0.5004 g of Irgarol 1051[®] in a volume of 250 ml of methanol. An Irgarol 1051[®] working solution was sequentially prepared by diluting 1 ml of the Irgarol 1051[®] stock solution into 100 ml of filtered seawater (0.45 μm Millipore filter), resulting in a $0.02 \mu\text{g } \mu\text{l}^{-1}$ solution. Test-solutions were prepared by adding 50 μl sub-stock aliquots into 2 l bottles filled with seawater from the L4 station. A working solution of methanol was prepared by diluting 1 ml of methanol into 100 ml of filtered seawater (0.45 μm Millipore filter). Carrier controls were prepared by adding 50 μl aliquots of the diluted methanol to the 2 l bottles.

6.1.2.2. Experiment with a natural phytoplankton assemblage

In February 2001, surface seawater was collected from the L4 sampling station. A temporal biological and physico-chemical dataset of this station is available (<http://www.pml.ac.uk/L4>). Seawater was stored in 50 litre Nalgene carboys and was taken to the laboratory within 2 h. After complete homogenisation, seawater was filtered through a 200 μm mesh net to remove larger zooplankton grazers and then distributed in 26 2 l-borosilicate bottles. Bottles were then randomly placed in a walk-in controlled temperature culture room and left for 24 h for phytoplankton acclimatisation to light and temperature conditions. After 24 h, all bottles received essential metals and silicate according to the enrichment f/2 described in Guillard (1975), modified by diluting enrichment concentrations to 1/5 (v/v), giving a final enrichment of f/10. Concentrations

of vitamins were used following Schone and Schone (1982). Essential metals, silicate and vitamins were added to the 2 l bottles using a 0.2 μm sterile filter. The experimental design is illustrated in the Figure 6.1.

Nutrients were added according to the following (modified from Graneli *et al.*, 1999): 39 μM NO_3^{-2} and 1.5 μM PO_4^{-3} for N treated microcosms; 3 μM NO_3^{-2} and 17 μM PO_4^{-3} for P treated microcosms; 39 μM NO_3^{-2} and 17 μM PO_4^{-3} for N+P treated microcosms; and no addition of NO_3^{-2} or PO_4^{-3} for TSV microcosms. Nitrate was added as aliquots of NaNO_3 solution and phosphate as NaH_2PO_4 solution with ultra-pure water.

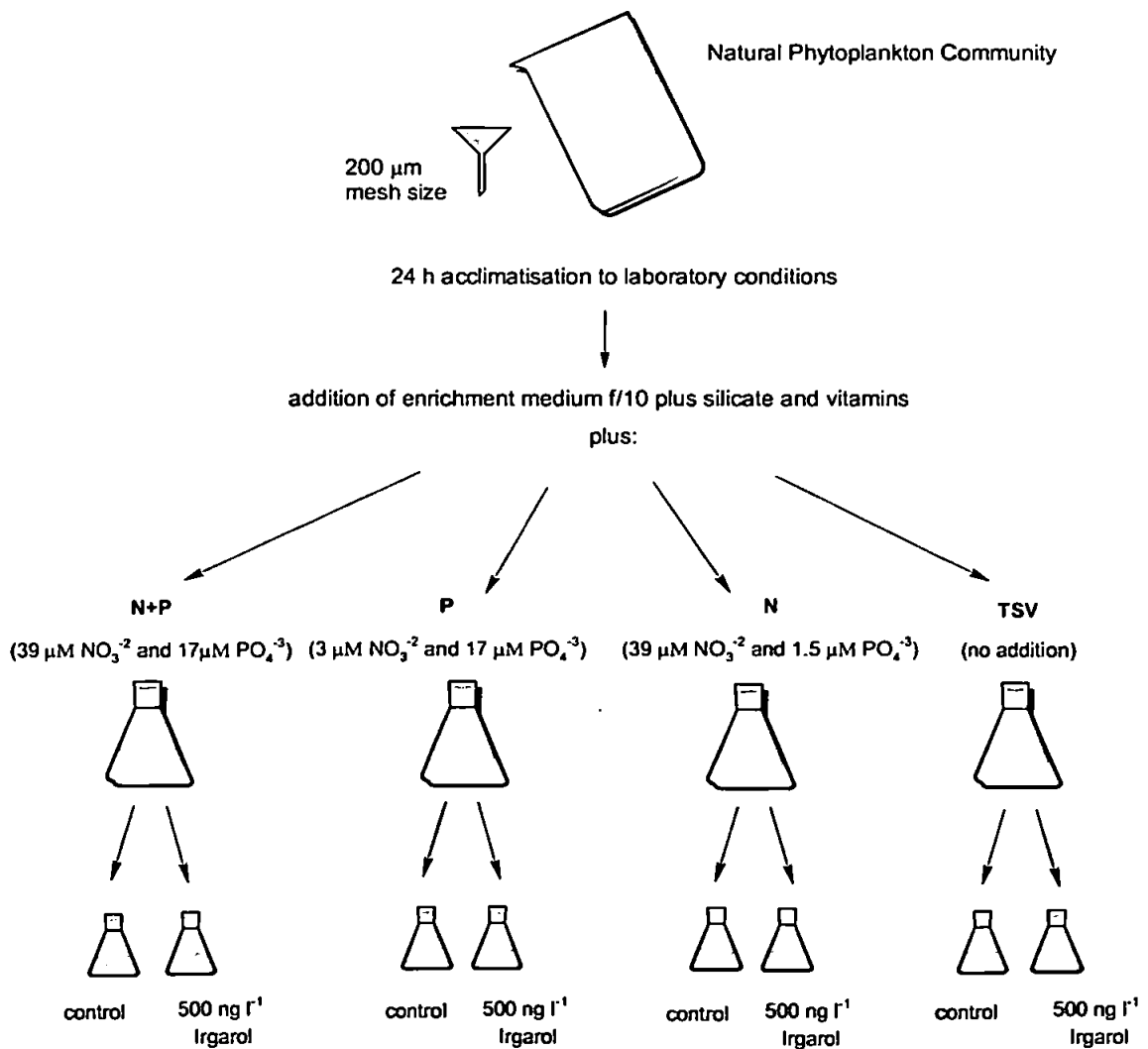


Figure 6.1. Experimental design to evaluate the potential influence of nitrate (N) and phosphate (P) additions on the toxicity of Irgarol 1051[®].

All treatments were investigated in triplicate. A 50 μl aliquot of sub-stock Irgarol 1051[®] solution ($0.02 \mu\text{g } \mu\text{l}^{-1}$) was added to each nutrient treatment bottle and nutrient controls, in order to obtain a nominal concentration of $0.5 \mu\text{g l}^{-1}$. The same amount of methanol was added to the carrier controls. No addition of either methanol or Irgarol 1051[®] was spiked to a third nutrient control (see Fig. 6.1). The bioassay was performed in batch conditions, *i.e.*, without renewal of the test medium, exposed to $100 \mu\text{E m}^{-2} \text{ s}^{-1}$ of photosynthetic active radiance (PAR), under a light/dark cycle of 12/12 h, at $17 \pm 2 \text{ }^\circ\text{C}$, for a period of 5 days. Samples for pigment analyses (1-1.5 l), Irgarol 1051[®] determination ($\sim 100 \text{ ml}$), and nutrient (PO_4^{-3} and NO_3^{-2}) analysis (60 ml) were taken at the beginning and the end of the experiment. Samples for flow cytometry analyses (20 ml), were taken daily during the 5 day experiment. These samples were fixed in buffered formaldehyde (to a final concentration of 2 %) and were stored as described in Chapter 2, section 2.5.7.1, until analysis. Salinity (36 PSU) was measured using a manual refractometer (ATAGO S/Mill-E). Light was supplied by Phillips Cool White bulbs and the intensity was measured using a LT Lutron LX-101 Digital Lux Meter.

6.1.2.3. Data analysis

Cell abundances data were analysed by two-way ANOVA (Factorial 4x2). The objective was to evaluate the effects of Irgarol 1051[®] addition on both total cells and group abundances grown under the selected nutrient conditions (excess of nitrate and/or phosphate). In addition to the 'main effects', a *post hoc* test was undertaken to determinate interactions between treatments using the Least Significant Difference (LSD) test ($\alpha = 0.05$). All data were tested for homocedasticity (Cochran's test) and normality (χ^2 test) and 'rank' values transformed when necessary to meet the assumptions for parametric tests ($p > 0.05$). These tests were made using the statistical package Statistica for Windows version 5.1 (1996 edition, StatSoft Inc., Tulsa, USA).

6.1.3. Results

Phytoplankton composition on the day of sampling (27th February 2001), as characterised by microscopy (cell abundance), was 13% flagellates (66% flagellates $2 \mu\text{m}$; 28% flagellates $5 \mu\text{m}$, and 6% cryptomonads), 0.03% diatoms (mainly *Navicula sp.*, *Paralia sulcata*, and *Nitzschia closterium*), 0.17% colourless Dinophyceae (98% colourless flagellates), $< 0.001\%$ Dinophyceae (*Scropsiella sp.*), 87% picoplankton, with a complete absence of Coccolithophorids (Fig. 6.2A). Ciliate abundances contributed

0.01% (mainly *Strombidium* sp.). Highest carbon biomass was attributed to flagellates (61%), picoplankton (18%), ciliates (8%), colourless Dinophyceae (6%), diatoms (5.1%), and Dinophyceae (0.4%) (Fig. 6.2B) (data from the Plymouth Marine Laboratory dataset <http://www.pml.ac.uk/L4/Index.htm>).

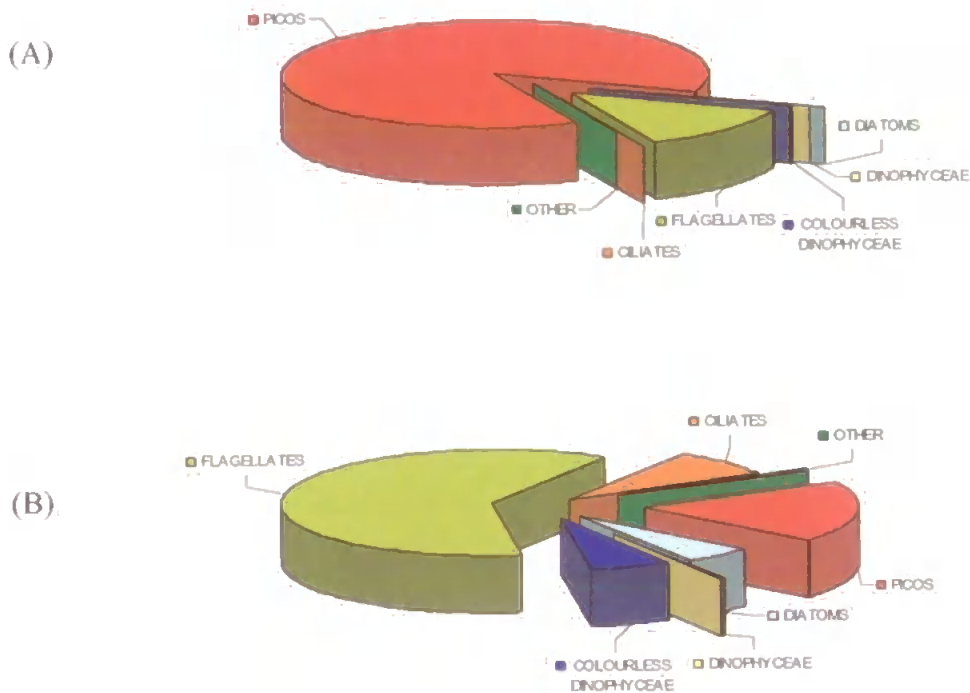
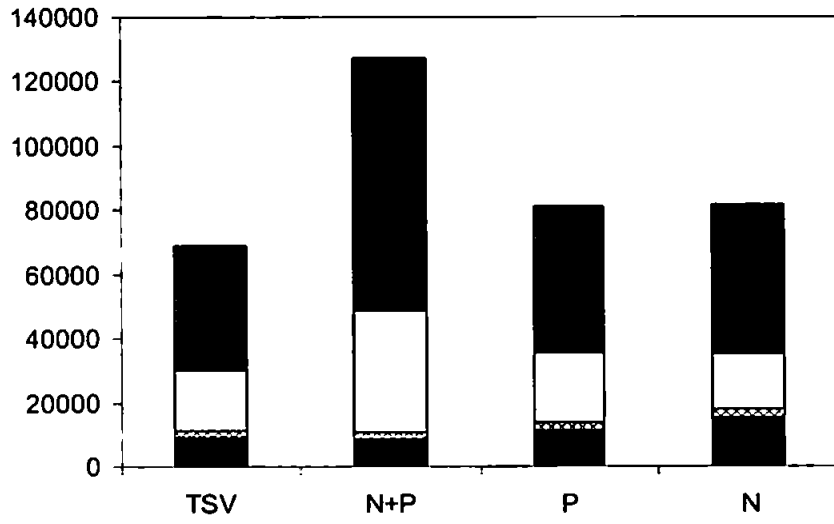


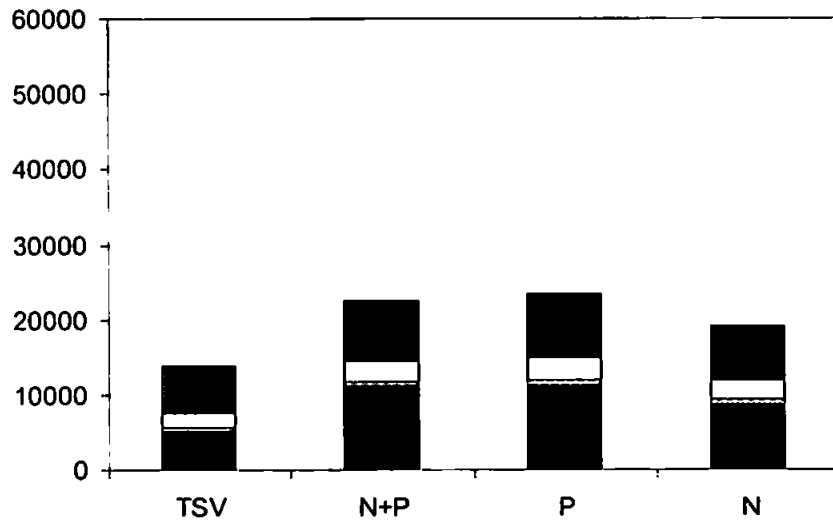
Figure 6.2. Phytoplankton composition determined by microscopy at the sampling station L4 shown as (A) percentage of total cell numbers and (B) percentage of total carbon content. Data obtained from L4 dataset (Plymouth Marine Laboratory).

Two-way ANOVA analysis of AFC measurements showed that, after 4 days of experiment, total cell abundances were significantly influenced by the different nutrient regimes ($p = 0.012$) and with the addition of Irgarol 1051[®] ($p < 0.0001$), although no significant interaction between effects of nutrient and Irgarol 1051[®] were observed ($p = 0.624$) (Appendix Table III.i.a). Amongst treatments without Irgarol 1051[®], only the microcosms treated with nitrate plus phosphate (N+P) showed significant increases in total cell abundances compared to the non-treated microcosms (TSV) ($p = 0.0043$; LSD *post hoc* test) and to the nitrate only treated (N) microcosm ($p = 0.0417$; LSD *post hoc* test) (Fig. 6.3 and Appendix Table III.i.b). After four days of exposure to 500 ng l⁻¹ Irgarol 1051[®], cellular density of all groups was severely affected with the exception of

(A)



(B)



■ Cyanophytes ▨ Cryptophytes □ Picoeukaryotes ■ Nanoeukaryotes

Figure 6.3. Cell abundances (cell ml^{-1}) for picoeukaryotes, nanoeukaryotes, and cyanophytes determined by AFC in (A) controls and (B) treated with 500 ng l^{-1} Irgarol 1051[®], grown under different nutrient conditions after 4 days of experiment. TSV: no nitrate or phosphate added; N+P: nitrate plus phosphate addition; P: only phosphate addition; N: only nitrate addition.

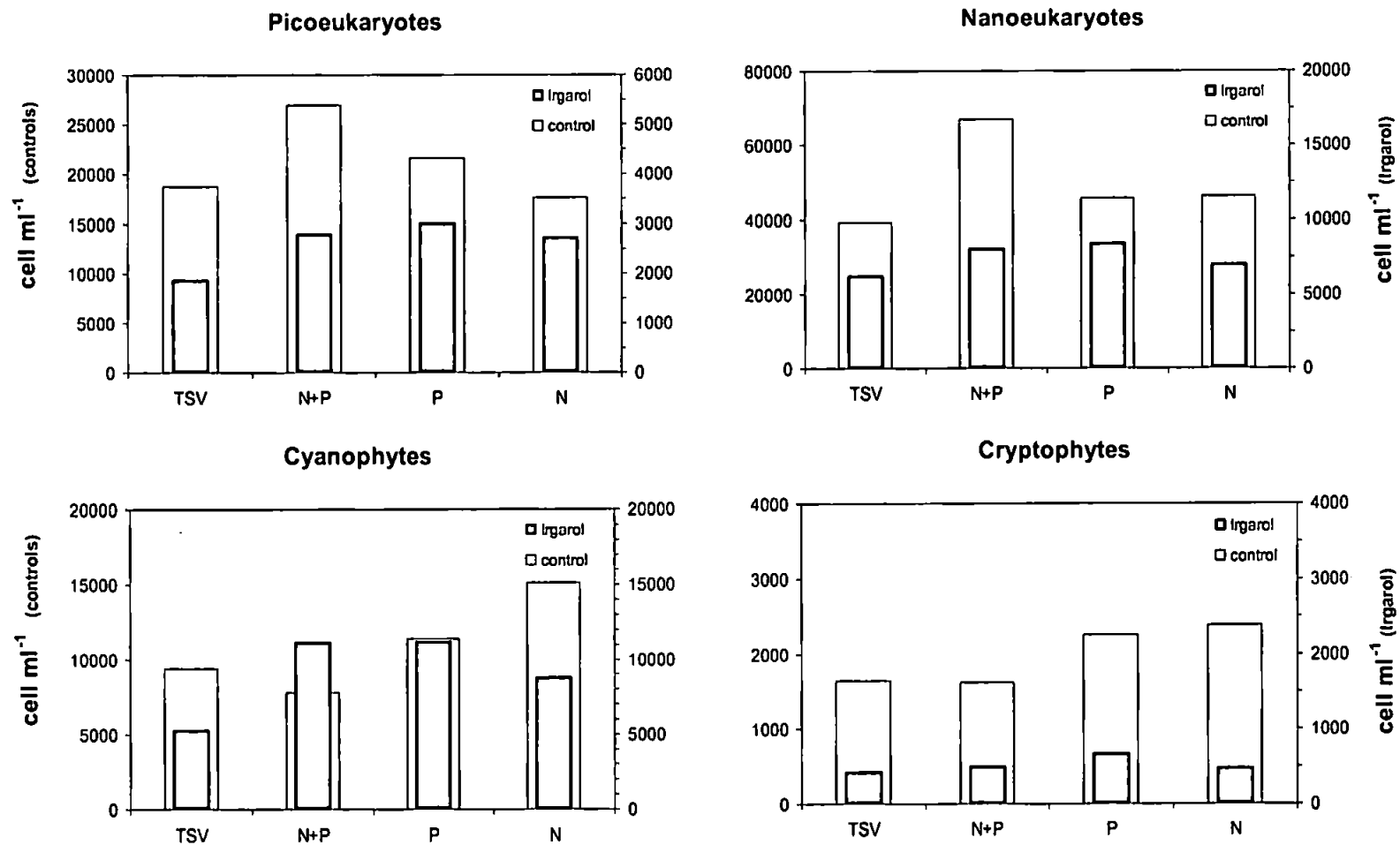


Figure 6.4. Cell densities (cell ml⁻¹) of controls (empty bars) and Irgarol 1051[®] treatment (filled bars) showing the effects of nutrient addition. TSV: no nitrate or phosphate added; N+P: nitrate plus phosphate addition; P: only phosphate addition; N: only nitrate addition. Values on the right y-axis are for Irgarol 1051[®] treatment and values on the left y-axis are for controls.

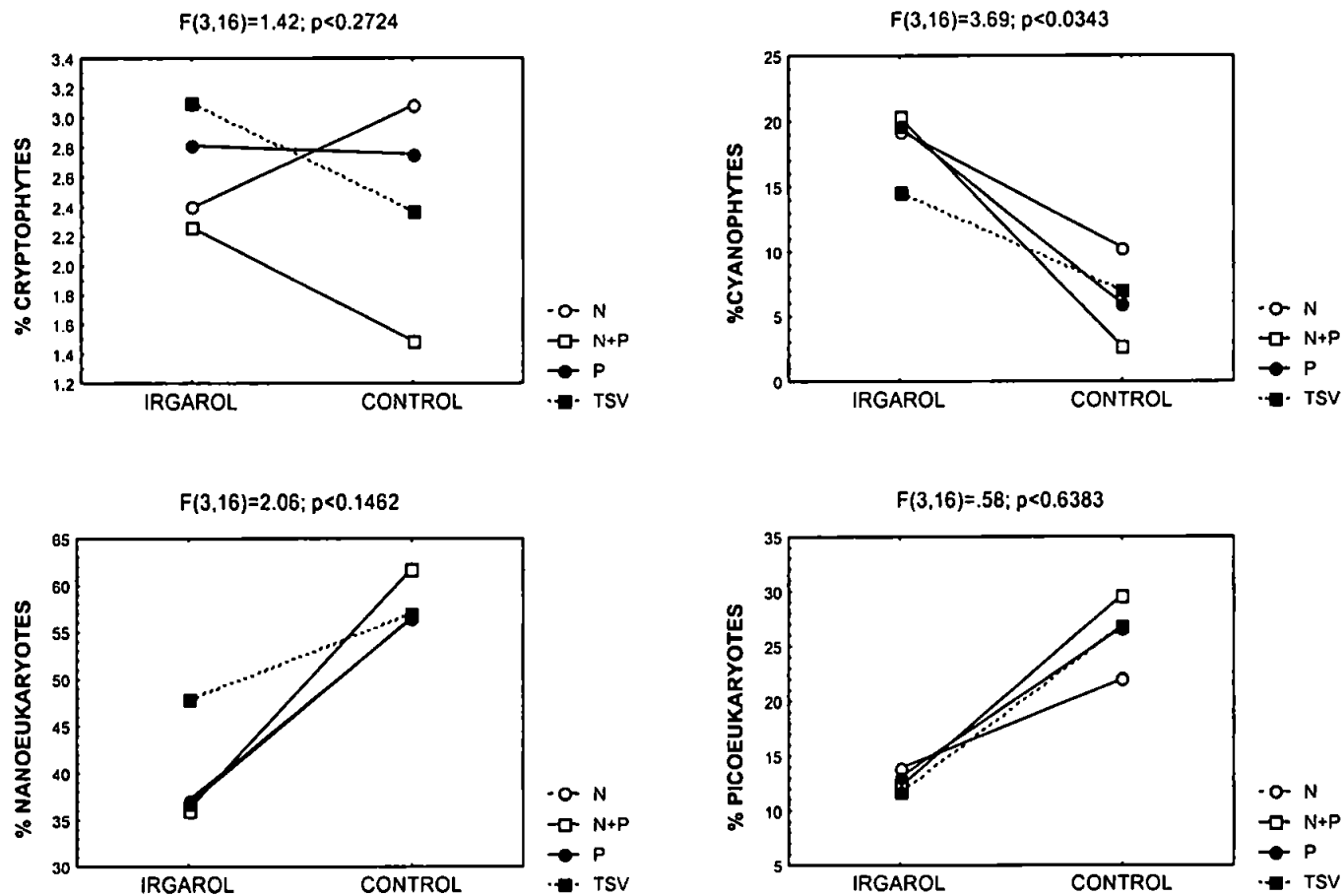


Figure 6.5. Plots of the results of interaction analysis (two-way ANOVA) of percentages of cyanophytes, nanoeukaryotes, and picoeukaryotes to total cells grown under different nutrient regimes and exposure to Irgarol 1051[®]. N: nitrate addition; N+P: nitrate plus phosphate addition; P: phosphate addition, TSV: no nitrate or phosphate added. Nutrient x Irgarol 1051[®] interactions are significant ($p < 0.05$) only for cyanophytes.

the cyanophytes, which appeared to be the least sensitive group and maintained approximately the same density as the controls (Fig. 6.4 and Fig. 6.5).

Nutrients influenced Irgarol 1051[®] toxicity by increasing the percentage of cyanophytes to total cells ($p = 0.0343$) (Appendice Table III.ii.a and Fig. 6.5). The percentage of cryptophytes to the total cells, however, was not affected by either Irgarol 1051[®] ($p = 0.4574$) or nutrient ($p = 0.1102$) treatments (Appendice Table III.iii.a). Picoeucaryotes and nanoeukaryotes responded similarly to nutrient addition and Irgarol 1051[®] toxicity. The percentages of picoeucaryotes and nanoeukaryotes were both affected only by Irgarol 1051[®] exposures ($p < 0.0001$). Neither nutrient treatment alone nor the nutrient in combination with Irgarol 1051[®] affected the response of these parameters (Appendice Table III.iv.a and Table III.v.a). When exposed to Irgarol 1051[®], the percentage of nanoeukaryotes were significantly higher in the TSV treatment when compared to P, N, or N+P treatments. Compared to controls, addition of Irgarol 1051[®] did not affect the percentage of nanoeukaryotes in the TSV treatment (Appendice Table III.v.b, Fig. 6.5), whilst other treatments (P, N, or N+P) were significantly affected by Irgarol 1051[®] addition.

Phytoplankton biomass, in terms of chlorophyll-*a*, was more affected by Irgarol 1051[®] under nutrient depleted conditions than in nitrate plus phosphate enriched conditions, with inhibitions of 28% at TSV, 24% at P, 17% at N, and 4.3% at N+P treatments ($p < 0.05$) (Fig. 6.6). Chlorophyll *c*₁*c*₂ (16-23%), fucoxanthin (19-27%), diadinoxanthin (26-29%), and β -carotene (21-27%) in the TSV, N, and P treatments were significantly more inhibited by Irgarol 1051[®] when compared to N+P treated microcosms (4.5%, 5.5%, 10%, and 7%, for the respective pigments) ($p < 0.05$). Also, alloxanthin was significantly more inhibited by Irgarol 1051[®] in TSV (28%) and N treatments (19%) when compared to 7% inhibition found in N+P treated microcosms. 19'-butanoyloxyfucoxanthin, however, was significantly more inhibited in P treated microcosms (68%) when compared to 39% inhibition in N+P microcosms ($p < 0.05$). The other pigments did not show significant difference from N+P treated microcosms ($p > 0.05$) (Fig. 6.6).

Spiked concentrations of Irgarol 1051[®] for this experiment are in agreement with GC-MS analyses (Table 6.1). Contamination in small quantities ($< 19 \text{ ng l}^{-1}$) was

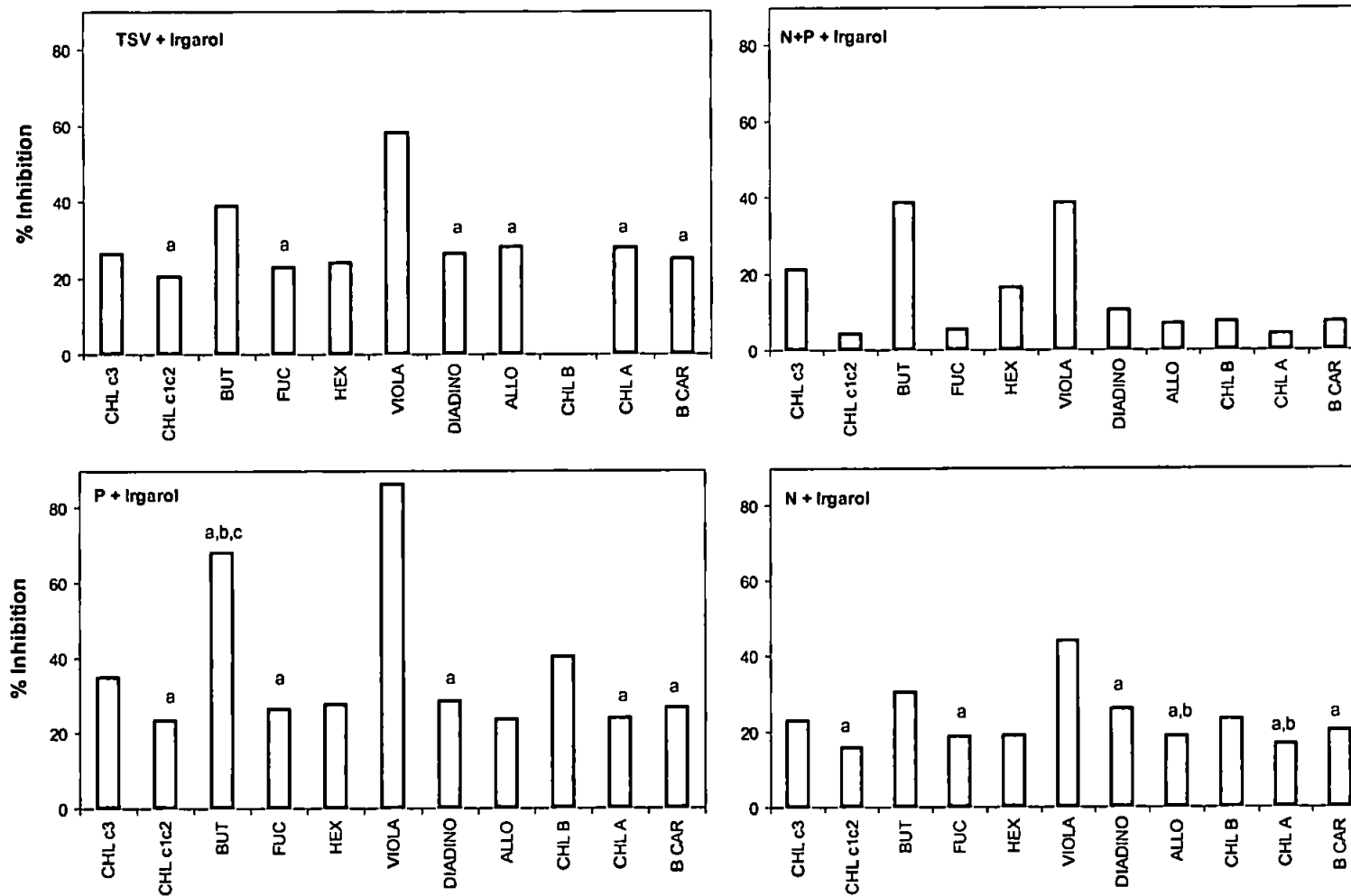


Figure 6.6. Percentage of reduction related to the controls in pigment concentrations ($\mu\text{g l}^{-1}$) by exposure to Irgarol 1051[®] (500 ng l^{-1}) after 5 days of experiment conducted under different nutrient additions: NP, nitrate+phosphate; P, phosphate and N, nitrate. Letters over bars indicate significant difference at $p < 0.05$ for % pigment to each Irgarol 1051[®] treatment: a, \neq N+P; b, \neq TSV; c, \neq N (one-way ANOVA followed by LSD post hoc test).

Table 6.1. Mean concentrations of Irgarol 1051[®] (ng l⁻¹), nitrate (μM) and phosphate (μM) from day 0 (time of sampling at site L4), day 1 and day 5 (experiment). Abbreviations shown are: TSV, trace-metal, silicate and vitamins added; NP, nitrate and phosphate added; P, only phosphate added; N, only nitrate added; n, number of replicates. Standard deviations of mean are shown in parentheses. Time of collection: day 0, sampling from site L4; day 1, nutrient and Irgarol 1051[®] additions; day 5, end of experiment.

TIME (days)	TREATMENT	n	IRGAROL 1051 [®] (ng l ⁻¹)	N-(NO ₃) ⁻² (μM)	P-(PO ₄) ⁻³ (μM)	N:P ratio ^a
0	sampling site L ₄	3	0 (0.0)	20.5 (0.3)	4.3 (0.2)	4.8
1	TSV	3		20.1 (0.8)	3.5 (0.1)	5.7
1	N+P	2		58.3 (0.3)	21.0 (0.2)	2.8
1	P	3		32.5 (17.5)	21.7 (0.5)	1.5
1	N	3		60.1 (0.2)	5.3 (0.2)	11.3
1	controls (no Irgarol 1051 [®])	4	14 (24)	-	-	-
1	Irgarol 1051 [®] addition	4	535 (42)	-	-	-
5	control TSV	2; 4 ^b	19 (19)	1.1 (1.4)	0.2 (0.1)	6.5
5	control N+P	3	14 (10)	10.3 (3.1)	1.5 (0.4)	7.1
5	control P	3	66 (95)	4.2 (3.0)	9.4 (1.0)	0.5
5	control N	2; 3 ^b	17 (15)	45.8 (1.0)	0.2 (0.1)	251.1
5	Irgarol 1051 [®] TSV	2; 3 ^b	558 (12)	17.4 (1.1)	2.4 (0.4)	7.2
5	Irgarol 1051 [®] N+P	2; 3 ^b	571 (68)	53.1 (0.0)	19.7 (0.4)	2.7
5	Irgarol 1051 [®] P	3	524 (37)	22.4 (0.0)	19.3 (0.6)	1.2
5	Irgarol 1051 [®] N	3	575 (120)	54.1 (0.2)	3.8 (0.1)	14.3

^a N quantified as nitrate only. ^b Number of replicated samples taken for phosphate and nitrate analyses.

however detected in control treatments. Irgarol 1051[®] concentrations recorded at the beginning of the experiment were similar to those at the end of the 5 day experiment.

This indicates negligible degradation or removal of the compound through adsorption/absorption processes. Nutrient concentrations obtained from the sampling site at time 0 (t₀) were 20.5 μM NO₃-N, and 4.3 μM PO₄-P with a N:P ratio of 4.8 (Table 6.1). In treated microcosms, mean concentrations after nutrient additions (day 1) were 59 μM of NO₃-N (N and N+P treatments), and 21 μM of PO₄-P (P and N+P treatments). On day 5, concentrations of nitrate and phosphate were higher for Irgarol 1051[®] treated

microcosms than for untreated (Table 6.1). Concentrations in the range of 1.2 to 16 times higher for $\text{NO}_3\text{-N}$ and 2 to 19 times higher for $\text{PO}_4\text{-P}$ were observed in the microcosms. The relatively high concentration of nitrate found in the N treatment on day 5 was not explained.

6.1.4. Discussion

Estuarine and coastal waters can be subjected to pulsed or continuous releases of xenobiotics, such as antifouling booster biocides, potentially leading to impacts on the natural phytoplankton communities. In addition to the direct effects, it is likely that nutrient availability will modify toxic responses. So far, toxicity of antifouling biocides on microalgae have been assessed as single compounds or mixtures of two or more compounds, although no work has been done so far concerning the influence of the nutrient status on their toxicity response. The current investigation represents a more realistic approach, which simulates a situation of a nutrient loading event associated with releasing of toxicants from antifouling paints.

Results from this study focussed on changes occurring in a single phytoplankton population that, at the time of sampling, was rich in flagellates ($<5 \mu\text{m}$) and picoplankton in terms of both carbon content and cell numbers. After 4 days of incubation in microcosms containing 500 ng l^{-1} Irgarol 1051[®], flow cytometry results demonstrated that phytoplankton groups were selectively affected and that total phytoplankton abundances were significantly reduced. Nutrient status also had a significant effect on total phytoplankton abundances, in which additions of nitrate plus phosphate stimulated significant increase in phytoplankton total numbers relative to the controls (TSV) and additions of nitrate alone (N), but did not differ from phosphate additions (P). Nutrient status, however, did not appear to significantly influence Irgarol 1051[®] toxicity, except in the case of cyanophytes.

Cyanophytes were the least sensitive phytoplankton group to Irgarol 1051[®] exposure compared to picoeukaryotes and nanoeukaryotes. Nutrient status influenced Irgarol 1051[®] toxicity in this group. In microcosms with no Irgarol 1051[®] added, the percentage of cyanophytes to total cells in the nitrate plus phosphate treatment were lower compared to nitrate treatment alone. Under Irgarol 1051[®] exposure, however, this pattern was changed, with N+P treatment significantly different only to the TSV treatment (no addition of nutrients). Deprivation of N has showed the formation of non-

functional PSII centres in the cyanobacterium *Prochlorococcus marinus*, accompanied by a continuous reduction in D1 protein (Steglich *et al.*, 2001), which might have interacted negatively under exposure to Irgarol 1051[®], a PSII inhibitor. However, cyanophytes possess the light-harvesting pigment phycoerythrin which functions as a dynamic N storage pool that is rapidly degraded when N becomes limiting (Wyman *et al.*, 1985; Collier and Grossman, 1992). This mechanism may have alleviated the toxic effects in nitrogen depleted microcosms, since N depletion (P treatment) did not show significant reductions in cell numbers of cyanophytes. Previous studies (see Chapters 3 and 5) corroborate with the identification of cyanophyte as the most resistant group to the effects of Irgarol 1051[®]. Other studies concerning herbicides, however, had identified cyanophytes as the most sensitive group to diquat (Pratt and Barreiro, 1998) and symetrine exposure (Kasai *et al.*, 1993). Both diquat and symetrine are photosynthetic inhibitors, but act at distinctive photosystems, PSI and PSII, respectively. Such discrepancies could be related to several factors, such as different communities studied, different culture conditions, herbicide structures, mode of action of the herbicide, and physiological state of the cells.

Unlike cyanophytes, picoeukaryote and nanoeukaryote contributions to the total cell abundance were affected by Irgarol 1051[®] additions alone, whilst cryptophytes contributions were not affected by neither nutrient status nor Irgarol 1051[®] additions. No influences of nutrient status on the toxicity of Irgarol 1051[®] was therefore identified for these three groups. Comparing nutrient treatments within the Irgarol 1051[®] controls (*i.e.*, treatments with no addition of Irgarol 1051[®]), results indicated that nutrient addition had no significant effect on group contributions, although the nitrate plus phosphate enriched culture appear to show an increase in picoeucaryotes and nanoeucaryotes contributions to total cells (Fig. 6.3).

According to the nutrient analysis after four days of incubation, dissolved nutrients in water appeared to be limiting phytoplankton growth in the N-treated and P-treated microcosms. Nitrate concentrations in the N treatment were not reduced to similar levels as observed in all other treatments (TSV, P, N+P) at the end of the incubations. The results showed that nutrients in non-limited microcosms were removed faster than in the P- or N- limited microcosms. This suggests that the phytoplankton community grown under non-limited nutrient conditions developed more rapidly than in nutrient limited conditions, reflecting a highly-responsive phytoplankton community. In the presence of

Irgarol 1051[®], microcosm nutrient concentrations were similar to day 1, when nutrients were added, suggesting slow biomass development of the phytoplankton community due to the blockage of PSII electron transport under Irgarol 1051[®], impairing the utilisation of P for ATP.

Nutrient additions can result in stimulation or inhibition of photosynthesis and respiration (DeLorenzo *et al.*, 2001). Studies of natural periphyton communities in low-nutrient conditions were found to be less likely to recover from herbicide stress than those in medium- and high- nutrient treatments (Lozano and Pratt, 1994). Intracellular competition between nutrients and toxicants, which may reduce toxic effects, has also been investigated (Wangberg and Blanck, 1990; Twiss and Nalewajko, 1992; Pratt and Barreiro, 1998). Consequences of N-deficient conditions include a higher proportion of lipids and include changes in cell shape, weight and volume (Halling-Sørensen *et al.*, 2000), which may alter pesticide toxicity.

Phytoplankton cells, on average, assimilate C, N and P in the approximate ratio 106:16:1 (Redfield ratio), and this elemental proportion has been used as a potential index of nutrient limitation, although it has recently been pointed out that the ratio is far from constant (Falkowski, 2000). An indication of nutrients being a limiting factor in the original water is when stimulation of production and/or growth is observed by a particular nutrient addition (Beardall *et al.*, 2001). In phytoplankton cultures, the physiological range of N:P in phytoplankton is from < 5 under severe N-limitation to > 100 under severe P-limitation (Geider and LaRoche, 2002). The N:P ratio of nutrient-replete phytoplankton ranges from about 5 to 19, with most observations falling below the Redfield ratio of 16. The range of N:P values under nutrient-replete conditions appeared to arise largely from interspecific or clonal variability rather than from differences in growth conditions or analytical techniques (Geider and LaRoche, 2002). The critical N:P ratio that marks the transition between N- and P-limitation appears to be in the range 20-50, and thus exceeds the Redfield ratio of 16 (Geider and LaRoche, 2002).

Toxicity of Irgarol 1051[®] was also detected through phytoplankton biomass, in terms of chlorophyll-*a*, under nutrient depleted conditions (TSV, N and P treatments) when compared to N+P treated conditions. The least impact of Irgarol 1051[®] addition was under the nitrate plus phosphate enrichment (N+P treatment). Besides chlorophyll-*a*,

pigment composition had also been significantly affected by Irgarol 1051[®] under varying nutrient conditions.

The addition of Irgarol 1051[®] in combination with nitrate plus phosphate resulted in reduction of inhibition of the following signature pigments: chlorophyll *c*₁*c*₂ (pigment signature for cryptophytes, diatoms, dinophytes, prymnesiophytes, chrysophytes), fucoxanthin (pigment signature for diatoms), diadinoxanthin (pigment signature for euglenophytes, diatoms, dinophytes, prymnesiophytes, chrysophytes) and β -carotene (pigment shared by several groups) compared to the other nutrient treatments; alloxanthin (pigment characteristic of cryptophytes) compared to TSV- and N-treatments; 19'-butanoyloxyfucoxanthin (pigment signature of prymnesiophytes and chrysophytes) compared to P-treated microcosms. Overall pigment inhibitions were more severe in P-treated microcosms than in the other nutrient condition.

Nutrient conditions are relevant when assessing herbicide toxicity as shown in this experiment. It is known that phytoplankton under N or P depleted conditions show changes in quality and quantity of their cellular content, which might affect toxicity, bioaccumulation, tolerance capacity, and detoxification characteristics inherent in each phytoplankton group or strain. For instance, P-starved algae increase their cell size, probably due to arrested cell division and accumulation of intracellular glycogen compounds (Van Donk and Hessen, 1993). Most phytoplankton species accumulate excess C in starch granules, whereas in some phytoplankton and bacteria species, mineral deficiency leads to accumulation of excess C as extracellular polysaccharides (Sondergaard and Schierup, 1982; Mykkestad, 1977). This strategy also seems to occur for phytoplankton exposed to pollutants, where extracellular C plays an important role in reducing the toxicant bioavailability.

Evidence that atrazine becomes more toxic to phytoplankton under nutrient-enriched conditions has been reported (deNoyelles *et al.*, 1982). However, high nutrient concentrations investigated here reduced the toxicity of Irgarol 1051[®], which is also a triazine herbicide. From an ecological point of view, nutrient-deficient systems slow phytoplankton growth rate and change species composition. However, the presence of pollutants interacting with nutrients can modify toxicity and possibly the community composition.

Functional tests for assessing impact due to the release of chemicals into an aquatic system have obvious advantages for providing ecologically relevant information on toxic effects. However, the whole-system complexity that makes these approaches attractive can also complicate interpretations of the results (McCarthy and Bartell, 1988). Although these results cannot be used to predict changes in natural assemblages, they provide a more realistic assessment of which phytoplankton groups are affected by inputs of Irgarol 1051[®]. These results should not be extrapolated to make any statements about the environmental effects of Irgarol 1051[®] in estuarine/marine habitats. The limited scope of this study does not reflect the inherent variability in phytoplankton community composition or the wide range of environmental conditions in estuarine and coastal waters. The timing of herbicide loading could be very important for determining the impacts on phytoplankton (Pinckney *et al.*, 2002).

6.1.5. Conclusions

This study is a preliminary investigation on the influence of nutrient status over the antifouling booster biocide (Irgarol 1051[®]) toxicity. Results gave an indication of the possible interaction between these two factors, particularly for cyanophytes. More studies, however, should be conducted to reveal interactions using different phytoplankton communities and also monoalgal cultures including species from the groups affected. Moreover, it would be important to investigate the capacity for recovery of the phytoplankton population developed under different nutrient conditions.

Even though the concentration of Irgarol 1051[®] tested was high, similar environmental concentrations have been detected in the most contaminated areas in UK and Europe (see Chapter 1).

6.2. Spatial distribution patterns of antifouling biocides and phytoplankton structures within Plymouth waters

6.2.1. Introduction

Estuarine and coastal areas are subjected to degradation from pollution as a result of recreational, industrial and shipping activities. The proximity of large urban and

industrial disturbances renders estuaries and coastal areas particularly vulnerable to such influences. The integrity of biotic communities is directly affected by changes in environmental characteristics (Griffith *et al.*, 2002), in which anthropogenic discharges play a significant role in modifying chemical/physical processes. These alterations, individually and interactively, induce responses within communities that are complex and not easily discerned solely by experimental manipulations, such as laboratory-based bioassays (Griffith *et al.*, 2002).

Because environmental effects are integrated by biotic communities, biological monitoring is a useful approach for assessing disturbance and pollution in aquatic ecosystems (Fore *et al.*, 1996). Biomonitoring is the repeated measurement of biological parameters to determine existing conditions, pollutant levels, or species in the environment, which aids in the assessment of the overall health of the environment. Manipulative approaches, as described earlier (Chapters 4, 5 and 6), could be supplemented with survey data whereby many sites are sampled and analysed using measurements of community composition as response variables (Griffith *et al.*, 2002). Although survey data are complex, multivariate statistical methods can extract patterns at regional scales relevant to environmental management (Omernik, 1995) and can be used to identify the main environmental stressors. Measures based on taxonomic or functional group composition of selected multi-species assemblages are often used to summarize abundance data and then tested for their relationship to natural or anthropogenic environmental gradients. Having first established the relevance of these measurements in laboratory-tests they can then be applied to field studies. Therefore, the use of manipulative approaches, such as microcosm experiments, combined with field data would enable a more realistic assessment of ecosystem health.

The study area for this investigation was the Tamar Estuary and Plymouth Sound (Fig. 6.7). The major run off into this estuary comes from the River Tamar and the coastal area surrounding the city of Plymouth, with a smaller contribution from the River Plym (Readman *et al.*, 1982; Siddorn *et al.*, 2003). The Tamar is a medium-sized, partially mixed estuary, 31 km long from its boundary with Plymouth Sound to its limit of tidal influence and salinity intrusion at Weir Head (Uncles and Lewis, 2001). The main physico-chemical variables (e.g. particulate carbon, salinity, turbidity, dissolved oxygen) and nutrient chemistry of the Tamar are well described (Morris *et al.*, 1978, 1981, 1982). Plymouth Sound is characterized by a maximum width of 6 km and a width of approximately 5 km at its mouth. There are three extensive marinas around Plymouth:

Queen Anne's Battery (QAB), Mayflower and the enclosed Sutton Harbour. Variability in dominant phytoplankton species and the timing of the seasonal cycle in the Plymouth area have been documented by Boalch (1987). There is high species diversity and the patterns of occurrence are dominated by the seasonal cycle. Although the species composition changes annually, the long-term changes in the overall pattern shows considerable degree of persistence in the community from one season to the next (Maddock *et al.*, 1989).

The distribution of xenobiotics and their environmental fate along the Tamar estuary and Plymouth Sound have been investigated. For example, polycyclic aromatic hydrocarbon concentrations have been reported with the highest values associated with turbidity (at the turbidity maximum zone) and anthropogenic inputs (localized at the industrial areas) to the estuary (Readman *et al.*, 1982). Environmental concentrations of antifouling biocides have only recently been studied in the U.K. (Zhou *et al.*, 1996; Scarlett *et al.*, 1997; Thomas *et al.*, 2002). Although no detailed survey has been carried out in the Tamar Estuary, Irgarol 1051[®] and diuron have been detected in Plymouth waters (marinas and Plymouth Sound) (Thomas *et al.* 2001). The measured concentrations of Irgarol 1051[®] are known to affect macroalgae (Scarlett *et al.*, 1997), but it is not known whether antifouling biocides influence the indigenous phytoplankton communities.

The main aim of this pilot study was to characterise the spatial distribution patterns of phytoplanktonic pigments and abundances, antifouling booster biocides, and various physico-chemical parameters within the estuary and Plymouth Sound, and to assess the possible influence of pollutant sources on phytoplankton composition. A survey was carried out at high tide along the Tamar Estuary, including marinas which have intensive recreational and commercial usage. Phytoplankton pigment chemotaxonomy coupled with analytical flow cytometry (for pico and nanophytoplankton determinations) were used to monitor spatial patterns in phytoplankton abundance and composition. The physico-chemical parameters, suspended particulate matter, carbon, and nitrogen (which indicates living and/or relatively undegraded primary production products) alongside the antifouling/herbicidal compounds (Sea-Nine 211[®], Irgarol 1051[®], and atrazine, a common herbicide used in agriculture) were determined for water characterization. The intention was to undertake further survey work at other times of the year to provide a more robust time-based dataset, but this proved not to be possible in the time available.

Thus, interpretation of the data should be treated with caution. The results are included as a indication of the approach that could be taken for future *in situ* studies.

6.2.2. Methods

6.2.2.1. Study area and sampling procedures

A pilot survey was carried out at the high tide on 20th September 2001 at 9 stations, covering the Tamar Estuary, Sutton Harbour Marina, Queen Anne's Battery Marina, and Plymouth Sound, and commencing at station 1 (Fig. 6.7). Spatial sampling was designed to characterize the potential effects of antifouling/herbicide compounds and concentrations at sites with varying water retention times and phytoplankton composition. Areas with similar salinity values were selected to minimise variability of freshwater and seawater phytoplankton composition. Surface samples were collected using a plastic bucket (except for antifouling biocide analyses). Bottom samples were collected using a glass bottle mounted on a weighted stainless steel frame and deployed just above the bottom by means of a nylon rope. Water samples were filtered on board, with additional filtration performed in the laboratory prior to pigment extraction. Water samples were analysed for HPLC-pigment determination (see 2.4.3), eukaryotic and prokaryotic phytoplankton (< 20 μm) enumeration by AFC (see 2.4.8), and for physico-chemical characteristics: salinity, suspended particulate matter (SPM), particulate nitrogen, organic carbon and total carbon (see 2.4.10), as well as measurements of the antifouling/herbicide compounds Sea-Nine 211[®], Irgarol 1051[®], and atrazine (see 2.4.4).

6.2.2.2. Data analysis and statistical approach

A Pearson correlation matrix between pigment composition ($\mu\text{g l}^{-1}$), chlorophyll-*a* and cell abundances (cell ml^{-1}) of nanoeukaryotes, picoeukaryotes, cryptophytes, and total cell numbers was generated to determine trends between the parameters measured. All these variables might be linearly correlated because they correspond to phytoplankton measurements, including pigment composition, which could be used to estimate phytoplankton composition. Correlations were expressed as the correlation coefficient at a significance level of 5% ($\alpha = 0.05$). Data were analysed using the statistical package Statistica for Windows version 5.1 (1996 edition, StatSoft Inc., Tulsa, USA). Data were further treated by generating a distance matrix (Bray Curtis similarity) using fourth root transformed pigment and cell abundances data. Subsequently, this matrix was submitted to an ordination by non-metric multidimensional scaling (MDS),

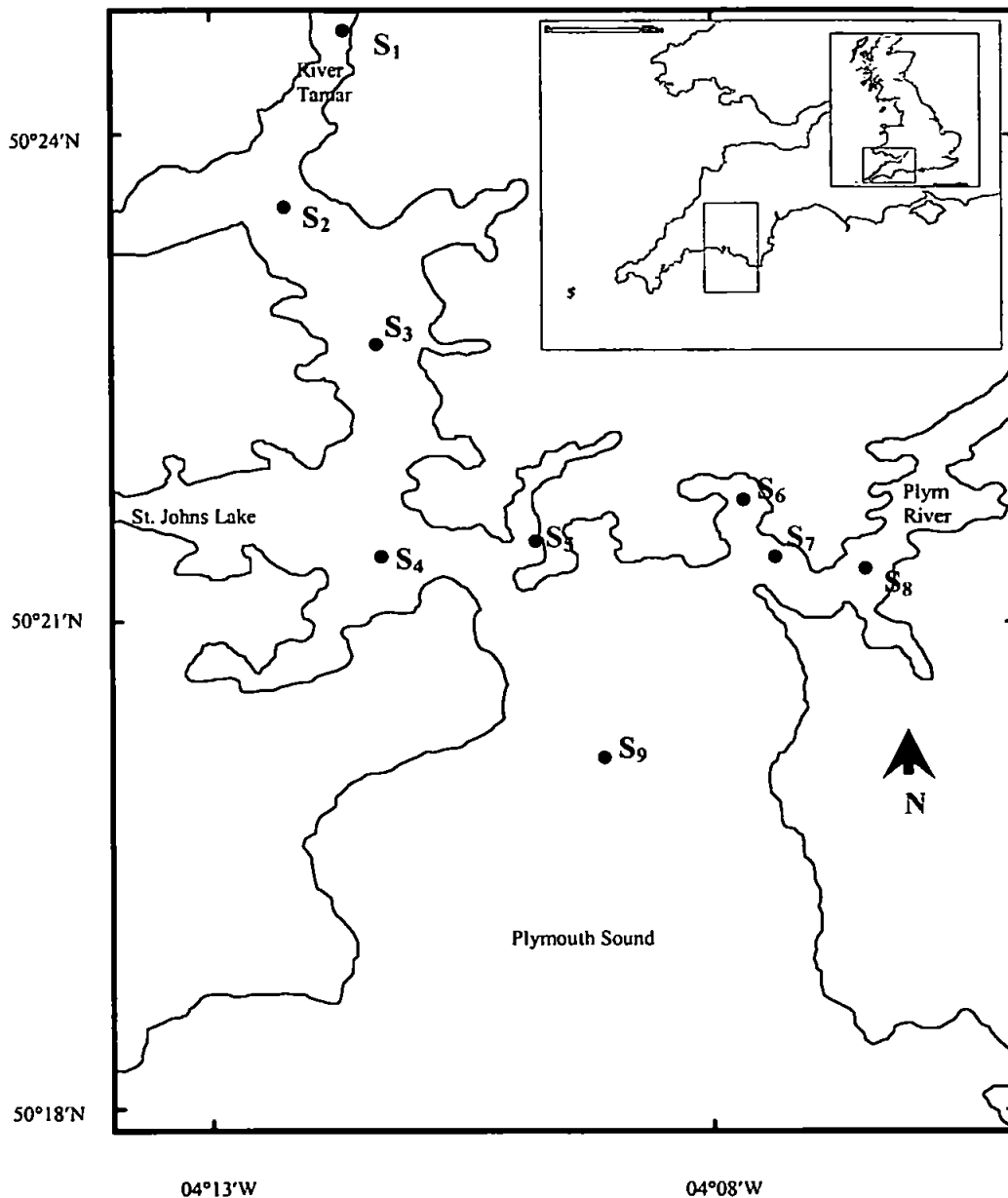


Figure 6.7. Sampling stations within the Tamar Estuary and Plymouth Sound area: Tamar River (S1: 50°24'48"N 4°12'16"W), Bull Point (S2: 50°23'31"N 4°12'00"W), Devonport (S3: 50°22'54"N 4°11'22"W), St. John's Lake (S4: 50°21'45"N 4°11'06"W), Mayflower Marina (S5: 50°21'48"N 4°09'52"W), Sutton Harbour (S6: 50°22'04"N 4°07'50"W), Queen Anne's Battery (QAB) (S7: 50°21'56"N 4°08'00"W), Plym River (S8: 50°21'39"N 4°07'13"W), and Plymouth Sound (S9: 50°20'32"N 4°08'48"W).

using the statistical software PRIMER for Windows version 5.2.9 (Clarke and Gorley 2001).

6.2.3. Results

6.2.3.1. Chemical-physical parameters

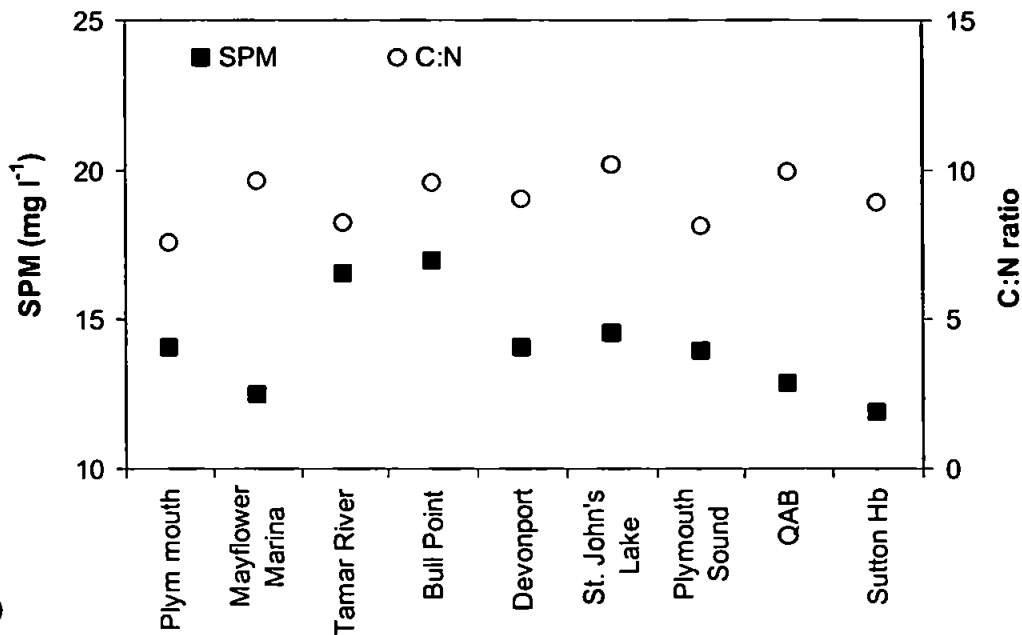
No strong freshwater influence was evident due to the absence of a salinity gradient between the stations. Salinity varied between 32.8 and 33.5 PSU and temperature was between 17 °C and 18 °C. Suspended particulate matter (SPM) from surface samples was slightly higher at Tamar River (S1) and Bull Point (S2) with 16.5-17 mg l⁻¹, and declined to 12.8 mg l⁻¹ at QAB (S7), 12.4 mg l⁻¹ at Mayflower Marina (S5), and to 11.8 mg l⁻¹ at Sutton Harbour (S6) (Fig. 6.8A). Organic carbon contribution was highest at Bull Point (3.8%), Tamar River (3.3%), and QAB (3.1%), whilst Sutton Harbour (2.5%) and Plymouth Sound (2.3%) showed the lowest values (Fig. 6.8B), which appear to coincide with variations in SPM values (Fig. 6.8A and 6.8B). Nitrogen values were higher for Bull Point (0.4%) and Tamar River (0.4%), with the other stations showing lower values.

Of the antifouling/herbicides analysed, only Irgarol 1051[®] and atrazine were detected in this survey. The highest values of Irgarol 1051[®] were detected in the marinas, with 21 ng l⁻¹ at Sutton Harbour (S6), 11.7 ng l⁻¹ at QAB (S7) and 3.7 ng l⁻¹ at Mayflower Marina (S5). No Irgarol 1051[®] was detected at the Plymouth Sound (S9) or at the mouth of Plym River (S8), whereas at the other stations values of ≤ 2 ng l⁻¹ were detected (Table 6.2).

6.2.3.2. Biological parameters

Pico- and nanophytoplankton cell numbers were lowest at the stations Sutton Harbour with 1.3 x 10⁴ cells ml⁻¹, Queen Anne's Battery with 1.79 x 10⁴ cells ml⁻¹ and Tamar River with 1.88 x 10⁴ cells ml⁻¹ (Fig. 6.9). The highest values detected were 2.38 x 10⁴ cells ml⁻¹ for Mayflower Marina and 2.30 x 10⁴ cells ml⁻¹ for Plymouth Sound. The contribution of each group of phytoplankton differed between stations (Fig. 6.10). Picoeucaryotes were the most important contributors to all stations, except Plymouth Sound and St. John's Lake, where cyanophytes predominated. The highest contributions of cyanophytes were found at Plymouth Sound (55.6%), Mayflower Marina (49.5%),

(A)



(B)

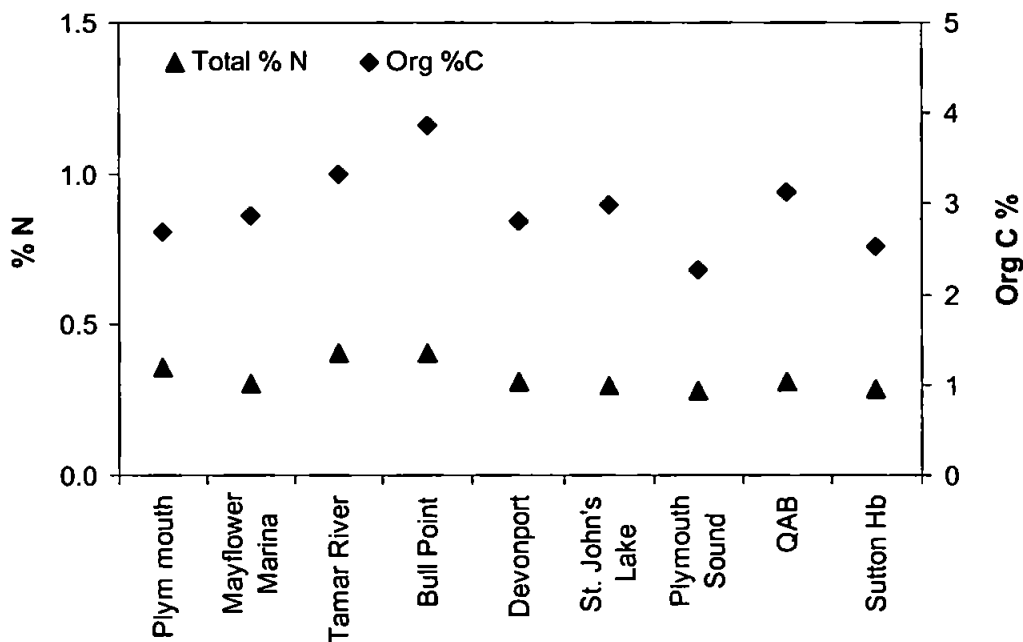


Figure 6.8. Mean data obtained for the 9 stations in Tamar Estuary and Plymouth Sound: (A) Suspended Particulate Material (SPM) in mg l⁻¹ and C:N ratio, and (B) percentage of particulate nitrogen (%N) and organic carbon (Org C%) (n = 2).

Table 6.2. Atrazine and Irgarol 1051[®] (ng l⁻¹) concentrations at 9 stations from Tamar Estuary and Plymouth Sound. *Note: Sea-Nine 211[®] was not detected at these locations.*

Station	Atrazine	Irgarol 1051 [®]
Sutton Harbour (S6)	< 1	21
QAB (S7)	< 1	11.7
Plymouth Sound (S9)	< 1	< 1
St. Jones Lake (S4)	< 1	0.5
Devonport (S3)	1	2
Bull Point (S2)	< 1	2
Tamar River (S1)	3	1
Mayflower Marina (S5)	2.3	3.7
Plym River mouth (S8)	< 1	< 1

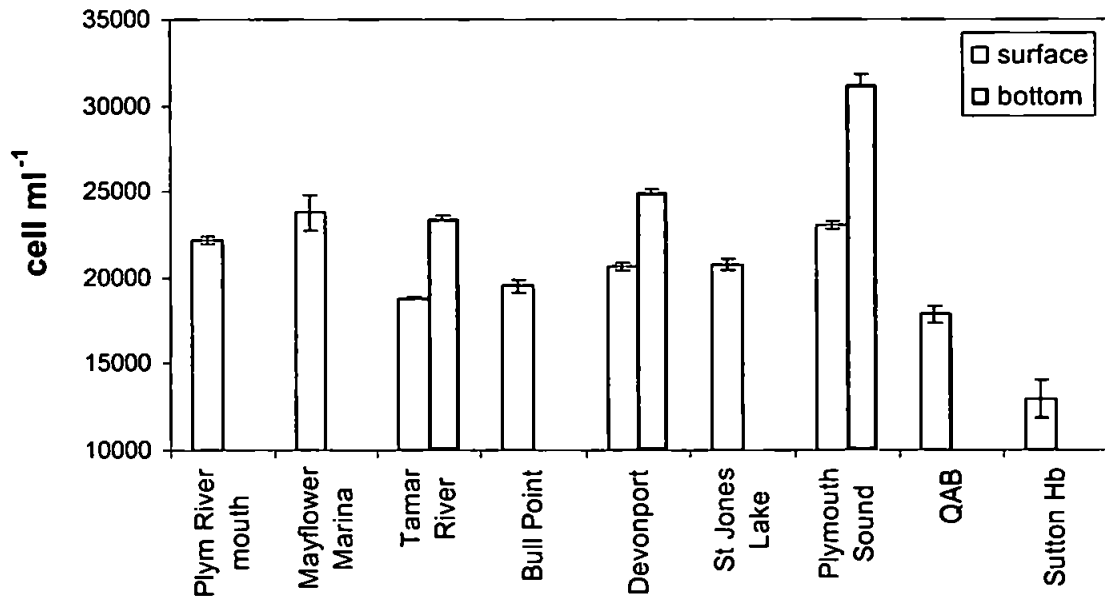


Figure 6.9. Total cell numbers for nanoeukaryotes + picoeukaryotes + cyanophytes measured by AFC at 9 sampling stations within Tamar Estuary and Plymouth Sound.

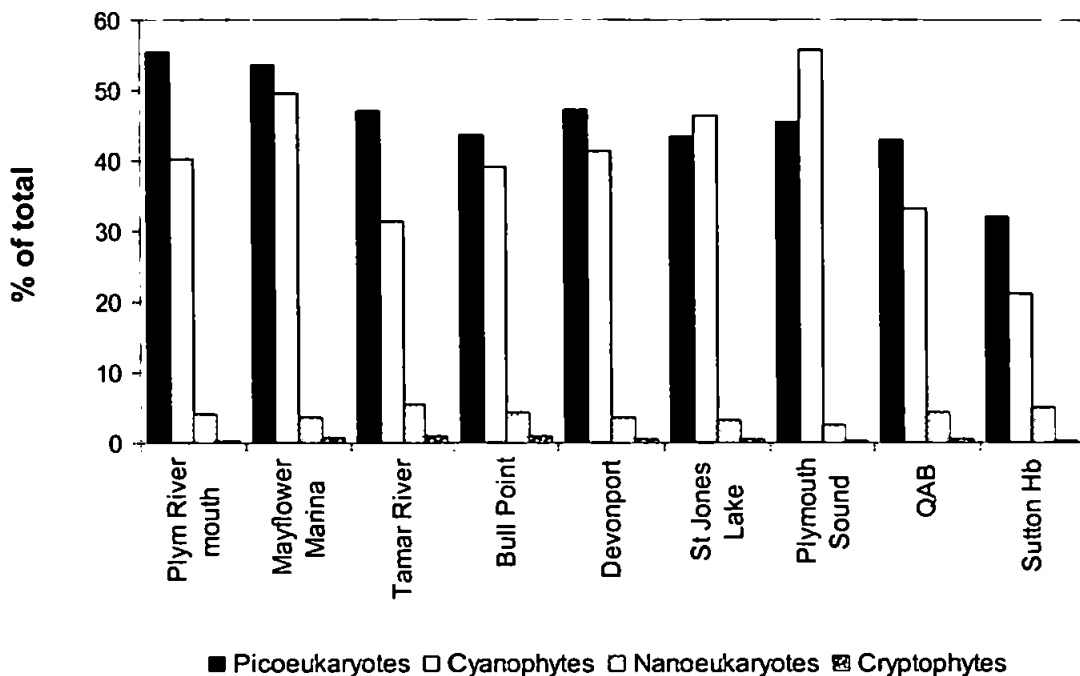


Figure 6.10. Contribution of picoeukaryotes, nanoeukaryotes, cyanophytes and cryptophytes measured by AFC, to the total cell number for each surface sampling station.

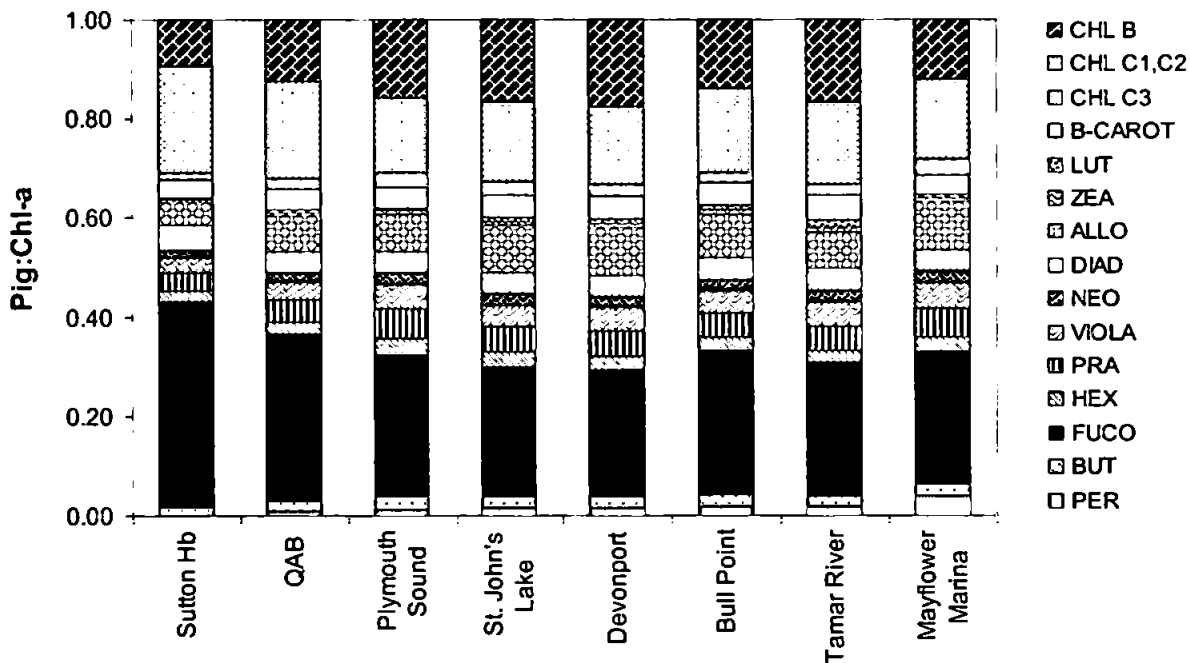


Figure 6.11. Pigment composition on a chlorophyll-a basis along 8 sampling stations (surface samples). CHL: chlorophylls *b*, *c*₁*c*₂ or *c*₃; B-CAROT: β -carotene; LUT: lutein; ZEA: zeaxanthin; ALLO: alloxanthin; DIADINO: diadinoxanthin; NEO: neoxanthin; VIOLA: violaxanthin; PRA: prasinoxanthin; HEX: 19'-hexanoyloxyfucoxanthin; FUCO: fucoxanthin; BUT: 19'-butanoyloxyfucoxanthin; PER: peridinin.

and St. John's Lake (46.5%). Highest picoeukaryote contributions were found for the Plym River mouth (55.5%) station and Mayflower Marina (53.6%) and lowest value were found at Sutton Harbour (32.1%). Contributions of nanoeukaryotes ranged from 5.4% (Tamar River) to 2.6% (Plymouth Sound), with Sutton Harbour showing a relatively high value (5.1%). The contribution by cryptophytes was very low at all stations (< 1%).

Highest values of pigment:chl-*a* were found at Mayflower Marina for chl *c*₃:chl-*a* (0.0304), peridinin:chl-*a* (0.0353), prasinoxanthin:chl-*a* (0.0527), violaxanthin:chl-*a* (0.0495), neoxanthin:chl-*a* (0.0216), alloxanthin:chl-*a* (0.0876); at Sutton Harbour for fucoxanthin:chl-*a* (0.3295) and diadinoxanthin:chl-*a* (0.0410); at QAB for chl *c*₁*c*₂:chl-*a* (0.1594); at Plymouth Sound for 19'-butanoyloxyfucoxanthin:chl-*a* (0.0245), 19'-hexanoloxyfucoxanthin:chl-*a* (0.0305), chl *b*:chl-*a* (0.1389); and at Tamar River for zeaxanthin:chl-*a* (0.0094), lutein:chl-*a* (0.0111), β -carotene:chl-*a* (0.0396) (Fig. 6.11). Highest phytoplankton biomass in terms of chlorophyll-*a* was found at Sutton Harbour, QAB, and at the Tamar River stations with concentrations of 2.05, 2.19 and 2.5 $\mu\text{g l}^{-1}$, respectively.

A Pearson correlation matrix resulting from contrasting comparisons between all pigments and chlorophyll-*a* or cell numbers (measured by AFC) of eukaryote picoplankton and prokaryotes (cyanophytes) is presented in Table 6.3. Most of the diagnostic pigments were significantly correlated to chlorophyll-*a* ($p < 0.05$) (Table 6.3). By comparison between diagnostic pigments and phytoplankton groups (<20 μm), results show no significant correlation between zeaxanthin concentrations measured by HPLC and number of cells of cyanophytes measured by AFC analysis ($r = 0.24$; $p = 0.448$). However, a significant correlation was found between zeaxanthin concentrations and cryptophyte abundances ($r = 0.71$; $p = 0.010$), and alloxanthin concentrations and cryptophyte abundances ($r = 0.73$; $p = 0.008$). Although a significant correlation was found between 19'-hexanoyloxyfucoxanthin and picoeukaryotes ($r = 0.74$; $p = 0.006$), prymnesiophytes are not known to be included in the picoplankton group (Jeffrey and Hallegraeff, 1990). Good correlations were also found between fucoxanthin and nanoeukaryotes ($R^2 = 0.76$; $p = 0.004$), chlorophyll *c*₁*c*₂ and nanoeukaryotes ($R^2 = 0.82$; $p = 0.001$), peridinin and nanoeukaryotes ($R^2 = 0.88$; $p < 0.001$), prasinoxanthin and picoeukaryotes ($R^2 = 0.77$; $p = 0.003$), chlorophyll *b* and picoeukaryotes ($R^2 = 0.70$; $p = 0.010$). A linear correlation ($R^2 = 0.711$, $p = 0.0171$; $n = 7$; not shown) was found

Table 6.3. Pearson correlation matrix between pigments determined by HPLC (ng l^{-1} ; rows) and chlorophyll-*a* (ng l^{-1} ; columns) and cell numbers of picoeukaryotes, nanoeukaryotes, cyanophytes, cryptophytes, and total cells determined by AFC (cell ml^{-1} ; columns). Data are expressed as correlation coefficient (*r*) and significance level (*p*). Marked correlations (in bold) are significant at $p < 0.05$. $n = 12$.

	CHL- <i>a</i>	PICO	NANO	CYANOPHYTES	CRYPTOPHYTES	TOTAL CELLS
C3	0.186 <i>p</i> =0.563	0.709 <i>p</i> = 0.010	-0.199 <i>p</i> =0.536	0.456 <i>p</i> =0.136	0.471 <i>p</i> =0.122	0.594 <i>p</i> = 0.041
C1C2	0.726 <i>p</i> = 0.008	-0.509 <i>p</i> =0.091	0.818 <i>p</i> = 0.001	-0.887 <i>p</i> = 0.000	-0.060 <i>p</i> =0.854	-0.785 <i>p</i> = 0.003
PER	0.383 <i>p</i> =0.219	0.881 <i>p</i> = 0.000	-0.222 <i>p</i> =0.489	0.553 <i>p</i> =0.062	0.868 <i>p</i> = 0.000	0.734 <i>p</i> = 0.007
BUT	0.559 <i>p</i> =0.059	0.672 <i>p</i> = 0.017	-0.128 <i>p</i> =0.691	0.323 <i>p</i> =0.306	0.773 <i>p</i> = 0.003	0.493 <i>p</i> =0.104
FUCO	0.434 <i>p</i> =0.158	-0.759 <i>p</i> = 0.004	0.760 <i>p</i> = 0.004	-0.934 <i>p</i> = 0.000	-0.322 <i>p</i> =0.308	-0.921 <i>p</i> = 0.000
HEX	0.595 <i>p</i> = 0.041	0.744 <i>p</i> = 0.006	-0.085 <i>p</i> =0.794	0.352 <i>p</i> =0.262	0.760 <i>p</i> = 0.004	0.544 <i>p</i> =0.067
PRA	0.549 <i>p</i> =0.065	0.774 <i>p</i> = 0.003	-0.224 <i>p</i> =0.485	0.430 <i>p</i> =0.163	0.685 <i>p</i> = 0.014	0.602 <i>p</i> =0.038
VIOLA	0.598 <i>p</i> = 0.040	0.729 <i>p</i> = 0.007	-0.056 <i>p</i> =0.863	0.327 <i>p</i> =0.299	0.706 <i>p</i> = 0.010	0.522 <i>p</i> =0.082
NEO	0.699 <i>p</i> = 0.011	0.678 <i>p</i> = 0.015	-0.002 <i>p</i> =0.996	0.260 <i>p</i> =0.414	0.760 <i>p</i> = 0.004	0.458 <i>p</i> =0.135
DIAD	0.815 <i>p</i> = 0.001	-0.321 <i>p</i> =0.309	0.873 <i>p</i> = 0.000	-0.772 <i>p</i> = 0.003	0.203 <i>p</i> =0.526	-0.622 <i>p</i> = 0.031
ALLO	0.635 <i>p</i> = 0.026	0.748 <i>p</i> = 0.005	-0.065 <i>p</i> =0.841	0.337 <i>p</i> =0.284	0.726 <i>p</i> = 0.008	0.536 <i>p</i> =0.073
ZEA	0.592 <i>p</i> = 0.042	0.690 <i>p</i> = 0.013	0.015 <i>p</i> =0.964	0.242 <i>p</i> =0.448	0.709 <i>p</i> = 0.010	0.450 <i>p</i> =0.142
LUT	0.523 <i>p</i> =0.081	0.749 <i>p</i> = 0.005	0.011 <i>p</i> =0.972	0.321 <i>p</i> =0.309	0.898 <i>p</i> = 0.000	0.532 <i>p</i> =0.075
CHLB	0.640 <i>p</i> = 0.025	0.705 <i>p</i> = 0.010	-0.070 <i>p</i> =0.829	0.337 <i>p</i> =0.284	0.747 <i>p</i> = 0.005	0.519 <i>p</i> =0.084
BCAR	0.841 <i>p</i> = 0.001	0.460 <i>p</i> =0.133	0.262 <i>p</i> =0.412	-0.018 <i>p</i> =0.957	0.712 <i>p</i> = 0.009	0.190 <i>p</i> =0.555
CHL- <i>a</i>		0.067 <i>p</i> =0.836	0.576 <i>p</i> =0.050	-0.451 <i>p</i> =0.141	0.385 <i>p</i> =0.216	-0.259 <i>p</i> =0.417

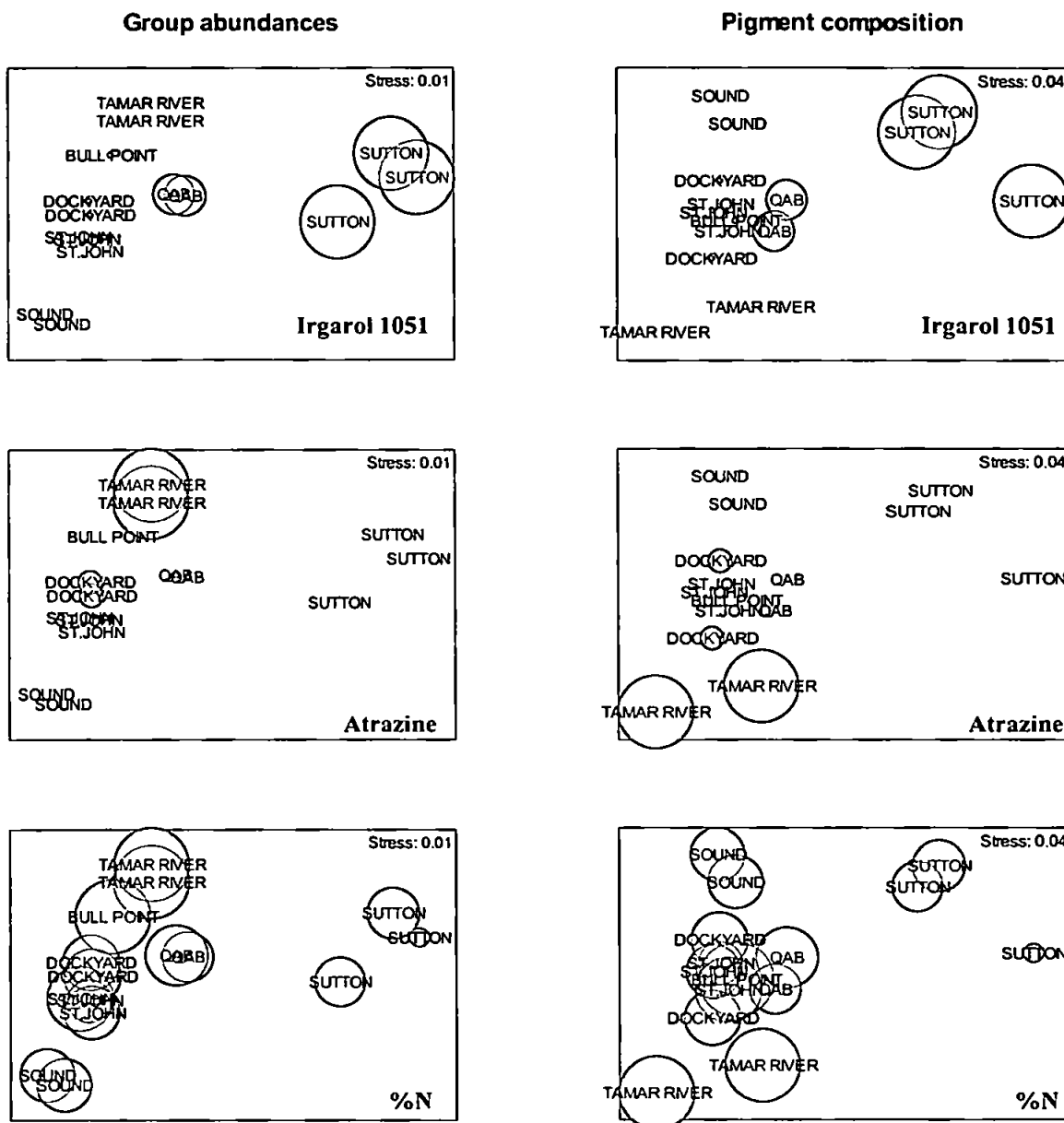


Figure 6.12. Multi-Dimensional Scaling (MDS) of Bray-Curtis similarities of \sqrt{x} -transformed group abundances data (graphs on the left) and of \sqrt{x} -transformed pigment composition data (graphs on the right) for 7 stations investigated (missing data for Mayflower Marina and Plym River stations). Small distances between observations indicate high similarity in community structure. Stress levels (above each graph) of <0.05 indicate an excellent representation of the relationship between observations (*i.e.*, they have not being arbitrarily placed). Both MDS set of graphs show superimposed circles which sizes indicate concentrations of Irgarol 1051[®] and atrazine, the percentage of nitrogen (%N), organic carbon (% Org C) and total carbon (%Total C), and the concentration of suspended particulate matter (SPM). (*cont. next page*)

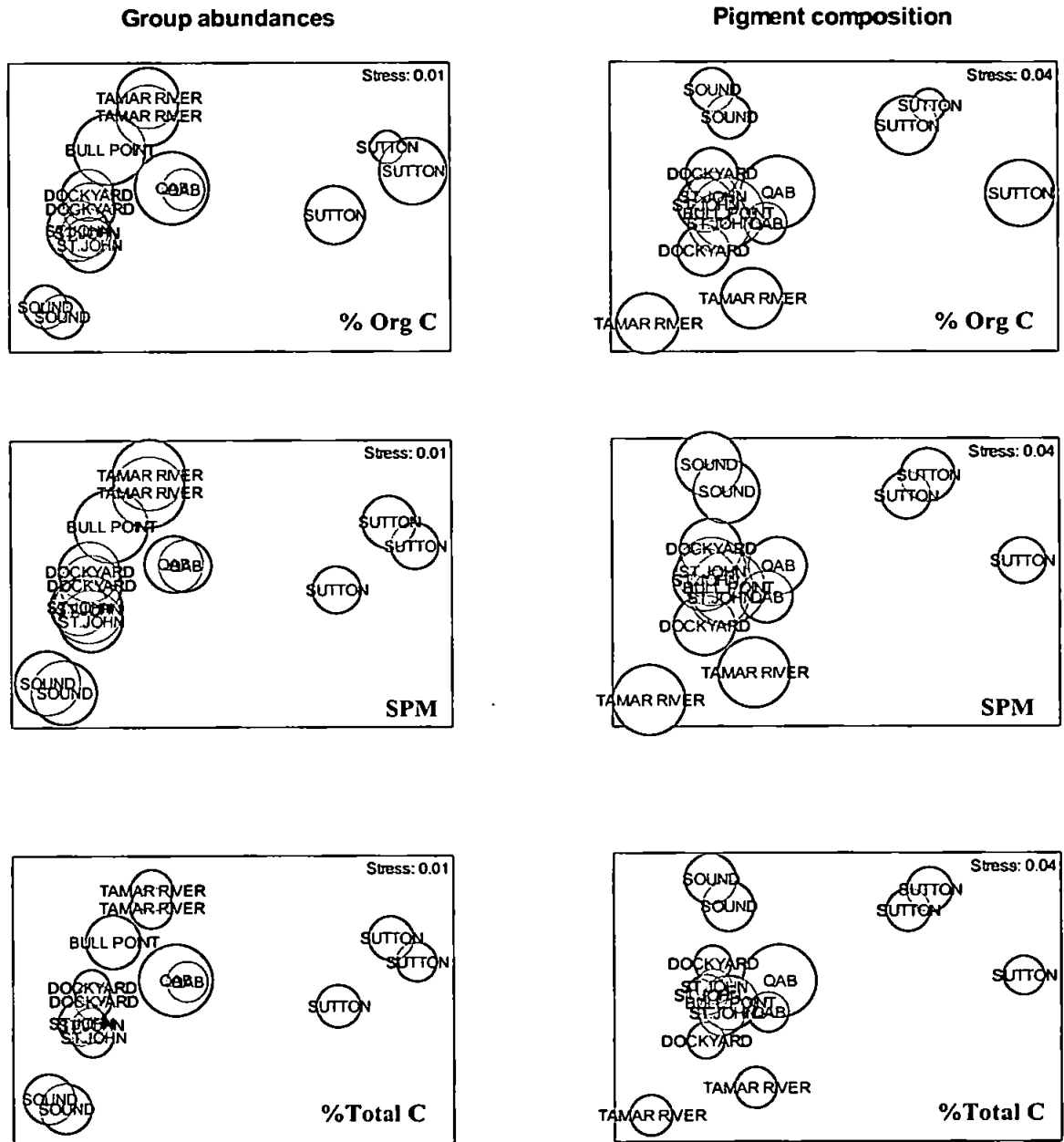


Figure 6.12 (cont.). Multi-Dimensional Scaling (MDS) of Bray-Curtis similarities of \sqrt{x} -transformed group abundances data (graphs on the left) and of \sqrt{x} -transformed pigment composition data (graphs on the right) for 7 stations investigated (missing data for Mayflower Marina and Plym River stations). Small distances between observations indicate high similarity in community structure. Stress levels (above each graph) of <0.05 indicate an excellent representation of the relationship between observations (*i.e.*, they have not being arbitrarily placed). Both MDS set of graphs show superimposed circles which sizes indicate concentrations of Irgarol 1051[®] and atrazine, the percentage of nitrogen (%N), organic carbon (% Org C) and total carbon (%Total C), and the concentration of suspended particulate matter (SPM).

between total cells (cell ml⁻¹) (measured by AFC) and chlorophyll-*a* (µg l⁻¹) (determined by HPLC) within the seven stations, Mayflower Marina, Tamar River, Bull Point, Devonport, St. John's Lake, Plymouth Sound and QAB, resulting in the equation 9:

$$\text{Cell_numbers} = -4.83 \times \text{Chla} + 29992 \quad \text{Eq. (9)}$$

6.2.3.3. Linking biological and environmental parameters

Concentrations of particulate organic carbon and chlorophyll-*a* in the surface of the water column did not show a significant correlation ($R^2 = 0.39$, $p = 0.1356$, $N = 7$; regression not shown). Linear regression of mean values of particulate organic carbon against mean values of chlorophyll-*a* is shown in the equation 10:

$$\text{POC} = 0.0007 \times \text{Chla} + 1.708 \quad \text{Eq. (10)}$$

By applying the chemical-physical parameters to the MDS ordination between groups (based on abundances of pico- and nanoeukaryotes and prokaryotes) and pigment composition (based on concentrations of carotenoids and chlorophylls), a comparison between the biological distribution and the influences of the parameters could be made (Fig. 6.12). A reasonably clear pattern could be noted for both biological based distributions, (group abundances and pigment composition) showing 3 defined groups: Sutton Harbour, Plymouth Sound and Tamar River. A fourth group, QAB, could be identified only in the abundances based group. Correlations of the biotic pattern with the variables measured are illustrated by superimposing circles (with size indicating the relative concentrations of the measured variable) on the MDS plots. Stations Sutton Harbour and QAB showed a possible separation due to Irgarol 1051[®] for distributions based on group abundances, but the same is not clear for distributions based on pigment composition. Atrazine concentrations did not have a matching distribution pattern. The % N seems to decrease with distance from the Tamar River (S1), shown as circles of varying diameters. No relationship was observed amongst the patterns of distribution and the parameters % total carbon, % organic carbon, and SPM.

6.2.4. Discussion

This pilot study was conducted to characterise the spatial variability of antifoulant/herbicides within the Tamar Estuary and Plymouth area and to investigate

whether these pollutants might influence the spatial distribution of phytoplankton. As additional sampling was not carried out, interpretation of the results is limited and the interpretations are speculative and preliminary. They do, however, provide an indication of the approach.

Similar salinity values amongst the stations sampled indicate similar water masses at high tide. Water quality, however, can differ due to localised inputs. The highest SPM values, found at the stations Tamar River and Bull Point, could be related to higher river runoff when compared to marinas, which have lower hydrodynamics. Maximum SPM recorded for the Tamar Estuary occurs at turbidity maxima with typically 200-300 mg l⁻¹ (Uncles and Stephens, 1993) and is characterised by much lower fractional proportions of organic and inorganic carbon (Morris *et al.*, 1982). In contrast, low suspended particulate loads (< 2.5 mg l⁻¹) have been found in both freshwater and marine waters of the Tamar Estuary with the fractional contribution made by organic carbon to the particulate composition generally high (45-170 mgC g⁻¹) (Morris *et al.*, 1982). High fractional contributions of organic carbon to the SPM, as shown in this study for Bull Point, Tamar River and QAB stations, indicated that living and/or relatively undegraded primary production products comprised a high proportion of the particulate inputs to the estuary (Morris *et al.*, 1982), along with nitrogen contributions (Bull Point and Tamar River stations). Within the Tamar Estuary, the fractional contribution of organic carbon decrease in an approximately linear correlation with decreasing salinity (Morris *et al.*, *op. cit.*), indicating the importance of marine biological contributions to this area.

Based on group abundances and pigment composition, Sutton Harbour was very different to the other stations sampled. It was characterized by the lowest cell abundances, with a lower contribution of cyanophytes, picoeucaryotes and a higher contribution of nanoeukaryotes to the total cell numbers (< 20 µm). Although abundances (cell numbers) of larger sized phytoplanktonic cells (> 20 µm) have not been investigated, they might have been a relevant component of the phytoplankton. Higher fucoxanthin:chl-*a* and chlorophyll *c*₁:*c*₂:chl-*a* ratios at Sutton Harbour compared to the other stations could indicate the presence of diatoms, prasinophytes, dinophytes, cryptophytes and/or chrysophytes. These groups are included in the nanoplankton (2-20 µm) and microplankton (20->200 µm) size classes (Jeffrey and Hallegraeff, 1990). Although fucoxanthin is shared by several phytoplankton groups, it is the main pigment component of diatoms. Chlorophylls *c*₁:*c*₂ are, however, shared amongst prasinophytes, dinophytes, cryptophytes and chrysophytes, and demonstrated a significant relationship

with nanoplankton ($r = 0.8$; $p = 0.001$). Such changes in concentrations of the detected pigments between stations can be used for assessing the development of the pigment-related group, as an indicator of the effects of toxicants.

The comparison between community structure and environmental gradients or biocide levels did not reveal clearly defined relationships. Due to the higher Irgarol 1051[®] level present at the Sutton Harbour station when compared to other stations, it is possible that this compound has influenced phytoplankton composition, but as with most environmental surveys, causality is extremely difficult to demonstrate. In addition, the low levels of biocides found during this survey are unlikely to have had a significant effect on community structures (see Chapter 3 and Chapter 5). Other influences, such as complex mixtures of pollutants associated with marina/harbour activities (e.g. oils and surfactants), may have contributed to alterations in phytoplankton community structure in Sutton Harbour. Also, flushing regimes are very different at this location. The measurements obtained in this pilot study, based on single point-in-time sampling regime, may not reflect the true variability in concentrations of contaminants or the environmental variables measured. In addition to the natural variability between stations, other sources of contamination are believed to affect the pattern of phytoplankton distribution, e.g. inputs of macronutrients, with ammonium loads higher than nitrate in the Tamar Estuary (Uncles *et al.*, 2002), polycyclic aromatic hydrocarbons (Readman *et al.*, 1982), complexing polyphenols released from macroalgae, which can potentially influence the potential toxicity of metals due to changes in metal speciation (Ragan *et al.*, 1980; Gledhill *et al.*, 1997). Therefore, the extent of herbicidal/antifoulant impact on phytoplankton (<20 μm) and chemotaxonomic distributions cannot be ascertained from the present data. Further time-series surveys are needed to allow more consistent patterns of phytoplankton distributions to be established which may then be related to xenobiotic influences.

Coastal phytoplankton <20 μm have not been fully evaluated in terms of their natural variability or their responses to xenobiotic impact. The two recently developed techniques reported in this thesis, which have proven to be effective in demonstrating the impact of biocides on phytoplankton community structures, have been applied and provide a preliminary insight into variabilities in a coastal system. HPLC pigment analyses and AFC have allowed rapid estimation/measurement of small sized phytoplankton within these coastal waters. Sutton Harbour is shown to differ from the

other stations and could prove to be a good site for further studies on temporal variability.

6.2.5. Conclusions

This pilot study has provided positive information towards the design of an approach for further investigations. Additional data could provide conclusive results concerning relationships between environmental gradients, biocide concentrations and phytoplankton community structures in the estuarine and coastal water around Plymouth. However, as has been pointed out, in most environmental surveys of contaminant distribution and biological effect measurements, causality is extremely difficult to demonstrate. In addition, the low levels of biocides reported in the present study are unlikely to induce significant changes in community structures. However, previous surveys of the area have reported much higher concentrations of antifoulants, reaching $0.12 \mu\text{g l}^{-1}$ Irgarol 1051[®] that would undoubtedly cause changes in phytoplankton community structure (see previous chapters).

Despite the limitations of this survey, it did show that Sutton Harbour has a very different community structure compared to the other stations. This could be a result of the influence of xenobiotics as well as the reduced water exchange in this area. For this reason, it is suggested that Sutton Harbour could provide an interesting location (together with appropriate controls) for more detailed and seasonal surveys.

Chapter 7

General conclusions and future research

7.1. General conclusions

In this research, an assessment of the impact of selected antifouling biocides on phytoplankton was carried out by application and comparison of a number of different techniques. Assessment at different structural levels was incorporated into this research, involving responses on cellular, population and community structure through microcosm-based experiments. In addition, an investigation into factors influencing antifoulant toxicity, such as nutrient inputs, and preliminary results from a pilot field investigation are presented.

The techniques tested in this research successfully measured physiological stress of the phytoplankton as well as changes in their community structure following exposure to antifouling booster biocides. The major achievements of my investigations are summarized below:

- The impact of the antifouling booster biocides Irgarol 1051[®], Sea-Nine 211[®], diuron and zinc pyriithione was successfully assessed. Biocides affected photosynthesis, cell density, cell viability, individual pigment composition, and selectively altered phytoplankton composition in a natural community.
- Microcosm experiments clearly demonstrated that the levels of antifouling biocides reported in the local marinas would impair the physiology and modify the composition of phytoplankton.
- It was clearly demonstrated that the toxicity varied according to the type of biocide and between phytoplankton species/groups in both unialgal experiments and in microcosms containing a natural phytoplankton community. For the phytoplankton community studied, readily degradable biocides (Sea-Nine 211[®] and zinc pyriithione) were highly toxic during the

first 24 h of exposure. At 72 h of exposure, Irgarol 1051[®] was the most toxic booster biocide studied and diuron was the least toxic.

- Differences in group-specific sensitivity to biocide exposure were successfully detected through HPLC-pigment chemotaxonomic analysis and are compared to both analytical flow cytometry and optical microscopy. CHEMTAX-HPLC analyses and microscopy revealed that prasinophytes and prymnesiophytes were the most sensitive groups and chlorophytes and dinoflagellates were comparatively the least affected upon exposure to Irgarol 1051[®]. CHEMTAX-HPLC analyses and analytical flow cytometry revealed that cyanophytes were the least affected group upon exposure to zinc pyrithione, Sea-Nine 211[®] and Irgarol 1051[®].
- Monitoring phytoplankton responses to toxicants using HPLC-pigment analysis and AFC are less time-consuming than traditional optical measurements. The use of class-specific pigment determinations combined with AFC and limited microscopic screening provides a comprehensive evaluation of the effects on a phytoplankton community under stress from antifouling booster biocides.
- Microcosm-based preliminary results for a natural phytoplankton community indicated possible influence of nutrient status on Irgarol 1051[®] toxicity, particularly for cyanophytes. Additional experiments are, however, needed in order to obtain more definitive results.
- The preliminary study on spatial distribution pattern of antifouling booster biocides and their potential association with phytoplankton composition and biomass provided information towards the design of an approach for further research. A continuation of this investigation may afford discrimination of the most impacted areas.

7.2. Future research

As discussed in the final conclusions, environmental concentrations of antifouling booster biocides can affect phytoplankton at different organizational levels. Such high concentrations in the environment are still a matter for concern. In the UK, the use of

Irgarol 1051[®] was revoked by legislation in July 2003, and the only biocides currently permitted (apart from copper) are Sea-Nine 211[®], zinc pyrithione and zineb. However, such restrictions have not been adopted worldwide. The results presented here suggest that more research on Sea-Nine 211[®] and especially zinc pyrithione is required.

Another important aspect of this research is that using a combination of techniques affords a comprehensive approach to identify toxic impairment of phytoplankton. Early warning indicators of toxic response at lower levels of biological organisation in combination with responses at a higher organizational level (community structure) are required. These allow changes in community composition and interactions between species and other chemical factors to be identified. Single species experiments are relevant for investigating direct cause-effect relationships, but they lack the system complexity of natural communities, which are of particular environmental relevance (Kimball and Levin, 1985). Changes in species composition following chronic toxic exposure could be more pronounced than physiological responses, since community structure might subtly change in response to the toxicant. Attention should be directed to cyanophytes, which indicated to be resistant to certain biocides in this study. The Cyanophyceae is a group of particular concern given their occurrence as toxic blooms (Jacoby *et al.*, 2000). Thus, consequences of biocide pollution on marine diversity during conditions which promote toxic blooms require further investigation in mesocosm-type studies.

Amongst the techniques applied here, pigment composition as an estimate of phytoplankton classes remains under development. More investigations that take into account pigment variability under stress conditions are needed. These should be conducted to investigate inter-species variations in pigment to chlorophyll-*a* ratios. Validation of the use of this technique with measurement of phytoplankton composition is essential to reinforce the application of CHEMTAX as an ecotoxicological endpoint.

Another important aspect to be considered in toxicity assessment is the effect of simultaneous exposure of organisms to multiple toxicants. The wide range of environmental toxicants from multiple sources (*e.g.* sewage oil, surfactants, etc.) together with the antifoulants, each have differing environmental properties which control fate and behaviour. Indeed, toxicants usually occur as mixtures in the aquatic environment, but most investigation relate to single compound testing. Therefore, the question arises as to whether or not reliable predictions can be made through these

single compound tests. More studies are also needed to investigate interactions between anthropogenic and naturally occurring chemicals in the environment, for example, interactions between nutrient status and toxic exposures. A continuation of the preliminary research described in the Chapter 6 would therefore be advisable. Moreover, it would also be important to investigate the capacity for recovery of phytoplankton populations following exposure and under different nutrient conditions.

Further assessments of toxic effects, through both laboratory and field investigations, would enhance the reliability of the data for risk assessment purposes. In other words, ecotoxicology must go beyond the simplistic evaluation of individual endpoints, or of single-species populations at a given site or within a given region. A thorough ecotoxicological evaluation must consider what effect the stressor is having on the ecosystem as a whole and on the interactions between species within the communities. My research has provided important and fundamental data upon which future studies can build.

Appendices

Contents

Appendice I. Autotrophs and heterotrophs species list resulted from microscopical analyses of samples from the experiment described in Chapter 4. Cell abundances. _____	158
Appendice II. Autotrophs and heterotrophs species list resulted from microscopical analyses of samples from the experiment described in Chapter 4. Carbon estimates. _____	158
Appendice III. Effects of nutrient status on toxicity (Chapter 6). Results of the two-way ANOVA (factorial 4x2) to evaluate the effects of Irgarol 1051 [®] addition on both total cells and group abundances grown under the selected nutrient conditions. _____	158
Table III.i.a. Summary of all effects from a 2-Way ANOVA analysis of 'total cell numbers'. _____	158
Table III.i.b. Probabilities for interactions between the factors 'nutrient' and 'Irgarol 1051 [®] ' using LSD <i>post hoc</i> test (2-Way ANOVA) with the parameter 'total cell numbers'. _____	158
Table III.ii.a. Summary of all effects from a 2-Way ANOVA analysis of the parameter 'percentage of cyanophytes to total cells'. _____	158
Table III.ii.b. Probabilities for interactions between the factors 'nutrient' and 'Irgarol 1051 [®] ' using LSD <i>post hoc</i> test (2-Way ANOVA) with the parameter 'percentage of cyanophytes to total cells'. _____	158
Table III.iii.a. Summary of all effects from a 2-Way ANOVA analysis of the parameter 'percentage of cryptophyte to total cells'. _____	159
Table III.iii.b. Probabilities for interactions between the factors 'nutrient' and 'Irgarol 1051 [®] ' using LSD <i>post hoc</i> test (2-Way ANOVA) with the parameter 'percentage of cryptophyte to total cells'. _____	159
Table III.iv.a. Summary of all effects from a 2-Way ANOVA analysis of the parameter 'percentage of picoeukaryote to total cells'. _____	159
Table III.iv.b. Probabilities for interactions between the factors 'nutrient' and 'Irgarol 1051 [®] ' using LSD <i>post hoc</i> test (2-Way ANOVA) with the parameter 'percentage of picoeukaryote to total cells'. _____	159
Table III.v.a. Summary of all effects from a 2-Way ANOVA analysis of the parameter 'percentage of nanoeukaryote to total cells'. _____	160
Table III.v.b. Probabilities for interactions between the factors 'nutrient' and 'Irgarol 1051 [®] ' using LSD <i>post hoc</i> test (2-Way ANOVA) with the parameter 'percentage of nanoeukaryote to total cells'. _____	160

Appendix I. Autotrophs and heterotrophs species list resulted from microscopical analyses of samples from the experiment described in Chapter 4. Data are cell abundances (cell ml⁻¹) at time 0 (sampling day) and after 96 h of exposure to Irgarol 1051[®].

Sampling time	time 0 (sampling day)		96 h	
	no addition	control	0.5 µg l ⁻¹	1 µg l ⁻¹
Irgarol 1051[®] treated samples				
ABUNDANCES (cell ml⁻¹)				
Diatoms				
<i>Cerataulina pelagica</i>	0.16	0.00	0.02	0.00
<i>Chaetoceros affinis</i>	0.32	0.38	0.09	0.00
<i>Chaetoceros calcitrans</i>	52.96	55.29	29.70	0.00
<i>Chaetoceros compressus</i>	1.28	1.97	3.10	2.20
<i>Chaetoceros danicus</i>	0.28	0.04	0.04	0.02
<i>Chaetoceros debilis</i>	0.16	0.00	0.16	0.04
<i>Chaetoceros decipiens</i>	0.28	0.04	0.18	0.02
<i>Chaetoceros didymus</i>	0.28	0.63	0.96	0.36
<i>Chaetoceros lacinosus</i>	0.32	0.00	0.00	0.02
<i>Dactyliosolen blavyana</i>	0.12	0.34	0.20	0.04
<i>Detonula pumila</i>	0.16	0.38	0.54	0.31
<i>Eucampia zoodiacus</i>	0.76	0.20	0.65	0.54
<i>Guinardia delicatula</i>	6.56	1.10	6.05	7.35
<i>Guinardia flaccida</i>	0.01	0.01	0.01	0.00
<i>Guinardia striata (Rhizosolenia stolterfothii)</i>	1.52	0.02	0.07	0.00
<i>Leptocylindrus danicus</i>	59.66	115.55	76.61	40.43
<i>Leptocylindrus mediterranea</i>	2.24	0.07	0.04	0.00
<i>Lioloma delicatula</i>	0.32	0.27	0.25	0.02
<i>Nitzschia longissima</i>	6.46	9.58	4.04	2.22
<i>Odontella mobiliensis</i>	0.02	0.00	0.00	0.01
<i>Paralia sulcata</i>	1.04	0.11	0.11	0.03
<i>Proboscia alata</i>	1.12	0.58	0.87	0.27
<i>Pseudonitzschia sp. "delicatissima"</i>	7.98	30.75	3.94	0.13
<i>Pseudonitzschia sp. "pungens"</i>	0.40	0.31	0.00	0.00
<i>Pseudonitzschia sp. "seriata"</i>	4.04	3.20	1.34	0.58
<i>Rhizosolenia heb. f. semispina</i>	0.01	0.01	0.00	0.00
<i>Rhizosolenia setigera 5µm</i>	0.08	0.02	0.00	0.04
<i>Rhizosolenia shrubsolei 5µm</i>	1.04	0.41	0.29	0.13
<i>Rhizosolenia shrubsolei 10µm</i>	0.42	0.00	0.00	0.00
<i>Roperia tessellata</i>	0.01	0.00	0.00	0.02
<i>Skeletonema costatum</i>	0.16	0.58	0.49	0.25
<i>Stauroneis membranacea</i>	0.01	0.01	0.09	0.10
<i>Thalassionema nitzschiodes</i>	0.16	0.99	1.39	0.31
Centric diatom 2µm	83.22	160.98	190.64	182.17
Centric diatom 5µm cf <i>T. gravida</i>	5.32	4.47	6.58	1.81
Centric diatom 10µm cf <i>T. gravida</i>	0.40	1.23	1.93	0.54
Centric diatom 20µm cf <i>T. gravida</i>	0.64	0.78	0.43	1.43
Centric diatom 30µm cf <i>T. gravida</i>	0.52	0.29	0.29	0.20
Total Diatoms	240.43	390.61	331.11	241.61
Dinoflagellates				
<i>Ceratium fusus</i>	0.06	0.01	0.01	0.01
<i>Ceratium horridum</i>	0.17	0.01	0.03	0.02
<i>Ceratium macroceros</i>	0.03	0.01	0.01	0.00

<i>Ceratium tripos</i>	0.25	0.07	0.07	0.08
<i>Ceratium 'minutum'/C. gamete</i>	0.00	0.01	0.01	0.00
<i>Gymnodinium sp. A</i>	8.36	16.60	14.90	17.66
<i>Gymnodinium sp. B</i>	4.56	43.20	4.67	1.06
<i>Heterocapsa cachenina</i>	60.52	35.38	210.99	0.21
<i>Kerenia mikimotoi (Gyrodinium aureolum)</i>	39.52	41.92	36.60	25.96
<i>Mesoporos perforatus</i>	0.64	0.43	0.20	0.25
<i>Prorocentrum micans</i>	0.20	0.39	0.28	0.20
<i>Prorocentrum minimum</i>	46.74	56.74	61.71	8.72
<i>Scripsiella sp.</i>	0.64	0.31	0.27	0.02
Total Dinoflagellates	161.69	195.07	329.74	54.20
Flagellates				
Chlorophyceae				
? <i>Dunaliella sp.</i>	30.26	122.86	80.49	512.60
<i>Eutreptia sp.</i>	3.80	10.85	14.47	10.43
Total Chlorophyceae	34.06	133.71	94.96	523.03
Chrysophyceae				
<i>Dinobryon</i>		0.85	0.58	0.00
<i>Meringosphaera</i>		12.71	12.71	8.47
Total Chrysophyceae	0.00	13.56	13.29	8.47
Cryptophyceae				
Total Cryptophyceae	37.83	50.84	38.34	0.00
Prasinophyceae				
1-4µm (? <i>Micromonas sp.</i>)	302.60	2732.48	1262.45	902.35
<i>Tetraselmis sp.</i>	0.38	4.89	13.13	0.00
>10µm	0.38	1.70	1.92	1.49
<i>Halosphaera sp.</i>		0.01	0.00	0.01
<i>Pterasperma spp.</i>	0.04	0.00	0.09	0.01
Total Prasinophyceae	303.40	2739.09	1277.59	903.86
Prymnesiophyceae				
1-4µm	340.43	533.79	504.13	233.00
5-10µm	408.51	2118.20	584.62	309.26
>10µm		45.79	44.94	8.47
? <i>Emiliana huxleyi</i>	295.04	355.86	220.29	254.18
Total Prymnesiophyceae	1043.97	3053.63	1353.98	804.92
Unidentified				
Unidentified Flagellates 1-4µm	1240.66	4130.49	3024.79	2647.75
Unidentified Flagellates 5-10µm	317.73	635.46	432.11	249.95
Total Unidentified Flagellates	1558.39	4765.95	3456.90	2897.70
Cyanobacteria				
Total Cyanobacteria	29500.00	61880.00	55720.00	33040.00
Heterotrophs				
" <i>Strombidium</i> " <20µm	1.96	0.54	0.18	0.16
" <i>Strombidium</i> " 20-30µm	0.52	0.00	0.00	0.00
<i>Amphidinium sp.</i>		0.22	0.02	0.07
<i>cf. Cafeteria</i>		127.09	186.40	334.68

Choanoflagellates		0.00	16.95	50.84
Gymnodinioid	52.96	16.95	0.00	0.00
<i>Gyrodinium sp. cf G. fusiformis</i>	1.28	0.76	0.52	0.31
<i>Katodinium sp.</i>	0.76	0.52	0.52	0.25
<i>Mesodinium >30µm</i>	0.20	0.00	0.09	0.00
<i>Pronoctiluca sp.</i>	0.64	0.36	0.25	0.13
<i>Protoberidinium bipes</i>	0.08	0.20	0.02	0.00
<i>Protoberidinium cf. P. steinii</i>	0.12	0.01	0.02	0.00
Unidentified Peridinians	1.60	1.52	1.52	1.39
<i>Torodinium sp. B</i>	0.32	0.04	0.00	0.02
<i>Torodinium sp. Cf T. robustum</i>	0.36	0.11	0.09	0.00
Total Heterotrophs	60.80	148.33	206.57	387.84
Nauplei in 100ml	8.00		5.60	6.72

Appendice II. Autotrophs and heterotrophs species list resulted from microscopical analyses of samples from the experiment described in Chapter 4. Data are carbon estimates (mg m^{-3}) at time 0 (sampling day) and after 96 h of exposure to Irgarol 1051[®].

Sampling time	time 0 (sampling day)		96 h	
	Irgarol 1051 [®] treated samples	no addition	control	0.5 $\mu\text{g l}^{-1}$
CARBON ESTIMATES (mg m^{-3})				
Diatoms				
<i>Cerataulina pelagica</i>	0.29	0.00	0.04	0.00
<i>Chaetoceros affinis</i>	0.01	0.01	0.00	0.00
<i>Chaetoceros calcitrans</i>	0.23	0.24	0.13	0.00
<i>Chaetoceros compressus</i>	0.02	0.03	0.04	0.03
<i>Chaetoceros danicus</i>	0.06	0.01	0.01	0.00
<i>Chaetoceros debilis</i>	0.02	0.00	0.02	0.01
<i>Chaetoceros decipiens</i>	0.04	0.01	0.02	0.00
<i>Chaetoceros didymus</i>	0.02	0.04	0.06	0.02
<i>Chaetoceros lacinosus</i>	0.01	0.00	0.00	0.00
<i>Dactyliosolen blavyana</i>	0.40	1.12	0.67	0.15
<i>Detonula pumila</i>	0.08	0.18	0.26	0.15
<i>Eucampia zoodiacus</i>	0.21	0.06	0.18	0.15
<i>Guinardia delicatula</i>	2.22	0.37	2.04	2.48
<i>Guinardia flaccida</i>	0.06	0.04	0.07	0.00
<i>Guinardia striata (Rhizosolenia stolterfothii)</i>	2.48	0.04	0.12	0.00
<i>Leptocylindrus danicus</i>	0.84	1.62	1.07	0.57
<i>Leptocylindrus mediterranea</i>	0.03	0.00	0.00	0.00
<i>Lioloma delicatula</i>	0.01	0.01	0.01	0.00
<i>Nitzschia longissima</i>	0.13	0.19	0.08	0.04
<i>Odontella mobiliensis</i>	0.06	0.00	0.00	0.02
<i>Paralia sulcata</i>	0.21	0.02	0.02	0.01
<i>Proboscia alata</i>	0.37	0.19	0.28	0.09
<i>Pseudonitzschia sp. "delicatissima"</i>	0.07	0.28	0.04	0.00
<i>Pseudonitzschia sp. "pungens"</i>	0.02	0.02	0.00	0.00
<i>Pseudonitzschia sp. "seriata"</i>	0.21	0.16	0.07	0.03
<i>Rhizosolenia heb. f. semispina</i>	0.01	0.01	0.00	0.00
<i>Rhizosolenia setigera 5μm</i>	0.01	0.00	0.00	0.01
<i>Rhizosolenia shrubsolei 5μm</i>	0.34	0.14	0.09	0.04
<i>Rhizosolenia shrubsolei 10μm</i>	0.39	0.00	0.00	0.00
<i>Roperia tessellata</i>	0.01	0.00	0.00	0.01
<i>Skeletonema costatum</i>	0.00	0.00	0.00	0.00
<i>Stauroneis membranacea</i>	0.01	0.01	0.06	0.06
<i>Thalassionema nitzschiodes</i>	0.00	0.02	0.03	0.01
Centric diatom 2 μm	0.08	0.16	0.19	0.18
Centric diatom 5 μm cf <i>T. gravida</i>	0.05	0.04	0.06	0.02
Centric diatom 10 μm cf <i>T. gravida</i>	0.02	0.05	0.08	0.02
Centric diatom 20 μm cf <i>T. gravida</i>	0.13	0.16	0.09	0.29
Centric diatom 30 μm cf <i>T. gravida</i>	0.27	0.15	0.15	0.10
Total Diatoms	9.40	5.37	6.00	4.50
Dinoflagellates				
<i>Ceratium fusus</i>	0.09	0.01	0.01	0.01
<i>Ceratium horridum</i>	1.12	0.04	0.18	0.15
<i>Ceratium macroceros</i>	0.13	0.02	0.05	0.00
<i>Ceratium tripos</i>	3.60	1.07	1.07	1.15

<i>Ceratium 'minutum'/C. gamete</i>	0.00	0.02	0.02	0.00
<i>Gymnodinium sp. A</i>	0.04	0.08	0.07	0.09
<i>Gymnodinium sp. B</i>	0.21	2.03	0.22	0.05
<i>Heterocapsa cathonina</i>	0.30	0.17	1.03	0.00
<i>Kerenia mikimotoi (Gyrodinium aureolum)</i>	19.99	21.20	18.51	13.13
<i>Mesoporos perforatus</i>	0.08	0.05	0.03	0.03
<i>Prorocentrum micans</i>	0.34	0.66	0.47	0.34
<i>Prorocentrum minimum</i>	1.22	1.48	1.60	0.23
<i>Scropsiella sp.</i>	0.29	0.14	0.12	0.01
Total Dinoflagellates	27.40	26.98	23.39	15.19
Chlorophyceae				
?Dunaliella sp.	1.46	5.92	3.88	24.68
Eutreptia sp.	0.93	2.65	3.53	2.54
Total Chlorophyceae	2.38	8.56	7.41	27.22
Chrysophyceae				
Dinobryon	0.00	0.01	0.01	0.00
Meringosphaera	0.00	0.17	0.17	0.11
Total Chrysophyceae	0.00	0.18	0.17	0.11
Cryptophyceae				
Total Cryptophyceae	0.49	0.66	0.50	0.00
Prasinophyceae				
1-4µm (? <i>Micromonas sp.</i>)	0.30	2.73	1.26	0.90
<i>Tetraselmis sp.</i>	0.00	0.06	0.17	0.00
>10µm	0.03	0.15	0.17	0.13
<i>Halosphaera sp.</i>	0.00	0.01	0.00	0.01
<i>Pterasperma spp.</i>	0.01	0.00	0.02	0.00
Total Prasinophyceae	0.35	2.96	1.62	1.05
Prymnesiophyceae				
1-4µm	0.34	0.53	0.50	0.23
5-10µm	5.23	27.11	7.48	3.96
>10µm	0.00	4.12	4.04	6.10
? <i>Emiliania huxleyi</i>	3.78	4.55	2.82	3.25
Total Prymnesiophyceae	9.35	36.32	14.85	13.55
Unidentified				
Unidentified Flagellates 1-4µm	1.24	4.13	3.02	2.65
Unidentified Flagellates 5-10µm	4.07	8.13	5.53	3.20
Total unidentified flagellates	5.31	12.26	8.56	5.85
Flagellates				
Total Flagellates	17.88	60.95	33.10	47.78
Cyanobacteria				
Total Cyanobacteria	6.74	14.15	12.74	7.55
Heterotrophs				
" <i>Strombidium</i> " <20µm	0.18	0.05	0.02	0.01
" <i>Strombidium</i> " 20-30µm	0.62	0.00	0.00	0.00
<i>Amphidinium sp.</i>	0.00	0.03	0.00	0.01

<i>cf. Cafeteria</i>	0.00	0.13	0.19	0.33
Choanoflagellates	0.00	0.00	0.17	0.51
Gymnodinioid	0.69	0.22	0.00	0.00
<i>Gyrodinium sp. cf G. fusiformis</i>	0.47	0.28	0.19	0.12
<i>Katodinium sp.</i>	0.03	0.02	0.02	0.01
<i>Mesodinium >30µm</i>	0.40	0.00	0.18	0.00
<i>Pronoctiluca sp.</i>	0.21	0.12	0.08	0.04
<i>Protoberidinium bipes</i>	0.04	0.10	0.01	0.00
<i>Protoberidinium cf. P. steinii</i>	0.06	0.01	0.01	0.00
Unidentified Peridinians	0.04	0.04	0.04	0.04
<i>Torodinium sp. B</i>	0.16	0.02	0.00	0.01
<i>Torodinium sp. Cf T. robustum</i>	0.98	0.31	0.24	0.00
Total Heterotrophs	3.89	1.33	1.16	1.09

Appendix III. Effects of nutrient status on toxicity (Chapter 6). Results of the two-way ANOVA (Factorial 4x2) to evaluate the effects of Irgarol 1051[®] addition on both total cells and group abundances grown under the selected nutrient conditions (excess of nitrate and/or phosphate). Tables illustrate (a) the main effects and (b) the interactions between treatments (LSD *post hoc*; $\alpha = 0.05$).

* Significant difference at $\alpha = 0.05$

III.i.a. Summary of all effects from a 2-Way ANOVA analysis of 'total cell numbers'.

	df	MS	df	MS	F	p-level
	Effect	Effect	Error	Error		
NUTRIENT	3	43.7	16	8.7	5.0	0.01223*
IRGAROL	1	864.0	16	8.7	99.2	0.00001*
NUTRIENT x IRGAROL	3	5.2	16	8.7	0.60	0.62448

III.i.b. Probabilities for interactions between the factors 'nutrient' and 'Irgarol 1051[®]' using LSD *post hoc* test (2-Way ANOVA) with the parameter 'total cell numbers'.

	{1}	{2}	{3}	{4}	{5}	{6}	{7}
	6.3	17.7	8.3	23.0	8.0	18.3	3.3
N IRG {1}							
N CON {2}	0.00024*						
N+P_IRG_{3}	0.41872	0.00135*					
N+P_CON_{4}	0.00000*	0.04174*	0.00002*				
P IRG {5}	0.49903	0.00101*	0.89170	0.00001*			
P CON {6}	0.00014*	0.78556	0.00075*	0.07063	0.00056*		
TSV IRG {7}	0.23103	0.00002*	0.05446	0.00000*	0.07063	0.00001*	
TSV_CON_{8}	0.00242*	0.28477	0.01375*	0.00433*	0.01033*	0.18553	0.00018*

III.ii.a. Summary of all effects from a 2-Way ANOVA analysis of the parameter 'percentage of cyanophytes to total cells'.

	df	MS	df	MS	F	p-level
	Effect	Effect	Error	Error		
NUTRIENT	3	18.7	16	8.5	2.2	0.1282
IRGAROL	1	864.0	16	8.5	101.6	0.0001*
NUTRIENT x IRGAROL	3	31.3	16	8.5	3.7	0.0343*

III.ii.b. Probabilities for interactions between the factors 'nutrient' and 'Irgarol 1051[®]' using LSD *post hoc* test (2-Way ANOVA) with the parameter 'percentage of cyanophytes to total cells'.

	{1}	{2}	{3}	{4}	{5}	{6}	{7}
	19.3	10.3	20.3	2.7	19.7	6.0	14.7
N IRG {1}							
N CON {2}	0.00164*						
N+P IRG {3}	0.68001	0.00068*					
N+P_CON_{4}	0.00001*	0.00534*	0.00001*				
P IRG {5}	0.89039	0.00122*	0.78302	0.00001*			
P CON {6}	0.00004*	0.08746	0.00002*	0.18052	0.00003*		
TSV IRG {7}	0.06760	0.08746	0.03006*	0.00012*	0.05190	0.00220*	
TSV_CON_{8}	0.00009*	0.18052	0.00004*	0.08746	0.00007*	0.68001	0.00534*

III.iii.a. Summary of all effects from a 2-Way ANOVA analysis of the parameter 'percentage of cryptophyte to total cells'.

	df	MS	df	MS	F	p-level
	Effect	Effect	Error	Error		
NUTRIENT	3	1.16	16	0.49	2.36	0.11017
IRGAROL	1	0.29	16	0.49	0.58	0.45744
NUTRIENT x IRGAROL	3	0.70	16	0.49	1.42	0.27239

III.iii.b. Probabilities for interactions between the factors 'nutrient' and 'Irgarol 1051[®]' using LSD post hoc test (2-Way ANOVA) with the parameter 'percentage of cryptophyte to total cells'.

	{1}	{2}	{3}	{4}	{5}	{6}	{7}
	2.4	3.1	2.3	1.5	2.8	2.8	3.1
N IRG {1}							
N CON {2}	0.25092						
N+P IRG {3}	0.81359	0.17167					
N+P CON {4}	0.13291	0.01353*	0.19783				
P IRG {5}	0.47752	0.64896	0.34790	0.03451*			
P CON {6}	0.53808	0.58188	0.39772	0.04182*	0.92305		
TSV IRG {7}	0.23729	0.97133	0.16162	0.01255*	0.62359	0.55785	
TSV CON {8}	0.96485	0.23429	0.84788	0.14345	0.45130	0.50994	0.22136

III.iv.a. Summary of all effects from a 2-Way ANOVA analysis of the parameter 'percentage of picoeukaryote to total cells'.

	df	MS	df	MS	F	p-level
	Effect	Effect	Error	Error		
NUTRIENT	3	9.3	16	40.58	0.23	0.87442
IRGAROL	1	1106.6	16	40.58	27.27	0.00008*
NUTRIENT x IRGAROL	3	23.4	16	40.58	0.58	0.63828

III.iv.b. Probabilities for interactions between the factors 'nutrient' and 'Irgarol 1051[®]' using LSD post hoc test (2-Way ANOVA) with the parameter 'percentage of picoeukaryote to total cells'.

	{1}	{2}	{3}	{4}	{5}	{6}	{7}
	13.9	22.0	12.2	29.6	13.1	26.7	11.8
N IRG {1}							
N CON {2}	0.13753						
N+P IRG {3}	0.75508	0.07834					
N+P CON {4}	0.00794*	0.16137	0.00407*				
P IRG {5}	0.87780	0.10478	0.87402	0.00572*			
P CON {6}	0.02537*	0.38035	0.01330*	0.57907	0.01850*		
TSV IRG {7}	0.69075	0.06659	0.93115	0.00339*	0.80661	0.01110*	
TSV CON {8}	0.02346*	0.36060	0.01227*	0.60525	0.01709*	0.96936	0.01023*

III.v.a. Summary of all effects from a 2-Way ANOVA analysis of the parameter 'percentage of nanoeukaryote to total cells'.

	df Effect	MS Effect	df Error	MS Error	F	p-level
NUTRIENT	3	43.7	16	34.15	1.28	0.31550
IRGAROL	1	2050.8	16	34.15	60.1	0.00001*
NUTRIENT x IRGAROL	3	70.3	16	34.15	2.06	0.14620

III.v.b. Probabilities for interactions between the factors 'nutrient' and 'Irgarol 1051®' using LSD post hoc test (2-Way ANOVA) with the parameter 'percentage of nanoeukaryote to total cells'.

	{1}	{2}	{3}	{4}	{5}	{6}	{7}
	37.1	56.5	36.2	61.8	36.7	56.6	47.9
N IRG {1}							
N CON {2}	0.00092*						
N+P IRG {3}	0.84332	0.00061*					
N+P CON {4}	0.00009*	0.28059	0.00006*				
P IRG {5}	0.93341	0.00077*	0.90910	0.00008*			
P CON {6}	0.00089*	0.98379	0.00058*	0.28925	0.00074*		
TSV IRG {7}	0.03908*	0.08988	0.02627*	0.00997*	0.03308*	0.08658	
TSV CON {8}	0.00073*	0.91126	0.00048*	0.33054	0.00061*	0.92738	0.07307

References

- Aiken, J., Fishwick, J., Moore, G., Pemberton, K., 2004. The annual cycle of phytoplankton photosynthetic quantum efficiency, pigment composition and optical properties in the western English Channel. *Journal of the Marine Biological Association of the United Kingdom*, 84: 301-313.
- Allison, D. G., 2003. The biofilm matrix. *Biofouling*, 19: 139-150.
- Andersen, R. A., Bidigare, R. R., Keller, M. D., Latasa, M., 1996. A comparison of HPLC pigment signatures and electron microscopy observations for oligotrophic waters of the North Atlantic and Pacific Oceans. *Deep-Sea Research*, 43: 517-537.
- Anderson, J. M., Park, Y-I., Chow, W. S., 1997. Photoinactivation and photoprotection of photosystem II in nature. *Physiologia Plantarum*, 100: 214-223.
- Arsenault, G., Cvetkovic, A. D., Popovic, R., 1993. Toxic effects of copper on *Selenastrum capricornutum* measured by a flow cytometry-based method. *Water Pollution Research Journal of Canada*, 28: 757-765.
- Aveline, B. M., Kochevar, I. E., Redmond, R. W., 1996. Photochemistry of N-hydroxy-2(1H)-pyridone, a more selective source of hydroxyl radicals than N-hydroxypyridine-2(1H)-thione. *Journal of the American Chemical Society*, 118:10124-10133.
- Barber, J., Malkin, S., Telfer, A., 1989. The origin of chlorophyll fluorescence in vivo and its quenching by the photosystem II reaction centre. *Philosophical Transactions of the Royal Society of London Series B*, 323:227-239.
- Barlow, R. G., Cummings, D. G., Gibb, S. W., 1997. Improved resolution of mono- and divinyl chlorophylls a and b and zeaxanthin and lutein in phytoplankton extracts using reverse phase C-8 HPLC. *Marine Ecology-Progress Series*, 161: 303-307.
- Barlow, R.G., Mantoura, R.F.C., Gough, M.A., Fileman, T.W., 1993. Pigment signatures of the phytoplankton composition in the northeastern Atlantic during the 1990 spring bloom. *Deep-Sea Research*, 41: 459-477.
- Beardall, J., Young, E., Roberts, S., 2001. Approaches for determining phytoplankton nutrient limitation. *Aquatic Sciences*, 63: 44-69.

- Beaumont, A. R., Newman, P. B., 1986. Low-levels of tributyl tin reduce growth of marine microalgae. *Marine Pollution Bulletin*, 17: 457-461.
- Beers, J. R., Reid, F. M. H., Stewart, G. L., 1975. Microplankton of the North Pacific central gyre. Population structure and abundance, June 1973. *Internationale Revue Der Gesamten Hydrobiologie*, 60: 607-638.
- Behra, R., Genoni, G. P., Joseph, A. L., 1999. Effect of atrazine on growth, photosynthesis, and between-strain variability in *Scenedesmus subspicatus* (Chlorophyceae). *Archives of Environmental Contamination and Toxicology*, 37: 36-41.
- Bennett, A., Bianchi, T. S., Means, J.C., 2000. The Effects of PAH Contamination and Grazing on the Abundance and Composition of Microphytobenthos in Salt Marsh Sediments (Pass Fourchon, LA, U.S.A.): II: The Use of Plant Pigments as Biomarkers. *Estuarine, Coastal and Shelf Science*, 50: 425-439.
- Bentley-Mowat, J. A., 1982. Application of fluorescence microscopy to pollution studies on marine phytoplankton. *Botanica Marina*, 25: 203-204.
- Bérard, A., Benninghoff, C., 2001. Pollution-induced community tolerance (PICT) and seasonal variations in the sensitivity of phytoplankton to atrazine in nanocosms. *Chemosphere*, 45: 427-437.
- Bérard, A., Dorigo, U., Mercier, I., Slooten, K. B., Grandjean, D., Leboulanger, C., 2003. Comparison of the ecotoxicological impact of the triazines Irgarol 1051 and atrazine on microalgal cultures and natural microalgal communities in Lake Geneva. *Chemosphere*, 53: 935-944.
- Berglund, D. L., Eversman, S., 1988. Flow cytometric measurement of pollutant stresses on algal cells. *Cytometry*, 9: 150-155.
- Blaise, C., Menard, L., 1998. A micro-algal solid phase test to assess the toxic potential of freshwater sediments. *Water Quality Research Journal of Canada*, 33: 133-151.
- Blanck, H., 1985. A simple community level, ecotoxicological test system using samples of periphyton. *Hydrobiologia*, 12: 251-261.
- Boalch, G. T., 1987. Changes in the phytoplankton of the western English Channel in recent years. *British Phycological Journal*, 22: 225-235.

- Boxall, A. B. A., Comber, S. D., Conrad, A. U., Howcroft, J., Zaman, N., 2000. Inputs, monitoring and fate modelling of antifouling biocides in UK estuaries. *Marine Pollution Bulletin*, 40: 898-905.
- Boxall, A., Conrad, A. Reed, S., 1998. Environmental Problems from Antifouling Agents: Survey of manufacturers, Chandlers (Suppliers) and Treatment Sites. Environment Agency R&D Technical Report P215.
- Breton, E., Brunet, C., Sautour, B., Brylinski, J-M., 2000. Annual variations of phytoplankton biomass in the Eastern English Channel: comparison by pigment signatures and microscopic counts. *Journal of Plankton Research*, 22: 1423-1440.
- Brown, L. S., Lean, D. R. S., 1995. Toxicity of selected pesticides to lake phytoplankton measured using photosynthetic inhibition compared to maximal uptake rates of phosphate and ammonium. *Environmental Toxicology and Chemistry*, 14: 93-98.
- Burkill, P. H., Mantoura, R. F. C., 1990. The rapid analysis of single marine cells by flow-cytometry. *Philosophical transactions of the Royal Society of London series A - Mathematical Physical and Engineering Sciences*, 333: 99-112.
- Burkill, P. H., Mantoura, R. F. C., Llewellyn, C. A., Owens, N. J. P., 1987. Microzooplankton grazing and selectivity of phytoplankton in coastal waters. *Marine Biology*, 93: 581-590.
- Campbell, D., Clarke, A. K., Gustafsson, P., Öquist, G., 1996. D1 exchange and the Photosystem II repair cycle in the cyanobacterium *Synechococcus*. *Plant Science*, 115: 183-190.
- Campbell, D., Eriksson, M-J., Öquist, G., Gustafsson, P., Clarke, A. K., 1998. The cyanobacterium *Synechococcus* resists UV-B by exchanging photosystem II reaction-center D1 proteins. *Proceedings of the National Academy of Sciences of the USA*, 95: 364-369.
- Campbell, L., 2001. Flow cytometric analysis of autotrophic picoplankton. *Methods in Microbiology*, 30: 317-343.
- Carpenter, E. J., Chang, J., 1988. Species-specific phytoplankton growth-rates via diel DNA-synthesis cycles. 1. Concept of the method. *Marine Ecology-Progress Series*, 43: 105-111.
- Carr, M. R., Tarran, G. A., Burkill, P. H., 1996. Discrimination of marine phytoplankton species through the statistical analysis of their flow cytometric signatures. *Journal of Plankton Research*, 18: 1225-1238.

- Carreto, J. I., Montoya, N. G., Benavides, H. R., Guerrero, R., Carignan, M. O., 2003. Characterization of spring phytoplankton communities in the Rio de La Plata maritime front using pigment signatures and cell microscopy. *Marine Biology*, 143: 1013-1027.
- Chesworth, J. C., Donkin, M. E., Brown, M. T., 2004. The interactive effects of the antifouling herbicides Irgarol 1051 and Diuron on the seagrass *Zostera marina* (L.). *Aquatic Toxicology*, 66: 293-305.
- Ciba-Geigy Corporation, 1996. YSDEC Registration of Irgarol Algicide 7/96, <http://pmep.cce.cornell.edu>.
- Clarke, K. R., Gorley, R. N., 2001. PRIMER v5 – Plymouth Routines in Multivariate Ecological Research. Statistical software. PRIMER-E Ltd, 91 pp.
- Collier, J. L., Campbell, L., 1999. Flow cytometry in molecular aquatic ecology. *Hydrobiologia*, 401: 33-53.
- Collier, J. L., Grossman, A. R., 1992. Chlorosis induced by nutrient deprivation in *Synechococcus sp* strain pcc-7942 - not all bleaching is the same. *Journal of Bacteriology*, 174: 4718-4726.
- Collier, P. J., Ramsey, A., Waigh, R. D., Douglas, K. T., Austin, P., Gilbert, P., 1990. Chemical reactivity of some isothiazolone biocides. *Journal of Applied Bacteriology*, 69: 578-584.
- Communauté Européenne (1989) Directive du Conseil. *Journal Officiel des Communautés Européennes*, No. L398/19, 19-23.
- Connelly, D. P., Readman, J. W., Knap, A. H., Davies, J., 2001. Contamination of the coastal waters of Bermuda by organotins and the triazine herbicide Irgarol 1051. *Marine Pollution Bulletin*, 42: 409-414.
- Cremlyn, R. J., 1991. *Agrochemicals: Preparation and Mode of Action*. Wiley, New York.
- Cucci, T. L., Shumway, S. E., Brown, W. S., Newell, C. R., 1989. Using phytoplankton and flow cytometry to analyze grazing by marine organisms. *Cytometry*, 10: 659-669.
- Da Gama, B. A. P., Pereira, R. C., Carvalho, A. G. V., Coutinho, R., Yoneshigue-Valentin, Y., 2002. The effects of seaweed secondary metabolites on biofouling. *Biofouling*, 18: 13-20.
- Dahl, B., Blanck, H., 1996. Toxic effects of the antifouling agent Irgarol 1051 on periphyton communities in coastal water microcosms. *Marine Pollution Bulletin*, 32: 342-350.

- De Jong, L., Admiraal, W., 1984. Competition between three estuarine benthic diatom species in mixed cultures. *Marine Ecology-Progress Series*, 18: 269-275.
- DeLorenzo, M. E., Scott, G. I., Ross, P. E., 1999. Effects of the agricultural pesticides atrazine, deethylatrazine, endosulfan, and chlorpyrifos on an estuarine microbial food web. *Environmental Toxicology and Chemistry*, 18: 2824-2835.
- DeLorenzo, M. E., Scott, G. I., Ross, P. E., 2001. Toxicity of pesticides to aquatic microorganisms: a review. *Environmental Toxicology and Chemistry*, 20: 84-98.
- DeLorenzo, M. E., Taylor, L. A., Lund, S. A., Pennington, P. L., Strozier, E. D., Fulton, M. H., 2002. Toxicity and bioconcentration potential of the agricultural pesticide endosulfan in phytoplankton and zooplankton. *Archives of Environmental Contamination and Toxicology*, 42: 173-181.
- Demming-Adams, B., 1990. Carotenoids and photoprotection in plants: a role for the xanthophylls zeaxanthin. *Biochimica et Biophysica Acta*, 1020: 1-24.
- DeNoyelles, F., Kettle, W. D., Sinn, D. E., 1982. The responses of plankton communities in experimental ponds to atrazine, the most heavily used pesticide in the United-States. *Ecology*, 63: 1285-1293.
- Derbyshire, R. L., Jacobson, A. H., O'Dowd, M. L., Santangelo, M. A., 1991. Metabolism of RH-5287 in bluegill sunfish. Rohm and Haas Company Technical Report n° 34-90-71, Rohm and Haas Company, Spring House, PA.
- Devilla, R. A., Brown, M. T., Donkin, M. E., Tarran, G., Aiken, J., Readman, J. W. (*in press*). Impact of antifouling booster biocides on single microalgal species and on a natural marine phytoplankton community. *Marine Ecology-Progress Series*.
- Dinning, A. J., Al-Adham, I. S. I., Eastwood, I. M., Austin, P., Collier, P. J., 1998. Pyrithiones as inhibitors of bacterial ATP synthesis. *Journal of Applied Microbiology*, 85: 141-146.
- Dorigo, U., Leboulanger, C., 2001. A pulse-amplitude modulated fluorescence-based method for assessing the effects of photosystem II herbicides on freshwater periphyton. *Journal of Applied Phycology*, 13: 509-515.
- Dorsey, J., Yentsch, C. M., Mayo, S., McKenna, C., 1989. Rapid analytical technique for the assessment of cell metabolic activity in marine microalgae. *Cytometry*, 10: 622-628.
- Dubelaar, G. B. J., Jonker, R. R., 2000. Flow cytometry as a tool for the study of phytoplankton. *Scientia Marina*, 64: 135-156.

- Dubinsky, Z., Falkowski, P. G., Wyman, K., 1986. Light harvesting and utilization by phytoplankton. *Plant and Cell Physiology*, 27: 1335-1349.
- Eppley, R.W., Reid, F.M.H., Strickland, J.D.H., 1970. Estimates of phytoplankton crop size, growth rate and primary production. In: Strickland, J.D.H. (Ed.), *The ecology of the plankton off La Jolla, California in the period April through September, 1967*. Bulletin of the Scripps Institution of Oceanography, 17, 33-42.
- Eriksson, M., 2001. Effects of six antifouling agents (Irgarol 1051, Sea-Nine, chlorothalonil, diuron, dichlofluanide, zinc pyrithione) on photosynthetic activities in marine phytoplankton communities. Master Thesis, Goteborg University.
- Evans, S. M., Birchenough, A. C., Brancato, M. S., 2000. The TBT Ban: Out of the Frying Pan Into the Fire? *Marine Pollution Bulletin*, 40: 204-211.
- Faber, M. J., Thompson, D. G., Stephenson, G. R., Boermans, H. J., 1998. Impact of glufosinate-ammonium and bialaphos on the phytoplankton community of a small eutrophic northern lake. *Environmental Toxicology and Chemistry*, 17: 1282-1290.
- Falkowski, P. G., 1991. Molecular ecology of phytoplankton photosynthesis. In: P. G. Falkowski and A. D. Woodhead (Eds.). *Primary productivity and biogeochemical cycles in the sea*. Plenum. pp. 47-67.
- Falkowski, P. G., 2000. Rationalizing elemental ratios in unicellular algae. *Journal of Phycology*, 36: 3-6.
- Falkowski, P. G., Raven, J. A., 1997. *Aquatic photosynthesis*. Blackwell Science. Malden. 375 pp.
- Faust, M., Altenburger, R., Backhaus, T., Blanck, H., Boedeker, W., Gramatica, P., Hamer, V., Scholze, M., Vighi, M., Grimme, L. H., 2003. Joint algal toxicity of 16 dissimilarity acting chemicals is predictable by the concept of independent action. *Aquatic Toxicology*, 63: 43-63.
- Fernández-Alba, A. R., Hernando, M. D., Piedra, L., Chisti, Y., 2002. Toxicity evaluation of single and mixed antifouling biocides measured with acute toxicity bioassays. *Analytica Chimica Acta*, 456: 303-312.
- Ferrer, I., Ballesteros, B., Marco, M. P., Barcélo, D., 1997. Pilot survey for the determination of the antifouling agent Irgarol 1051 in enclosed sea water samples by a direct enzyme-linked-immunosorbent assay and solid-phase-extraction following by LC-DAD detection. *Environmental Science and Technology*, 31: 3530-3555.

- Fietz, S., Nicklish, A., 2004. An HPLC analysis of the summer phytoplankton assemblage in Lake Baikal. *Freshwater Biology*, 49: 332-345.
- Folt, C. L., Chen, C. Y., Moore, M. V., Burnaford, J., 1999. Synergism and antagonism among multiple stressors. *Limnology and Oceanography*, 44: 864-877.
- Forbis, A. D., Georgie, L., Bunch, B., 1985. Uptake, depuration and bioconcentration of ^{14}C -RH-5287 by bluegill sunfish (*Lepomis macrochirus*). Rohm and Haas Company Technical Report No. 310-86-33, ABC Labs, Inc., Columbia, MO.
- Fore, L. S., Karr, J. R., Wisseman, R. W., 1996. Assessing invertebrate responses to human activities: Evaluating alternative approaches. *Journal of the North American Benthological Society*, 15: 212-231.
- Franklin, N. M., Stauber, J. L., Lim, R. P., 2001a. Development of flow cytometry-based algal bioassays for assessing toxicity of copper in natural waters. *Environmental Toxicology and Chemistry*, 20: 160-170.
- Franklin, N. M., Adams, M. S., Stauber, J. L., Lim, R. P., 2001b. Development of an improved rapid enzyme inhibition bioassay with marine and freshwater microalgae using flow cytometry. *Archives of Environmental Contamination and Toxicology*, 40: 469-480.
- Franklin, N. M., Stauber, J. L., Apte, S. C., Lim, R. P., 2002. Effect of initial cell density on the bioavailability and toxicity of copper in microalgal bioassays. *Environmental Toxicology and Chemistry*, 21: 742-751.
- Franqueira, D., Orosa, M., Torres, E., Herrero, C., Cid, A., 2000. Potential use of flow cytometry in toxicity studies with microalgae. *The Science of the Total Environment*, 247: 119-126.
- Furuya, K., Li, W. K. W., 1992. Evaluation of photosynthetic capacity in phytoplankton by flow cytometric analysis of DCMU-enhanced chlorophyll fluorescence. *Marine Ecology-Progress Series*, 88: 279-287.
- Gala, W. R., Giesy, J. P., 1994. Flow cytometric determination of the photoinduced toxicity of anthracene to the green-alga *Selenastrum capricornutum*. *Environmental Toxicology and Chemistry*, 13: 831-840.
- Garibotti, I. A., Vernet, M., Kozłowski, W. A., Ferrario, M. E., 2003. Composition and biomass of phytoplankton assemblages in coastal Antarctic waters: a comparison of chemotaxonomic and microscopic analyses. *Marine Ecology-Progress Series*, 247: 27-42.

- Geider, R. J., LaRoche, J., 2002. Redfield revisited: variability of C:N:P in marine microalgae and its biochemical basis. *European Journal of Phycology*, 37: 1-17.
- Gieskes, W.W.C., Kraay, G.W., 1983. Dominance of Cryptophyceae during the phytoplankton spring bloom in the central North Sea detected by HPLC analysis of pigments. *Marine Biology*, 75: 179-185.
- Gilbert, F., Galgani, F., Cadiou, Y., 1992. Rapid assessment of metabolic activity in marine microalgae: application in ecotoxicological tests and evaluation of water quality. *Marine Biology*, 112: 199-205.
- Gin, K.Y.H., Zhang, S., Lee, Y.K., 2003. Phytoplankton community structure in Singapore's coastal waters using HPLC pigment analysis and flow cytometry. *Journal of Plankton Research*, 25: 1507-1519.
- Gledhill, M., Nimmo, M., Hill, S. J., Brown, M. T., 1997. The toxicity of copper(II) species to marine algae, with particular reference to macroalgae. *Journal of Phycology*, 33, 2-11.
- Goericke, R., Montoya, J. P., 1998. Estimating the contribution of microalgal taxa to chlorophyll-*a* in the field – variations of pigment ratios under nutrient- and light-limited growth. *Marine Ecology-Progress Series*, 169: 97-112.
- Goldman, J. G., Caron, D. A., Dennett, M. R., 1987. Nutrient cycling in a microflagellate food chain. IV. Phytoplankton-microflagellate interactions. *Marine Ecology-Progress Series*, 38: 75-87.
- Goldsborough, L. G., Robinson, G. G. C., 1986. Changes in periphytic algal community structure as a consequence of short herbicide exposures. *Hydrobiologia*, 139: 177-192.
- Gough, M. A., Fothergill, J., Hendrie, J. D., 1994. A survey of southern England coastal waters for the s-triazine antifouling compound Irgarol 1051. *Marine Pollution Bulletin* 28: 613-620.
- Graneli, E., Carlsson, P., Turner, J. T., Tester, P. A., Bechemin, C., Dawson, R., Funari, E., 1999. Effects of N:P:Si ratios and zooplankton grazing on phytoplankton communities in the northern Adriatic Sea. I. Nutrients, phytoplankton biomass, and polysaccharide production. *Aquatic Microbial Ecology*, 18: 37-54.
- Grasshoff, K., 1976. *Methods of seawater analysis*. Verlag Chemie, Weinheim/New York.
- Gray, J. S., 1989. Using ecological criteria for improving efficiency in marine benthic monitoring: A short review. *Oceanic Processes in Marine Pollution*, 4: 103-111.

- Greene, R. M., Geider, R. J., Falkowski, P. G., 1991. Effect of iron limitation on photosynthesis in a marine diatom. *Limnology and Oceanography*, 36: 1772-1782.
- Greene, R. M., Geider, R. J., Kolber, Z., Falkowski, P. G., 1992. Iron-induced changes in light-harvesting and photochemical energy conversion processes in eukaryotic marine algae. *Plant Physiology*, 100: 565-575.
- Greene, R. M., Kolber, Z. S., 1994. Physiological limitation of phytoplankton photosynthesis in the eastern equatorial Pacific determined from variability in the quantum yield of fluorescence. *Limnology and Oceanography*, 39: 1061-1074.
- Griffith, M. B., Hill, B. H., Herlihy, A. T., Kaufmann, P. R., 2002. Multivariate analysis of periphyton assemblages in relation to environmental gradients in Colorado rocky mountains streams. *Journal of Phycology*, 38: 83-95.
- Guillard R. R. L., 1975. Culture of phytoplankton for feeding marine invertebrates animals. In: W. L. Smith and M.H. Chanley (Eds.). *Culture of marine invertebrates animals*. Plenum Press. pp 29-60.
- Gustavson, K., Wängberg, S., 1995. Tolerance induction and succession in microalgae communities exposed to copper and atrazine. *Aquatic Toxicology*, 32: 283-302.
- Hall, L. W., Giddings, J. M., Solomon, K. R., Balcomb, R., 1999. An ecological risk assessment for the use of Irgarol 1051 as an algaecide for antifoulant paints. *Critical Reviews In Toxicology*, 29: 367-437.
- Halling-Sørensen, B., Nyholm, N., Kusk, K. O., Jacobsson, E., 2000. Influence of nitrogen status on the bioconcentration of hydrophobic organic compounds to *Selenastrum capricornutum*. *Ecotoxicology and Environmental Safety*, 45: 33-42.
- Hamilton, P. B., Jackson, G. S., Kaushik, N. K., Solomon, K. R., Stephenson, G. L., 1988. The impact of two applications of atrazine on the plankton communities of *in situ* enclosures. *Aquatic Toxicology*, 13: 123-140.
- Harris, G. P., 1986. *Phytoplankton ecology: Structure, function and fluctuation*. Chapman and Hall, London.
- Hellio, C., De La Broise, D., Dufosse, L., Le Gal, Y., Bourgoignon, N., 2001. Inhibition of marine bacteria by extracts of macroalgae: potential use for environmentally friendly antifouling paints. *Marine Environmental Research*, 52: 231-247.

- Henriksen, P., Riemann, B., Kaas, H., Sørensen, H. M., Sørensen, H. L., 2002. Effects of nutrient-limitation and irradiance on marine phytoplankton pigments. *Journal of Plankton Research*, 24: 835-858.
- Hoagland, K., Carder, J., Spawn, R., 1996. Effects of organic toxic substances. In: Stevenson, R., Bothwell, M., Lowe, R. (Eds.). *Algal ecology: Freshwater benthic ecosystems*. Academic, San Diego, pp 469-496.
- Holligan, P. M., Fernández, E., Aiken, J., Balch, W. M., Boyd, P., Finch, M., Groom, S. B., Malin, G., Muller, K., Purdie, D. A., Robinson, C., Trees, C. C., Turner, S. M., Wal, P. van der, 1993. A biogeochemical study of the coccolithophore *Emiliania huxleyi* in the north Atlantic. *Global Biogeochemical Cycles*, 7: 879-900.
- Horton, P., Ruban, A. V., Walters, R. G., 1996. Regulation of light harvesting in green plants. *Annual Review of Plant Physiology and Plant Molecular Biology*, 47: 655-684.
- Howard, P. H., 1991. Handbook of environmental fate and exposure data for organic chemicals. Vol. III. Pesticides. Lewis Publ. 684 pp.
- HSE – Health and Safety Executive (2002a) Information Document. HSE 730/15. 13 pp
- HSE – Health and Safety Executive (2002b) Guidelines on the efficacy data requirements for approval of non-agricultural pesticide products. 18 pp
- Irigoien, X., Head, R.N., Harris, R.P., Cummings, D., Harbour, D., 2000. Feeding selectivity and egg production of *Calanus helgolandicus* in the English Channel. *Limnology and Oceanography*, 45: 44-54.
- Jacobson, A. H., Willingham, G. L., 2000. Sea-Nine antifoulant: an environmentally acceptable alternative to organotin antifoulants. *The Science of the Total Environment*, 258: 103-110.
- Jacobson, A., 1993. RH-5287: Octanol:water partition coefficient. Rohm and Hass Company, Research Laboratories, Pennsylvania.
- Jacoby, J. M., Collier, D. C., Welch, E. B., Hardy, F. J., Crayton, M., 2000. Environmental factors associated with a toxic bloom of *Microcystis aeruginosa*. *Canadian Journal of Fisheries and Aquatic Sciences*, 57: 231-240.
- Jak, R. G., Maas, J. L., Scholten, M. C. T., 1998. Ecotoxicity of 3,4-dichloroaniline in enclosed freshwater plankton communities at different nutrient levels. *Ecotoxicology*, 7: 49-60.

- Jeffrey, S. W., Hallegraeff, G. M., 1990. Phytoplankton ecology of Australian waters. In: Clayton, M. N., King, R. J. (Eds.). *Biology of Marine Plants*, Longman-Cheshire, Melbourne, pp. 310-348.
- Jeffrey, S. W., Mantoura, R. F. C., Wright, S. W., 1997. *Phytoplankton pigments in oceanography*. UNESCO. Paris. 661 pp.
- Jeffrey, S.W., Vesk, M., 1997. Introduction to marine phytoplankton and their pigment signatures. In: Jeffrey, S.W., Mantoura, R.F.C., Wright, S.W., (Eds.), *Phytoplankton pigments in oceanography: Guidelines to modern methods*. UNESCO, Paris, pp. 37-84.
- Jochem, F. J., 1999. Dark survival strategies in marine phytoplankton assessed by cytometric measurement of metabolic activity with fluorescein diacetate. *Marine Biology*, 135: 721-728.
- Jochem, F. J., 2000. Probing the physiological state of phytoplankton at the single-cell level. *Scientia Marina*, 64: 183-195.
- Johnsen, G., Sakshaug, E., 1993. Bio-optical characteristics and photoadaptive responses in the toxic and bloom-forming dinoflagellates *Gyrodinium aureolum*, *Gymnodinium galatheanum*, and two strains of *Prorocentrum minimum*. *Journal of Phycology*, 29: 627-642.
- Jones, R. J., Kerswell, A. P., 2003. Phytotoxicity of photosystem II (PSII) herbicides to coral. *Marine Ecology-Progress Series*, 261: 149-159.
- Jørgensen, E., Christoffersen, K., 2000. Short-term effects of linear alkylbenzene sulfonate on freshwater plankton studied under field conditions. *Environmental Toxicology and Chemistry*, 19: 904-911.
- Kasai, F., Takamura, N., Hatakeyama, S., 1993. Effects of simetryne on growth of various freshwater algal taxa. *Environmental Pollution*, 79: 77-83.
- Kayser, H., 1979. Growth interactions between marine dinoflagellates in multispecies culture experiments. *Marine Biology*, 52: 357-369.
- Kimball, K. D., Levin, S. A., 1985. Limitations of laboratory bioassays – The need for ecosystem-level testing. *Bioscience*, 35: 165-171.
- Kleppel, G. S., Frazel, D., Pieper, R. E., Holliday, D. V., 1988. Natural diets of zooplankton off southern California. *Marine Ecology-Progress Series*, 49: 231-241.

- Kolber, Z. S., Falkowski, P. G., 1993. Use of active fluorescence to estimate phytoplankton photosynthesis *in situ*. *Limnology and Oceanography*, 38: 1646-1665.
- Kolber, Z. S., Prášil, O., Falkowski, P. G., 1998. Measurements of variable chlorophyll fluorescence using fast repetition rate techniques: defining methodology and experimental protocols. *Biochimica et Biophysica Acta*, 1367: 88-106.
- Kolber, Z. S., Zehr, J., Falkowski, P. G., 1988. Effects of growth irradiance and nitrogen limitation on photosynthetic energy conversion in photosystem 2. *Plant Physiology*, 88: 923-929.
- Konstantinou, I. K., Albanis, T. A., 2004. Worldwide occurrence and effects of antifouling paint booster biocides in the aquatic environment: a review. *Environmental International*, 30: 235-248.
- Krause, G. H., Weiss, E., 1991. Chlorophyll fluorescence and photosynthesis: the basics. *Annual Review of Plant Physiology and Plant Molecular Biology*, 42: 313-349.
- Kromkamp, J. C., Forster, R. M., 2003. The use of variable fluorescence measurements in aquatic ecosystems: differences between multiple and single turnover measuring protocols and suggested terminology. *European Journal of Phycology*, 38: 103-112.
- Kromkamp, J. C., Mur, L. R., 1984. Buoyant density changes in the cyanobacterium *Microcystis aeruginosa* due to changes in the cellular carbohydrate content. *FEMS Microbiology Letters*, 25: 105-109.
- Landry, M. R., Constantinou, J., Kirshtein, J., 1995. Microzooplankton grazing in the Central Equatorial Pacific during February and August, 1992. *Deep-Sea Research*, 42: 657-671.
- Langston, W. J., Bryan, G. W., Burt, G. R., Gibbs, P. E., 1990. Assessing the impact of tin and tbt in estuaries and coastal regions. *Functional Ecology*, 4: 433-443.
- Laopaiboon, L., Smith, R. N., Hall, S. J., 2001. A study of the effect of isothiazolones on the performance and characteristics of a laboratory-scale rotating biological contactor. *Journal of Applied Microbiology*, 91: 93-103.
- Larsen, D. K., Wagner, I., Gustavson, K., Forbes, V. E., Lund, T., 2003. Long-term effect of Sea-Nine on natural coastal phytoplankton communities assessed by pollution induced community tolerance. *Aquatic Toxicology*, 62: 35-44.

- Law, R. J., Fileman, T. W., Portmann, J. E., 1988. Methods of analysis of hydrocarbons in marine and other samples. *Aquatic Environ Protect: Anal. Methods* (3), MAFF, Lowestoft, pp 25.
- Leboulanger, C., Rimet, F., de Lacotte, M. H., Bérard, A., 2001. Effects of atrazine and nicosulfuron on freshwater microalgae. *Environmental International*, 26: 131-135.
- Lewis, M. A., 1995. Algae and vascular plant tests. In: *Fundamentals of Aquatic Toxicology. Effects, Environmental Fate, and Risk Assessment*. Rand, G. M. (Ed.), North Palm Beach, Florida, 2nd edition. pp 135-169.
- Li, W. K. W., Goldman, J. C., 1981. Problems in estimating growth rates of marine phytoplankton from short-term C-14 assays. *Microbial Ecology*, 7: 113-121.
- Liu, D., Maguire, R. J., Lau, Y. L., Pacepavicius, G. J., Okamura, H., Aoyama, I., 1997a. Transformations of the new antifouling compound Irgarol 1051 by *Phanerochaete chrysosporium*. *Water Research*, 31: 2363-2369.
- Liu, H., Nolla, H. A., Campbell, L., 1997b. *Prochlorococcus* growth rate and contribution to primary production in the equatorial and subtropical North Pacific Ocean. *Aquatic Microbial Ecology*, 12: 39-47.
- Liu, H., Campbell, L., Landry, M. R., Nolla, H. A., Brown, S. L., Constantinou, J., 1998. *Prochlorococcus* and *Synechococcus* growth rates and relative contributions to production in the Arabian Seas during Southwest and Northeast Monsoons. *Deep-Sea Research II*, 45: 2327-2352.
- Lodish, H., Berk, A., Matsudaira, P., Kaiser, C. A., Krieger, M., Scott, M. P., Zipursky, S. L., Darnell, J., 2004. Cellular energetics. In: Lodish, H., Berk, A., Matsudaira, P., Kaiser, C. A., Krieger, M., Scott, M. P., Zipursky, S. L., Darnell, J., (Eds.). *Molecular Cell Biology*. Freeman and Company, New York, pp 301-347.
- Longhurst, A., Sathyendranath, S., Platt, T., Caverhill, C., 1995. An estimate of global primary production in the ocean from satellite radiometer data. *Journal of Plankton Research*, 17: 1245-1271.
- Lozano, R. B., Pratt, J. R., 1994. Interaction of toxicants and communities - the role of nutrients. *Environmental Toxicology and Chemistry*, 13: 361-368.
- Lytle, J. S., Lytle, T. F., 2001. Use of plants for toxicity assessment of estuarine ecosystems. *Environmental Toxicology and Chemistry*, 20: 68-83.

- Mackey, D. J., Higgins, H. W., Mackey, M. D., Holdsworth, D., 1998. Algal class abundance in the western equatorial Pacific: estimation from HPLC measurements of chloroplast pigments using CHEMTAX. *Deep-Sea Research I*, 45: 1441-1468.
- Mackey, M. D., Mackey, D. J., Higgins, H. W., Wright, S. W., 1996. CHEMTAX - A program for estimating class abundances from chemical markers: Application to HPLC measurements of phytoplankton. *Marine Ecology-Progress Series*, 144: 265-283.
- Maddock, L., Harbour, D. S., Boalch, G. T., 1989. Seasonal and Year-to-Year Changes in the Phytoplankton from the Plymouth Area, 1963-1986. *Journal of the Marine Biological Association of the United Kingdom*, 69: 229-244.
- Margalef, R., 1958. Temporal succession and spatial heterogeneity in phytoplankton. In: *Perspectives in Marine Biology*. Buzzati-Traverso, A.A., (Ed.), Berkley: University of California Press, pp 323-350.
- Marino Balsa, J. C., Perez, P., Estevez-Blanco, P., Saco Alvarez, L., Fernandez, E., Beiras, R., 2003. Assessment of the toxicity of sediment and seawater polluted by the Prestige fuel spill using bioassays with clams (*Venerupis pullastra*, *Tappes decussatus*, and *Venerupis rhomboideus*) and the microalga *Skeletonema costatum*. *Ciencias marinas*, 29: 115-122.
- Marwood, C. A., Solomon, K. R., Greenberg, B. M., 2001. Chlorophyll fluorescence as a bioindicator of effects on growth in aquatic macrophytes from mixtures of polycyclic aromatic hydrocarbons. *Environmental Toxicology and Chemistry*, 20: 890-898.
- Maxwell, K., Johnson, G. N., 2000. Chlorophyll fluorescence – a practical guide. *Journal of Experimental Botany*, 51: 659-668.
- McCarthy, J. F., Bartell, S. M., 1988. How the trophic status of a community can alter the bioavailability and toxic effects of contaminants. In: *Functional Testing of Aquatic Biota for Estimating Hazards of Chemicals*. ASTM STP 988. J. Cairns, Jr., and J. R. Pratt (Eds.), ASTM, Philadelphia, 1988. pp 3-16.
- McCormick, P. V., Cairns, J. J., 1994. Algae as indicator of environmental change. *Journal of Applied Phycology*, 6: 509-526.
- Metaxas, A., Lewis, A. G., 1991. Interactions between 2 species of marine diatoms – effects on their individual copper tolerance. *Marine Biology*, 109: 407-415.
- Millard, E. S., Halfon, E., Minns, C. K., Charlton, C. C., 1993. Effect of primary productivity and vertical mixing on PCB dynamics in planktonic model-ecosystems. *Environmental Toxicology And Chemistry*, 12: 931-946.

- Molander, S., Blanck, H., 1992. Detection of pollution-induced community tolerance (PICT) in marine periphyton communities established under diuron exposure. *Aquatic Toxicology*, 22: 129-144.
- Molander, S., Dahl, B., Blanck, H., 1992. Combined effects of tri-normal-butyl tin (TBT) and diuron on marine periphyton on communities detected as pollution-induced community tolerance. *Archives of Environmental Contamination and Toxicology*, 22: 419-427.
- Montagnes, D.J.S., Franklin, D.J., 2001. Effect of temperature on diatom volume, growth rate, and carbon and nitrogen content: reconsidering some paradigms. *Limnology and Oceanography*, 46: 2008-2018.
- Morris, A. W., Bale, A. J., Howland, R. J. M., 1981. Nutrient distributions in an estuary: evidence of chemical precipitation of dissolved silicate and phosphate. *Estuarine, Coastal and Shelf Science*, 12: 205-216.
- Morris, A. W., Loring, D. H., Bale, A. J., Howland, R. J. M., Mantoura, R. F. C., Woodward, E. M. S., 1982. Particulate dynamics, particulate carbon and the oxygen minimum in an estuary. *Oceanologica Acta*, 5: 349-353.
- Morris, A. W., Mantoura, R. F. C., Bale, A. J., Howland, R. J. M., 1978. Very low salinity regions of estuaries: important sites for chemical and biological reactions. *Nature*, 274: 678-680.
- Myklestad, S., 1977. Production of carbohydrates by marine planktonic diatoms. II. Influence of the N/P ratio in the growth medium on the assimilation ration, growth rate and production of cellular and extracellular carbohydrates by *Chaetocerus affinis* var. *willei* (Gran) Hustedt and *Skeletonema costatum* (Grev.) Cleve. *Journal of Experimental Marine Biology and Ecology*, 29: 161-179.
- Nelson, A. C., Kursar, T. A., 1999. Interactions among plant defense compounds: a method for analysis. *Chemoecology*, 9: 81-92.
- Nyström, B., Becker-van Slooten, K., Bérard, A., Grandjean, D., Druart, J. C., Leboulanger, C., 2002. Toxic effects of Irgarol 1051 on phytoplankton and macrophytes in Lake Geneva. *Water Research*, 36: 2020-2028.
- Nyström, B., Paulsson, M., Almgren, K., Blanck, H., 2000. Evaluation of the capacity for development of atrazine tolerance in periphyton from a swedish freshwater site as determined by inhibition of photosynthesis and sulfolipid synthesis. *Environmental Toxicology and Chemistry*, 19: 1324-1333.

- Olesen, T. D., Ganf, G. G., 1986. Photosynthate partitioning – a labile, adaptive phenomenon in *Microcystis aeruginosa*. *Archiv fur Hydrobiologie*, 108: 55-76.
- Olin, 1997. Evaluation of the safety and efficacy of zinc omadine industrial fungicide. Technical summary submitted by Olin. Arch Chemicals.
- Omernik, J. M., 1995. Ecoregions: a spatial framework for environmental management. In: W. S. Davis and T. P. Simon (Eds.). *Biological Assessment and Criteria: Tools for Water Resource Planning and Decision Making*. Lewis Publishers, Boca Raton, Florida, pp. 49-62.
- Pennington, P. L., Scott, G. I., 2001. Toxicity of atrazine to the estuarine phytoplankter *Pavlova* sp. (PRYMNESIOPHYCEAE): increased sensitivity after long-term, low-level population exposure. *Environmental Toxicology and Chemistry*, 20: 2237-2242.
- Peperzak, L., Colijn, F., Vrieling, E. G., Gieskes, W. W. C., Peeters, J. C. H., 2000. Observations of flagellates in colonies of *Phaeocystis globosa* (Prymnesiophyceae): a hypothesis for their position in the life cycle. *Journal of Plankton Research*, 22: 2181-2203.
- Peterson, B. J., 1980. Aquatic primary productivity and the ¹⁴C-CO₂ method: A history of the productivity problem. *Annual Review of Ecology and Systematics*, 11: 359-385.
- Pinckney, J. L., Örnólfsson, R. B., Lumsden, S. E., 2002. Estuarine phytoplankton group-specific responses to sublethal concentrations of the agricultural herbicide, atrazine. *Marine Pollution Bulletin*, 44: 1109-1116.
- Pingree, R. D., Holligan, P. M., Mardell, G. T., 1978. The effects of vertical stability on phytoplankton distributions in the summer on the northwest European Shelf. *Deep-Sea Research*, 25: 1011-1028.
- Plumley, F. G., Davis, D. E., 1980. Effects of the photosynthetic inhibitor atrazine on salt marsh edaphic algae in culture, microecosystems and in the field. *Estuaries*, 3: 271-277.
- Pollehne, F., Jost, G., Kerstan, E., Meyer-Harms, B., Reckermann, M., Nausch, M., Wodarg, D., 1999. Triazine herbicides and primary pelagic interactions in an estuarine summer situation. *Journal of Experimental Marine Biology and Ecology*, 238: 243-257.
- Porra, R. J., Pfundel, E. E., Engel, N., 1997. Metabolism and function of photosynthetic pigments. In: Jeffrey, S.W., Mantoura, R.F.C., Wright, S.W., (Eds.). *Phytoplankton pigments in oceanography: Guidelines to modern methods*. UNESCO, Paris, pp. 327-341.

- Pratt, J. R., Barreiro, R., 1998. Influence of trophic status on the toxic effects of a herbicide: A microcosm study. *Archives of Environmental Contamination and Toxicology*, 35: 404-411.
- Pratt, J. R., Cairns, C. Jr., 1996. Ecotoxicology and the redundancy problem: Understanding effects on community structure and function. In: Newman, M. C. and Jagoe, C. H. (Eds.). *Ecotoxicology: A hierarchical treatment*. Lewis, New York, pp 347-370.
- Ragan, M. A., Ragan, C. M., Jensen, A., 1980. Natural chelators in seawater: detoxification of Zn²⁺ by brown algal polyphenols. *Journal of Experimental Marine Biology and Ecology*, 44: 261-267.
- Ranke, J., Jarstorff, B., 2000. Multidimensional risk analysis of antifouling biocides. *Environmental Science and Pollution Research*, 7: 105-114.
- Rau, W., 1988. Functions of carotenoids other than in photosynthesis. In: Goodwin, T. W. (Ed.). *Plant pigment*. New York: Academic, pp 231-255.
- Raven, J. A., 1993. Global overview of carbon and nitrogen-metabolism in plants and related organisms. *Plant Physiology*, 102: 3-3.
- Readman, J. W., Devilla, R. A., Tarran, G., Llewellyn, C. A., Fileman, T. W., Easton, A., Burkill, P. H., Mantoura, R. F. C., 2004. Flow cytometry and pigment analyses as tools to investigate the toxicity of herbicides to natural phytoplankton communities. *Marine Environmental Research*, 58: 353-358.
- Readman, J. W., Kwong, L. L. W., Grondin, D., Bartocci, J., Villeneuve, J. P., Mee, L. D., 1993. Coastal water contamination from a triazine herbicide used in antifouling paints. *Environmental Science and Technology*, 27: 1940-1942.
- Readman, J. W., Mantoura, R. F. C., Rhead, M. M., Brown, L., 1982. Aquatic distribution and heterotrophic degradation of polycyclic aromatic hydrocarbons (PAH) in the Tamar Estuary. *Estuarine, Coastal and Shelf Science*, 14: 369-389.
- Regel, R. H., Ferris, J. M., Ganf, G. G., Brookes, J. D., 2002. Algal esterase activity as a biomeasure of environmental degradation in a freshwater creek. *Aquatic Toxicology*, 59: 209-223.
- Reynolds, J. L., 1995. Aqueous photolysis of [pyridine-2,6-¹⁴C] zinc omadine in pH 9 buffer and artificial seawater. XenoBiotic Laboratories, Inc, Plainsboro, NJ. Arch Chemicals.

References

- Rioboo, C., González, O., Herrero, C., Cid, A., 2002. Physiological response of freshwater microalga (*Chlorella vulgaris*) to triazine and phenylurea herbicides. *Aquatic Toxicology*, 59: 225-235.
- Ritter, J. C., 1999. Summary of the aerobic and anaerobic aquatic metabolism of [pyridine-2,6-14C] copper omadine and [pyridine-2,6-14C] zinc omadine in marine water and sediment. Olin Research Centre, Cheshire, CT. Arch Chemicals.
- Rodriguez, F., Fernandez, E., Head, R. N., Harbour, D. S., Bratbak, G., Heldal, M., Harris, R. P., 2000. Temporal variability of viruses, bacteria, phytoplankton and zooplankton in the western English Channel off Plymouth. *Journal of the Marine Biological Association United Kingdom*, 80: 575-586.
- Rodriguez, F., Varela, M., Zapata, M., 2002. Phytoplankton assemblages in the Gerlache and Bransfield Straits (Antartic Peninsula) determined by light microscopy and CHEMTAX analysis of HPLC pigment data. *Deep-Sea Research II*, 49: 723-747.
- Sakshaug, E., Bricaud, A., Dandonneau, Y., Falkowski, P. G., Kiefer, D. A., Legendre, L., Morel, A., Parslow, J., Takahashi, M., 1997. Parameters of photosynthesis: definitions, theory and interpretation of results. *Journal of Plankton Research*, 19: 1637-1670.
- Sandmann, G., Kuhn, M., Boger, P., 1993. Carotenoids in photosynthesis: protection of D1 degradation in the light. *Photosynthesis Research*, 35: 185-190.
- Sane, P. V., Ivanov, A. G., Sveshnikov, D., Huner, N. P. A., 2002. A transient exchange of the photosystem II reaction center protein D1:1 with D1:2 during low temperature stress of *Synechococcus* sp. PCC 7942 in the light lowers the redox potential of Q_B. *The Journal of Biological Chemistry*, 277: 32739-32745.
- Sargent, C. J., Bowman, J. C., Zhou, J. L., 2000. Levels of antifoulant irgarol 1051 in the Conwy Marina, North Wales. *Chemosphere*, 41: 1755-1760.
- Scarlett, A., Donkin, M. E., Fileman, T. W., Donkin, P., 1997. Occurrence of the marine antifouling agent Irgarol 1051[®] within the Plymouth Sound locality: Implications for the green macroalga *Enteromorpha intestinalis*. *Marine Pollution Bulletin*, 34: 645-651.
- Scarlett, A., Donkin, P., Fileman, T. W., Evans, S. V., Donkin, M. E., 1999. Risk posed by the antifouling agent Irgarol 1051[®] to the seagrass, *Zostera marina*. *Aquatic Toxicology*, 45: 159-170.
- Schindler, D. W., 1987. Detecting ecosystem responses to anthropogenic stress. *Canadian Journal of Fisheries and Aquatic Sciences*, 44: 6-25.

- Schlüter, L., Møhlenberg, F., Havskum, H., Larsen, S., 2000. The use of phytoplankton pigments for identifying and quantifying phytoplankton groups in coastal areas: testing the influence of light and nutrients on pigment/chlorophyll-*a* ratios. *Marine Ecology-Progress Series*, 192: 49-63.
- Schmidt, J. M., Head, L. L., 1991. Aerobic aquatic metabolism of ¹⁴C-Irgarol 1051. ABC Report 38886. Analytical Bio-Chemistry Laboratories, Inc. Columbia, MO. 1194 pp.
- Schone, H. K., Schone, A., 1982. MET 44: Weakly Enriched Sea-Water Medium for Ecological Studies on Marine Plankton Algae, and Some Examples of Its Application. *Botanica Marina*, 15: 117-122.
- Schone, H. K., Schone, A., 1982. MET 44: Weakly Enriched Sea-Water Medium for Ecological Studies on Marine Plankton Algae, and Some Examples of Its Application. *Botanica Marina*, 15: 117-122.
- Seguin, F., Le Bihan, F., Leboulanger, C., Bérard, A., 2002. A risk assessment of pollution: induction of atrazine tolerance in phytoplankton communities in freshwater outdoor mesocosms, using chlorophyll fluorescence as an endpoint. *Water Research*, 36: 3227-3236.
- Selvig, T. A., Leavitt, R. I., Powers, W. P., 1999. Marine antifouling methods and compositions. United States Patent h1h35,919,989.
- Shade, W. D., Hurt, S. H., Jacobson, A. H., Reinert, K. H., 1993. Ecological risk assessment of a novel marine antifoulant. *Environmental toxicology and risk assessment*. 2nd vol. ASTM STP 1216. J. W. Gorsuch, F. J. Dwyer, C. G. Ingersoll and T. W. La Point (Eds.), American Society for Testing and Materials, Philadelphia.
- Sharp, J. H., Underhill, P. A., Hughes, D. J., 1979. Interaction (allelopathy) between marine diatoms: *Thalassiosira pseudonana* and *Phaeodactylum tricorutum*. *Journal of Phycology*, 15: 353-362.
- Siddorn, J. R., Allen, J. I., Uncles, R. J., 2003. Heat, salt and tracer transport in the Plymouth Sound coastal region: a 3-D modelling study. *Journal of Marine Biological Association of United Kingdom*, 83: 673-682.
- Simon, N., Barlow, R.G., Marie, D., Partensky, F., Vaultot, D., 1994. Characterization of oceanic photosynthetic picoeukaryotes by flow cytometry. *Journal of Phycology*, 30: 922-935.

- Søndergaard, M., Schierup, H. H., 1982. Release of extracellular organic carbon during a diatom bloom in lake Mossø: molecular weight fractionation. *Freshwater Biology*, 12: 313-320.
- Steglich, C., Behrenfeld, M., Koblizek, M., Claustre, H., Penno, S., Prasil, O., Partensky, F., Hess, W. R., 2001. Nitrogen deprivation strongly affects Photosystem II but not phycoerythrin level in the divinyl-chlorophyll *b*-containing cyanobacterium *Prochlorococcus marinus*. *Biochimica et Biophysica Acta*, 1503: 341-349.
- Strathmann, R. R., 1967. Estimating the organic carbon content of phytoplankton from cell volume or plasma volume. *Limnology and Oceanography*, 12: 411-418.
- Strickland, J. D. H., Parsons, T. R., 1968. A practical handbook of sea water analysis. *Bulletin Fisheries Research Board of Canada*, 167: 310.
- Strickland, J. D. H., Parsons, T. R., 1972. A practical manual of seawater analysis. 2nd ed. *Bulletin Fisheries Research Board of Canada*, 167: 1-310.
- Suggett, D. J., Oxborough, K., Baker, N. R., MacIntyre, H. L., Kana, T. M., Geider, R. J., 2003. Fast repetition rate and pulse amplitude modulation chlorophyll-*a* fluorescence measurements for assessment of photosynthetic electron transport in marine phytoplankton. *European Journal of Phycology*, 38: 371-384.
- Suggett, D., Kraay, G., Holligan, P., Davey, M., Aiken, J., Geider, R., 2001. Assessment of photosynthesis in a spring cyanobacterial bloom by use of a fast repetition rate fluorometer. *Limnology and Oceanography*, 46: 802-810.
- Tang, J., Hoagland, K. D., Siegfried, B. D., 1998. Uptake and bioconcentration of atrazine by selected freshwater algae. *Environmental Toxicology and Chemistry*, 17: 1085-1090.
- Thomas, K. V., 1999. Determination of the antifouling agent zinc pyrithione in water samples by copper chelate formation and high-performance liquid chromatography atmospheric pressure chemical ionisation mass spectrometry. *Journal of Chromatography A*, 833: 105-109.
- Thomas, K. V., 2001. The environmental fate and behaviour of antifouling paint booster biocides: a review. *Biofouling*, 17: 73-86.
- Thomas, K. V., Fileman, T. W., Redman, J. W., Waldock, M. J., 2001. Antifouling paint booster biocides in the UK coastal environment and potential risks of biological effects. *Marine Pollution Bulletin*, 42: 677-688.

- Thomas, K. V., McHugh, M., Waldock, M., 2002. Antifouling paint booster biocides in UK coastal waters: inputs, occurrence and environmental fate. *The Science of the Total Environment*, 293: 117-127.
- Tixier, C., Sancelme, M., Bonnemoy, F., Cuer, A., Veschambre, H., 2001. Degradation Products of a phenylurea herbicide, diuron: synthesis, ecotoxicity, and biotransformation. *Environmental Toxicology and Chemistry*, 20: 1381-1389.
- Townsin, R. L., 2003. The ship hull fouling penalty. *Biofouling*, 19: 9-15.
- Turley, P. A., Fenn, R. J., Figura, P. M., Ritter, J. C., 2000. Pyrithiones as antifoulants: environmental chemistry and risk assessment. *Biofouling*, 15: 175-182.
- Twiss, M. R., Nalewajko, C., 1992. Influence of phosphorus-nutrition on copper toxicity to 3 strains of *Scenedesmus acutus* (CHLOROPHYCEAE). *Journal of Phycology*, 28: 291-298.
- Uncles, R. J., Fraser, A. L., Butterfield, D., Johnes, P., Harrod, T. R., 2002. The prediction of nutrients into estuaries and their subsequent behaviour: application to the Tamar and comparison with the Tweed, UK. *Hydrobiologia*, 475: 239-250.
- Uncles, R. J., Lewis, R. E., 2001. The transport of fresh water from river to coastal zone through a temperate estuary. *Journal of Sea Research*, 46: 161-175.
- Uncles, R. J., Stephens, J. A., 1993. The freshwater-saltwater interface and its relationship to the turbidity maximum in the Tamar Estuary, United Kingdom. *Estuaries*, 16: 126-141.
- UNESCO, 1974. A review of methods used for quantitative phytoplankton studies. *Unesco Technical Papers in Marine Science*, 18: 1-27.
- Van Donk, E., Hessen, D. O., 1993. Grazing resistance in nutrient stressed phytoplankton. *Oecologia*, 93: 508-511.
- Vanleeuwe, M. A., Stefels, J., 1998. Effects of iron and light stress on the biochemical composition of Antarctic *Phaeocystis* sp. (Prymnesiophyceae). ii. Pigment composition. *Journal of Phycology*, 34: 496-503.
- Vaulot, D., Courties, C., Partensky, F., 1989. A simple method to preserve oceanic phytoplankton for flow cytometric analyses. *Cytometry*, 10: 629-635.
- Vaulot, D., Marie, D., Olson, R. J., Chisholm, S. W., 1995. Growth of *Prochlorococcus*, a photosynthetic prokaryote, in the equatorial pacific ocean. *Science*, 268: 1480-1482.

- Vinebrooke, 2003. <http://www.biology.ualberta.ca>.
- Vouvoulis, N., Scrimshaw, M. D., Lester, J. N., 2000. Comparative environmental assessment of biocides used in antifouling paints. *Chemosphere*, 47: 789-795.
- Walsh, G. E., 1988. Methods for toxicity tests of single substances and liquid complex waters with marine unicellular algae. EPA/600/8-87/043. 64 pp.
- Walsh, G. E., Deans, C. H., MacLaughlin, L. L., 1987. Comparison of the EC50s of algal toxicity tests calculated by four methods. *Environmental Toxicology and Chemistry*, 6: 767-770.
- Wängberg, S., Blanck, H., 1990. Arsenate sensitivity in marine periphyton communities established under various nutrient regimes. *Journal of Experimental Marine Biology and Ecology*, 139: 119-134.
- Weisse, T., 1993. Dynamics of autotrophic picoplankton in marine and freshwater ecosystems. *Advances in Microbial Ecology*, 13:327-370.
- Williams, M., Hargadine, S., 1990. Soil/sediment adsorption-desorption of ¹⁴C-Irgarol 1051. ABC Report 38884. Analytical Bio-Chemistry Laboratories Inc., Columbia, MO, 465 pp.
- Williams, P. J. leB., Robinson, C., Sondergaard, M., Jespersen, A. -M., Bentley, T. L., Lefevre, D., Richardson, K., Riemann, B., 1996. Algal ¹⁴C and total carbon metabolisms. 2. Experimental observations with the diatom *Skeletonema costatum*. *Journal of Plankton Research*, 18: 1961-1974.
- Williams, P. J. leB., 1993. Chemical and tracer methods of measuring planktons production. *ICES Marine Science Symposium*, 197: 20-36.
- Wilson, J. G., Elkaim, B., 1991. A comparison of the pollution status of twelve Irish and French estuaries. *Estuaries and Coasts: Spatial and Temporal Intercomparisons*. pp. 317-322.
- Woodward, E. M. S., 1994. Analysis of nutrients in seawater. Plymouth Marine Laboratory Technical Report.
- Wright, S.W., Jeffrey, S.W., 1997. High resolution HPLC system for chlorophylls and carotenoids of marine phytoplankton. In: Jeffrey, S.W., Mantoura, R.F.C., Wright, S.W., (Eds.), *Phytoplankton pigments in oceanography: Guidelines to modern methods*. UNESCO, Paris, pp. 327-341.

References

- Wyman, M., Gregory, R. P. F., Carr, N. G., 1985. Novel role for phycoerythrin in a marine cyanobacterium, *Synechococcus* strain DC2. *Science*, 230: 818-820.
- Zhou, J. L., Fileman, T. W., Evans, S., Donkin, P., Mantoura, R. F. C., Rowland, S. J., 1996. Seasonal distribution of dissolved pesticides and polynuclear aromatic hydrocarbons in the Humber Estuary and Humber coastal zone. *Marine Pollution Bulletin*, 32: 599-608.

Impact of antifouling booster biocides on single microalgal species and on a natural marine phytoplankton community

Rosângela A. Devilla^{1,2,*}, Murray T. Brown², Maria Donkin², Glen A. Tarran¹, James Aiken¹, James W. Readman¹

¹Plymouth Marine Laboratory, Prospect Place, West Hoe, Plymouth, Devon PL1 3DH, UK

²Dept. of Biological Sciences, Plymouth Environmental Research Centre, University of Plymouth, Drake Circus, Plymouth, Devon PL4 8AA, UK

ABSTRACT: Phytoplankton were exposed to 4 antifouling booster biocides (Sea-Nine 211[®], Irgarol 1051[®], diuron and zinc pyrithione) to investigate toxicological responses. Initially, single species/single biocide exposure experiments revealed changes in pigment ratios under all biocide exposures for the prymnesiophyte *Emiliana huxleyi*, but not for the cyanophyte *Synechococcus* sp. Growth inhibition results following 72 h exposures indicated that *Synechococcus* sp. was more tolerant to zinc pyrithione (NOEC of 1.0 µg l⁻¹) and Sea-Nine 211[®] (NOEC of 0.9 µg l⁻¹) than *E. huxleyi* (EC₅₀ of 0.54 and EC₅₀ of 0.35 µg l⁻¹, respectively). In contrast, *Synechococcus* sp. was more sensitive to diuron (EC₅₀ of 0.55 µg l⁻¹) than *E. huxleyi* (EC₅₀ of 2.26 µg l⁻¹), whereas exposure to Irgarol 1051[®] similarly impacted both species (EC₅₀ of 0.16 and 0.25 µg l⁻¹, respectively). In addition, the impact on photosynthesis and on pigment chemotaxonomy was investigated through a laboratory exposure experiment using a natural phytoplankton community. Pigment signatures were measured by High Performance Liquid Chromatography (HPLC) and densities of size-classified phytoplankton groups were monitored using Analytical Flow Cytometry (AFC). Group-specific sensitivity of the natural phytoplankton community was detected through pigment composition after 72 h exposure to 5 µg l⁻¹ zinc pyrithione and 10 µg l⁻¹ Sea-Nine 211[®]. Zeaxanthin increased proportionally, indicating a relative increase in Cyanophyceae. This result was corroborated using AFC. Primary production, estimated by ¹⁴C-HCO₃⁻ uptake, was compared to maximum quantum yield of Photosystem II (F_v/F_m), which was quantified by Fast Repetition Rate Fluorimetry (FRRF). The 2 techniques were in good agreement ($R^2 = 0.89$, $p = 0.0001$), both primary production and F_v/F_m being impaired by exposure to all biocides tested. These results are discussed in the context of the potential environmental impact of biocides on phytoplankton communities and the ecological implications of any modifications in species composition.

KEY WORDS: Marine phytoplankton · Antifouling booster biocides · *Emiliana huxleyi* · *Synechococcus* sp. · Analytical Flow Cytometry · Pigments · Fast Repetition Rate Fluorescence · ¹⁴C-HCO₃⁻ uptake

Resale or republication not permitted without written consent of the publisher

INTRODUCTION

The application of antifouling paints to the hulls of ships or boats is to prevent attachment and growth of fouling biota, but these chemical applications pose a threat to non-target organisms (Readman et al. 1993).

Most contain organic biocides, which are used singly or as an additional component to copper-based formulations (Health and Safety Executive, HSE 2002). Such organic biocides enhance the efficacy of the formulation and are commonly referred to as 'booster' biocides. Since tri-*n*-butyltin (TBT) restrictions were intro-

*Email: roadev@yahoo.co.uk

duced in the late 1990s (HSE 2002), the use of booster biocides has become more widespread and, worldwide, around 18 compounds have been used (Thomas 2001). Among them, Irgarol 1051[®] and diuron were, until recently, the most commonly used, with levels up to 1.42 and 6.74 $\mu\text{g l}^{-1}$ respectively being reported in UK marinas (Thomas et al. 2001).

Phytoplankton are highly susceptible to herbicidal antifouling compounds due to the latter's damaging effects on photosynthesis. Due to their short generation times and differential responses and susceptibilities to biocides, algae can be affected over time scales from hours to days, leading to changes in community structure. Therefore, toxicological studies on phytoplankton are particularly relevant when safe environmental regulations are to be established. These are typically based on unialgal tests, but toxic responses of natural phytoplankton communities are more environmentally relevant, yet such studies are scarce (e.g. Dahl & Blanck 1996, Nyström et al. 2002, Readman et al. 2004).

The aims of this study were to investigate changes in biochemical and physiological function of selected microalgal species and in the structure of a marine phytoplankton community, induced by exposure to 4 antifouling biocides, two of which have been reported in Plymouth waters (diuron and Irgarol 1051[®]) and two of which are in common usage (Sea-Nine 211[®] and zinc pyrithione). Diuron and Irgarol 1051[®] are PSII inhibitors and impair photosynthesis by displacing a plastoquinone (Q_B) from its binding site in the D1 protein of photosystem II (Cremllyn 1991). Sea-Nine 211[®] has a broad spectrum activity (e.g. against fungi, algae, bacteria and marine invertebrates) and reacts with thiol-containing enzymes (Collier et al. 1990). Zinc pyrithione inhibits bacterial ATP synthesis and membrane transport (Dinning et al. 1998) and generates hydroxyl radicals when photolysed with visible or UV light (Aveline et al. 1996). Since the detection of sensitive toxicological endpoints is crucial for accurately determining toxic effects on communities, we also assessed the suitability of several biomarkers, growth, photosynthesis, pigment:chlorophyll *a* (chl *a*) ratios and chemotaxonomy.

MATERIAL AND METHODS

Preparation of biocide solutions and chemical reagents. Authentic analytical standards were acquired: Irgarol 1051[®] (2-methylthio-4-tert-butylamino-6-cyclopropylamino-s-triazine; Ciba-Geigy), diuron Pestanal[®] ([3-(3,4-Dichlorophenyl)-1,1 dimethyl-urea]; 99% purity; Riedel-de Haën), Sea-Nine 211[®] (4,5-dichloro-2-n-octyl-4-isothiazolin-3-one; Institute for Environmen-

tal Science, The Netherlands), and zinc pyrithione (1-Hydroxypyridine-2-thione (pyrithione) zinc salt; 95% purity; Sigma Chemical). Stock solutions of Irgarol 1051[®], diuron Pestanal[®] and Sea-Nine 211[®] were dissolved in methanol and their working solutions prepared with sterile seawater. The zinc pyrithione stock and working solutions were prepared by dilutions into sterile seawater at the start of the experiment.

Algal cultures and single-species experiments. The prymnesiophyte *Emiliana huxleyi* (PCC 92D) and the cyanophyte *Synechococcus* sp. (PCC 543) were obtained from the Plymouth Culture Collection, UK. Species selection was based on previous studies (Readman et al. 2004) that showed *E. huxleyi* to be highly sensitive to, and *Synechococcus* sp. to be comparatively resistant to, Irgarol 1051[®] exposure.

Non-axenic cultures were maintained in f/2 culture medium (Guillard 1975), without Trizma, and prepared with filtered (0.45 μm) seawater (salinity of 33‰; initial pH of 8.3 to 8.4). Ideal growth rates (~ 1 division d^{-1}) were achieved by varying culture conditions in both species. *Emiliana huxleyi* was grown in a 12:12 h light:dark cycle at $15.5 \pm 2.5^\circ\text{C}$ under an average irradiance of 160 $\mu\text{mol photons m}^{-2} \text{s}^{-1}$ photosynthetic active radiation (PAR), provided by cool white light bulbs (Sylvania; 70 W); *Synechococcus* sp. was grown on a 12:12 h light:dark cycle at $20.5 \pm 1.5^\circ\text{C}$ under an average irradiance of 80 $\mu\text{mol photons m}^{-2} \text{s}^{-1}$ PAR. Cultures were grown for at least 4 d to ensure cell acclimatisation prior to experimentation. Sterile techniques were used for all culture work in an attempt to minimize bacterial growth.

Experiments were conducted using 2 l borosilicate bottles containing 1 l of f/2 medium spiked with aliquots of biocide working solutions. *Emiliana huxleyi* was exposed to the nominal concentrations of 0.2, 0.4, 0.6, 0.8, 1.0 $\mu\text{g l}^{-1}$ zinc pyrithione; 0.4, 0.8, 1.5 $\mu\text{g l}^{-1}$ Sea-Nine 211[®]; 0.1, 0.2, 0.5 $\mu\text{g l}^{-1}$ Irgarol 1051[®]; and 0.2, 0.5, 5.0, 10, 50 $\mu\text{g l}^{-1}$ diuron. *Synechococcus* sp. was exposed to 0.4, 0.6, 1 $\mu\text{g l}^{-1}$ zinc pyrithione; 0.2, 0.4, 0.9 $\mu\text{g l}^{-1}$ Sea-Nine 211[®]; 0.2, 0.5, 1 $\mu\text{g l}^{-1}$ Irgarol 1051[®]; 0.2, 0.4, 2.2 and 3.3 $\mu\text{g l}^{-1}$ diuron. Exponentially growing cells were inoculated into bottles to obtain $\sim 1 \times 10^4$ cells ml^{-1} . Controls and carrier controls were included in all experiments. Final concentrations of methanol for each treatment did not exceed 0.00036% (v/v). Experiments were static and carried out in triplicate over 72 h. Samples for pigment analyses and biocide determinations were taken at the beginning and end of the experiments, while samples for Analytical Flow Cytometry (AFC) were taken daily.

Experiment with a natural phytoplankton community. Coastal water was collected from the well characterised station L4 (<http://www.pml.ac.uk/L4>), Plymouth, UK ($50^\circ 15' \text{N}$, $04^\circ 13' \text{W}$) in August 2001. The

in situ temperature was 15°C and salinity was 33‰. Phytoplankton composition on the day of sampling, as characterised by cell abundance, was 15.6% flagellates ($\leq 5 \mu\text{m}$), 3.5% diatoms, 2.2% colourless Dinophyceae, 0.2% Dinophyceae, 0.05% coccolithophorids, and 78.5% picoplankton. Highest carbon biomass was attributed to Dinophyceae (35%), flagellates (24%), colourless Dinophyceae (16%), diatoms (18%), and picoplankton (6%) (<http://www.pml.ac.uk/L4>).

Seawater containing phytoplankton ($< 63 \mu\text{m}$) was transferred into 2 l borosilicate bottles and spiked with the biocide working solutions, in triplicate. The concentrations tested were selected from a previous scaling experiment and were: 0.03 and 0.05 $\mu\text{g l}^{-1}$ Irgarol 1051[®], 0.5 and 5 $\mu\text{g l}^{-1}$ zinc pyriithione, 1 and 10 $\mu\text{g l}^{-1}$ diuron, and 1 and 10 $\mu\text{g l}^{-1}$ Sea-Nine 211[®], including controls and carrier controls (methanol). Bottles were incubated for 72 h under a 12:12 h light:dark cycle, an average temperature of 17°C and irradiance of 230 $\mu\text{mol photons m}^{-2} \text{s}^{-1}$ PAR. Daily sampling was carried out for AFC and FRRF determinations. After 72 h, samples were filtered (0.5 to 1.5 l; 0.7 μm GF/F) for pigment analyses. Samples for biocide determination were taken at the sampling station and at the beginning and end of the experiment. A set of 60 ml transparent polycarbonate bottles containing the phytoplankton community under the same exposure concentrations was also incubated to determine carbon dioxide fixation by $^{14}\text{C-HCO}_3^-$ uptake.

Determination of biological parameters. The rate of carbon fixation was estimated from the incorporation of $^{14}\text{C-HCO}_3^-$ (Joint et al. 2002). Aliquots of $^{14}\text{C-HCO}_3^-$ were added to each 60 ml bottle, giving a final activity of 5 $\mu\text{Ci } ^{14}\text{C-HCO}_3^-$ per bottle. After 24 h, incubations were terminated by filtration through Nuclepore polycarbonate membrane filters (0.2 μm) and samples were counted in a liquid scintillation counter (LSC) LKB Wallac 1219 Rackbeta.

In vivo fluorescence measurements were determined by a FAST^{track} fluorometer (FRRF) (Chelsea Instruments) operated as a benchtop unit (Suggett et al. 2001). Samples (25 ml) were dark-adapted (30 min) and data were analysed by FRRF software FRS 1.8 to provide values for the maximum quantum yield of PSII (F_v/F_m). The FRRF was configured with only the dark chamber activated, with auto-ranging mode gain and 20 discrete acquisitions.

Pigment composition was determined by filtering seawater samples (1 to 2 l) onto Whatman glass fiber filters (0.7 μm GF/F) and frozen in liquid nitrogen (-196°C). Pigments were extracted with 90% acetone (containing internal standard) by ultrasonication. Extracts were clarified by centrifugation and supernatants were mixed with 1 M ammonium acetate (50%:50% v/v) before injection into the HPLC. Analy-

ses of pigments were conducted using the reverse phase HPLC procedure outlined by Barlow et al. (1997) using a 3 μm Hypersil MOS2 C-8 column (100 mm \times 4.6 mm; Alltech Associates) on a Shimadzu HPLC system coupled to a photo-diode array detector (UV6000). Calibration was performed with standards purchased from DHI Water and Environment and Sigma-Aldrich.

Samples for AFC were fixed with 1 to 2% glutaraldehyde (final concentration) (microscopy grade; Merck). Samples were fast-frozen in liquid nitrogen and stored at -80°C in the dark to preserve their fluorescence. *In vivo* samples derived from the unialgal cultures were analysed immediately after sample collection and therefore did not require fixation. Phytoplankton samples were analysed for enumeration and size classification using a Becton Dickinson FACSort[™] flow cytometer as described in Readman et al. (2004).

Antifouling booster biocides analyses. Seawater samples were collected from sub-surface (0.5 m depth) at the sampling station (2.7 l) and from the experiments (1 to 2 l), spiked with an internal standard (Ametryn or Atrazine- d_5), and were stored at 4°C awaiting extraction. Extractions and analyses of Irgarol 1051[®] and Sea-Nine 211[®] were based on the methods described in Zhou et al. (1996) (for solid-phase extraction) and Sargent et al. (2000) (for liquid-liquid extraction). Extracts (1 to 2 μl) were injected into a GC-MS (6890 N Network GC System) coupled to a 5973 Mass Selective Detector (Agilent Technologies) and operated in selective ion monitoring (SIM) mode using m/z values of 182 for Irgarol 1051[®], 169 for Sea-Nine 211[®], and 227 for Ametryn or 205 for Atrazine- d_5 . Spiked recoveries were 85% ($\pm 3\%$; $n = 5$) for Sea-Nine 211[®] and 81% ($\pm 6\%$; $n = 5$) for Irgarol 1051[®]. Samples for diuron determination were analysed using an Enzyme-Linked ImmunoSorbent Assay (ELISA) kit (Sension). Zinc pyriithione is notoriously difficult to analyse, and for this reason, nominal concentrations were used.

Data analyses. For the unialgal experiments, the effective concentration which reduces growth by 50% (EC_{50}) was calculated by graphical interpolation (Walsh 1988). The lowest observable effective concentration (LOEC) and the non-observable effective concentration (NOEC) after 72 h exposure to biocides were determined by one-way ANOVA, followed by Tukey honest significant difference test (HSD; $\alpha = 0.05$), in which LOEC represented $p < 0.05$ and NOEC represented $p > 0.05$. Growth rates (μ) were estimated from the slope of linear fitting curves between \log_2 of cell number versus time and were expressed as divisions d^{-1} . Cell number, μ and pigment ratio data were analysed by 1-way ANOVA followed by the Tukey HSD test ($\alpha = 0.05$). All data were tested for homoscedasticity (Cochran's test) and normality (χ^2 test) and 'rank' values transformed when necessary to meet the

assumptions for parametric tests. All tests were carried out using the statistical package Statistica for Windows v 5.1 (StatSoft).

For the experiment with natural phytoplankton, a distance matrix (Bray Curtis similarity) was generated using fourth root transformed pigment data and submitted to analysis of similarities (ANOSIM analysis). The contribution of individual pigments to each biocide exposure was determined by SIMPER analysis (Similarity Percentages–Species Contributions) using the statistical software PRIMER for Windows v 5.2.9.

Estimates of biomass, as chl *a*, for each phytoplankton group were obtained using the matrix factorisation program CHEMTAX (Mackey et al. 1996). The pigment:chl *a* ratios used to create the initial matrix were derived from published literature (Mackey et al. 1996, Schlüter et al. 2000) as well as from the unialgal culture data obtained in this study. The pigment data were run under 3 different pigment:chl *a* ratios for Prymnesiophytes, obtained from the *Emiliana huxleyi* cultures exposed to biocides (see Table 2). For Cyanophyceae, zeaxanthin:chl *a* ratios were constant, as determined for *Synechococcus* sp. throughout biocide exposures (see Table 2). The pigments β -carotene, diadinoxanthin and chlorophyll c_1c_2 were excluded from the matrix as recommended by Mackey et al. (1996). Algal classes were selected according to the phytoplankton composition on the day of sampling (see section above 'Experiment with a natural phytoplankton community').

RESULTS

Unialgal experiments

Growth inhibition

The EC_{50} (72 h) values for cell numbers of *Emiliana huxleyi* indicated differences in the sensitivity to the 4 biocides. EC_{50} values were $2.26 \mu\text{g l}^{-1}$ for diuron, $0.54 \mu\text{g l}^{-1}$ for zinc pyriithione, $0.35 \mu\text{g l}^{-1}$ for Sea-Nine 211[®] and of $0.25 \mu\text{g l}^{-1}$ for Irgarol 1051[®] (Table 1). At concentrations of $0.5 \mu\text{g l}^{-1}$ diuron and $0.2 \mu\text{g l}^{-1}$ zinc pyriithione, no effect was observed at 72 h (NOEC) ($p > 0.05$) (Table 1). The LOEC (cell numbers) was $0.4 \mu\text{g l}^{-1}$ for zinc pyriithione and $0.1 \mu\text{g l}^{-1}$ for Irgarol 1051[®] ($p < 0.05$).

Under the selected experimental conditions, *Synechococcus* sp. was not inhibited by the concentrations of zinc pyriithione and Sea-Nine 211[®] tested ($p > 0.05$), whereas diuron (EC_{50} of $0.55 \mu\text{g l}^{-1}$) and Irgarol 1051[®] (EC_{50} of

$0.16 \mu\text{g l}^{-1}$) significantly affected cell density ($p < 0.05$) (Tables 1 & 2). The NOEC for diuron was $0.21 \mu\text{g l}^{-1}$, $1.0 \mu\text{g l}^{-1}$ for zinc pyriithione, and $0.9 \mu\text{g l}^{-1}$ for Sea-Nine 211[®] ($p > 0.05$) (Table 1). Results indicated that the carrier solvent did not significantly influence growth compared to the controls ($p > 0.05$).

Pigment composition

For *Emiliana huxleyi*, all marker pigment to chl *a* ratios changed significantly when exposed to diuron and zinc pyriithione ($p < 0.05$); whereas chlorophyll c_3 (chl c_3):chl *a*, fuco:chl *a* (fucoxanthin:chl *a*) and 19'-hex:chl *a* (19'-hexanoyloxyfucoxanthin:chl *a*) varied with Sea-Nine 211[®] concentrations, and only the fuco:chl *a* ratio varied with Irgarol 1051[®] concentrations ($p < 0.05$) (Table 2). A pattern of reduction in pigment to chl *a* ratio was observed with increasing exposure to biocides, except for the 19'-hex:chl *a*, diadino:chl *a* and chl c_3 :chl *a* ratios, which increased at intermediate concentrations of biocides, followed by a decline at the highest concentrations ($\geq 5 \mu\text{g l}^{-1}$ diuron) (Table 2). However, when these ratios were normalised to the number of cells, a general pattern of decreased pigment per cell with increasing toxicant concentrations was apparent.

For *Synechococcus* sp., there was no significant difference in marker pigment to chl *a* ratios within the concentration range of the biocides tested ($p > 0.05$) except for Irgarol 1051[®], where significant differences in β -carotene:chl *a* and also in chl *a*:cell were recorded ($p < 0.05$) (Table 2).

Natural phytoplankton community experiment

Toxic effects on pigment composition

Biocide treatments significantly affected the pigment composition ($R = 0.477$; $p = 0.001$; ANOSIM analysis). Largest differences in pigment proportions were found at concentrations of $5 \mu\text{g l}^{-1}$ zinc pyriithione and $10 \mu\text{g l}^{-1}$

Table 1. EC_{50} , NOEC, and LOEC ($\mu\text{g l}^{-1}$) 72 h as cell number inhibition of *Emiliana huxleyi* and *Synechococcus* sp. exposed to the 4 biocides tested. Numbers in parentheses indicate the percentage of inhibition at the given concentration. nd: not determined due to insufficient data

	<i>Emiliana huxleyi</i>			<i>Synechococcus</i> sp.		
	EC_{50}	NOEC	LOEC	EC_{50}	NOEC	LOEC
Zinc pyriithione	0.54	0.2	0.4 (21%)	nd	1.0	nd
Diuron	2.26	0.54	nd	0.55	0.21	0.43 (45%)
Irgarol 1051 [®]	0.25	nd	0.1 (21%)	0.16	nd	nd
Sea-Nine 211 [®]	0.35	nd	nd	1.25	0.9	nd

Table 2. Growth rate (μ , divisions d^{-1}), cell numbers (cell ml^{-1}), chlorophyll *a* to cell (pg $cell^{-1}$) and marker pigment to chlorophyll *a* ratios for the prymnesiophyte *Emiliana huxleyi* and the cyanophyte *Synechococcus* sp. exposed to different type and concentrations of antifouling biocides. Data represent means of 3 replicated cultures. *Significant differences in pigment ratios and growth rates due to different concentrations of biocides for each marked column ($p < 0.05$)

Species	Biocide type	Biocide ($\mu g\ l^{-1}$)	μ^a (div d^{-1})	Cell ml^{-1} ($\times 10^4$)	Chl <i>a</i> : cell	Chl ₁ C ₂ : chl <i>a</i>	Chl ₃ : chl <i>a</i>	Fuc: chl <i>a</i>	19'-Hex: chl <i>a</i>	Diad: chl <i>a</i>	β -Car: chl <i>a</i>	Zea: chl <i>a</i>
<i>Emiliana huxleyi</i> (Prymnesiophyceae)	Diuron	0	1.12	7.23	0.40	0.28	0.20	0.60	0.19	0.17	0.032	
		MEOH	1.11	7.48	0.40	0.27	0.20	0.57	0.18	0.17	0.032	
		0.2	1.05	6.38	0.37	0.26	0.22	0.50	0.25	0.16	0.030	
		0.5	1.02	6.54	0.26	0.25	0.22	0.48	0.27	0.17	0.031	
		5	0.51	2.23	0.25	0.24	0.21	0.48	0.27	0.17	0.029	
		12	0.42	1.74	0.23	0.23	0.21	0.50	0.24	0.18	0.031	
		50	0.38	1.70	0.16	0.16	0.19	0.45	0.23	0.19	0.025	
		
	Zinc pyriithione	0	1.15	5.86	0.46	0.24	0.11	0.42	0.19	0.19	0.022	
		0.2	1.13	5.63	0.52	0.23	0.11	0.39	0.20	0.18	0.024	
		0.4	1.06	4.55	0.23	0.24	0.12	0.37	0.31	0.34	0.022	
		0.6	0.84	2.54	0.16	0.19	0.17	0.23	0.35	0.38	0.026	
		0.8	0.18	6.88	0.11	1.37	0.61	1.98	3.27	0.94	0.004	
		1	-0.62	1.23	0.12	4.70	1.25	7.05	10.37	2.09	0.000	
			
	SeaNine 211 [®]	0	1.17	3.02	0.81	0.25	0.17	0.51	0.15	0.11	0.024	
		MEOH	1.13	2.91	0.80	0.23	0.12	0.58	0.19	0.14	0.019	
		0.4	0.74	1.24	0.69	0.26	0.14	0.45	0.22	0.12	0.023	
		0.8	-1.33	0.02	0.76	0.19	0.07	0.43	0.35	0.16	0.011	
			
	Irgarol 1051 [®]	0	1.17	3.02	0.81	0.25	0.17	0.50	0.15	0.11	0.024	
		MEOH	1.13	2.91	0.80	0.23	0.12	0.58	0.19	0.14	0.019	
		0.1	1.02	2.33	0.37	0.82	0.29	2.15	0.83	0.28	0.009	
		0.2	0.86	1.61	0.46	0.21	0.17	0.39	0.23	0.13	0.022	
0.5		0.52	0.80	0.40	0.31	0.16	0.72	0.35	0.24	0.015		
			
<i>Synechococcus</i> sp. (Nostocophyceae)	Diuron	0	1.23	12.85	0.0033						0.12	0.61
		MEOH	1.26	11.89	0.0034						0.12	0.64
		0.2	1.03	8.76	0.0037						0.14	0.64
		0.4	1.07	7.82	0.0043						0.12	0.56
		2.2	0.53	2.96	0.0025						0.18	0.64
		3.3	0.29	1.80	0.0035						0.13	0.65
			
	Zinc pyriithione	0	1.18	5.37	0.0049						0.11	0.71
		0.4	1.18	5.15	0.0042						0.13	0.64
		0.6	1.15	7.10	0.0046						0.11	0.66
		1	1.02	4.76	0.0054						0.11	0.64
	SeaNine 211 [®]	0	1.18	5.37	0.0049						0.11	0.71
		MEOH	1.19	5.15	0.0045						0.11	0.68
		0.2	1.23	5.60	0.0042						0.12	0.69
		0.4	1.18	6.70	0.0040						0.12	0.67
		0.9	0.91	3.61	0.0046						0.11	0.71
	Irgarol 1051 [®]	0	1.13	8.39	0.0036						0.14	0.74
		MEOH	0.97	6.11	0.0050						0.13	0.83
		0.2	0.58	3.07	0.0022						0.21	0.65
		0.5	0.08	1.08	0.0037						0.12	0.71
1		-0.10	0.77	0.0031						0.14	0.81	
			

^a μ was estimated by taking into account the 3 days of the experiment

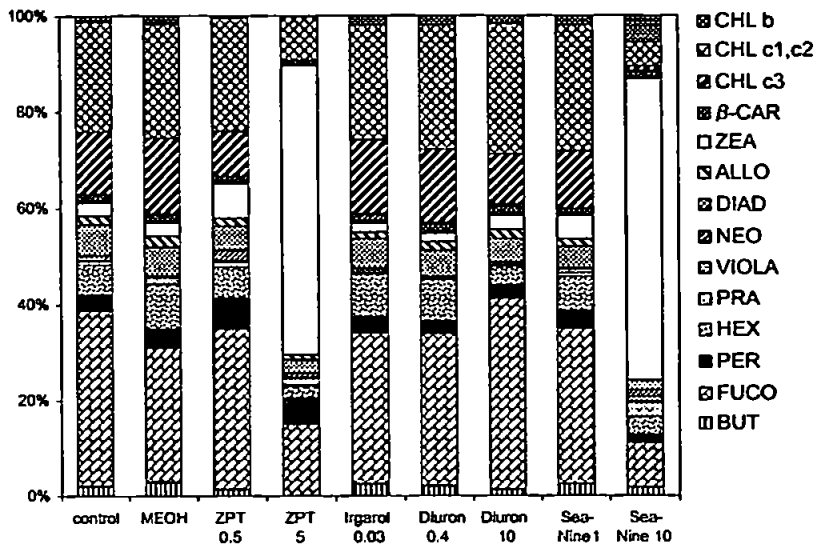


Fig. 1. Pigment composition (% of total) of phytoplankton after 72 h exposure to concentrations ($\mu\text{g l}^{-1}$) of zinc pyrithione (ZPT), Irgarol 1051[®] (Irgarol), diuron, Sea-Nine 211[®] (SeaNine), including control (no biocide addition) and the carrier control (MEOH). Data are mean values ($n = 3$). Samples from the $0.05 \mu\text{g l}^{-1}$ Irgarol 1051[®] were lost during analyses. CHL b: chlorophyll b; CHL c₁, c₂: chlorophyll c₁, c₂; CHL c₃: chlorophyll c₃; β -CAR: β -carotene; ZEA: zeaxanthin; ALLO: alloxanthin; DIAD: diadinoxanthin; NEO: neoxanthin; VIOLA: violaxanthin; PRA: prasinolanthin; HEX: 19'-hexanoyloxyfucoxanthin; PER: peridinin; FUCO: fucoxanthin; BUT: 19'-butanoyloxyfucoxanthin

Sea-Nine 211[®] (Fig. 1). Whilst the contribution of chl a to total pigments was reduced drastically, zeaxanthin levels either increased (Sea-Nine 211[®] exposure) or remained unchanged (zinc pyrithione exposure) resulting in an increase in its relative contribution (Fig. 1). There was a trend towards dissimilarity (>40%) between untreated samples and those treated with $5 \mu\text{g l}^{-1}$ zinc pyrithione and $10 \mu\text{g l}^{-1}$ Sea-Nine 211[®] (SIMPER analysis). The pigments chl c₃, fucoxanthin, 19'-butanoyloxyfucoxanthin and 19'-hexanoyloxyfucoxanthin contributed to 54% of the dissimilarity between $5 \mu\text{g l}^{-1}$ zinc pyrithione and controls; whilst fucoxanthin, chl c₃, alloxanthin, peridinin and 19'-hexanoyloxyfucoxanthin contributed to 54% of the dissimilarity between $10 \mu\text{g l}^{-1}$ Sea-Nine 211[®] and the controls. Dissimilarities amongst treatments (>30%) were observed for concentrations of (1) $5 \mu\text{g l}^{-1}$ zinc pyrithione with diuron (0.4 and $10 \mu\text{g l}^{-1}$), Irgarol 1051[®] ($0.03 \mu\text{g l}^{-1}$), Sea-Nine 211[®] ($1 \mu\text{g l}^{-1}$) and zinc pyrithione ($0.5 \mu\text{g l}^{-1}$); and (2) $10 \mu\text{g l}^{-1}$ Sea-Nine 211[®] with zinc pyrithione ($0.5 \mu\text{g l}^{-1}$), Irgarol 1051[®] ($0.03 \mu\text{g l}^{-1}$), diuron (0.4 and $10 \mu\text{g l}^{-1}$) and Sea-Nine 211[®] ($1 \mu\text{g l}^{-1}$). All other comparisons showed dissimilarities lower than 30%.

Estimation of the community structure using CHEMTAX identified diatoms, dinoflagellates, prymnesio-

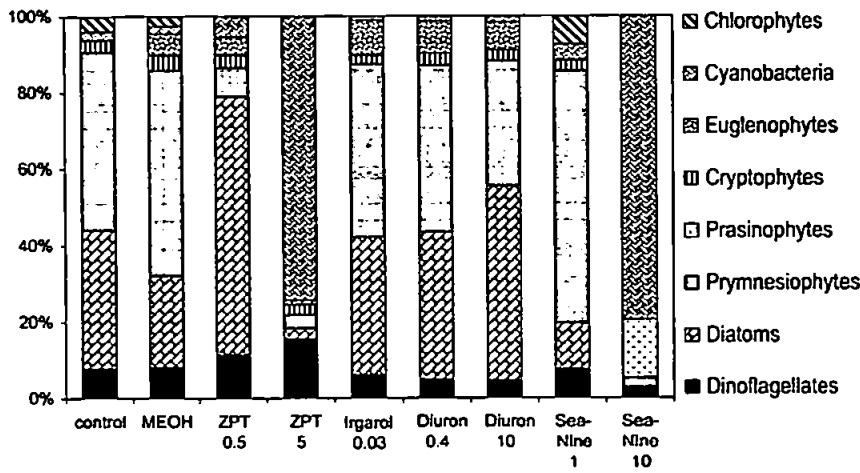
phytes and cyanophytes as the main contributors to the total chl a biomass of the phytoplankton community. Cyanophytes contributed 74 and 79% to the total biomass (as chl a), respectively, at the highest concentrations of zinc pyrithione and Sea-Nine 211[®] (Fig. 2). The contribution of dinoflagellates to biomass increased at 0.5 and $5 \mu\text{g l}^{-1}$ zinc pyrithione (11 and 15%, respectively) when compared to the controls (8%), although it remained almost unchanged under the other biocide treatments. At $10 \mu\text{g l}^{-1}$ diuron and $0.5 \mu\text{g l}^{-1}$ zinc pyrithione, a reduction in prymnesiophytes (15 and 40%, respectively) and an increase in diatoms (21 and 38%, respectively), relative to controls, were observed. At $1 \mu\text{g l}^{-1}$ Sea-Nine 211[®], a reduction in diatoms and an increase in prymnesiophytes were observed.

Toxic effect on phytoplankton growth

AFC results demonstrated a reduction in total cell numbers compared to the controls from 7 to 95% under all biocide concentrations after 72 h ($p < 0.05$), except for $0.03 \mu\text{g l}^{-1}$ Irgarol 1051[®] and $0.4 \mu\text{g l}^{-1}$ diuron ($p > 0.05$; 1-way ANOVA, Least Significant Difference post hoc test) (Fig. 3). Compared to controls, results indicated a decrease in nanoeukaryotes following exposures to zinc pyrithione, Sea-Nine 211[®] and $10 \mu\text{g l}^{-1}$ diuron ($p < 0.05$), a reduction in picoeukaryote numbers in all biocide exposures ($p < 0.05$) except for $1 \mu\text{g l}^{-1}$ Sea-Nine 211[®], and no changes in Cyanophyte abundances in all treatments ($p > 0.05$), except for $10 \mu\text{g l}^{-1}$ diuron (data not shown). The relative contributions of cyanophyte to the population increased at the highest levels of zinc pyrithione and Sea-Nine 211[®]; picoeukaryotes appeared to contribute similarly ($5 \mu\text{g l}^{-1}$ zinc pyrithione) or more ($10 \mu\text{g l}^{-1}$ Sea-Nine 211[®]) compared to the controls, whilst the contribution of nanoeukaryotes decreased (Fig. 4).

Toxic effect on photosynthesis

The development of the phytoplankton community was followed daily using *in vivo* chlorophyll fluorescence. All 4 antifouling biocides impaired photosynthesis at the concentrations tested (Fig. 5). After 72 h exposure, reductions between 20 and 90% in F_v/F_m

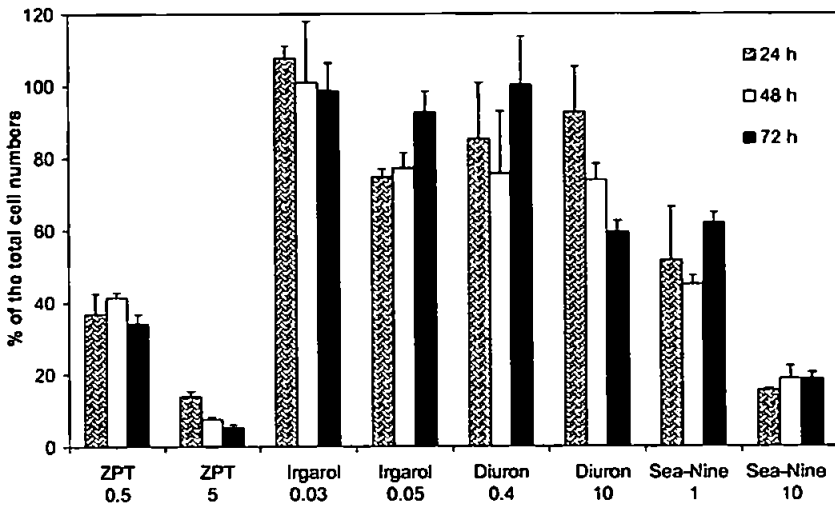


Changes in antifouling biocide concentrations with time

In the single species experiments, measured concentrations of Irgarol 1051[®] and diuron were within $\pm 3\%$ of the nominal concentration at time zero, and did not change substantially after 72 h ($\pm 3\%$ of the measured initial values). Measured Sea-Nine 211[®] concentrations were lower than the nominal concentrations and probably relate to the rapid degradation of Sea-Nine 211[®] (half-life ≤ 24 h). Indeed, after 72 h no Sea-Nine 211[®] was detected in the samples. Therefore, nominal concentrations were used for the calculations of toxicological endpoints.

Fig. 2. Contribution of different algal groups, as determined from pigment: chlorophyll a ratios using CHEMTAX, after 72 h exposure to concentrations ($\mu\text{g l}^{-1}$) of zinc pyrithione (ZPT), Irgarol 1051[®] (Irgarol), diuron, Sea-Nine 211[®] (Sea-Nine), including the control (no biocide addition) and the carrier control (MEOH)

No Irgarol 1051[®] was detected at the sampling site ($n = 3$) or in the control treatments ($n = 3$). For the natural phytoplankton, concentrations of Irgarol 1051[®] in the carrier controls on Day 1 of the experiment were close to the detection limit. Initial Irgarol 1051[®] concentrations were within $\pm 5\%$ of the nominal concentrations ($n = 2$). Diuron concentrations on Day 1 were 0.4 and 9.7 $\mu\text{g l}^{-1}$ and after 72 h were 0.4 and 6.0 $\mu\text{g l}^{-1}$, respectively.



DISCUSSION

Unialgal experiments

Fig. 3. Percentage of total cell numbers (measured by Analytical Flow Cytometry) related to carrier controls (MEOH) after 24 h, 48 h and 72 h exposure to concentrations ($\mu\text{g l}^{-1}$) of zinc pyrithione (ZPT), Irgarol 1051[®] (Irgarol), diuron, and Sea-Nine 211[®] (Sea-Nine). Data are mean values \pm SD ($n = 3$)

The intensity of toxic effects on growth and pigmentation differed according to the type of biocide and the species tested. For *Emiliania huxleyi*, Irgarol 1051[®] was the most toxic ($EC_{50} = 0.25 \mu\text{g l}^{-1}$) with respect to growth and diuron the least toxic ($EC_{50} = 2.26 \mu\text{g l}^{-1}$). Although Sea-Nine 211[®] is readily degraded (Jacobson & Willingham

2000), and is therefore suggested to be less harmful to non-target species, it impaired *E. huxleyi* growth to a similar extent to that of Irgarol 1051[®] ($EC_{50} = 0.35 \mu\text{g l}^{-1}$). Values of NOEC for Sea-Nine 211[®] and zinc pyrithione in *Synechococcus* sp. were higher than the EC_{50} s calculated for *E. huxleyi*, which suggests that *Synechococcus* sp. is more tolerant to these 2 biocides. Comparing the EC_{50} s of the 2 species, *Synechococcus* sp. was more sensitive to diuron than *E. huxleyi*, whereas both showed similar sensitivities to Irgarol

were apparent depending on the concentration of the biocide. For zinc pyrithione, inhibition was more pronounced at 24 h exposure, contrasting with Sea-Nine 211[®], where inhibition appeared to decrease with time of exposure (Fig. 5). *In vivo* inhibition of fluorescence measured using FRRF was compared with inhibition of $^{14}\text{C-HCO}_3^-$ incorporation after a 24 h incubation period (Fig. 6). Linear regression indicates a significant correlation between them ($R^2 = 0.89$; $p = 0.0001$).

2000), and is therefore suggested to be less harmful to non-target species, it impaired *E. huxleyi* growth to a similar extent to that of Irgarol 1051[®] ($EC_{50} = 0.35 \mu\text{g l}^{-1}$). Values of NOEC for Sea-Nine 211[®] and zinc pyrithione in *Synechococcus* sp. were higher than the EC_{50} s calculated for *E. huxleyi*, which suggests that *Synechococcus* sp. is more tolerant to these 2 biocides. Comparing the EC_{50} s of the 2 species, *Synechococcus* sp. was more sensitive to diuron than *E. huxleyi*, whereas both showed similar sensitivities to Irgarol

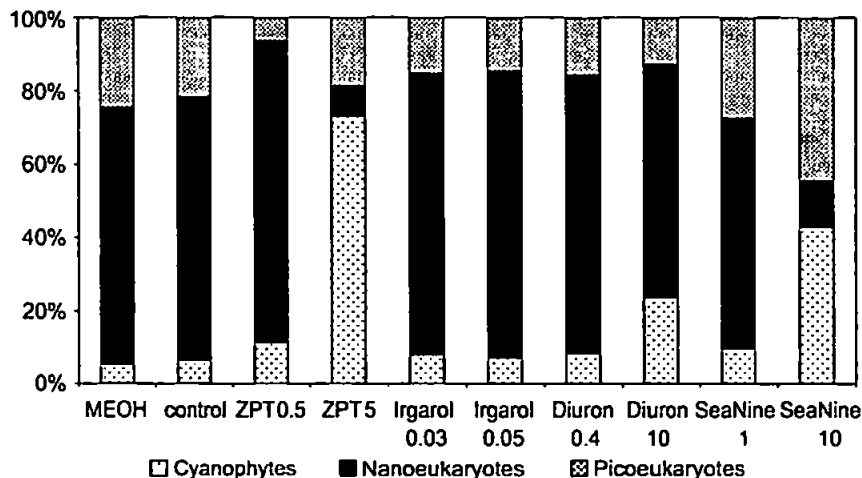


Fig. 4. Cell number of picoeukaryotes, nanoeukaryotes and cyanophytes measured by Analytical Flow Cytometry after 72 h exposure to concentrations ($\mu\text{g l}^{-1}$) of zinc pyriithione (ZPT), Irgarol 1051[®] (Irgarol), diuron, Sea-Nine 211[®] (Sea-Nine), including the control (no biocide addition) and the methanol control (MEOH). Data are mean values ($n = 3$)

1051[®]. Our data indicate higher sensitivities in the species tested than those reported for the freshwater alga *Selenastrum capricornutum* exposed to Sea-Nine 211[®] ($\text{EC}_{50} = 3 \mu\text{g l}^{-1}$), diuron ($\text{EC}_{50} = 45 \mu\text{g l}^{-1}$), and Irgarol 1051[®] ($\text{EC}_{50} = 11 \mu\text{g l}^{-1}$) (Fernández-Alba et al. 2002). Differences in sensitivities observed in this study and compared to the literature are probably related to the species studied, culture conditions and the measures of toxic response, and are further discussed.

In cultures of *Emiliana huxleyi*, changes in pigment: chl *a* ratios showed increase in 19'-hexanoyloxyfucoxanthin, diadinoxanthin and chl c_3 per chl *a* with increasing concentrations of biocides, and resulted from a relative reduction of chl *a*. Increases in 19'-hex:chl *a* and diadino:chl *a* ratios have also been reported by Schlüter et al. (2000) for *Phaeocystis* sp. and *E. huxleyi* in response to increasing light levels. The relative increase of 19'-hexanoyloxyfucoxanthin might be related to hydroxylation of fucoxanthin to 19'-hexanoyloxyfucoxanthin, causing a reduced efficiency of energy supply by the light harvesting complex (Vanleeuwe & Stefels 1998, Schlüter et al. 2000). This coincides with a decrease in fucoxanthin: chl *a* and an increase in 19'-hex:chl *a* ratios under diuron exposures in this study.

In contrast to *Emiliana huxleyi*, *Synechococcus* sp. showed no overall differences in pigment ratios at the concentrations of biocides tested, owing mostly to the lack of inhibitory response of growth (zinc pyriithione and Sea-Nine 211[®] exposures). For Irgarol 1051[®], however, where growth inhibition was more pronounced, the changes in β -carotene:chl *a* and chl *a*:cell ratios might have been related to protective mechanisms. When exposed to PSII inhibitors (such

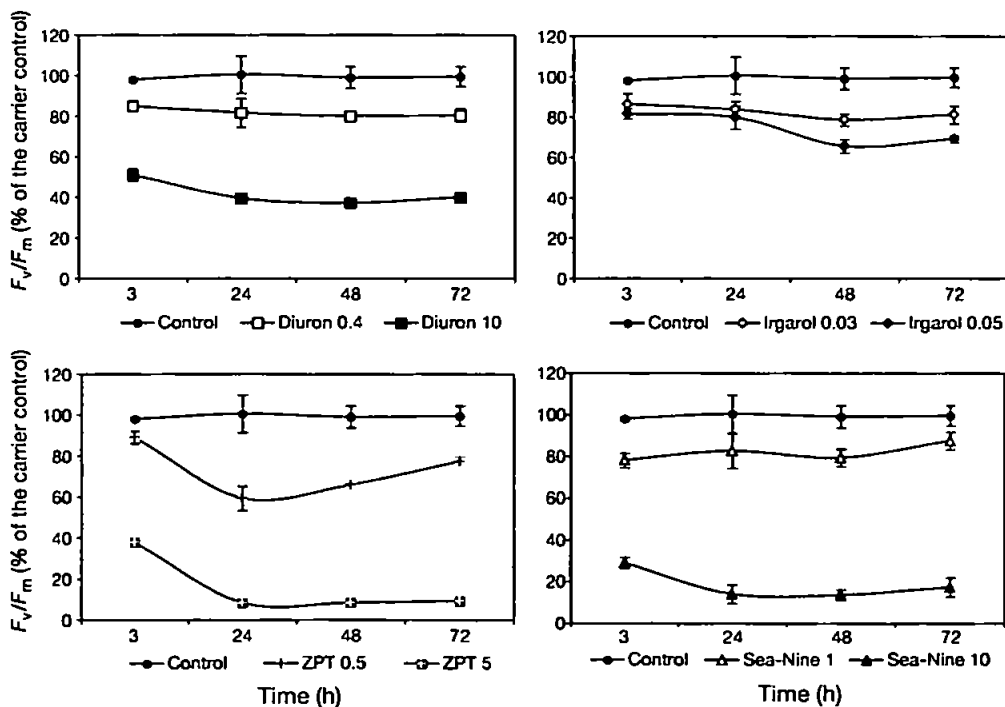


Fig. 5. Photosynthetic efficiency (F_v/F_m) responses of phytoplankton exposed to concentrations ($\mu\text{g l}^{-1}$) of zinc pyriithione (ZPT), Irgarol 1051[®] (Irgarol), diuron and Sea-Nine 211[®] (Sea-Nine) for the period of the experiment (72 h). Data are mean values \pm SD ($n = 3$)

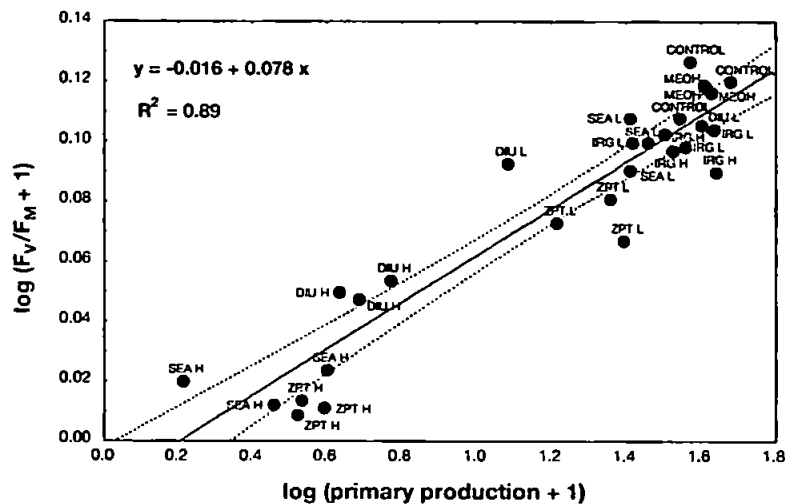


Fig. 6. A linear model relating primary production and F_v/F_m data after 24 h exposure of natural phytoplankton to Irgarol 1051[®], zinc pyrithione, Sea-Nine 211[®] and diuron ($p = 0.0001$). The confidence intervals (95%) correspond to the outer bounds on the graph. Controls, carrier controls (MEOH), diuron 0.4 $\mu\text{g l}^{-1}$ (DIU L) and 10 $\mu\text{g l}^{-1}$ (DIU H), Irgarol 1051[®] 0.03 $\mu\text{g l}^{-1}$ (IRG L) and 0.05 $\mu\text{g l}^{-1}$ (IRG H), zinc pyrithione 0.5 $\mu\text{g l}^{-1}$ (ZPT L) and 5 $\mu\text{g l}^{-1}$ (ZPT H), Sea-Nine 211[®] 1 $\mu\text{g l}^{-1}$ (SEA L) and 10 $\mu\text{g l}^{-1}$ (SEA H)

as Irgarol 1051[®] and diuron), algae decrease their electron transport capacity and increase the production of oxy-radicals, giving rise to destructive effects when the protective mechanisms are overwhelmed (Dahl & Blanck 1996). In contrast to algae, cyanobacteria lack the zeaxanthin cycle-dependent antenna quenching, and so other mechanisms of energy dissipation, such as D1 exchange might be involved in cell protection (Sane et al. 2002). The unialgal culture studies reported here indicated that, under the selected experimental conditions, *Synechococcus* was more sensitive to PSII inhibitors than *E. huxleyi*. Elucidating why the biochemical mechanisms appear more susceptible to PSII inhibitors in *Synechococcus* sp. requires further investigation.

The values of pigment to chl *a* ratios obtained in controls for *Emiliania huxleyi* and *Synechococcus* sp. are in close agreement with those reported in the literature (Schlüter et al. 2000, Henriksen et al. 2002). While it is well documented that changes in natural environmental conditions (e.g. nutrient-limitation, irradiance and cell growth phase) can alter pigment to chl *a* ratios (Schlüter et al. 2000, Henriksen et al. 2002), our results indicate that anthropogenically derived substances such as biocides may also influence pigment to chl *a* ratios and therefore must be taken into account when estimating phytoplankton composition from group-specific pigment ratios used in programmes such as CHEMTAX.

Natural phytoplankton community experiment

Toxic impairment on phytoplankton composition

Estimation of phytoplankton composition using CHEMTAX provides an indication of the structural changes following exposures to biocides. Our results showed a selective toxicity to the natural phytoplankton assemblage, especially following exposure to the highest concentrations of zinc pyrithione and Sea-Nine 211[®] tested. A relative increase in peridinin indicated an increase of dinoflagellates and a relative increase in zeaxanthin denoting a greater proportion of Cyanophyceae present in the community under exposure to zinc pyrithione. Similar structural changes to these were also noted at 10 $\mu\text{g l}^{-1}$ Sea-Nine 211[®], although the relative proportion of peridinin in this case remained almost unchanged. Such tolerance to both

biocides (zinc pyrithione and Sea-Nine 211[®]) is corroborated by the lack of sensitivity found in *Synechococcus* sp. toxicity experiments.

Under almost all biocide exposures, cyanophycean cell numbers remained unchanged compared to controls, even though marked reductions in other phytoplankton groups occurred. For instance, picoeukaryotes were sensitive to almost all biocide treatments, possibly as a result of their large surface:volume ratio, absorbing more chemical per body mass. The selective reduction of other groups resulted in a relative increase in Cyanophyceae abundance mainly at zinc pyrithione and Sea-Nine 211[®] exposures. Moreover, AFC results and CHEMTAX estimates were in good agreement in detecting these changes in Cyanophyceae. Such relative lack of sensitivity of Cyanophyceae in comparison to other groups could possibly lead to development of potentially toxic Cyanophyceae species with environmental consequences.

Cyanophycean cell numbers increased under exposure to 10 $\mu\text{g l}^{-1}$ diuron; this was not detected from the pigment results, due probably to them being masked by major algal groups. *Synechococcus* sp. has been reported to be capable of exchanging the D1:1 and D1:2 proteins, triggered by diuron treatments (Campbell et al. 1996), therefore conferring resistance to PSII inhibitors. Cells containing the D1:2 form generally have a higher quantum yield of oxygen evolution and lower non-photochemical quenching than cells

containing only D1:1 protein (Campbell et al. 1996). The transient exchange of the D1:1 protein, which appears to be the initial response, may thus provide the time required for full cellular acclimation to an increased excitation pressure by modification in protein and lipid composition. This mechanism might have aided cyanophytes to outcompete other algal groups in the community, when exposed to high diuron concentrations.

Although the concentrations of Irgarol 1051[®] tested were too low to induce any detectable impact under the selected experimental conditions, it is likely that environmental concentrations (of up to 1.42 $\mu\text{g l}^{-1}$; Thomas et al. 2001) would modify phytoplankton composition (Readman et al. 2004). Other studies have demonstrated that, depending on the concentrations, Irgarol 1051[®] (0.07 to 2.5 $\mu\text{g l}^{-1}$) can modify algal community structure, by reduction in prymnesiophytes and development of pennate diatoms, cryptophytes, chrysophytes and cyanophytes (Bérard et al. 2003, Readman et al. 2004). A similar pattern was observed in this study for 0.5 $\mu\text{g l}^{-1}$ zinc pyriithione and 10 $\mu\text{g l}^{-1}$ diuron, where the relative contribution of diatoms increased, while prymnesiophytes (indicated by 19'-hexanoxyfucoxanthin) were reduced. Reported environmental concentrations of diuron (up to 6.74 $\mu\text{g l}^{-1}$; Thomas et al. 2001) also pose a threat to phytoplankton, as indicated in this study. Very little data is available on environmental concentrations of Sea-Nine 211[®] and zinc pyriithione (www.pml.ac.uk/ace).

Phytoplankton were more sensitive to antifoulants than other planktonic groups, such as bacteria and crustaceans (Fernández-Alba et al. 2002). However, phytoplankton toxic responses such as compositional changes and low productivity might have an indirect impact on grazers by reducing their food resources. These compositional changes also affect nutrient cycling through the microbial food web and subsequent flow to higher trophic levels (Goldman et al. 1987). Bioaccumulation and consequent trophic transfer of antifoulants is unlikely to be of major significance.

Toxic effect on photosynthesis

The quantum efficiency of PSII (F_V/F_M) was diminished by all concentrations of all biocides tested on the natural phytoplankton community. Diminished F_V/F_M can indicate a large proportion of inactive PSII reaction centres due to oxidation, degradation of D1 proteins (Anderson et al. 1997) or severely reduced pigment concentrations (Marwood et al. 2001). Based on F_V/F_M measurements, the phytotoxicity of the biocides for the natural phytoplankton community can be ranked: Irgarol 1051[®] > zinc pyriithione ~ Sea-Nine 211[®] >

diuron. Variations in this toxicity ranking of biocides might differ for other communities depending on species composition or physiological state.

Irgarol 1051[®] affected F_V/F_M at very low (0.03 $\mu\text{g l}^{-1}$) and environmentally relevant concentrations. Even though a higher concentration of diuron was required to impair photosynthesis (10 $\mu\text{g l}^{-1}$), similar levels (up to 6.74 $\mu\text{g l}^{-1}$) have been detected in the environment (Thomas et al. 2001). Degradation products of diuron can also pose a toxic threat to the environment (Tixier et al. 2001). However, since Irgarol 1051[®] and diuron are not easily degraded, exposures and toxicity were not significantly reduced over time during the experiments in this study. Zinc pyriithione and Sea-Nine 211[®] are, however, transformed more rapidly than diuron and Irgarol 1051[®] (Thomas 2001) reducing exposure concentrations and toxic response. Reversibility of the F_V/F_M impairment was faster for zinc pyriithione than for Sea-Nine 211[®], which was observed at the lower concentrations tested, most likely due to the fact that these compounds undergo degradation within hours. Biological processes appear to be more important than abiotic processes for the transformation of the active substance of Sea-Nine 211[®] (DCOI), with half-lives varying from <1 to 24 h according to the matrices and temperature investigated (Jacobson & Willingham 2000). In contrast to Sea-Nine 211[®], zinc pyriithione is rapidly transformed by photolysis with a half-life of <1 h in natural seawater. Toxicity of metabolites is lower than zinc pyriithione and this may have contributed to the F_V/F_M recovery observed after 24 h exposure (Turley et al. 2000).

FRRF versus $^{14}\text{C-HCO}_3^-$ uptake

Photosynthesis-related endpoints are sensitive measures for assessing short-term responses to antifouling biocides. Although F_V/F_M and $^{14}\text{C-HCO}_3^-$ uptake measure different phases of the photosynthetic process, a good correlation between both methods was found ($R^2 = 0.89$). Analysis of chlorophyll fluorescence is a sensitive and early indicator of damage to the photosynthetic apparatus (Krause & Weis 1991), whilst $^{14}\text{C-HCO}_3^-$ uptake measures the end result of the photosynthetic process, i.e. carbon assimilation. A 1:1 relationship between $^{14}\text{C-HCO}_3^-$ measurements and FRRF estimates of carbon fixation has been reported by the originators of the technique (Kolber & Falkowski 1993). Good comparability between a pulse-amplitude modulated fluorometer and $^{14}\text{C-HCO}_3^-$ -based primary production has also been reported by Dorigo & Le Boulanger (2001) for freshwater periphyton exposed to herbicides and for natural phytoplankton exposed to Irgarol 1051[®] (Nyström et al. 2002).

CONCLUSIONS

The differential toxicity of the tested biocides to algae induced modifications to the community structure of the natural phytoplankton under investigation, which resulted in changes to the taxonomic composition of natural seawater. The cyanophyte *Synechococcus* sp. was more resistant than the prymnesiophyte *Emiliana huxleyi* to zinc pyriithione and Sea-Nine 211[®] in culture experiments. In contrast, *Synechococcus* sp. was more sensitive than *E. huxleyi* to diuron, while exposure to Irgarol 1051[®] showed a similar impact on both species. Irgarol 1051[®] toxicity was up to twice that of zinc pyriithione and Sea-Nine 211[®], whilst diuron was the least toxic of the biocides studied.

The biocides impact on the selected natural phytoplankton community and the differences in group-specific sensitivity were detected through pigment composition. Following exposure to zinc pyriithione and Sea-Nine 211[®], the pigment zeaxanthin proportionally increased indicating a relative increase in Cyanophyceae, which was corroborated with AFC results. Cyanophyceae is a group of particular concern because of toxic blooms. Consequences of biocide pollution on marine diversity during conditions which promote toxic blooms require further investigation in mesocosm-type studies.

However, further investigations should be conducted on inter-species variations in pigment to chl *a* ratios under the influence of toxicants. Biocidal effects were detected by both ¹⁴C-HCO₃⁻ uptake and F_v/F_m measurements at very low concentrations. F_v/F_m is considered to be a sensitive and rapid endpoint to assess the impact of antifouling booster biocides.

Concentrations of antifouling booster biocides in the environment are still a matter for concern. In the UK, the use of Irgarol 1051[®] was revoked by legislation in July 2003. While both Sea-Nine 211[®] and zinc pyriithione are readily degradable, our results suggest that the consequences of continuous use, providing persistent contamination, could be environmentally damaging. The effects of short-term pulses needs to be more researched.

Acknowledgements. This research was supported by the Brazilian Research Council (CNPq), through a studentship to R.A.D., and by the European Commission under the ACE (Assessment of Antifouling Agents in Coastal Environments) contract (MAS3-CT98-0178) (a component of the EC IMPACTS cluster). The authors thank the PML for the L4 microscopy data and also H. W. Higgins for providing a copy of the CHEMTAX program.

LITERATURE CITED

- Anderson JM, Park Y-I, Chow WS (1997) Photoinactivation and photoprotection of photosystem II in nature. *Physiol Plant* 100:214-223
- Aveline BM, Kochevar IE, Redmond RW (1996) Photochemistry of N-hydroxy-2(1H)-pyridone, a more selective source of hydroxyl radicals than N-hydroxypyridine-2(1H)-thione. *J Am Chem Soc* 118:10124-10133
- Barlow RG, Cummings DG, Gibb SW (1997) Improved resolution of mono- and divinyl chlorophylls *a* and *b* and zeaxanthin and lutein in phytoplankton extracts using reverse phase C-8 HPLC. *Mar Ecol Prog Ser* 161:303-307
- Bérard A, Dorigo U, Mercier I, Slooten KB, Grandjean D, Leboulanger C (2003) Comparison of the ecotoxicological impact of the triazines Irgarol 1051 and atrazine on microalgal cultures and natural microalgal communities in Lake Geneva. *Chemosphere* 53:935-944
- Campbell D, Clarke AK, Gustafsson P, Öquist G (1996) D1 exchange and the Photosystem II repair cycle in the cyanobacterium *Synechococcus*. *Plant Sci* 115:183-190
- Collier PJ, Ramsey A, Waigh RD, Douglas KT, Austin P, Gilbert P (1990) Chemical reactivity of some isothiazolone biocides. *J Appl Bacteriol* 69:578-584
- Cremllyn RJ (1991) *Agrochemicals: preparation and mode of action*. Wiley, New York
- Dahl B, Blanck H (1996) Toxic effects of the antifouling agent Irgarol 1051 on periphyton communities in coastal water microcosms. *Mar Pollut Bull* 32:342-350
- Dinning AJ, Al-Adham ISI, Eastwood IM, Austin P, Collier PJ (1998) Pyriithiones as inhibitors of bacterial ATP synthesis. *J Appl Microbiol* 85:141-146
- Dorigo U, Leboulanger C (2001) A pulse-amplitude modulated fluorescence-based method for assessing the effects of photosystem II herbicides on freshwater periphyton. *J Appl Phycol* 13:509-515
- Fernández-Alba AR, Hernando MD, Piedra L, Chisti Y (2002) Toxicity evaluation of single and mixed antifouling biocides measured with acute toxicity bioassays. *Anal Chim Acta* 456:303-312
- Goldman JG, Caron DA, Dennett MR (1987) Nutrient cycling in a microflagellate food chain. IV. Phytoplankton-microflagellate interactions. *Mar Ecol Prog Ser* 38:75-87
- Guillard RRL (1975) Culture of phytoplankton for feeding marine invertebrates animals. In: Smith WL, Chanley MH (eds) *Culture of marine invertebrates animals*. Plenum Press, New York, p 29-60
- Henriksen P, Riemann B, Kaas H, Sørensen HM, Sørensen HL (2002) Effects of nutrient-limitation and irradiance on marine phytoplankton pigments. *J Plankton Res* 24:835-858
- HSE (Health and Safety Executive) (2002) Information Document. HSE 730/15. www.hse.gov.uk/toi/internalops/fod/oc/700-799/730_15.pdf
- Jacobson AH, Willingham GL (2000) Sea-Nine antifoulant: an environmentally acceptable alternative to organotin antifoulants. *Sci Total Environ* 258:103-110
- Joint I, Groom SB, Wollast R, Chou L, Tilstone GH, Figueiras FG, Loijens M, Smyth TJ (2002). The response of phytoplankton production to periodic upwelling and relaxation events at the Iberian shelf break: estimates by the ¹⁴C method and by satellite remote sensing. *J Mar Syst* 32: 219-238
- Kolber ZS, Falkowski PG (1993) Use of active fluorescence to estimate phytoplankton photosynthesis in situ. *Limnol Oceanogr* 38:1646-1665
- Krause GH, Weiss E (1991) Chlorophyll fluorescence and photosynthesis: the basics. *Annu Rev Plant Physiol* 42: 313-349
- Mackey MD, Mackey DJ, Higgins HW, Wright SW (1996) CHEMTAX—a program for estimating class abundances from chemical markers: application to HPLC measurements of phytoplankton. *Mar Ecol Prog Ser* 144:265-283

- Marwood CA, Solomon KR, Greenberg BM (2001) Chlorophyll fluorescence as a bioindicator of effects on growth in aquatic macrophytes from mixtures of polycyclic aromatic hydrocarbons. *Environ Toxicol Chem* 20:890–898
- Nyström B, Becker-van Slooten K, Bérard A, Grandjean D, Druart JC, Leboulanger C (2002) Toxic effects of Irgarol 1051 on phytoplankton and macrophytes in Lake Geneva. *Water Res* 36:2020–2028
- Readman JW, Kwong LLW, Grondlin D, Bartocci J, Vielle-neuve JP, Mee L (1993) Coastal water contamination from a triazine herbicide used in antifouling paints. *Environ Sci Technol* 27:1940–1942
- Readman JW, Devilla RA, Tarran G, Llewellyn CA, Fileman TW, Easton A, Burkill PH, Mantoura RFC (2004) Flow cytometry and pigment analyses as tools to investigate the toxicity of herbicides to natural phytoplankton communities. *Mar Environ Res* 58:353–358
- Sane PV, Ivanov AG, Sveshnikov D, Huner NPA, Öquist G (2002) A transient exchange of the photosystem II reaction center protein D1:1 with D1:2 during low temperature stress of *Synechococcus* sp. PCC 7942 in the light lowers the redox potential of Q_B . *J Biol Chem* 277:32739–32745
- Sargent CJ, Bowman JC, Zhou JL (2000) Levels of antifoulant Irgarol 1051® in the Conwy Marina, North Wales. *Chemosphere* 41:1755–1760
- Schlüter L, Mohlenberg F, Havskum H, Larsen S (2000) The use of phytoplankton pigments for identifying and quantifying phytoplankton groups in coastal areas: testing the influence of light and nutrients on pigment/chlorophyll-*a* ratios. *Mar Ecol Prog Ser* 192:49–63
- Suggett D, Kraay G, Holligan P, Davey M, Aiken J, Geider R (2001) Assessment of photosynthesis in a spring cyanobacterial bloom by use of a fast repetition rate fluorometer. *Limnol Oceanogr* 46:802–810
- Thomas (2001) The environmental fate and behaviour of antifouling paint booster biocides: a review. *Biofouling* 17: 73–86
- Thomas KV, Fileman TW, Readman JW, Waldock MJ (2001) Antifouling paint booster biocides in the UK coastal environment and potential risks of biological effects. *Mar Pollut Bull* 42:677–688
- Tixier C, Sancelme M, Bonnemoy F, Cuer A, Veschambre H (2001) Degradation products of a phenylurea herbicide, diuron: synthesis, ecotoxicity, and biotransformation. *Environ Toxicol Chem* 20:1381–1389
- Turley PA, Fenn RJ, Figura PM, Ritter JC (2000) Pyrithiones as antifoulants: environmental chemistry and risk assessment. *Biofouling* 15:175–182
- Vanleeuwe MA, Stefels J (1998) Effects of iron and light stress on the biochemical composition of Antarctic *Phaeocystis* sp. (Prymnesiophyceae). ii. Pigment composition. *J Phycol* 34: 496–503
- Walsh GE (1988) Methods for toxicity tests of single substances and liquid complex waters with marine unicellular algae. EPA/600/8–87/043, Cincinnati, OH
- Zhou JL, Fileman TW, Evans S, Donkin P, Mantoura RFC, Rowland SJ (1996) Seasonal distribution of dissolved pesticides and polynuclear aromatic hydrocarbons in the Humber Estuary and Humber coastal zone. *Mar Pollut Bull* 32:599–608

Editorial responsibility: Otto Kinne (Editor-in-Chief), Oldendorf/Luhe, Germany

Submitted: February 20, 2004; Accepted: September 2, 2004
Proofs received from author(s): January 14, 2005

The effects of a PSII inhibitor on phytoplankton community structure as assessed by HPLC pigment analyses, microscopy and flow cytometry

Rosângela A. Devilla^{a,b,*}, Murray T. Brown^b, Maria Donkin^b, James W. Readman^a

^a Plymouth Marine Laboratory, Prospect Place, West Hoe, Plymouth PL1 3DH, UK

^b School of Biological Sciences, University of Plymouth, Drake Circus, Plymouth PL4 8AA, UK

Received 16 July 2004; received in revised form 7 October 2004; accepted 8 October 2004

Abstract

Measurements of the stress imposed by a PSII inhibiting herbicide (Irgarol 1051[®]) on the composition of a phytoplankton community was investigated by comparing chemotaxonomy, as determined by high performance liquid chromatography (HPLC), optical microscopy and analytical flow cytometry (AFC). Changes in community structure were induced in microcosms containing a natural marine phytoplankton community exposed to different concentrations of Irgarol 1051[®] (0.5 and 1.0 $\mu\text{g l}^{-1}$). Microcosms were maintained under controlled laboratory conditions in semi-continuous culture over 120 h. Class-specific phytoplankton biomass (chlorophyll *a*) was estimated using CHEMTAX analyses of pigment concentrations. Microscopic identification and carbon content estimates were cross-correlated with CHEMTAX and also with AFC enumeration/size classifications of major phytoplankton groups. CHEMTAX–HPLC analyses and microscopy results demonstrated that prasinophytes and prymnesiophytes were the most affected groups following exposure to Irgarol 1051[®]. The selective reductions in both classes as estimated by both techniques revealed similar trends. Results for chlorophytes and dinoflagellates showed these groups to be most tolerant to Irgarol 1051[®]. Indeed, class-specific biomass for chlorophytes as determined by CHEMTAX and microscopy were correlated ($R^2 = 0.53$) which demonstrated an increase in both abundance and carbon content following exposures to Irgarol 1051[®]. Abundances of nanoeukaryotes as determined by microscopy afforded good agreement with results from AFC ($R^2 = 0.8$), although for picoeukaryotes, abundances were underestimated by microscopy ($R^2 = 0.43$). The relative performance of the selected techniques is discussed.

© 2004 Elsevier B.V. All rights reserved.

Keywords: Marine phytoplankton; Toxicity; Antifouling booster biocides; Flow cytometry; Pigments; CHEMTAX; Microscopy

1. Introduction

Irgarol 1051[®] is an *s*-triazine photosynthetic inhibitor used in antifouling paints to prevent attachment

* Corresponding author. Tel.: +44 1752 633460;

fax: +44 1752 633101.

E-mail address: roadev@yahoo.co.uk (R.A. Devilla).

and growth of algae on the hulls of ships or boats. After painting, the chemical is continuously released to the surrounding water and remains active for approximately 1–2 years (HSE, 2002a), posing a threat to non-target organisms in the environment. Concerns over the use of antifouling ‘booster’ biocides have increased since TBT restrictions were introduced in the late 1990s (HSE, 2002b; Readman et al., 1993) and their use became more widespread. Irgarol 1051[®] was, until recently, one of the most commonly used booster biocides in the UK (Thomas et al., 2002), with levels up to 1421 ng l⁻¹ being reported in UK marinas (Thomas et al., 2001). As a consequence, concerns have been raised about the environmental impact they may have on indigenous organisms (Readman et al., 2004).

Algal species comprising the phytoplankton are highly susceptible to herbicidal antifouling compounds which damage photosynthetic pathways. Due to their short generation times and differential responses and susceptibilities to the biocides, algae can, potentially, be affected over time scales from hours to days (McCormick and Cairns, 1994; Jørgensen and Christoffersen, 2000), with resultant changes in algal communities (Hamilton et al., 1988). As modifications to phytoplankton communities can alter the functional structure of the food web, the detection of such changes imposed by toxicants is crucial to determine the extent of damage to the ecosystem.

Several techniques have been employed to investigate phytoplankton community composition. Light microscopy is the classical method for identifying and enumerating phytoplankton, allowing estimations of carbon content from biovolume determinations (Strathmann, 1967; Montagnes and Franklin, 2001). While detailed information about species and size can be acquired, this method is very time consuming and requires considerable taxonomic expertise. Moreover, light microscopy examination does not easily lend itself to identification of small-sized organisms (e.g. nanoplanktonic flagellates). Furthermore, fixation can alter the structure of fragile cells of many species (Gieskes and Kraay, 1983; Simon et al., 1994). Analytical flow cytometry (AFC) provides a more rapid assessment and quantification of phytoplankton communities, but lacks detailed compositional information. Based on the optical properties of cells, AFC can only discriminate phytoplankton communities into picoplanktonic prokaryotes, pi-

coeukaryotes, and nanoeukaryotes (Readman et al., 2004).

A chemotaxonomic approach has provided an additional tool that overcomes some of the limitations of microscopy and AFC. Based on analyses of pigments using high performance liquid chromatography (HPLC), taxon-specific markers can discriminate between the main algal classes contributing to the phytoplankton community (e.g. Barlow et al., 1993; Jeffrey et al., 1997). For example, peridinin has been used as a diagnostic pigment marker for dinoflagellates, 19'-hexanoyloxyfucoxanthin for prymnesiophytes, alloxanthin for cryptophytes, while other pigments are shared within more than one algal class, e.g. chlorophyll *b* which occurs in chlorophytes, prasinophytes and prochlorophytes (Andersen et al., 1996; Jeffrey et al., 1997). However, the use of specific biomarkers in coastal waters is more complicated than in open ocean, since inland inputs can change the chemical, physical and consequently the biological characteristics more intensively.

Several recent studies have compared microscopic and chemotaxonomic approaches on natural communities (Breton et al., 2000; Rodriguez et al., 2002; Carreto et al., 2003; Garibotti et al., 2003; Fietz and Nicklish, 2004), with some also including flow cytometry analyses (e.g. Gin et al., 2003). Studies have demonstrated that HPLC pigment analysis is a valuable tool for phytoplankton studies and that it can generate a good approximation of carbon biomass. However, more research is needed to assess the chemotaxonomic approach, since the use of chlorophyll *a* as a biomass indicator must be undertaken with caution as it is susceptible to changes in environmental conditions. To date, few investigations on community changes under anthropogenic stressors have been reported (Readman et al., 2004). Data on single species exposures and preliminary data on natural phytoplankton community changes have been reported by Devilla et al. (in press). In this study, we examine the consequences of environmental disturbances on phytoplankton composition by manipulating a natural algal community in microcosms exposed to the PSII inhibitor Irgarol 1051[®]. The aim is to compare and contrast changes in community structure as determined by HPLC-class specific pigment analyses, optical microscopy and AFC and use these techniques to monitor the effects of Irgarol 1051[®] in microcosms.

2. Materials and methods

2.1. Sampling and experimental design

One hundred litres of coastal surface water was collected from the well-characterised L4 station (Pingree et al., 1978; Rodriguez et al., 2000) off Plymouth, UK (50°15'N, 04°13'W) on 11 August 2003. The in situ temperature was 16 °C and salinity 35 PSU. At the laboratory, the seawater was filtered through a 150 µm nylon mesh net and 4 l were transferred into each of 15 microcosms comprising 5 l borosilicate glass Erlenmeyer flasks.

A stock solution of 0.503 µg µl⁻¹ Irgarol 1051[®] (2-methylthio-4-tertiary-butylamino-6-cyclopropylamino-*s*-triazine) was prepared by dissolution in methanol (HPLC grade). The working solution (1 µg ml⁻¹) was prepared at the start of the experiment from dilutions of the stock solution into filtered (0.45 µm) and autoclaved seawater to reduce carrier solvent concentration. Microcosms were spiked with aliquots of the Irgarol 1051[®] working solution to give nominal concentrations of 0.5 and 1.0 µg l⁻¹ (which were selected from a preliminary scaling experiment). It was ensured that all microcosms (including the controls) were spiked with the same amount of methanol. Final concentrations of methanol for each treatment did not exceed 0.0002% (v/v). There were five replicate microcosms for each treatment and control. Flasks were randomly placed in a walk-in controlled temperature room on a 12 h:12 h light:dark cycle under an average temperature of 17 °C and an irradiance of 160 µmol photons m⁻² s⁻¹ photosynthetic active radiation (PAR), provided by cool white fluorescent light bulbs (Sylvania; 70 W). The experiment was conducted over 120 h. After 48 h, the water in all microcosms was partially renewed with the original seawater (sterilized by filtration through 0.2 µm Track-Etch membrane filters following collection, with or without Irgarol 1051[®] addition) to compensate for any nutrient depletion. This was adjusted to result in a dilution of phytoplankton content of 1.4 times. To minimise changes due to light variability, flasks were randomly repositioned each day. Flasks were swirled by hand once daily prior to sample removal. Samples for AFC were taken daily to monitor phytoplankton growth. Samples for pigments, microscopy and Irgarol 1051[®] analyses were taken at days 0, 2 and 4 of the experimental period.

2.2. Chemical and biological analyses

2.2.1. HPLC pigment analyses

Phytoplankton samples (1–1.5 l) were concentrated under gentle vacuum onto 25 mm GF/F Whatman filters and were then frozen in liquid nitrogen. Pigments were extracted into 2 ml of 90% acetone:10% Milli-Q water (v/v) solution (containing apo-carotenal as an internal standard) with the aid of an ultrasonication probe (20 s; 60 W). Extracts were then centrifuged (3000 rpm, 5 min followed by 14 000 rpm, 2 min). Supernatants were mixed with 1 M ammonium acetate (50%:50% v/v) before injection into the HPLC. Analyses of pigments were conducted using the reverse phase HPLC procedure outlined by Barlow et al. (1997) using a 3 µm Hypersil MOS2 C-8 column (100 mm × 4.6 mm; Alltech Associates Ltd.) fitted to an Agilent HPLC system with a diode-array detector. Solvent A consisted of 70:30 (v/v) methanol:1 M ammonium acetate and solvent B was 100% methanol. Pigments were separated at a flow rate of 1 ml min⁻¹ by a linear gradient programmed as follows (minutes; % solvent A; % solvent B): (0; 75; 25), (1; 50; 50), (20; 30; 70), (25; 0; 100), and (32; 0; 100). Calibration was performed with the following standards (from DHI, Water and Environment, and Sigma-Aldrich Co.): chlorophylls *a*, *b*, *c*₁*c*₂, and *c*₃, peridinin, 19'-butanoyloxyfucoxanthin, fucoxanthin, 19'-hexanoyloxyfucoxanthin, violaxanthin, neoxanthin, diadinoxanthin, antheraxanthin, diatoxanthin, alloxanthin, zeaxanthin, lutein, apo-carotenal, phaeophytin and β-carotene. All solvents were of HPLC grade.

2.2.2. Flow cytometry analysis

In vivo samples for AFC were analysed immediately after sample collection and therefore did not require fixation. Phytoplankton samples were analysed for enumeration and size classification using a Becton Dickinson FACSort[™] flow cytometer as described by Readman et al. (2004). Chlorophyll *a* fluorescence (>650 nm), phycoerythrin fluorescence (585 ± 21 nm) and side scatter (light scattered at 90° to the plane of a vertically polarised argon ion laser exciting at 488 nm) were the parameters used to discriminate between cells. Flow rate was calibrated with each run of samples using a 10%:90% (v/v) solution of polystyrene beads (Coulter[™] Flow-Set[™] Fluorospheres; 3.6 µm diameter; 1 × 10⁶ beads ml⁻¹) and particle free ultra-pure

water. Bivariate scatter-plots of side scatter against phycoerythrin and chlorophyll fluorescence were plotted to discriminate between picoplanktonic cyanophytes and the nanoplanktonic cryptophytes. The picoeukaryotes and nanoeukaryotes were resolved using bivariate scatter-plots of side scatter against chlorophyll fluorescence (Fig. 1). Data plots were obtained using

the Software WinMDI (Version 2.6; Joseph Trotter, 1998).

2.2.3. Microscopy

Phytoplankton samples were preserved with Lugol's iodine solution to 2% (final concentration) and counting was carried out on settled (Utermöhl) 100 ml samples using an inverted microscope at magnifications of 187× and 750×. Algal cells were identified to species level when possible, except for the small fragile algae (e.g. nanoplanktonic flagellates) for which only the genus or class was recorded. Carbon estimates for each species were derived from volume determinations according to Kovala and Larrance (1966) and the cell volume:carbon relationships were obtained from Eppley et al. (1970) (see also UNESCO, 1974), except for ciliates whose conversion factors were derived from Beers et al. (1975).

2.2.4. Irgarol 1051[®] analyses

Actual concentrations of Irgarol 1051[®] were measured by collecting 1 l of seawater from the microcosms. Samples were spiked with an internal standard (Ametryn) and were stored at 4 °C (Thomas et al., 2001) awaiting extraction.

Extractions and analyses of Irgarol 1051[®] were based on the method described in Sargent et al. (2000). Liquid-liquid extraction was performed using glass separation funnels with dichloromethane as the extracting solvent. Extractions were performed twice by shaking the sample plus solvent for 2 min. All solvents were of HPLC grade (Rathburn Chemicals Ltd., UK). Water-free solvent extracts containing the internal standard were sequentially concentrated down to 1 ml in a rotary-evaporator (Büchi Rotavapor R-205; 30–35 °C) and to <1 ml under a gentle N₂ stream in a turbo-evaporator (Zymark Turbo Vap[®] LV; 30 °C; 2.5 PSI N₂). Extracts (1–2 µl) were injected into a 6890 N gas chromatograph system coupled to a 5973 mass selective detector (Agilent Technologies, UK). The instrument was operated in selective ion monitoring (SIM) mode using *m/z* values of 182 for Irgarol 1051[®] and 227 for Ametryn. Calibration curves displayed a determination coefficient of 0.98–0.99 (R^2). Analytical performance was assessed by analyses of blanks and standard solutions. Recovery of Irgarol 1051[®] was 81% ($\pm 6\%$; $n = 5$).

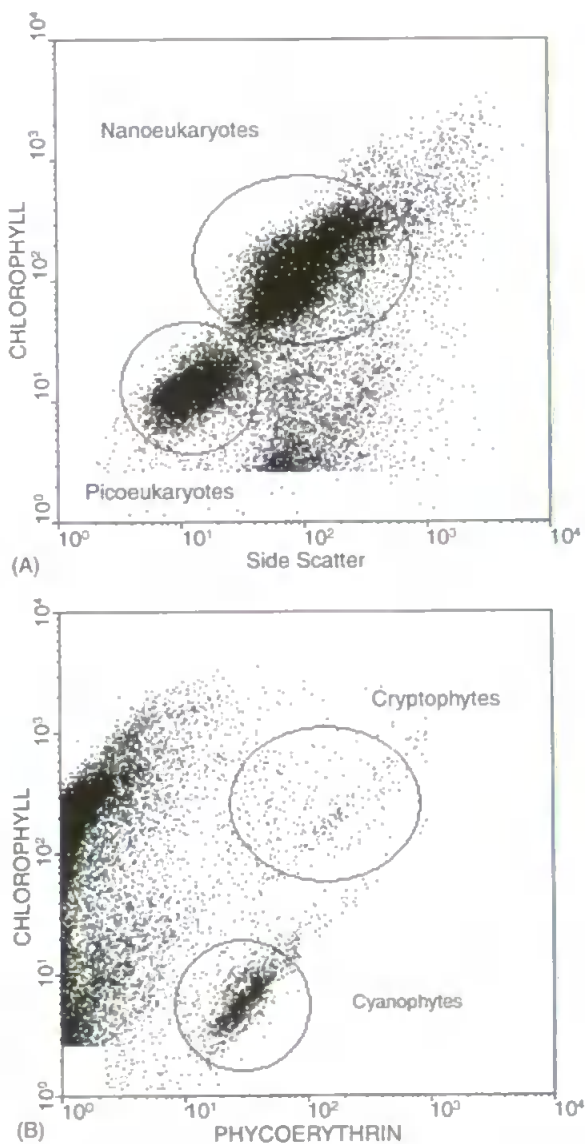


Fig. 1. Bivariate scatter-plots (AFC) of chlorophyll fluorescence vs. side-angle light scatter (A) and phycoerythrin (B) showing phytoplankton separation for (A) nanoeukaryotes and picoeukaryotes and (B) cyanophytes and cryptophytes.

2.3. Data analyses

2.3.1. Evaluation of phytoplankton diversity

Comparisons between the effects of Irgarol 1051[®] on community structure were performed using average Margalef's diversity index (Margalef, 1958) and the number of species or groups of autotrophs enumerated by microscopy. The diversity index was calculated from the following equation: $D = (S - 1) / \ln N$, where D is the Margalef's diversity index, S the number of species in a sample, and N the number of individuals in a community.

A matrix using Bray–Curtis dissimilarity was generated using fourth root transformed abundance data from microscopy observations. Subsequently, non-metric multi-dimensional scaling (MDS) ordinations were conducted for species abundances and species aggregated into groups (diatoms, dinoflagellates, chlorophyceae, chrysophyceae, cryptophyceae, prasinophyceae, prymnesiophyceae, unidentified flagellates). These analyses were performed using the statistical software PRIMER for Windows, Version 5.2.9 (Plymouth, UK).

2.3.2. Estimates of class-specific biomass

Estimates of biomass from chlorophyll *a* for each phytoplankton group were obtained using the matrix factorisation program CHEMTAX run under MATLAB[™] (Mackey et al., 1996). Algal classes were selected according to the phytoplankton composition obtained from microscopic analysis. The pigment:chlorophyll *a* ratio input matrix was derived from the literature (Mackey et al., 1996; Irigoien et al., 2000). In addition to the dinoflagellates, a separate initial marker pigment:chlorophyll *a* ratio was required for the dinoflagellate *Karenia mikimotoi* (formerly *Gyrodinium aureolum*) (80% carbon), because its pigment composition differs from the normal pigment composition of dinoflagellates, which have peridinin as the marker carotenoid (Wright and Jeffrey, 1997). This species has 19'-hexanoyloxyfucoxanthin and fucoxanthin instead of peridinin (Johnsen and Sakshaug, 1993). The light protecting carotenoids β -carotene, diadinoxanthin, diatoxanthin and other pigments only detected in trace amounts were excluded from the matrix, as recommended by Mackey et al. (1996).

2.3.3. Comparisons between methods

Linear regression models between chlorophyll *a* biomass estimated through CHEMTAX and carbon content obtained from microscopy for each phytoplankton group were obtained using the statistical package Statistica for Windows, Version 5.1 (1996 edition, StatSoft Inc., Tulsa, USA). Regressions were considered significant at a level of 0.05. The effects of Irgarol 1051[®] exposures were analysed by one-way ANOVA followed by the least significant difference test (LSD; $\alpha = 0.05$). All data were tested for homocedasticity (Cochran's test) and normality (χ^2 test) and transformed ($\log x + 1$; rank) when necessary to meet the assumptions for parametric tests.

3. Results

3.1. Analytical flow cytometry

Growth of nanophytoplankton and picophytoplankton was monitored by AFC for 120 h. Nanoplanktonic cryptophytes were at insignificant numbers and were therefore omitted in the results. Picoeukaryotes were exponentially growing until 96 h in the controls (Fig. 2), therefore data resulting from this day were selected for comparisons. Results showed a decline in cell numbers relative to controls with increasing concentrations of Irgarol 1051[®] throughout the experimental period (Fig. 2). After 96 h, relative to the controls, picoeukaryotes exposed to 0.5 and 1.0 $\mu\text{g l}^{-1}$ Irgarol 1051[®] were significantly ($P < 0.05$) inhibited by 38% and 73%, respectively, and nanoeukaryotes were inhibited by 52% and 78%, respectively. Cyanophyceae cell numbers steadily declined throughout the experimental period (Fig. 2), with cell numbers being reduced by 53% following a 96 h exposure to 1.0 $\mu\text{g l}^{-1}$ Irgarol 1051[®] (Fig. 2).

3.2. Microscopy

As shown in Fig. 3, 96 h exposures to concentrations of 0.5 and 1.0 $\mu\text{g l}^{-1}$ Irgarol 1051[®] induced changes in autotroph composition by modifying either phytoplankton species or group compositions. Similar species composition could be readily separated into three clusters representing the different treatments and controls at 96 h of incubation (Fig. 3A). For sim-

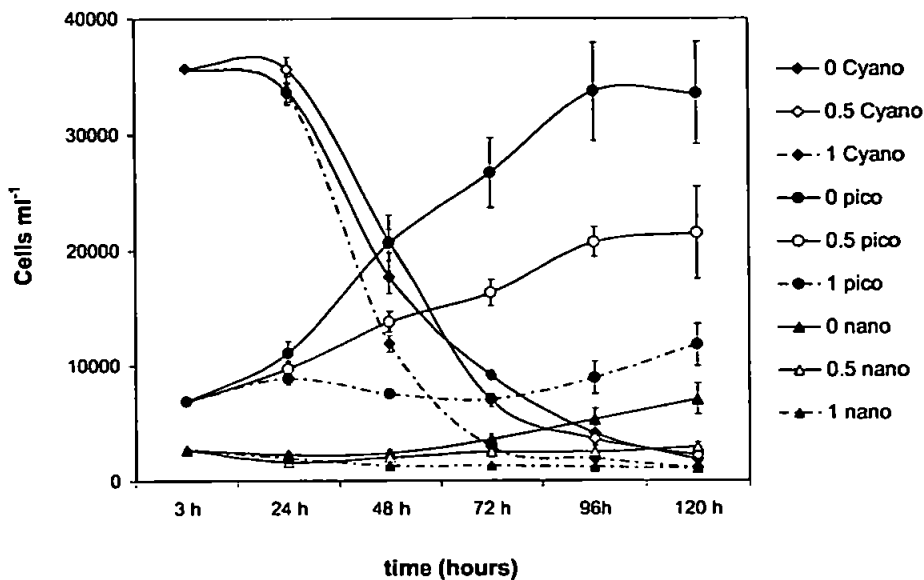


Fig. 2. Growth responses of picoeukaryotes (pico), nanoeukaryotes (nano), and cyanophytes (Cyano) under exposures to 0.5 and 1.0 $\mu\text{g l}^{-1}$ Irgarol 1051[®] and the controls (no Irgarol 1051[®] added) over a 120 h period of incubation. Data are expressed as mean cell abundances (measured by AFC). Bars indicate standard deviations ($n=5$).

ilar group composition clustering only isolated the 1.0 $\mu\text{g l}^{-1}$ exposure (Fig. 3B). All treated and control clusters after 96 h of incubation were different from the 'initial' composition, i.e., time 0 of incubation (Fig. 3A and B).

Microscopy observations revealed that the number of autotrophic species (S) and autotrophic groups (G) significantly declined ($S=36$; $G=7$) relative to the controls ($S=45$; $G=9$) following a 96 h exposure to 1.0 $\mu\text{g l}^{-1}$ Irgarol 1051[®] ($P<0.01$) (Fig. 4). A significant reduction in the Margalef's diversity index was also observed for the community studied under exposure to 1.0 $\mu\text{g l}^{-1}$ Irgarol 1051[®] ($P<0.01$) (Fig. 4). Both parameters also showed significant differences between 0.5 and 1.0 $\mu\text{g l}^{-1}$ Irgarol 1051[®] ($P<0.05$).

Relative to the controls, autotroph species abundances were significantly reduced by 39% and 52% following exposure to 0.5 and 1.0 $\mu\text{g l}^{-1}$ Irgarol 1051[®], respectively ($P<0.05$). No significant difference in autotroph abundance was, however, found between the Irgarol 1051[®] treatments ($P>0.05$). Abundance of prasinophytes and prymnesiophytes were significantly reduced after exposure to 0.5 and 1.0 $\mu\text{g l}^{-1}$ Irgarol 1051[®] ($P<0.05$) when compared to the controls (Fig. 5A). Diatoms, dinoflagellates, cryptophytes, and

unidentified flagellates were significantly reduced only under 1.0 $\mu\text{g l}^{-1}$ Irgarol 1051[®]. In contrast, chlorophyte abundances significantly increased following exposure to this concentration ($P<0.05$) (Fig. 5A). No significant differences ($P>0.05$) were observed for diatoms, dinoflagellates, chlorophytes, chrysophytes, cryptophytes and unidentified flagellates exposed to 0.5 $\mu\text{g l}^{-1}$ Irgarol 1051[®]. Also, no changes were observed for chrysophytes at both exposure concentrations ($P>0.05$).

Carbon estimates indicated similar patterns of response amongst groups to both Irgarol 1051[®] exposures, except for diatoms, in which the carbon content did not differ between treatments. The relative carbon contribution of chlorophytes increased from 6% (controls) to 24% (1.0 $\mu\text{g l}^{-1}$ Irgarol 1051[®]), dinoflagellates increased from 18% (controls) to 24% (0.5 $\mu\text{g l}^{-1}$ Irgarol 1051[®]). Reductions in the relative proportion of carbon content were observed mainly for the prymnesiophytes from 23% (controls) to 11% (1.0 $\mu\text{g l}^{-1}$ Irgarol 1051[®]). Heterotrophs, however, increased in numbers under 1.0 $\mu\text{g l}^{-1}$ Irgarol 1051[®] ($P<0.05$), whilst no difference was observed in their carbon content ($P>0.05$) (data not shown). Carbon contents of total autotrophs exposed to 0.5 and 1.0 $\mu\text{g l}^{-1}$ Irgarol

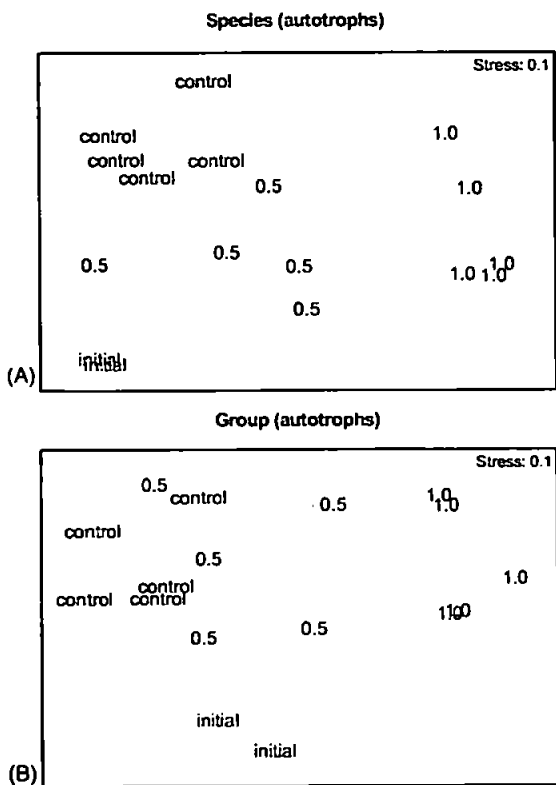


Fig. 3. Non-metric multi-dimensional scaling (MDS) ordination of (A) species abundances and (B) species abundances aggregated into groups of autotrophs. Data were fourth-root-transformed for Bray–Curtis dissimilarities analysis. Autotrophs present in the controls (no Irgarol 1051[®] added) and in the microcosms treated with 0.5 and 1.0 $\mu\text{g l}^{-1}$ Irgarol 1051[®] at 96 h of experiment (five replicates). Autotrophs at time of collection (time 0) is expressed as 'initial'. Small distances between observations indicate high similarity in community structure. Stress levels (above each graph) indicate a good representation of the relationship between observations.

1051[®] decreased significantly relative to the controls ($P=0.0034$ and 0.0338 , respectively), but no significant difference was observed between Irgarol 1051[®] treatments ($P=0.236$) (Fig. 5B). A value of 80% of the carbon content relative to dinoflagellates was attributed to *K. mikimotoi*.

3.3. Pigment composition

All diagnostic pigments were significantly correlated to chlorophyll *a* ($P<0.05$) (Table 1). The highest correlations were found for fucoxanthin ($R^2=0.96$), alloxanthin ($R^2=0.84$), chlorophyll *c*₃ ($R^2=0.73$),

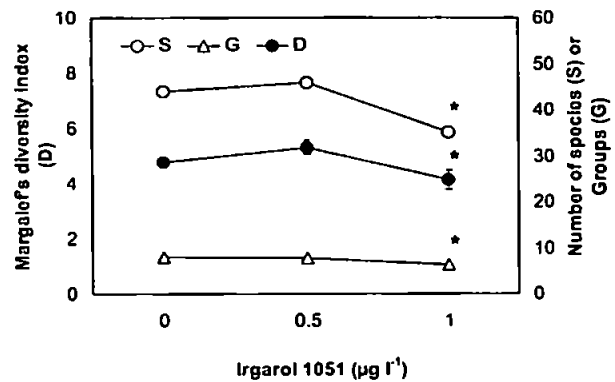


Fig. 4. Effects of Irgarol 1051[®] on community structure expressed as average ($n=5$) Margalef's diversity index (*D*) and number of species (*S*) and groups (*G*) of autotrophs. Data obtained from microscopy observations at 96 h of experimental period. (*) Significant difference compared to controls (i.e. no addition of Irgarol 1051[®]). ANOVA one-way followed by LSD post hoc comparison of means ($P<0.01$; data were rank transformed for the parameter *S*).

chlorophyll *b* ($R^2=0.62$), 19'-hexanoyloxyfucoxanthin ($R^2=0.55$), and 19'-butanoyloxyfucoxanthin ($R^2=0.52$) ($P<0.01$). Zeaxanthin proved to be an exception to this pattern, being inversely proportional to chlorophyll *a* ($R^2=0.73$; $P<0.0001$) (Table 1). It is demonstrated, therefore, that chlorophyll *a* biomass is linearly related to prymnesiophytes, chrysophytes and diatoms (fucoxanthin-containing groups), the cryptophytes (alloxanthin), and the chlorophytes (chlorophyll *b*). Other phytoplankton diagnostic pigments presented weak correlations with chlorophyll standing stocks.

After 96 h, an apparent 10% increase in chlorophyll *a* was observed at exposures to 0.5 $\mu\text{g l}^{-1}$ Irgarol 1051[®] ($P>0.05$), with a subsequent significant decrease of 30% at 1.0 $\mu\text{g l}^{-1}$ Irgarol 1051[®] ($P<0.05$) compared to the controls (Fig. 6A). No pattern of strong dominance of a specific pigment was observed in the microcosms. Fucoxanthin was the main pigment and constituted 26% of the total pigments in the controls, followed by 19'-hexanoyloxyfucoxanthin, which constituted 17%. In the treated microcosms (0.5 and 1.0 $\mu\text{g l}^{-1}$ Irgarol 1051[®]), zeaxanthin and antheraxanthin proportionally increased up to two and six times, respectively, relative to the controls (Fig. 6A).

Estimation of the community structure using the CHEMTAX calculations identified four groups as the main contributors to the total chlorophyll *a* biomass of

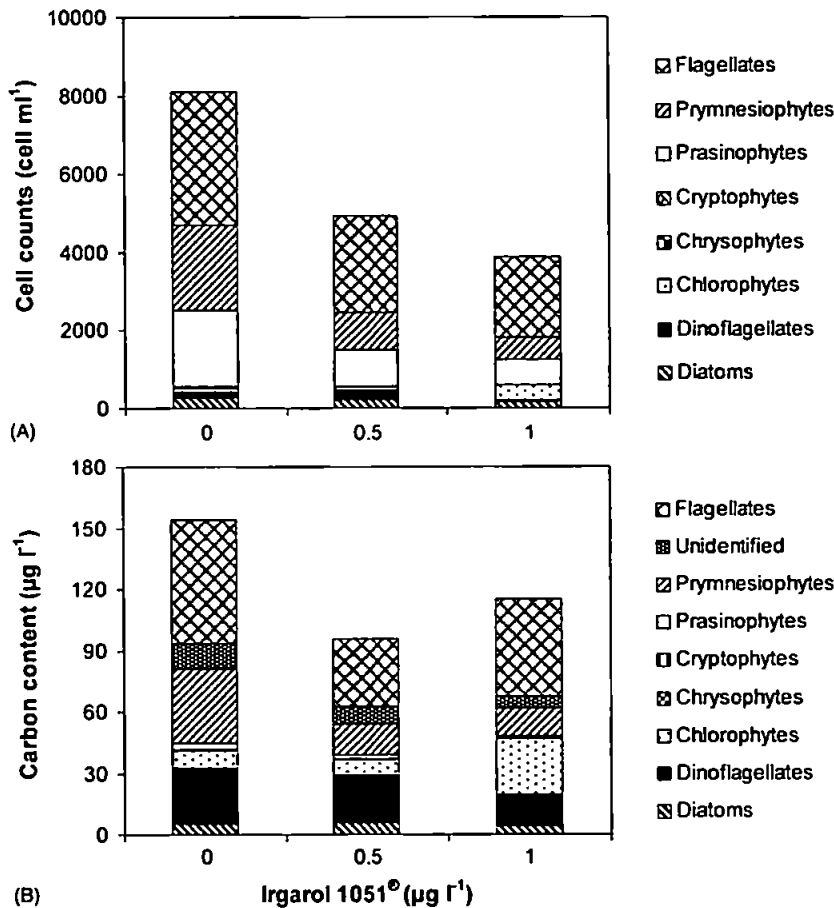


Fig. 5. Phytoplankton response after 96 h exposure to 0.5 and 1.0 µg l⁻¹ Irgarol 1051[®] expressed from microscopy results as (A) cell abundances and (B) carbon content estimates ($n=5$).

the phytoplankton community. Dinoflagellates '1' (as discriminated by *K. mikimotoi*), chrysophytes, cryptophytes, and prymnesiophytes contributed to 36%, 21%, 18%, 11%, respectively, for the chlorophyll *a* biomass in the controls after 96 h (Fig. 6B). The contribution of chlorophytes estimated by CHEMTAX increased with increasing concentrations of Irgarol 1051[®], from 4% of

the total biomass in the controls to 21% at 1.0 µg l⁻¹ ($P < 0.05$) (Fig. 6B). Also, the relative contributions of diatoms and dinoflagellates increased with increasing exposure to Irgarol 1051[®], from 5% (controls) to 18% (1.0 µg l⁻¹) and from 4% (controls) to 6% (1.0 µg l⁻¹), respectively. The dinoflagellate *K. mikimotoi*, for which the main diagnostic carotenoid is

Table 1
Correlations derived from linear regression between each pigment and chlorophyll *a*

	Chl <i>c</i> ₃	Chl <i>c</i> ₁ <i>c</i> ₂	PER	BUT	FUCO	HEX	ANTH	VIOLA	ALLO	ZEA	Chl <i>b</i>	DIATO	DIADINO	β-CAR
R^2	0.73	0.94	0.41	0.52	0.96	0.55	0.48	0.29	0.84	0.73	0.62	0.50	0.29	0.90
P	0.0000	0.0000	0.0096	0.0025	0.0000	0.0016	0.0041	0.0038	0.0000	0.0000	0.0005	0.0030	0.0378	0.0000

Data were obtained from all treatments (control, 0.5 and 1.0 µg l⁻¹ Irgarol 1051[®]) at 96 h of experiment; $n=15$. Chl, chlorophylls *b*, *c*₁*c*₂ or *c*₃; PER, peridinin; BUT, 19'-butanoyloxyfucoxanthin; FUCO, fucoxanthin; HEX, 19'-hexanoyloxyfucoxanthin; ANTH, antheraxanthin; VIOLA, violaxanthin; ALLO, alloxanthin; ZEA, zeaxanthin; DIATO, diatoxanthin; DIADINO, diadinoxanthin; β-CAR, β-carotene.

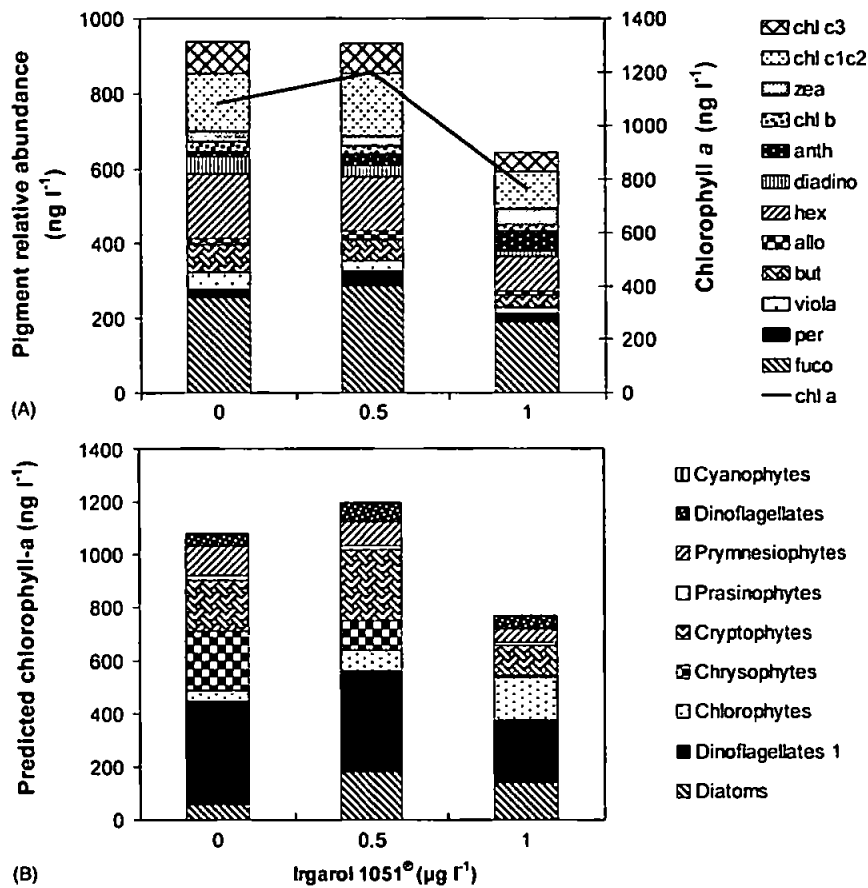


Fig. 6. Phytoplankton response after 96 h exposure to 0.5 and 1.0 µg l⁻¹ Irgarol 1051[®] expressed as (A) diagnostic pigment relative abundance and (B) predicted chlorophyll *a* from CHEMTAX calculations ($n=5$). The abbreviations used follow: Chl: chlorophylls *a*, *b*, *c*₁*c*₂ or *c*₃; per, peridinin; but, 19'-butanoyloxyfucoxanthin; fuco, fucoxanthin; hex, 19'-hexanoyloxyfucoxanthin; anth, antheraxanthin; viola, violaxanthin; allo, alloxanthin; zea, zeaxanthin; diadino, diadinoxanthin (A). 'Dinoflagellates 1' correspond to *K. mikimotoi* (B).

19'-hexanoyloxyfucoxanthin instead of peridinin, was confirmed by CHEMTAX analyses to be a major contributor to the dinoflagellate biomass. The biomass of prymnesiophytes, chrysophytes and dinoflagellates '1' was significantly reduced with increasing concentrations of Irgarol 1051[®] (Fig. 6B) with reductions from 11% (controls) to 7% (1.0 µg l⁻¹), from 21% (controls) to 1% (1.0 µg l⁻¹), and from 36% (controls) to 31% (1.0 µg l⁻¹), respectively for the three groups.

3.4. Comparisons between methods

Comparisons of CHEMTAX estimates of chlorophyll *a* and phytoplankton carbon (from microscopy) showed agreement mainly for chlorophytes

($R^2=0.53$; $P=0.002$), cryptophytes ($R^2=0.51$; $P=0.003$) and dinoflagellates (discriminated as *K. mikimotoi*) ($R^2=0.48$; $P=0.004$) (Fig. 7). Unidentified flagellates enumerated by microscopy also showed agreement with prymnesiophytes ($R^2=0.56$; $P=0.001$), chrysophytes ($R^2=0.54$; $P=0.002$), and prasinophytes ($R^2=0.64$; $P<0.001$) (Fig. 7) estimated by CHEMTAX. Discrepancies were, however, observed for cryptophytes, which did not show a correlation with unidentified flagellates enumerated by microscopy. Also, no correlation was observed between total carbon and total chlorophyll *a* (data not shown).

Comparisons of cell enumeration by microscopy and by flow cytometry revealed good agreement for na-

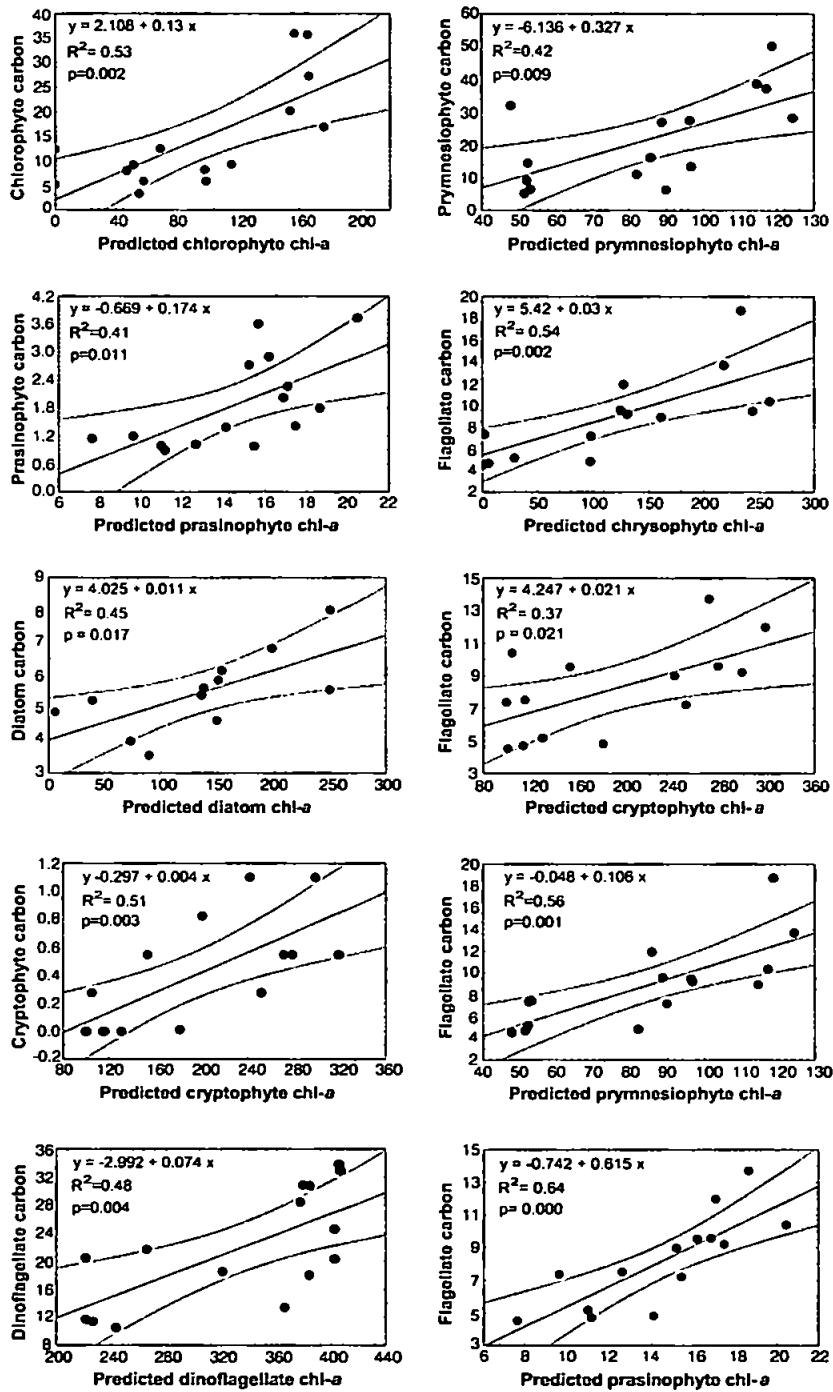


Fig. 7. Biomass of individual algal classes as chlorophyll *a* (chl-*a*) in ng l^{-1} estimated from CHEMTAX calculations (*x*-axis) and as carbon concentration in $\mu\text{g l}^{-1}$ estimated by microscopy (*y*-axis). Linear regressions are significant ($P < 0.05$) between biomass estimations ($n = 15$). Data are rank transformed (diatoms) and $\log(x + 1)$ transformed (cryptophyte \times flagellate).

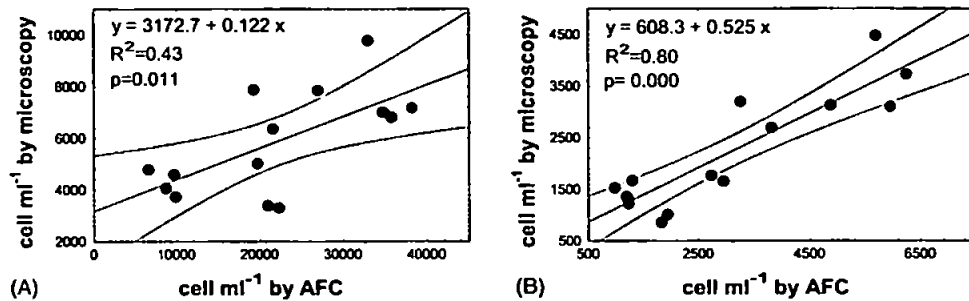


Fig. 8. Relationship between cell enumeration made by microscopy and analytical flow cytometry (AFC) for (A) picoeukaryotes and (B) nanoeukaryotes. Regressions are significant ($P < 0.05$; $n = 15$).

noeukaryotes ($R^2 = 0.80$; $P < 0.001$), although a lower coefficient of determination was found for picoeukaryotes ($R^2 = 0.43$; $P = 0.011$) (Fig. 8).

3.5. Irgarol 1051[®] analyses

At the beginning of the experiment, measured concentrations of Irgarol 1051[®] were 0.61 and 1.16 $\mu\text{g l}^{-1}$ for the two dosing concentrations. Following replenishment of the seawater (after 48 h), concentrations were measured to be 0.60 and 1.20 $\mu\text{g l}^{-1}$. At the end of the experiment, measured concentrations were 0.58 and 1.13 $\mu\text{g l}^{-1}$. Concentrations measured for the controls were close to the limit of detection of the method.

4. Discussion

Addition of the PSII inhibitor Irgarol 1051[®] to the microcosms induced marked changes in the phytoplankton community as revealed by microscopy, class-specific pigments and AFC. Nanoeukaryotes appeared to be more affected by Irgarol 1051[®] than picoeukaryotes. This higher sensitivity could be related to the presence of species- or class-specific algae which are more vulnerable to antifoulant stress. The decline in cyanophytes with time, as measured by AFC, may have resulted from the experimental conditions giving optimal conditions for other groups to develop. According to optical microscopy, chrysophytes were not sensitive to Irgarol 1051[®], whilst chlorophytes were stimulated with increasing Irgarol 1051[®] exposure concentrations. Despite efforts in reducing the heterotrophs present in the microcosms, their presence might have influenced the abundances of some classes due to selective her-

bivory. Prasinophytes and prymnesiophytes were the most sensitive groups to Irgarol 1051[®]. The sensitivity of prymnesiophytes to this biocide was also detected in recent studies (Readman et al., 2004; Devilla et al., in press).

Optical microscopy and class-specific pigment techniques identified changes in dominant microalgae groups amongst controls and treated microcosms. Significant correlations were found between chlorophyll *a* biomass and the diagnostic pigments. CHEMTAX–HPLC pigment data was used to quantify the contribution of the individual phytoplankton groups to total chlorophyll *a*. Estimation of phytoplankton composition using CHEMTAX indicated structural changes relative to the controls following exposures to Irgarol 1051[®]. Significant correlations were found between the group-specific chlorophyll *a* of several phytoplankton groups and their respective carbon biomass as estimated from optical microscopy. Results indicated an agreement between carbon content and chlorophyll biomass of chlorophytes ($R^2 = 0.53$). Significant amounts of 19'-hexanoyloxyfucoxanthin could be attributed to a particular species of dinoflagellate (*K. mikimotoi*), which was shown by optical microscopy to comprise 80% of the dinoflagellate carbon content. Good agreement was demonstrated between the two techniques for inhibition of this particular dinoflagellate following exposure to 1.0 $\mu\text{g l}^{-1}$ Irgarol 1051[®]. *K. mikimotoi* did not, however, show significant inhibition at the lower Irgarol 1051[®] concentration tested (0.5 $\mu\text{g l}^{-1}$), as shown by either microscopy or CHEMTAX estimations.

Light microscopic analyses confirmed the presence of phytoplankton groups which corresponded to the diagnostic pigments for dinoflagellates (mainly *K. miki-*

motoi, which contains 19'-hexanoyloxyfucoxanthin), diatoms (fucoxanthin), prymnesiophytes (19'-hexanoyloxyfucoxanthin), chlorophytes and prasinophytes (chlorophyll *b*). Following exposure, marked reductions in prymnesiophyte and flagellate carbon contents (estimated from microscopy) were observed, whilst chlorophytes increased in cell numbers and carbon content (compared to the controls) with increasing concentrations of Irgarol 1051®. A large quantity of small phytoflagellates (nanoplankton flagellates) could not be taxonomically identified by microscopy. These flagellates probably belong mostly to prasinophytes, haptophytes and chrysophytes. This is supported by the significant correlation found between small flagellate abundance and the CHEMTAX estimates.

Microscopy observations, together with AFC, did not corroborate the presence of cryptophytes as estimated by CHEMTAX. A possible explanation for this disagreement could be either problems in sample preservation which render microscopic observations difficult, or the presence of dinoflagellates or the ciliate *Mesodinium rubrum*, which can contain cryptophytes as endosymbionts (Gieskes and Kraay, 1983; Jeffrey and Vesik, 1997).

In general, correlations between carbon biomass and concentrations of the respective pigment marker co-vary between phytoplankton communities (Breton et al., 2000). The more an algal group is homogeneous in composition and size, the better is the correlation (Breton et al., 2000). Even though positive correlations were found between chlorophyll *a* and carbon content for some individual microalgal groups, quantitative comparison of total chlorophyll *a* to total carbon concentration indicated discrepancies. Total carbon and chlorophyll *a* decreased significantly under high ($1.0 \mu\text{g l}^{-1}$) Irgarol 1051® exposure. Under low exposure ($0.5 \mu\text{g l}^{-1}$), however, both parameters showed opposite trends, where chlorophyll biomass was not shown to be affected whereas the carbon content decreased. Irgarol 1051® is known to impair photosynthesis by displacing a plastoquinone (Q_B) from its binding site in the D1 protein of photosystem II (Cremlyn, 1991), and considered to be one of the most potent photosynthetic inhibitors (Dahl and Blanck, 1996). Cellular amounts of light-harvesting pigments may, however, increase under moderate photosynthetic inhibition by a herbicide, simulating the effects of light limitation (Plumley and Davis, 1980).

Although cell densities were significantly reduced with increasing concentrations of Irgarol 1051®, total carbon did not differ between concentrations of 0.5 and $1.0 \mu\text{g l}^{-1}$ Irgarol 1051®, probably owing to a volume increase relating to delayed cell division. As a consequence, no linear correlation between total carbon and total chlorophyll *a* was found.

Investigating the influence of toxicants in coastal areas requires rapid methods to detect subtle modifications in community structure. Flow cytometry and HPLC are both rapid methods that can identify changes in community and, with the aid of microscopy, can yield a comprehensive description which can be used to assess the effects of toxicants. Measuring pigment composition by HPLC affords a more rapid discrimination of algal types than microscopic analyses, especially for small-sized cells that are difficult to visualise. Group-specific chlorophyll *a* estimations may afford a good approximation of carbon biomass from HPLC pigment analyses (Breton et al., 2000), but algal class biomass estimations from pigment data in coastal waters should be treated cautiously since pigment per chlorophyll *a* measures can vary due to anthropogenic stressors (Devilla et al., in press). Cellular-intrinsic or environmental parameters can also influence this parameter (Mackey et al., 1996).

Cross-correlation analyses between diagnostic pigments and the presence of specific algal groups are necessary to understand the accuracy of chemotaxonomic estimations. Biomass estimations from pigments require a stable physiological state, which is difficult to achieve in the environment. Thus, variations in pigment content per chlorophyll *a* and carbon per chlorophyll *a* hamper class-specific biomass estimations. Even though a number of class-specific pigment ratios are available in the literature (Mackey et al., 1996; Goericke and Montoya, 1998; Schlüter et al., 2000; Henriksen et al., 2002), more research to evaluate the influence of environmental parameters on pigment:chlorophyll *a* ratios would enable more accurate predictions, especially when considering coastal areas with herbicidal inputs (Devilla et al., in press). Different responses for the various pigment:chlorophyll *a* ratios have been reported within the same phytoplankton group and even between species (Goericke and Montoya, 1998; Henriksen et al., 2002), where inter-species variability exceeds the differences in the ratios caused by the varying growth conditions (Schlüter et al.,

2000). Besides the influences of irradiance, nutritional state and growth phase, it is also necessary to understand the xenobiotic influences regulating dynamics in phytoplankton community-structures in coastal areas.

5. Conclusions

The toxicity of the PSII inhibitor Irgarol 1051[®] towards the phytoplankton community studied induced a restructuring of the community and therefore, changes in taxonomic composition. Group-specific sensitivity was detected through microscopy and was corroborated with CHEMTAX estimations. Results revealed that chlorophytes and dinoflagellates are comparatively resistant to Irgarol 1051[®]. Estimates from HPLC–CHEMTAX pigment analyses were correlated with chlorophytes ($R^2=0.53$), which increased in both abundance and carbon content under exposures to Irgarol 1051[®]. Both CHEMTAX–HPLC analyses and microscopy revealed that prasinophytes and prymnesiophytes are the most affected groups by exposure to Irgarol 1051[®]. Abundances determined by microscopy afforded good agreement with AFC in measuring nanoeukaryotes ($R^2=0.8$), but microscopy was shown to underestimate picoeukaryotes.

Monitoring phytoplankton responses to toxicants benefits from the assessment of a relatively large number of samples. Less time-consuming methods that evaluate all phytoplankton sizes are therefore beneficial. The use of class-specific pigment determinations combined with AFC and some microscopic screening is demonstrated to provide a comprehensive evaluation of the effects on a phytoplankton community under the stress of a PSII inhibitor.

Acknowledgements

This research was supported by a Brazilian Research Council (CNPq) studentship to R.A. Devilla, and was also supported by the European Commission under the ACE (Assessment of Antifouling Agents in Coastal Environments) contract (MAS3-CT98-0178) (a component of the EC IMPACTS cluster). The authors thank H.W. Higgins for a copy of CHEMTAX program and D. Harbour for microscopic analysis.

References

- Andersen, R.A., Bidigare, R.R., Keller, M.D., Latasa, M., 1996. A comparison of HPLC pigment signatures and electron microscopy observations for oligotrophic waters of the North Atlantic and Pacific Oceans. *Deep-Sea Res.* 43, 517–537.
- Barlow, R.G., Mantoura, R.F.C., Gough, M.A., Fileman, T.W., 1993. Pigment signatures of the phytoplankton composition in the northeastern Atlantic during the 1990 spring bloom. *Deep-Sea Res.* 41, 459–477.
- Barlow, R.G., Cummings, D.G., Gibb, S.W., 1997. Improved resolution of mono- and divinyl chlorophylls *a* and *b* and zeaxanthin and lutein in phytoplankton extracts using reverse phase C-8 HPLC. *Mar. Ecol. Prog. Ser.* 161, 303–307.
- Beers, J.R., Reid, F.M.H., Stewart, G.L., 1975. Microplankton of the North Pacific central gyre. Population structure and abundance, June 1973. *Int. Revue Ges Hydrobiol.* 60, 607–638.
- Breton, E., Brunet, C., Sautour, B., Brylinski, J.-M., 2000. Annual variations of phytoplankton biomass in the eastern English Channel: comparison by pigment signatures and microscopic counts. *J. Plankton Res.* 22, 1423–1440.
- Carreto, J.I., Montoya, N.G., Benavides, H.R., Guerrero, R., Carignan, M.O., 2003. Characterization of spring phytoplankton communities in the Rio de La Plata maritime front using pigment signatures and cell microscopy. *Mar. Biol.* 143, 1013–1027.
- Cremlyn, R.J., 1991. *Agrochemicals: Preparation and Mode of Action*. Wiley, New York.
- Dahl, B., Blanck, H., 1996. Toxic effects of the antifouling agent Irgarol 1051 on periphyton communities in coastal water microcosms. *Mar. Pollut. Bul.* 32, 342–350.
- Devilla, R.A., Brown, M.T., Donkin, M.E., Tarran, G.A., Aiken, J., Readman, J.W., in press. Impact of antifouling booster biocides on single microalgal species and on a natural marine phytoplankton community. *Mar. Ecol. Prog. Ser.*
- Eppley, R.W., Reid, F.M.H., Strickland, J.D.H., 1970. Estimates of phytoplankton crop size, growth rate and primary production. In: Strickland, J.D.H. (Ed.), *The Ecology of the Plankton off La Jolla, California in the Period April Through September, 1967*, Bull Scripps Inst. Oceanogr. 17, 33–42.
- Fietz, S., Nicklish, A., 2004. An HPLC analysis of the summer phytoplankton assemblage in Lake Baikal. *Freshwater Biol.* 49, 332–345.
- Garibotti, I.A., Vernet, M., Kozlowski, W.A., Ferrario, M.E., 2003. Composition and biomass of phytoplankton assemblages in coastal Antarctic waters: a comparison of chemotaxonomic and microscopic analyses. *Mar. Ecol. Prog. Ser.* 247, 27–42.
- Gieskes, W.W.C., Kraay, G.W., 1983. Dominance of *Cryptophyceae* during the phytoplankton spring bloom in the central North Sea detected by HPLC analysis of pigments. *Mar. Biol.* 75, 179–185.
- Gin, K.Y.H., Zhang, S., Lee, Y.K., 2003. Phytoplankton community structure in Singapore's coastal waters using HPLC pigment analysis and flow cytometry. *J. Plankton Res.* 25, 1507–1519.
- Goericke, R., Montoya, J.P., 1998. Estimating the contribution of microalgal taxa to chlorophyll *a* in the field – variations of pigment ratios under nutrient- and light-limited growth. *Mar. Ecol. Prog. Ser.* 169, 97–112.

- Hamilton, P.B., Jackson, G.S., Kaushik, N.K., Solomon, K.R., Stephenson, G.L., 1988. The impact of two applications of atrazine on the plankton communities of in situ enclosures. *Aquat. Toxicol.* 13, 123–140.
- Henriksen, P., Riemann, B., Kaas, H., Sorensen, H.M., Sorensen, H.L., 2002. Effects of nutrient-limitation and irradiance on marine phytoplankton pigments. *J. Plankton Res.* 24, 835–858.
- HSE, 2002a. Health and Safety Executive. Guidelines on the Efficacy Data Requirements for Approval of Non-agricultural Pesticide Products. p. 18.
- HSE, 2002b. Health and Safety Executive. Information Document, HSE 730/15, p. 13.
- Irigoien, X., Head, R.N., Harris, R.P., Cummings, D., Harbour, D., 2000. Feeding selectivity and egg production of *Calanus helgolandicus* in the English Channel. *Limnol. Oceanogr.* 45, 44–54.
- Jeffrey, S.W., Vesk, M., 1997. Introduction to marine phytoplankton and their pigment signatures. In: Jeffrey, S.W., Mantoura, R.F.C., Wright, S.W. (Eds.), *Phytoplankton Pigments in Oceanography: Guidelines to Modern Methods*. UNESCO, Paris, pp. 37–84.
- Jeffrey, S.W., Mantoura, R.F.C., Wright, S.W., 1997. *Phytoplankton Pigments in Oceanography*. UNESCO, Paris, p. 661.
- Johnsen, G., Sakshaug, E., 1993. Bio-optical characteristics and photoadaptive responses in the toxic and bloom-forming dinoflagellates *Gyrodinium aureolum*, *Gymnodinium galatheanum*, and two strains of *Prorocentrum minimum*. *J. Phycol.* 29, 627–642.
- Jorgensen, E., Christoffersen, K., 2000. Short-term effects of linear alkylbenzene sulfonate on freshwater plankton studied under field conditions. *Environ. Toxicol. Chem.* 19, 904–911.
- Kovala, P.E., Larrance, J.D., 1966. Computation of phytoplankton cell numbers, cell volume, cell surface and plasma volume per litre, from microscopical counts. University of Washington, Department of Oceanography, Spec. Rep. No. 38, 1–21.
- Mackey, M.D., Mackey, D.J., Higgins, H.W., Wright, S.W., 1996. CHEMTAX – a program for estimating class abundances from chemical markers: application to HPLC measurements of phytoplankton. *Mar. Ecol. Prog. Ser.* 144, 265–283.
- Margalef, R., 1958. Temporal succession and spatial heterogeneity in phytoplankton. In: Buzzati-Traverso, A.A. (Ed.), *Perspectives in Marine Biology*. University of California Press, Berkeley, pp. 323–350.
- McCormick, P.V., Cairns, J.J., 1994. Algae as indicator of environmental change. *J. Appl. Phycol.* 6, 509–526.
- Montagnes, D.J.S., Franklin, D.J., 2001. Effect of temperature on diatom volume, growth rate, and carbon and nitrogen content: re-considering some paradigms. *Limnol. Oceanogr.* 46, 2008–2018.
- Pingree, R.D., Holligan, P.M., Mardell, G.T., 1978. The effects of vertical stability on phytoplankton distributions in the summer on the northwest European Shelf. *Deep-Sea Res.* 25, 1011–1028.
- Plumley, F.G., Davis, D.E., 1980. Effects of the photosynthetic inhibitor atrazine on salt marsh edaphic algae in culture, microecosystems and in the field. *Estuaries* 3, 271–277.
- Readman, J.W., Kwong, L.L.W., Grondlin, D., Bartocci, J., Vielleuneuve, J.P., Mee, L., 1993. Coastal water contamination from a triazine herbicide used in antifouling paints. *Environ. Sci. Technol.* 27, 1940–1942.
- Readman, J.W., Devilla, R.A., Tarran, G., Llewellyn, C.A., Fileman, T.W., Easton, A., Burkill, P.H., Mantoura, R.F.C., 2004. Flow cytometry and pigment analyses as tools to investigate the toxicity of herbicides to natural phytoplankton communities. *Mar. Environ. Res.* 58, 353–358.
- Rodriguez, F., Fernandez, E., Head, R.N., Harbour, D.S., Bratbak, G., Heldal, M., Harris, R.P., 2000. Temporal variability of viruses, bacteria, phytoplankton and zooplankton in the western English Channel off Plymouth. *J. Mar. Biol. Assoc. UK* 80, 575–586.
- Rodriguez, F., Varela, M., Zapata, M., 2002. Phytoplankton assemblages in the Gerlache and Bransfield Straits (Antarctic Peninsula) determined by light microscopy and CHEMTAX analysis of HPLC pigment data. *Deep-Sea Res. II* 49, 723–747.
- Sargent, C.J., Bowman, J.C., Zhou, J.L., 2000. Levels of antifoulant Irgarol 1051® in the Conwy Marina, North Wales. *Chemosphere* 41, 1755–1760.
- Schlüter, L., Mohlenberg, F., Havskum, H., Larsen, S., 2000. The use of phytoplankton pigments for identifying and quantifying phytoplankton groups in coastal areas: testing the influence of light and nutrients on pigment/chlorophyll-*a* ratios. *Mar. Ecol. Prog. Ser.* 192, 49–63.
- Simon, N., Barlow, R.G., Marie, D., Partensky, F., Vaulot, D., 1994. Characterization of oceanic photosynthetic picocaryotes by flow cytometry. *J. Phycol.* 30, 922–935.
- Strathmann, R.R., 1967. Estimating the organic carbon content of phytoplankton from cell volume or plasma volume. *Limnol. Oceanogr.* 12, 411–418.
- Thomas, K.V., Fileman, T.W., Readman, J.W., Waldock, M.J., 2001. Antifouling paint booster biocides in the UK coastal environment and potential risks of biological effects. *Mar. Pollut. Bul.* 42, 677–688.
- Thomas, K.V., McHugh, M., Waldock, M., 2002. Antifouling paint booster biocides in UK coastal waters: inputs, occurrence and environmental fate. *Sci. Total Environ.* 293, 117–127.
- UNESCO, 1974. A review of methods used for quantitative phytoplankton studies. UNESCO Tech. Pap. Mar. Sci. 18, 1–27.
- Wright, S.W., Jeffrey, S.W., 1997. High resolution HPLC system for chlorophylls and carotenoids of marine phytoplankton. In: Jeffrey, S.W., Mantoura, R.F.C., Wright, S.W. (Eds.), *Phytoplankton Pigments in Oceanography: Guidelines to Modern Methods*. UNESCO, Paris, pp. 327–341.